PHENOMENOLOGICAL STUDY OF RARE SEMILEPTONIC B MESON DECAYS WITH LEPTOQUARKS

To be submitted in the partial fulfilment for the degree of
DOCTOR OF PHILOSOPHY IN PHYSICS

BY

SUCHISMITA SAHOO
13PHPH05

Under the supervision of
Prof. RUKMANI MOHANTA

School of Physics
University of Hyderabad
Hyderabad 500 046, INDIA

October 2017

DECLARATION

I hereby declare that, this thesis titled **Phenomenological Study of Rare Semileptonic *B* Meson Decays with Leptoquarks** submitted by me, under the guidance and supervision of **Prof. Rukmani Mohanta**, is a bonafide research work and is free from plagiarism. I also declare that it has not been submitted previously, in part or in full to this University or any other University or Institution, for the award of any degree or diploma. I hereby agree that my thesis can be deposited in Shodhganga/INFLIBNET.

A report on plagiarism statistics from the University Librarian is enclosed.

Hyderabad (Suchismita Sahoo)
Date: Reg. No.: 13PHPH05

CERTIFICATE

This is to certify that the thesis entitled **Phenomenological Study of Rare Semileptonic *B* Meson Decays with Leptoquarks** submitted by Suchismita Sahoo bearing registration number 13PHPH05 in partial fulfilment of the requirements for award of Doctor of Philosophy in the School of Physics is a bonafide work carried out by her under my supervision and guidance.

This thesis is free from plagiarism and has not been submitted previously in part or in full to this or any other University or Institution for award of any degree or diploma.

Further, the student has the following publications before the submission of the thesis for adjudication.

1) S. Sahoo, and R. Mohanta, Physical Review D **91**, 094019 (2015), (ISSN No: 2470-0029 (online)), Chapter 3.

2) S. Sahoo, and R. Mohanta, New Journal of Physics **18**, 013032 (2015), (ISSN No: 1367-2630 (online)), Chapter 3.

3) S. Sahoo, and R. Mohanta, Physical Review D **93**, 034018 (2015), (ISSN No: 2470-0029 (online)), Chapter 4.

4) S. Sahoo, R. Mohanta, and A. K. Giri, Physical Review D **95**, 035027 (2017), (ISSN No: 2470-0029 (online)), Chapter 5.

5) M. Duraisamy, S. Sahoo, and R. Mohanta, Physical Review D **95**, 035022 (2017), (ISSN No: 2470-0029 (online)), Chapter 6.

Further, the student has passed the following courses towards fulfilment of coursework requirement for Ph.D:

Course Code	Name	Credits	Pass/Fail
PY801	Advanced Quantum Mechanics	4	Pass
PY803	Advanced Statistical Mechanics	4	Pass
PY804	Advanced Electromagnetic Theory	4	Pass
PY821	Research Methodology	4	Pass

Prof. Rukmani Mohanta
Thesis Supervisor
School of Physics
University of Hyderabad

Prof. Bindu A. Bambah
Dean
School of Physics
University of Hyderabad

Date:

Acknowledgements

I would like to convey my heartful gratitude to many people for their continuous support and encouragement throughout my research career.

First among these is my supervisor, Prof. Rukmani Mohanta, whom I would like to thank for taking me in her team. Each and every aspect of this thesis has taken its present shape under her proper guidance and help in both research and in day-to-day life. It was a great pleasure to work with her. I also wish to thank her for her patience and understanding during my Ph.D. period.

I would like to convey my special thank to our Dean, Prof. Bindu A. Bambha for her encouraging words to pursue research in Particle Physics. With the same respect, I wish to thank our former Dean of the School, Prof. S. Chaturvedi and Prof. R. Singh.

I am extremely thankful to my doctoral committee members, Prof. E. Harikumar and Prof. Soma Sanyal for their support. In addition, I would like to convey my thanks to all the faculty members of our school.

I consider myself extremely fortunate to get the opportunity to collaborate with Prof. A. K. Giri, Indian Institute of Technology, Hyderabad and Prof. M. Duraisamy, Virginia Commonwealth University, USA. I would like to thank them for their scintillating and lively discussions. I would also like to thank Prof. Sudhanwa Patra, Indian Institute of Technology, Bhilai for his encouraging words.

I acknowledge all the non-teaching staff of our School. My special thank goes to Mr. T. Abraham and Ms. Deepika, for their patience and help in the academic activities.

I acknowledge the Science and Engineering Research Board (SERB), Government of India for the financial support during my research period. In this context, I would like to convey my gratitude to my supervisor for giving me this opportunity.

I would like to express my gratitude to my teachers (from School to University) for their support at different stages of my academic life. I am extremely thankful to Suresh babu, Ramesh babu, Sanju babu and all the family members for their blessings and financial support. I would like to thank my uncle Mr. Bharat Sahoo for his encouraging words.

I would like to thank my seniors Soumya Di and Sruthilaya Di for their useful suggestions and support. I am extremely thankful to Sanjeev Bhai for handling my computer related issues. I would like to convey my thank to my friends Jitu, Robertson, Aswathi, and all my classmates for their selfess support and beautiful friendship. A very special and heartful thank goes to my friend and labmate Shivaramkrishna for his constant support during up-down period of my research career. I am extremely thankful to my juniors, Saswati, Atasi, Pooja, Aishwarya, Akshay, Rudra, Mitesh, Lipu, Anubhab, Kunu, Manas, Subhasmita, Itishree, Purnima, Bijeta and Sujita.

I would like to thank my old friends Srabani, Nirakar, Biswaranjan, Pintu, Ranesh, Bikash, Aishwarya and Debadeepti. I would like to convey my heartful thank to my friend Jogesh for his constant support during my boring, lonely and bad periods of life.

My family has been a source of unwavering support, and no words in these acknowledgements can adequately thank them. I would like to convey my love and special gratitude to my family members, without whose support and understanding, the success of my life journey was impossible. A very special thank goes to my elder parents, Mr. Udayanath Sahoo and Mrs. Kamala Sahoo. My father and mother, Mr. Kailash Chandra Sahoo and Mrs. Shashirekha Sahoo are both models of love and compassion. They are my role models in everything I do. I would like to thank my brothers and sister-in-law: Mr. Satya Narayan Sahoo and Mrs. Parbati Sahoo, Mr. Pramod Sahoo and Mrs. Subhashree Sahoo for supporting me to continue my research. I am also thankful to all my sisters and brother-in-law: Sabita Di and Banku Bhai, Rasmita Di and Srimanta Bhai, Kuni Di and Kiran Bhai, Minu Di and Alok Bhai, Tuni Di and Jagan Bhai. Finally, I would like to express my love to all my nephew and nieces, Soumya, Priyanshu, Akash, Tisha, Disha and Pratyush who have always added happiness in my life.

Last but not at all the least, I would like to convey my love and deep gratitude to my friend Kanha for being my confidante.

Abstract

A search for new physics beyond the standard model in some rare semileptonic B meson decays has been precisely investigated in this thesis in the context of leptoquark model.

The SM describes the behavior of particles at the fundamental level and has capability to elucidate almost all the existing experimental data so far. Still we need physics beyond it in order to answer some of the open questions, such as the matter-antimatter asymmetry, neutrino oscillation, dark matter and dark energy components etc. Recently, the B factories BaBaR and Belle as well as the LHCb experiment have reported several anomalies in the semileptonic B meson decays, such as P_5' observable, the $R_{K^{(*)}}$ and $R_{D^{(*)}}$ etc. These observables have discrepancy of $(3-4)\sigma$ from the corresponding SM predictions. In order to resolve the anomalies in B meson, we extend the SM with an addition of a scalar/vector leptoquark.

We study the rare $\bar{B} \to \bar{K} l^+ l^-$ and $\bar{B} \to \bar{K}^{(*)} \nu\bar{\nu}$ processes, driven by the quark level transition $b \to s l^+ l^- (\nu\bar{\nu})$ by using $(3, 2, 7/6)$ scalar leptoquark model. We work out the constraint on the leptoquark couplings by using the branching ratios of $B_s \to l^+ l^-$ and $\bar{B} \to X_s l^+ l^-$ processes, measured by the CMS and LHCb experiments. Using the new couplings, we estimate the branching ratios, isospin asymmetries, lepton non-universality parameters and the flat term of $\bar{B} \to \bar{K} l^+ l^-$ processes in the full q^2 region except the intermediate region. The branching ratios of semileptonic B decays with neutrinos in the final state, $\bar{B} \to \bar{K}^{(*)} \nu\bar{\nu}$ are also computed in the scalar leptoquark model.

Furthermore, we investigate the effect of scalar leptoquarks $(3, 2, 7/6)$ and $(3, 2, 1/6)$ on the exclusive rare B meson decays $\bar{B} \to \bar{K}^*(\to K^- \pi^+) l^+ l^-$ in both the low and high q^2 region. In addition to the above constraint on leptoquark coupling, we also constrain the new parameters by considering the present experimental data on $B^0 - \bar{B}^0$ oscillation. We compute the branching ratio, forward-backward asymmetry and isospin asymmetry distribution using the constrained parameter space. We also look into various form factor independent observables like $P'_{4,5,6}$ and CP violating parameters of $\bar{B} \to \bar{K}^* l^+ l^-$ decay modes in the scalar leptoquark model.

We investigate a simultaneous explanation of $R_{D^{(*)}}$ and R_K anomalies by considering the vector leptoquarks $(3, 3, 2/3)$ and $(3, 1, 2/3)$ relevant for both $b \to c l \bar{\nu}_l$ and $b \to s l^+ l^-$ transitions. The leptoquark parameter space is constrained by using the experimentally measured branching ratios of $B_s \to l^+ l^-$, $\bar{B} \to X_s l^+ l^- (\nu\bar{\nu})$ and $B_u^+ \to l^+ \nu_l$ processes. Using the constrained leptoquark couplings, we compute the branching ratios, forward-backward asymmetries, τ and D^* polarization parameters in the $\bar{B} \to \bar{D}^{(*)} l \bar{\nu}_l$ processes. We found that vector leptoquarks can explain both the R_K and $R_{D^{(*)}}$ anomalies, simultaneously.

We also envisage the consequence of vector leptoquarks on the rare semileptonic lepton flavor violating decays of the B meson which are more promising and effective channels to probe the new physics signal. We assume that the resulting leptoquark couplings are real and constrain the new parameter space by using the branching ratios of $B_{s,d} \to l^+l^-$, $K_L \to l^+l^-$ and $\tau^- \to l^-\gamma$ processes. We estimate the branching ratios of rare lepton flavor violating $B^+ \to K^+(\pi^+)l_i^- l_j^+$ processes using the constrained leptoquark couplings. We also compute the forward-backward asymmetries and the lepton non-universality parameters of these decays in the vector leptoquark model. Furthermore, we study the effect of vector leptoquark on the $(g-2)_\mu$ anomaly.

Contents

List of Figures

List of Tables

Dedicated to my family,
specially to my beloved father

Chapter 1

Introduction

1.1 Standard model: Theory of fundamental particles

We being the followers of symmetry, endeavored to realize the symmetry in nature from the days of yore. In the class of all possible theoretical ideas to explore the symmetry in physics, the foremost success is the standard model (SM), which is a wonderful theoretical framework build up by the particle physicists in order to narrate the particles, their behavior, and interactions. Standard model, the one and only theoretical model which could accommodate most of the observed experimental data at the most fundamental level.

1.1.1 The particle content

In the SM, for every particle there exists an antiparticle which behaves in the same way as the particle, with an exception of opposite charge. Based on the quantum numbers, the particle spectrum in this model is categorized into two types: (i) Fermion, (ii) Boson. The fermions are subatomic particles with odd half-integral spin, which are characterized by the Fermi-Dirac statistics and obey the Pauli-exclusion principle. They are further divided into quarks and leptons, which are the fundamental constituents of all the visible matters. Quarks are massive half-spin elementary particles, which have fractional electric charge as $\pm\frac{2}{3}$ (for up type) or $\mp\frac{1}{3}$ (for down type). There exist 6 flavors of quarks in nature namely, *up* (u), *down* (d), *strange* (s), *charm* (c), *bottom* (b) and *top* (t), which are classified into three generations. Quarks of different flavors combine with each other to form composite particles called hadrons, which in general are of two types (i) Baryons, which contain three quarks and (ii) Mesons, which contain a quark-antiquark pair. Imposing Pauli-exclusion principle to the triquark state, a new quantum number called "color" charge has been introduced. All flavors of quarks come in three colors, namely red (R), green (G) and blue (B) and the corresponding antiquarks have anticolors. The composite particles should be colorless. Leptons are half-spin point like particles with no more internal structure. As like quarks, leptons are also arranged in three families but don't carry any color charge. Based on the electric charge, leptons are divided into two categories, (i) charged leptons: electron (e), muon (μ) and tau (τ) (ii) neutral leptons: electron neutrino (ν_e), muon neutrino (ν_μ) and tau neutrino (ν_τ). Each generation of leptons is associated with a corresponding lepton number (L_i), which is conserved in the SM.

The integral spin elementary particles, obeying the Bose-Einstein statistics are known as bosons. The observed fundamental bosons in the SM include the vector gauge bosons such as photon (γ), gluon (g), $W^\pm$ and Z^0, which mediate the elementary interactions, and the scalar Higgs boson, which generates masses of the SM particles. Strong, electromagnetic, weak and gravitational forces are the four fundamental forces of the universe. Of these, the strong force is strongest one and is also known as color or nuclear force. The massless bicolor gluon is the carrier of strong interactions, which can talk strongly with quarks and other gluons. This interaction is well explained by the theory of Quantum Chromodynamics (QCD) and the strength is represented in terms of the QCD coupling constant (α_s), which decreases with the increase of energy. This property is known as asymptotic freedom. The massless photon mediates the electromagnetic force. Quantum Electrodynamics (QED) is the theory of this force and the corresponding strength is represented by the fine structure constant ($\alpha_{\rm em}$). The weak force is the only interaction of the SM, which allows quarks to exchange their flavor with another. This force is mediated by the massive $W^\pm$ and Z^0 bosons and the corresponding strength is represented by the Fermi constant (G_F), which is experimentally extracted from the life time of muon. This interaction is unique in the sense that it allows the possibility of the change of flavor of the participating particles (quarks and leptons). Gravitational force is the weakest among all four fundamental interactions, which is mediated by a hypothetical massless gauge boson called Graviton, however there is no experimental evidence so far about its existence. This is an attractive force, which attracts all the massive objects towards each other.

Glashow, Salam, and Weinberg suggested the electroweak theory by unifying both the electromagnetic and weak interactions [1–3]. The unified electroweak theory along with the strong interaction form the SM of particle physics, which is represented by the $SU(3)_C \times SU(2)_L \times U(1)_Y$ gauge group. Here $SU(3)_C$ represents the strong interaction with C as the color charge, $SU(2)_L$ denotes the weak interaction where L stands for left-handedness and $U(1)_Y$ is for the electromagnetic force, where $Y = 2\,(Q - T_3)$ (Q is the electric charge and T_3 is the third component of the isospin) is called the weak hypercharge. The left (right) handed quarks and leptons are isospin doublets (singlets) of the $SU(2)_L$ gauge group. In the SM, the invariance of local gauge symmetry demands that all the fundamental particles should be massless, thus contradicting the experimental fact that all the SM particles have non-zero mass. In order to resolve this issue, Higgs mechanism [4–7] was introduced with a new scalar boson called Higgs. Due to the spontaneous symmetry breaking (SSB) of $SU(2)_L \times U(1)_Y \to U(1)_{\rm em}$, the expectation value of the scalar Higgs field (ϕ) in the ground state, i.e., the vacuum expectation value (VEV) is found to be non-zero, which thus, provides masses to all the three gauge bosons ($W^\pm, Z^0$) of weak interactions. The charged leptons also gain their masses through the interaction with Higgs field, whereas the neutrino, photon and gluon remain massless. The non-zero masses of the fermions and gauge bosons, strongly indicate the existence of the Higgs boson. On 4th July 2012, the LHC Collaboration [8, 9] announced the observation of a new particle, which was named as Higgs boson after Prof. Peter Higgs, a tribute for his theoretical contribution to understanding the origination of particle masses. The discovery of Higgs boson has strengthened the foundation of SM.

1.1.2 The interaction Lagrangian in the SM

There are 18 unknown free parameters in the SM, whose numerical values are evaluated by various experiments. In order to get knowledge about the free parameters, we need to elaborate the utmost general Lagrangian of the SM. More explicitly, the general renormalizable Lagrangian of the SM can be written as [10–15]

$$\mathcal{L}^{\rm SM} = \mathcal{L}^{\rm SM}_{\rm kinetic} + \mathcal{L}^{\rm SM}_{\rm Higgs} + \mathcal{L}^{\rm SM}_{\rm Yukawa}, \tag{1.1}$$

where $\mathcal{L}^{\rm SM}_{\rm kinetic}$ carries the fermion kinetic terms along with the gauge interactions, the $\mathcal{L}^{\rm SM}_{\rm Higgs}$ part is responsible for the Higgs mechanism and the Yukawa interaction, i.e., the interaction of fermion with scalar is described by $\mathcal{L}^{\rm SM}_{\rm Yukawa}$.

- $\underline{\boldsymbol{\mathcal{L}^{\rm SM}_{\rm kinetic}}}$:

  The $\mathcal{L}^{\rm SM}_{\rm kinetic}$ part of the SM Lagrangian is given by

$$\begin{aligned} -\mathcal{L}^{\rm SM}_{\rm kinetic} &= i\overline{Q_{L_i}}\not{D}_{Q_L} Q_{L_i} + i\overline{U_{R_i}}\not{D}_{U_R} U_{R_i} + i\overline{D_{R_i}}\not{D}_{D_R} D_{R_i} \\ &\quad + i\overline{L_{L_i}}\not{D}_{L_L} L_{L_i} + i\overline{E_{R_i}}\not{D}_{E_R} E_{R_i}, \end{aligned} \tag{1.2}$$

  where $\not{D} = D^\mu \gamma_\mu$ and

$$Q_{L_i}(3,2,+\frac{1}{6}), \quad U_{R_i}(3,1,+\frac{2}{3}), \quad D_{R_i}(3,1,-\frac{1}{3}), \quad L_{L_i}(1,2,-\frac{1}{2}), \quad E_{R_i}(1,1,-1), \tag{1.3}$$

are the representations of various particles (left-handed quark (lepton) doublet Q_{L_i} (L_{L_i}), right-handed up and down type quark singlets (U_{R_i} and D_{R_i}), right-handed charged-lepton singlet (E_{R_i})) under the SM $SU(3)_C \times SU(2)_L \times U(1)_Y$ gauge group. For the sake of conservation of the local gauge symmetry, the derivatives (∂^μ) are replaced by covariant derivatives (D^μ). Here the covariant derivatives for all the quarks and leptons are related to the partial derivatives through the relations

$$\begin{aligned} D^\mu_{Q_L} &= \partial^\mu + \frac{i}{2} g_s G^\mu_a \lambda_a + \frac{i}{2} g W^\mu_b \tau_b + \frac{i}{6} g' B^\mu, \qquad D^\mu_{L_L} = \partial^\mu + \frac{i}{2} g W^\mu_b \tau_b - \frac{i}{2} g' B^\mu, \\ D^\mu_{U_R} &= \partial^\mu + \frac{i}{2} g_s G^\mu_a \lambda_a + \frac{2i}{3} g' B^\mu, \qquad D^\mu_{E_R} = \partial^\mu - i g' B^\mu, \\ D^\mu_{D_R} &= \partial^\mu + \frac{i}{2} g_s G^\mu_a \lambda_a - \frac{i}{3} g' B^\mu, \end{aligned} \tag{1.4}$$

where G^μ_a (W^μ_b and B^μ) are the neutral gluon fields of strong interaction (isotriplet and isosinglet vector fields of weak interaction) with coupling strength g_s (g and g') and λ_a (τ_b)'s are the $SU(3)_C$ ($SU(2)_Y$) generators.

N. B.: The $\mathcal{L}^{\rm SM}_{\rm kinetic}$ Lagrangian contributes three free parameters, $g_s,\ g$ and g'.

- $\underline{\boldsymbol{\mathcal{L}^{\rm SM}_{\rm Higgs}}}$:

The interaction Lagrangian for scalar Higgs boson is given by [14]

$$\mathcal{L}^{\rm SM}_{\rm Higgs} = \frac{1}{2} (\partial_\mu \phi)^2 - \mu^2 \phi^\dagger \phi - \lambda (\phi^\dagger \phi)^2, \tag{1.5}$$

where $\mu,\ \lambda$ are two free parameters with $\lambda > 0$.

N. B.: The $\mathcal{L}^{\rm SM}_{\rm Higgs}$ Lagrangian contributes two free parameters, μ and λ.

- $\underline{\boldsymbol{\mathcal{L}^{\rm SM}_{\rm Yukawa}}}$:

The $\mathcal{L}^{\rm SM}_{\rm Yukawa}$ part of the SM Lagrangian describes the Yukawa interaction between a Dirac fermion and the scalar Higgs boson and is given by [15]

$$\mathcal{L}^{\rm SM}_{\rm Yukawa} = Y^d_{ij} \overline{Q_{L_i}} \phi D_{R_j} + Y^u_{ij} \overline{Q_{L_i}} \tilde{\phi} U_{R_j} + Y^e_{ij} \overline{L_{L_i}} \phi E_{R_j} + h.c., \tag{1.6}$$

where $\tilde{\phi} = i\tau_2 \phi^\dagger$, Y^d_{ij} (Y^u_{ij}) is the Yukawa couplings of the down (up) type quark with the Higgs field and Y^e_{ij} is the lepton Yukawa couplings with i, j as the generation indices of quarks and leptons. If we expand the $SU(2)_L$ indices and change the basis, then one can easily see that this Lagrangian contains 13 unknown parameters. The detailed description about the above free SM parameters is provided in the section below.

N. B.: The $\mathcal{L}^{\rm SM}_{\rm Yukawa}$ Lagrangian contributes 13 free parameters: 6 quark masses, 3 charged lepton masses, 3 mixing angles, and one complex phase (δ).

1.2 CP violation and the CKM paradigm

CP is the combined operation of charge-conjugation (C) and parity (P), where C converts a particle into its antiparticle and P creates the mirror image. The CP conservation implies that the rate of particle $\Leftrightarrow$ antiparticle transitions should be equal. However, our existing matter dominated universe demands that the conversion rate of matter $\Leftrightarrow$ antimatter should not be equal. In this regard Sakharov has suggested three conditions [16, 17] to describe the present universe: (i) Interactions out of thermal equilibrium, (ii) Non-conservation of Baryon number and (iii) Violation of C and CP in both the quark and lepton sectors.

The investigation of beta decay has demonstrated the $V - A$ current structure for weak interactions, where the gauge bosons couple only to the left-handed fermions. The observation of flavor changing charge current (FCCC) $K^+ \to \mu^+\nu_\mu$ process ($u \to s$ transition) by various experiments contradicted the usual expectation that the flavor changing transitions occur within the same family of quarks only, i.e., $u \Leftrightarrow d$ and $c \Leftrightarrow s$. To settle this issue, Cabibbo proposed that the interaction eigenstates are (u, d') and (c, s') doublets, and are related to the flavor states (u, d) and (c, s) doublets by [18]

$$\begin{pmatrix} d' \\ s' \end{pmatrix} = \begin{pmatrix} \cos\theta_C & \sin\theta_C \\ -\sin\theta_C & \cos\theta_C \end{pmatrix} \begin{pmatrix} d \\ s \end{pmatrix} = \begin{pmatrix} V_{ud} & V_{us} \\ V_{cd} & V_{cs} \end{pmatrix} \begin{pmatrix} d \\ s \end{pmatrix}, \tag{1.7}$$

where θ_C is the quark mixing angle (Cabibbo angle) and $d^{(\prime)}$, $s^{(\prime)}$ are the flavor (weak) eigenstates. Here $|V_{ab}|^2$ implies the probability of transition of b flavor quark to the quark of a flavor.

The real tension arises in the study of rare $K_L \to \mu^+\mu^-$ process, which is mediated by the flavor changing neutral current (FCNC) $s \to d$ transition. Since u and d spectator quarks of $K^+ \to \mu^+\nu_\mu$ and $K_L \to \mu^+\mu^-$ processes are isospin partners, one should expect $\text{BR}(K^+ \to \mu^+\nu_\mu) \approx \text{BR}(K_L \to \mu^+\mu^-)$. However, the experimental measured values of the branching ratios of these processes are [19, 20]

$$\text{BR}(K^+ \to \mu^+\nu_\mu) = (63.44 \pm 0.14)\%, \quad \text{BR}(K_L \to \mu^+\mu^-) = (6.87 \pm 0.11) \times 10^{-9}. \tag{1.8}$$

One can notice that the branching ratio of leptonic decay of neutral K^0 meson is suppressed as compared to the $K^+ \to \mu^+\nu_\mu$ process. To account this suppression of strangeness violating K^0 meson decays, Glashow, Illiopoulous, and Maiani (GIM) [21] proposed the existence of an additional up type quark, namely "charm" ($\boldsymbol{c}$) before its discovery. Hence, u quark exchanged one loop diagram exactly gets canceled with the diagrams involving c quark, which instigates mass difference of u and c quark and put an upper limit on the charm quark mass. GIM mechanism [21] implies the FCNC transitions should be either absent or very much suppressed in weak interaction. In general, for n doublets of left handed quarks, the down type flavor interaction eigenstates can be written as

$$d'_i = \sum_{j=1}^{n} V_{ij} d_j, \qquad i = 1, 2, ..., n, \tag{1.9}$$

where V_{ij} is a $n \times n$ unitary matrix.

1.2.1 The CKM (Cabbibo-Kobayashi-Maskawa) matrix

Expanding all the $SU(2)_L$ doublets of the Lagrangian in Eqn. (1.6)

$$\phi = \begin{pmatrix} 0 \\ (v+h)/\sqrt{2} \end{pmatrix}, \qquad Q_{L_i} = \begin{pmatrix} U_{L_i} \\ D_{L_i} \end{pmatrix}, \tag{1.10}$$

the Yukawa Lagrangian in the mass eigenstate basis can be written as

$$\mathcal{L}_M = (M_d)_{ij}\, \overline{D}_{L_i} D_{R_j} + (M_u)_{ij}\, \overline{U}_{L_i} U_{R_j} + h.c., \tag{1.11}$$

where

$$M_u = \frac{v}{\sqrt{2}} Y^u, \qquad M_d = \frac{v}{\sqrt{2}} Y^d, \tag{1.12}$$

are the masses of up and down type quarks and $(M_{u,d})_{ij}$ are the 3×3 complex quark matrices in flavor space.

One can apply the unitary transformation on the Y^u and Y^d Yukawa couplings as

$$Y^u \to \hat{Y}^u = V_{uL} Y^u V^{\dagger}_{uR}, \qquad Y^d \to \hat{Y}^d = V_{dL} Y^d V^{\dagger}_{dR}, \tag{1.13}$$

where $\hat{Y}^u$ ($\hat{Y}^d$) are real and diagonal

$$\hat{Y}^u = \mathrm{diag}\,(y_u, y_c, y_t)\,, \qquad \hat{Y}^d = \mathrm{diag}\,(y_d, y_s, y_b)\,. \tag{1.14}$$

From the interaction basis of Y^u, one can write

$$Y^u = \hat{Y}^u, \qquad Y^d = V\hat{Y}^d, \tag{1.15}$$

and from the basis of Y^d

$$Y^d = \hat{Y}^d, \qquad Y^u = V^{\dagger}\hat{Y}^u. \tag{1.16}$$

Thus, from (1.15, 1.16), the matrix V can be written as

$$V = V_{uL} V_{dL}^{\dagger} = \begin{pmatrix} V_{ud} & V_{us} & V_{ub} \\ V_{cd} & V_{cs} & V_{cb} \\ V_{td} & V_{ts} & V_{tb} \end{pmatrix}. \tag{1.17}$$

Here, this matrix is called the CKM matrix [18, 22], which is physical and independent of basis.

1.2.1.1 Counting the no. of parameters in CKM matrix

A unitary $n \times n$ matrix can have $2n^2$ parameters, which can be written as

$$V_{ij} = A_{ij} + iB_{ij}, \tag{1.18}$$

where A_{ij} (B_{ij}) is the real (imaginary) part of the matrix elements. The unitarity of the matrix V implies

$$\delta_{ij} = (V^{\dagger}V)_{ij} = V_{ik}^{\dagger} V_{kj} = A_{ki}A_{kj} + B_{ki}B_{kj} + i(A_{ki}B_{kj} - A_{kj}B_{ki}). \tag{1.19}$$

Thus, we get

$$A_{ki}A_{kj} + B_{ki}B_{kj} = \delta_{ij}, \quad A_{ki}B_{kj} - A_{kj}B_{ki} = 0, \tag{1.20}$$

which provides $\frac{1}{2}n(n+1) + \frac{1}{2}n(n-1) = n^2$ independent conditions. Hence, the no. of remaining free parameters is

$$2n^2 - n^2 = n^2. \tag{1.21}$$

A physical observable should be independent of phase. Since quark fields are physical, $(2n-1)$ phases can be absorbed for n quark generations. Thus, the total no. of independent parameters are

$$n^2 - (2n-1) = (n-1)^2. \tag{1.22}$$

Of these, $\frac{1}{2}n(n-1)$ parameters are associated with the real rotation angles and the rest $\frac{1}{2}(n-1)(n-2)$ are the no. of complex phases. Hence, a 2×2 matrix has one rotational angle (Cabibbo angle) and the 3×3 matrix has three mixing angles and one complex phase, which is responsible for CP violation (CPV). Thus, to explain CPV Kobayashi and Maskawa proposed the existence of 3$^{\text{rd}}$ generation of quarks in 1973 [22] before they are experimentally observed.

1.2.1.2 CKM parametrization

Several parametrizations have been proposed for the CKM matrix in terms of the four parameters (three rotational angles and one phase), which differ from each other in the aspect that the freedom of phase rotation will leave a single complex phase. Of these, the most common parametrizations are (i) Standard parametrization [23–25], (ii) Wolfenstein parametrization [26].

- **Standard parametrization**:

$$V_{\rm CKM} = \begin{pmatrix} c_{12}c_{13} & s_{12}c_{13} & s_{13}e^{-i\delta} \\ -s_{12}c_{23} - c_{12}s_{23}s_{13}e^{i\delta} & c_{12}c_{23} - s_{12}s_{23}s_{13}e^{i\delta} & s_{23}c_{13} \\ s_{12}s_{23} - c_{12}c_{23}s_{13}e^{i\delta} & -c_{12}s_{23} - s_{12}c_{23}s_{13}e^{i\delta} & c_{23}c_{13} \end{pmatrix}, \quad (1.23)$$

  where $c_{ij} = \cos\theta_{ij}$, $s_{ij} = \sin\theta_{ij}$ with $i, j = 1, 2, 3$ and δ is the CP violating phase.

- **Wolfenstein parametrization**:

  This is another useful parametrization of CKM matrix, which is related to the standard parametrization by

$$s_{12} = \lambda, \quad s_{23} = A\lambda^2, \quad s_{13}e^{-i\delta} = A\lambda^3\left(\rho - i\eta\right), \quad (1.24)$$

  where A, λ, ρ, and η are four Wolfenstein parameters. With these relations, the new form of CKM matrix is given by [26]

$$V_{\rm CKM} = \begin{pmatrix} 1-\frac{\lambda^2}{2} & \lambda & A\lambda^3(\rho - i\eta) \\ -\lambda & 1-\frac{\lambda^2}{2} & A\lambda^2 \\ A\lambda^3(1-\bar\rho - i\bar\eta) & -A\lambda^2 & 1 \end{pmatrix} + \mathcal{O}(\lambda^4), \quad (1.25)$$

  where the $\bar\rho$ and $\bar\eta$ parameters are given by

$$\bar\rho = \rho\left(1 - \frac{\lambda^2}{2}\right), \quad \bar\eta = \eta\left(1 - \frac{\lambda^2}{2}\right), \quad (1.26)$$

  and η being the imaginary parameter should be nonzero for CP violation.

All the CP violating observables should be independent of the type of parametrization used. Thus, one can define the Jarlskog invariant ($J_{\rm CKM}$) [27] as

$$\mathrm{Im}\left(V_{ij}V_{kl}V^*_{il}V^*_{kj}\right) = J_{\rm CKM}\sum_{m,n=1}^{3}\epsilon_{ikm}\epsilon_{jln}, \qquad (i, j, k, l = 1, 2, 3) \quad (1.27)$$

where V_{ab}'s are the CKM elements and ϵ_{abc} is the Levi-Civita symbol. In the standard and Wolfenstein parametrizations, this invariant quantity is given as

$$J_{\rm CKM} = c_{12}c_{23}c_{13}^2 s_{12}s_{23}s_{13}\sin\delta \approx \lambda^6 A^2 \eta \ . \tag{1.28}$$

As we have already discussed that the only CP violating parameter in the SM, i.e., the complex phase is present in the Yukawa Lagrangian. Thus, the condition for CP violation can be expressed as [27]

$$\mathrm{Im}(\det[Y^d Y^{d\dagger}, Y^u Y^{u\dagger}]) \neq 0. \tag{1.29}$$

An interesting question arises here. Why do we need a complex parameter to describe the CP violation in the SM? To get the answer, lets again go back to the Yukawa Lagrangian. Operation of CP on the Yukawa Lagrangian (the quark doublet part of the Yukawa Lagrangian along with the corresponding hermitian conjugation)

$$\begin{aligned} \mathcal{L}_{\rm Yukawa} &= Y_{ij}\overline{\psi_{L_i}}\phi\psi_{R_j} + Y_{ij}^*\overline{\psi_{R_j}}\phi^\dagger\psi_{L_i} \\ &\xrightarrow{CP} Y_{ij}\overline{\psi_{R_j}}\phi^\dagger\psi_{L_i} + Y_{ij}^*\overline{\psi_{L_i}}\phi\psi_{R_j} \ , \end{aligned} \tag{1.30}$$

will leave the coefficients Y_{ij} and Y_{ij}^* unchanged. Therefore, CP violation requires $Y_{ij} \neq Y_{ij}^*$, i.e., Y_{ij} coefficients should be complex.

For the quark sector of the SM, the essential condition for CP violation in the mass basis (the condition in Eqn. (1.29) is translated to the mass basis) is given by

$$\Delta m_{tc}^2 \Delta m_{tu}^2 \Delta m_{cu}^2 \Delta m_{bs}^2 \Delta m_{bd}^2 \Delta m_{sd}^2 J_{\rm CKM} \neq 0, \tag{1.31}$$

where $\Delta m_{ij}^2 = m_i^2 - m_j^2$.

From the above discussion, we conclude that for CP violation in the SM, the following conditions are essential.

- The up (down) type quarks should not possess any mass degeneracy,
- Values of all the three mixing angles in the CKM matrix should neither be 0 nor $\pi/2$,
- The complex CP violating phase (δ) should not be equal to 0 or π.

1.2.2 Unitary triangle

The unitarity of CKM matrix implies $V_{\rm CKM}V_{\rm CKM}^{\dagger} = I$, which gives several relations between the CKM elements. Out of the twelve possible equations, six relations are of the form [28]

$$\sum_i V_{id}V_{is}^* = 0 , \tag{1.32}$$

which are the required geometrical conditions to construct a triangle. Thus, one can construct six unitary triangles in the complex $(\bar{\rho}, \bar{\eta})$ plane. Among these, the most relevant unitary triangle is constructed from the following relation

$$\underbrace{V_{ud}V_{ub}^*}_{A\lambda^3(\bar{\rho}+i\bar{\eta})} + \underbrace{V_{cd}V_{cb}^*}_{-A\lambda^3} + \underbrace{V_{td}V_{tb}^*}_{A\lambda^3(1-\bar{\rho}-i\bar{\eta})} = 0. \tag{1.33}$$

In Fig. 1.1, we show the unitary triangle formed by using the above relation, where the length of all the sides of the triangles are roughly of same order ($\sim \mathcal{O}(\lambda^3)$). Rescaling the length of one side of the triangle to 1, the remaining two sides become

$$R_u \equiv \left|\frac{V_{ud}V_{ub}^*}{V_{cd}V_{cb}^*}\right| = \sqrt{\bar{\rho}^2 + \bar{\eta}^2}, \qquad R_t \equiv \left|\frac{V_{td}V_{tb}^*}{V_{cd}V_{cb}^*}\right| = \sqrt{(1-\bar{\rho})^2 + \bar{\eta}^2} \, . \tag{1.34}$$

The associated angles of this triangle are

$$\alpha = \arg\left[-\frac{V_{td}V_{tb}^*}{V_{ud}V_{ub}^*}\right], \quad \beta = \arg\left[-\frac{V_{cd}V_{cb}^*}{V_{td}V_{tb}^*}\right], \quad \gamma = \arg\left[-\frac{V_{ud}V_{ub}^*}{V_{cd}V_{cb}^*}\right], \tag{1.35}$$

where $\alpha + \beta + \gamma = 180°$. The area of all the six unitary triangles are given by [29]

$$A_{\rm UT} = \frac{1}{2}\left|{\rm Im}\left(V_{ij}V_{kl}V_{il}^*V_{kj}^*\right)\right| = \frac{1}{2}J_{\rm CKM}. \tag{1.36}$$

However, $J_{\rm CKM}$ is constant irrespective of the CKM matrix parametrization, hence, all the six unitary triangles have equal area. Thus, twice the area of the triangle will be the measure of CP violation.

1.2.3 Role of K meson in CP violation

In 1964, the discovery of CP violation in the neutral K meson [30] is the first experimental observation of CPV in the meson sector. The K^0 meson contains a strange quark which is produced via the strong interaction and it decays via weak interaction. Thus, we can write the weak eigenstates ($|K^0_{1,2}\rangle$) as the reinforcement of the strong eigenstates

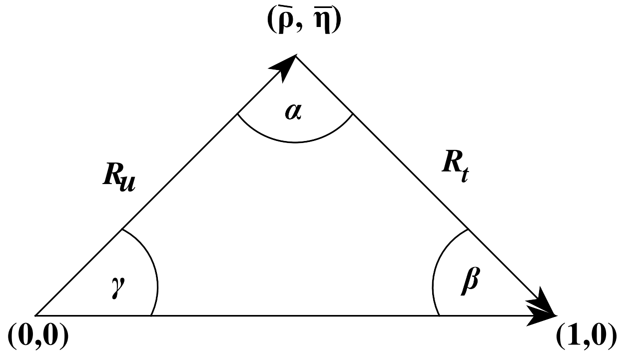

FIGURE 1.1: The resized unitary triangle constructed from the unitarity condition $V_{ud}V_{ub}^* + V_{cd}V_{cb}^* + V_{td}V_{tb}^* = 0$.

$(|K^0\rangle, |\bar{K}^0\rangle)$ as

$$|K_1^0\rangle = \frac{1}{\sqrt{2}}\left(|K^0\rangle - |\bar{K}^0\rangle\right), \qquad |K_2^0\rangle = \frac{1}{\sqrt{2}}\left(|K^0\rangle + |\bar{K}^0\rangle\right). \tag{1.37}$$

Now, applying CP symmetry on $|K_{1,2}^0\rangle$

$$\underbrace{\mathrm{CP}|K_1^0\rangle = +|K_1^0\rangle}_{\text{CP even}}, \qquad \underbrace{\mathrm{CP}|K_2^0\rangle = -|K_2^0\rangle}_{\text{CP odd}}, \tag{1.38}$$

we notice that K_1^0 (K_2^0) is CP even (odd). Thus, CP conservation implies K_1 will decay only to two pion state while K_2 should go to three pion state . However, in 1964, for the first time Cronin and his group have observed $K_2 \to 2\pi$ process, which is a clear indication of CP violation in weak decays. The detection of $K_2 \to 2\pi$ implies that the weak eigenstates differ from the CP eigenstates by a small admixture of other CP eigenstates. Thus, the physical states are represented as

$$K_S = \frac{K_1^0 + \bar{\varepsilon}K_2^0}{\sqrt{(1+|\bar{\varepsilon}|^2)}}, \qquad K_L = \frac{K_2^0 + \bar{\varepsilon}K_1^0}{\sqrt{(1+|\bar{\varepsilon}|^2)}}, \tag{1.39}$$

where $\bar{\varepsilon}$ is the mixing parameter with value $\bar{\varepsilon} \sim 2.3 \times 10^{-3}$.

1.3 Theory of B meson

Even though CP violation was observed in neutral K meson system, the order of CPV ($\sim \mathcal{O}(10^{-3})$) is not sufficient to explain the present matter-antimatter asymmetry. Later in 2001, Belle [31–34] and BaBar [35–38] experiments have observed CP violation in B meson system. The measured value of CPV in the B meson is $\sim \mathcal{O}(1)$. Besides this, the relative phase between the $B^0 - \bar{B}^0$ mixing parameter is much larger than the $K^0 - \bar{K}^0$

mixing. The B meson being much heavier in comparison to the K meson, thus, provides many decay channels to detect CP violation. The size of the mass difference (ΔM_K) of $K^0 - \bar{K}^0$ system predicts the upper mass limit on charm quark. Analogously, upper bound on the top quark mass is predicted from the size of ΔM_B. This provides strong motivation to look for CP violation and physics beyond the standard model in B system.

B meson is one of the most interesting particles of nature to elucidate our present universe, which was first observed in the decays of $\Upsilon(4s)$ resonance in 1983. The backbone of B meson is the bottom/beauty (b) quark, which combines with other light antiquarks ($\bar{u}, \bar{d}, \bar{c}, \bar{s}$) to form the B_u^-, $\bar{B}_d^0$, B_c^-, and $\bar{B}_s^0$ mesons, respectively. The quark content of the existing B mesons are

$$B_u^- = (b\bar{u})\,, \qquad \bar{B}_d^0 = \left(b\bar{d}\right), \qquad B_c^- = (b\bar{c})\,, \qquad \bar{B}_s^0 = (b\bar{s})\,. \tag{1.40}$$

To study CPV in the B system and to critically test the SM predictions, the LHCb at CERN and two asymmetric B factories: Belle at KEK and BaBar at SLAC have provided tremendous amount of data. The main objectives of these experiments are to test the SM results very precisely and to explore possible new physics (NP) beyond it. The spectacular performance of the B factories and LHCb has enhanced our understanding on CPV in B sector and the shape of flavor physics in the SM. The B factories have also observed various rare decay processes of B mesons and the associated CP violating observables. The high luminosity Belle II experiment is almost ready for operation to study the rare B decays more precisely. The recent experimental results on some new observables in the B sector have inconsistency with the SM predictions. The observation of lepton universality violation (LUV) at LHCb in $\bar{B} \to \bar{K}^{(*)} l^+ l^-$ processes [39, 40] involving $b \to s$ transitions and in $\bar{B} \to \bar{D}^{(*)} l \nu_l$ decay processes [41–46] mediated via $b \to c$ transitions become a challenge for B physics lovers. Furthermore, the upper limits on the branching ratios of lepton flavor violating (LFV) B decays [24], such as $B_{s,d} \to l_i^{\mp} l_j^{\pm}$, $B^+ \to K^+ l_i^{\mp} l_j^{\pm}$ strongly demand new theory apart from the SM.

Apart from unable to explain the observed anomalies in the B sector, the SM has also some other limitations. Though it is considered as the fundamental theory of particle physics, it fails to explain some of the important issues of particle physics [47–50], such as the neutrino oscillation, hierarchy problem, dark matter and dark energy components, gravitational force and so on. These above limitations of SM indicate that, the necessity of NP beyond the SM is very much crucial. In this context, B physics provides a very good platform to explain the baryon asymmetry of universe and to explore the NP domain beyond the standard model.

1.3.1 Effective Hamiltonian and the operator product expansion

The interchange of quarks and gluons inside the B meson couldn't explain the QCD effects for long distance hadronic states. Thus, we need to separate the low and high energy scales in our theory in order to take into account the QCD effects precisely. The method, which separates the full theory into two distinct parts: short and long range terms, is called the operator product expansion (OPE) [51–54]. In the OPE technique, the effective Hamiltonian is simply equal to the summation of point like effective operators multiplied with the corresponding couplings. Thus, the shape of the utmost general effective Hamiltonian illustrating the rare decays of B mesons at low energy is given by [55]

$$\mathcal{H}_{\rm eff} = \frac{G_F}{\sqrt{2}} V_{\rm CKM} \sum_i C_i(\mu)\mathcal{O}_i(\mu), \tag{1.41}$$

where $V_{\rm CKM}$ is the combination of CKM matrix elements [18, 22], $\mathcal{O}_i$'s are the dimension six effective operators and the C_i's are the coupling constants which characterize the strength of the operators in the Hamiltonian and are known as Wilson coefficients [51, 52, 54].

In weak interactions, the Feynman diagrams for the decay processes of B mesons in the full theory are sketched by the exchange of $W^{\pm}$, Z^0 among the initial and final state interacting quarks, which differs from the reality. In real, the B meson decays are more precisely described by the local point-like operators ($\mathcal{O}_i$) in the effective theory. The heavy bosons and quarks are removed from the operators and their effects are included in the corresponding Wilson coefficients in the effective field theory. The physics contributions into the short and long distance parts are separated by a renormalization scale factor μ. The physics contribution above μ are included in the Wilson coefficients and the effective operators constitute the theory below the renormalization scale μ, thus, the full theory is preserved. The matching scales (μ) is of the order of $\mathcal{O}(m_b)$ ($\mathcal{O}(m_c)$) for the case of B (D) meson decays, and $\mu \sim \mathcal{O}(1-2)$ GeV for the study of K decay processes. Since the Wilson coefficients include all the massive $W^{\pm}$, Z^0 bosons and the top quark contributions, these are at the scale of $M_{W,Z}$. However, the decay amplitudes should be independent of any scale. Thus, we have to evolve either the Wilson coefficients, $C(M_W) \to C(m_b)$ or the effective operators $\langle \mathcal{O}_i(M_W)\rangle \to \langle \mathcal{O}_i(m_b)\rangle$ such that the μ dependence of the Wilson coefficients will cancel with the scheme dependance in the effective operators. In general, we express $C(M_W)$ in terms of $C(m_b)$ by using the renormalization group equation (RGE) [55].

The effective operators are categorized into various types depending on the final state quarks and leptons, and the Dirac and color structure of quarks. The B meson decays can occur either at tree level or loop level (penguin and box) diagrams. All possible relevant operators [55] of the SM and the Feynman diagrams associated with these operators are presented below.

Tree level operators:

$$\mathcal{O}_1 = \left(\bar{q}'_\alpha b_\beta\right)_{V-A} \left(\bar{q}_\beta q''_\alpha\right)_{V-A}, \qquad \mathcal{O}_2 = \left(\bar{q}' b\right)_{V-A} \left(\bar{q} q''\right)_{V-A}, \tag{1.42}$$

QCD penguin operators:

$$\begin{aligned}\mathcal{O}_3 &= (\bar{q}b)_{V-A} \sum_{q_1=u,d,s,c,b} (\bar{q}_1 q_1)_{V-A}, \quad \mathcal{O}_4 = (\bar{q}_\alpha b_\beta)_{V-A} \sum_{q_1=u,d,s,c,b} (\bar{q}_{1\beta} q_{1\alpha})_{V-A}, \\ \mathcal{O}_5 &= (\bar{q}b)_{V-A} \sum_{q_1=u,d,s,c,b} (\bar{q}_1 q_1)_{V+A}, \quad \mathcal{O}_6 = (\bar{q}_\alpha b_\beta)_{V-A} \sum_{q_1=u,d,s,c,b} (\bar{q}_{1\beta} q_{1\alpha})_{V+A}, \end{aligned} \tag{1.43}$$

Magnetic penguin operators:

$$\mathcal{O}_{7\gamma} = \frac{e}{8\pi^2} m_b \bar{q}_\alpha \sigma^{\mu\nu}(1+\gamma_5) b_\alpha F_{\mu\nu}, \quad \mathcal{O}_{8G} = \frac{g}{8\pi^2} m_b \bar{q}_\alpha \sigma^{\mu\nu}(1+\gamma_5) T^a_{\alpha\beta} b_\alpha G^a_{\mu\nu}, \tag{1.44}$$

Semileptonic operators:

$$\mathcal{O}_9 = \frac{\alpha}{4\pi}(\bar{q}b)_{V-A}(\bar{\mu}\mu)_V, \qquad \mathcal{O}_{10} = \frac{\alpha}{4\pi}(\bar{q}b)_{V-A}(\bar{\mu}\mu)_A, \tag{1.45}$$

$$\mathcal{O}_L^\nu = \frac{\alpha}{2\pi}(\bar{q}b)_{V-A}(\bar{\nu}\nu)_{V-A}, \qquad \mathcal{O}_R^\nu = \frac{\alpha}{2\pi}(\bar{q}b)_{V+A}(\bar{\nu}\nu)_{V+A}, \tag{1.46}$$

$\Delta B = 2$ **operators**:

$$\mathcal{O}_{LL} = \left(\bar{b}d\right)_{V-A} \left(\bar{b}d\right)_{V-A}, \quad \mathcal{O}_{RR} = \left(\bar{b}d\right)_{V+A} \left(\bar{b}d\right)_{V+A}. \tag{1.47}$$

Here $\mathcal{O}_{1,2}$ represent the current-current operators, which arise from the simplest tree level diagrams mediated by the charged $W^\pm$ bosons in the SM. In these operators $q = d$ or s, $q' = q'' = u, c$ and α, β are the color indices of quarks. Here $V \mp A = \gamma^\mu(1 \mp \gamma_5)$ with V (A) is the vector (axial-vector) current structure of electroweak interactions. In Fig. 1.2, we have shown the tree level Feynman diagram for B decays. The tree level FCNC diagrams driven by Z^0 gauge boson are forbidden by GIM mechanism. The mediators of one loop penguin diagrams are gluon (QCD penguin), Z^0 and γ (Electroweak penguin) vector gauge bosons. The exchange of internal up type quarks and $W^\pm$ takes place inside the loop of penguin diagrams. The QCD penguins operators are denoted by $\mathcal{O}_{3,4,5,6}$ and the corresponding diagram is shown in the left panel of Fig. 1.3. The five dimensional $\mathcal{O}_{7\gamma}$ (mediated by photon) and $\mathcal{O}_{8G}$ (mediated by gluon) operators are known as magnetic operators. The schematic diagram corresponds to $\mathcal{O}_{7\gamma}$ operator is presented in the right panel of Fig. 1.3. The FCNC semileptonic $b \to q l^+ l^-$ processes occur via one loop box or penguin diagrams and the corresponding operators are symbolized by $\mathcal{O}_{9,10}$. These operators involve both quarks and leptons. In Fig. 1.4, we show the penguin (left panel) and box (right panel) diagrams for semileptonic processes. The operators for semileptonic B decays mediate via $b \to q\nu\bar{\nu}$ transitions are denoted by $\mathcal{O}^{\nu}_{L(R)}$ in Eqn. 1.46. The $\Delta B = 2$ operators are responsible for $B_q^0 - \bar{B}_q^0$ mixing, whose schematic diagram is given in Fig. 1.5. The left handed $\mathcal{O}_{LL}$ operator is only contribute in the SM.

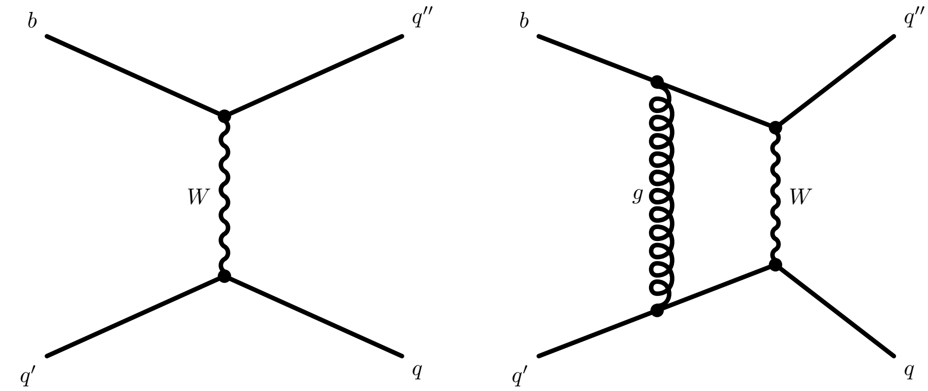

FIGURE 1.2: Tree level diagram for $b \to qq'q''$ processes in the SM.

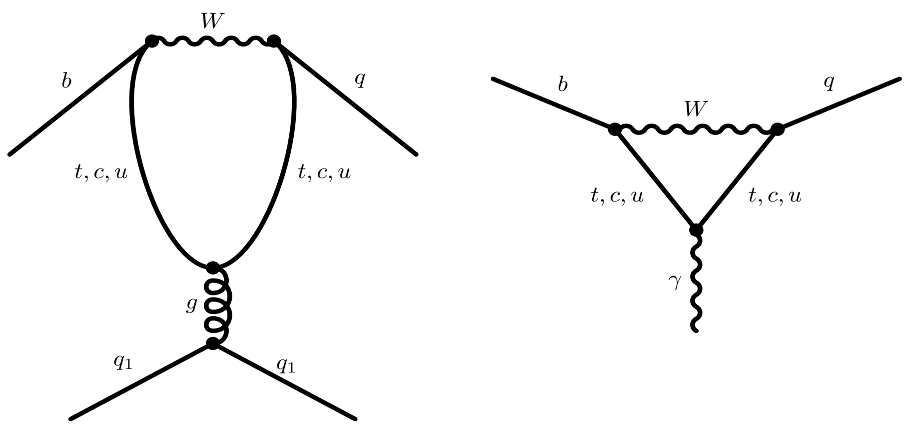

FIGURE 1.3: QCD penguin (left panel) and magnetic penguin (right panel) diagrams in the SM.

The decays of B mesons are of three types: (i) leptonic decays, which have only leptons in the final states, (ii) nonleptonic decays, whose final states are only hardons and (iii) semileptonic decays, which contain both hardons and leptons in the final state. In this thesis, we intend to study the theoretical tools for some rare semiletonic B decays and the NP associated with these processes.

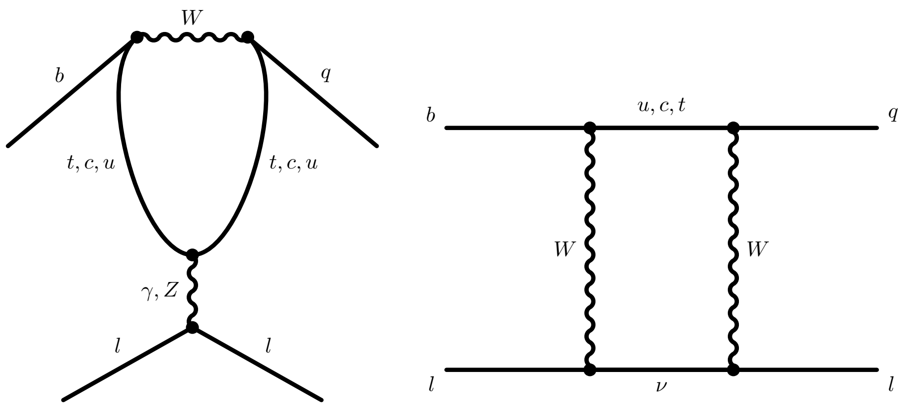

FIGURE 1.4: Penguin (left panel) and box (right panel) diagrams for semileptonic $b \to q l^+ l^-$ processes in the SM.

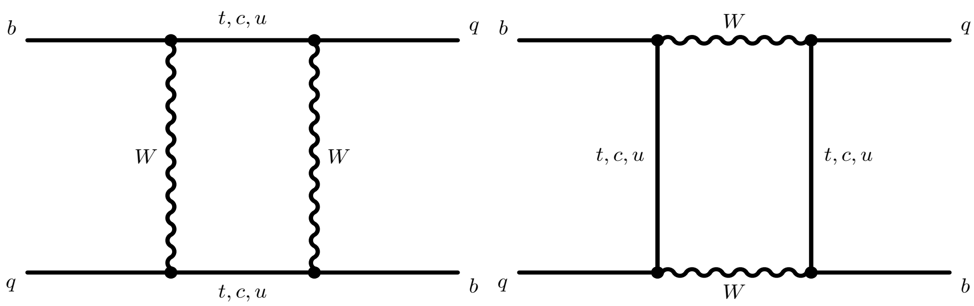

FIGURE 1.5: Schematic diagram for $B^0 - \bar{B}^0$ mixing in the SM.

1.3.2 Formalism of rare semileptonic B meson decays

The analysis of rare semileptonic decays of B mesons is one of the active research topic in recent times. The elements of CKM matrix can be precisely determined from the investigation of these decays. The semileptonic decays are of two types: (i) Exclusive decays (ii) Inclusive decays. The exclusive decays imply that we are measuring the energy, momentum and other physical observables of one particular decay channels, e.g., $\bar{B} \to \bar{K}^{(*)} ll$, $\bar{B} \to \bar{D}^{(*)} l\nu_l$ processes. However, inclusive decays involve the decays of a specific initial B meson to a couple of possible final states. In the $\bar{B} \to X l \nu_l$ inclusive decays, the initial B meson can decay to a $l\nu_l$ pair plus any hadrons.

The effective Hamiltonian of semileptonic decays with $b \to q l^+ l^-$ transitions in the SM is given by [55–58]

$$\mathcal{H}_{\rm eff} = -\frac{4G_F}{\sqrt{2}} \left[\lambda_t^{(q)} \mathcal{H}_{\rm eff}^{(t)} + \lambda_u^{(q)} \mathcal{H}_{\rm eff}^{(u)} \right] + h.c., \tag{1.48}$$

where

$$\begin{aligned}
\mathcal{H}_{\text{eff}}^{(u)} &= C_1\left(\mathcal{O}_1^c - \mathcal{O}_2^u\right) + C_2\left(\mathcal{O}_2^c - \mathcal{O}_2^u\right), \\
\mathcal{H}_{\text{eff}}^{(t)} &= C_1\mathcal{O}_1^c + C_2\mathcal{O}_2^c + \sum_{i=3}^{10} C_i\mathcal{O}_i,
\end{aligned} \tag{1.49}$$

with $\lambda_{q_2} = V_{q_2 b}V_{q_2 q}^* \quad (q_2 = t, u)$.

The effective Hamiltonian for $b \to q\nu\bar{\nu}$ processes is given by [59]

$$\mathcal{H}_{\text{eff}} = \frac{-4G_F}{\sqrt{2}} V_{tb}V_{tq}^* \left(C_L^\nu \mathcal{O}_L^\nu + C_R^\nu \mathcal{O}_R^\nu\right) + h.c., \tag{1.50}$$

where $C_L^\nu = -X(x_t)/\sin^2\theta_W$ [60, 61] is the SM Wilson coefficient associated with the left handed current and the C_R^ν Wilson coefficient corresponding to right handed current is negligible in the SM.

The effective Hamiltonian mediating the semileptonic decays $b \to q' l \bar{\nu}_l$, considering neutrinos only to be left handed, is given as [62]

$$\mathcal{H}_{\text{eff}} = \frac{4G_F}{\sqrt{2}} V_{q'b}\Big[\left(1 + C_{V_1}^l\right)\mathcal{O}_{V_1}^l + C_{V_2}^l\mathcal{O}_{V_2}^l + C_{S_1}^l\mathcal{O}_{S_1}^l + C_{S_2}^l\mathcal{O}_{S_2}^l\Big], \tag{1.51}$$

where $V_{q'b}$ is the CKM matrix element. The C_X^l coefficients, with $X = V_{1,2}, S_{1,2}$ are the Wilson coefficients and the corresponding operators are

$$\begin{aligned}
\mathcal{O}_{V_1}^l &= \left(\bar{c}_L\gamma^\mu b_L\right)\left(\bar{\tau}_L\gamma_\mu\nu_{lL}\right), \qquad & \mathcal{O}_{V_2}^l &= \left(\bar{c}_R\gamma^\mu b_R\right)\left(\bar{\tau}_L\gamma_\mu\nu_{lL}\right), \\
\mathcal{O}_{S_1}^l &= \left(\bar{c}_L b_R\right)\left(\bar{\tau}_R\nu_{lL}\right), & \mathcal{O}_{S_2}^l &= \left(\bar{c}_R b_L\right)\left(\bar{\tau}_R\nu_{lL}\right),
\end{aligned} \tag{1.52}$$

where $q_{L(R)} = L(R)q$ are the chiral quark fields with $L(R) = (1\mp\gamma_5)/2$ as the projection operators. In the standard model, the C_X^l Wilson coefficients are zero. These coefficients can only be generated in new physics models.

Now to estimate the decay rate of a semileptonic process, we should have knowledge on computing the hardonic matrix elements. For semileptonic decays, the hardonic matrix element of the current between the initial and final mesons can be described by various form factors. The form factors for B meson decays to any pseudoscalar meson ($P = K,\ \pi$) are given by [63, 64]

$$\langle P(p_P)|V_\mu|B(p_B)\rangle = (2p_B - q)_\mu F_1(q^2) + q_\mu \frac{M_B^2 - M_P^2}{q^2}\Big[F_0(q^2) - F_1(q^2)\Big], \tag{1.53}$$

$$\langle P(p_P)|i\sigma_{\mu\nu}q^\nu|B(p_B)\rangle = -\Big[(2p_B - q)_\mu q^2 - \left(M_B^2 - M_P^2\right)q_\mu\Big]\frac{F_T(q^2)}{M_B + M_P}, \tag{1.54}$$

where M_B (M_P) is the mass of the B (P) meson respectively and $q = p_B - p_P$ is the intermediate momentum transfer. Here $F_{0,1,T}(q^2)$ are the form factors which are estimated by using various methods such as heavy quark effective theory (HQET), lattice QCD, light cone sum rule (LCSR) etc. Similarly for $B \to V$ transitions, where $V = K^*,\ \rho,\ \phi$ are vector mesons, the hardonic matrix element can be parametrized as [63, 65]

$$\begin{aligned}
\langle V(p_V,\varepsilon)|V_\mu \mp A_\mu|B(p_B)\rangle &= i\frac{2V(q^2)}{M_B+M_V}\epsilon_{\mu\nu\alpha\beta}\varepsilon^{*\nu}p_B^\alpha q^\beta \\
&\mp\Bigg[(M_B+M_V)\,\varepsilon^*_\mu A_1(q^2) \\
&-\frac{\varepsilon^*\cdot q}{M_B+M_V}\left(2p_B-q\right)_\mu A_2(q^2) \\
&-\frac{2M_V}{q^2}\left(\varepsilon^*\cdot q\right)q_\mu\Big[A_3(q^2)-A_0(q^2)\Big]\Bigg], \qquad (1.55)\\
\langle V(p_V,\varepsilon)|i\sigma_{\mu\nu}q^\nu(1\mp\gamma_5)|B(p_B)\rangle &= -2i\epsilon_{\mu\nu\alpha\beta}\varepsilon^{*\nu}p_B^\alpha q^\beta T_1(q^2) \\
&\pm\Bigg[\Big(\varepsilon^*_\mu\left(M_B^2-M_V^2\right)-\left(\varepsilon^*\cdot q\right)\left(2p_B-q\right)_\mu\Big)T_2(q^2) \\
&+\left(\varepsilon^*\cdot q\right)\Big(q_\mu-\frac{q^2}{M_B-M_V}\left(2p_B-q\right)_\mu\Big)T_3(q^2)\Bigg], \qquad (1.56)
\end{aligned}$$

where M_V is the mass of vector meson, $q = p_B - p_V$ and ε^μ is the polarization vector of V meson. Here $A_{0,1,2}(q^2), V(q^2)$ and $T_{1,2,3}(q^2)$ are the form factors and $A_3(q^2)$ is related to $A_{1,2}(q^2)$ through

$$A_3(q^2) = \frac{M_B+M_V}{2M_V}A_1(q^2) - \frac{M_B-M_V}{2M_V}A_2(q^2). \qquad (1.57)$$

1.4 Mixing of neutral mesons

In the SM, the particle-antiparticle ($P^0 - \bar{P}^0$) mixing occurs in $B_s^0,\ B_d^0,\ K^0$ and D^0 neutral mesons by the box diagrams with the exchange of internal W boson and top quark. This in turn implies that the flavor eigenstates differ from the mass eigenstates. The time evolution of $P^0 - \bar{P}^0$ structure at the time of mixing of two flavor state is illustrated by [66, 67]

$$i\frac{d\psi(t)}{dt} = \mathcal{H}\psi(t), \qquad |\psi(t)\rangle = a(t)|P^0\rangle + b(t)|\bar{P}^0\rangle, \qquad (1.58)$$

where $\mathcal{H}$ is a 2×2 non-hermitian Hamiltonian written as

$$\mathcal{H} = M' - \frac{i}{2}\Gamma' = \begin{pmatrix} M_{11} & M_{12} \\ M_{21} & M_{22} \end{pmatrix} - \frac{i}{2}\begin{pmatrix} \Gamma_{11} & \Gamma_{12} \\ \Gamma_{21} & \Gamma_{22} \end{pmatrix}. \qquad (1.59)$$

Here the M' and Γ' hermitian matrices are the off-shell and on-shell intermediate states of $\Delta P = 2$ transition which carry the dispersive and absorptive part respectively. The hermicity implies, $M_{21} = M_{12}^*,\ \Gamma_{21} = \Gamma_{21}^*$ and imposing the invariance of CPT, we get $M_{11} = M_{22} = M,\ \Gamma_{11} = \Gamma_{22} = \Gamma$ [68]. Thus, the non-hermitian Hamiltonian (1.59) simplifies to

$$\mathcal{H} = \begin{pmatrix} M - \frac{i}{2}\Gamma & M_{12} - \frac{i}{2}\Gamma_{12} \\ M_{12}^* - \frac{i}{2}\Gamma_{12}^* & M - \frac{i}{2}\Gamma \end{pmatrix}. \tag{1.60}$$

Now diagonalizing the Hamiltonian, the obtained eigenstates are

$$|P_{L,H}\rangle = \frac{1}{\sqrt{|p|^2 + |q|^2}} \Big[p|P^0\rangle \pm q|\bar{P}^0\rangle \Big], \tag{1.61}$$

where the subscript L (H) stands for light (heavy) and $q,\ p$ are related to the mixing parameter ($\bar{\varepsilon}$) and the off-diagonal matrix elements by

$$\frac{q}{p} = \frac{1-\bar{\varepsilon}}{1+\bar{\varepsilon}} = \left(\frac{M_{12}^* - \frac{i}{2}\Gamma_{12}^*}{M_{12} - \frac{i}{2}\Gamma_{12}} \right)^{1/2}. \tag{1.62}$$

After diagonalization, the corresponding eigenvalues of $\mathcal{H}$ are simply the mass (real part) and decay width (imaginary part) of the neutral mesons. For CP conservation $|q/p| = 1$ and M_{12} (Γ_{12}) is real.

1.5 Classification of CP violation

After knowing the theoretical tools for B and K decays, we now discuss all possible ways to see CP violation. The decays of B and K mesons will occur either through decay or through mixing. Let's consider the decay processes, where the initial state i ($\bar{i}$) will decay to a final state f ($\bar{f}$). The amplitudes are given as

$$A_f = \langle f|\mathcal{H}|i\rangle, \quad \bar{A}_f = \langle f|\mathcal{H}|\bar{i}\rangle, \quad A_{\bar{f}} = \langle \bar{f}|\mathcal{H}|i\rangle, \quad \bar{A}_{\bar{f}} = \langle \bar{f}|\mathcal{H}|\bar{i}\rangle. \tag{1.63}$$

Using the above parameters, the following observables in B meson decays and mixing can be constructed to investigate CP violation

$$\left|\frac{q}{p}\right|, \quad \left|\frac{\bar{A}_{\bar{f}}}{A_f}\right|, \quad \lambda_f = \frac{q}{p}\frac{\bar{A}_f}{A_f}. \tag{1.64}$$

For two types of processes (decays and mixing), CP violation can be classified into three types as [11]

- **CP violation in decay (Direct CP violation)**:

The CP violation of this category appears in both the charged and neutral particles and arises due to the difference between the decay amplitudes of $P^+ \to f^+$ and $P^- \to f^-$ processes, i.e., $A(P^+ \to f^+) \neq A(P^- \to f^-)$. This CP asymmetry is given as

$$A_{\rm CP}^{\rm decay} = \frac{\Gamma(P^+ \to f^+) - \Gamma(P^- \to f^-)}{\Gamma(P^+ \to f^+) + \Gamma(P^- \to f^-)} = \frac{1 - |\bar{A}_{f^-}/A_{f^+}|^2}{1 + |\bar{A}_{f^-}/A_{f^+}|^2} \,. \tag{1.65}$$

In the A_{f^+} and $\bar{A}_{f^-}$ decay amplitudes two types of phases arise (i) weak phase which appears in the electroweak interaction of the SM and have opposite sign in A_{f^+} and $\bar{A}_{f^-}$ (ii) strong phase which appears in the decay amplitudes and have same sign. Thus, the decay amplitudes can be written as

$$A_{f^+} = \sum_i A_i e^{i(\delta_i + \phi_i)}, \qquad \bar{A}_{f^-} = \sum_i A_i e^{i(\delta_i - \phi_i)} \,. \tag{1.66}$$

From the above equations one can notice that for CP violation the following relation should hold

$$\left| \frac{\bar{A}_{f^-}}{A_{f^+}} \right| \neq 1. \tag{1.67}$$

Thus, $A_{\rm CP}^{\rm decay}$ is nonzero and is given by

$$A_{\rm CP}^{\rm decay} = \sum_{i,j} \left(\frac{-2A_i A_j \sin(\phi_i - \phi_j) \sin(\delta_i - \delta_j)}{A_i^2 + A_j^2 + 2A_i A_j \cos(\phi_i - \phi_j) \cos(\delta_i - \delta_j)} \right). \tag{1.68}$$

- **CP violation in mixing (Indirect CP violation)**:

Indirect CP violation occurs in neutral meson decays when the physical eigenstates differ from the CP eigenstates and is governed by the above defined $|q/p|$ parameter. Even though $\left|\bar{A}_{\bar{f}}/A_f\right| = 1$, this type of CP violation arises for

$$\left| \frac{q}{p} \right| \neq 1. \tag{1.69}$$

This asymmetry can be measured in semileptonic decays of P meson if one finds a wrong sign lepton in the final state. For example, the amplitudes of $P \to X l^+ \nu_l$ and $\bar{P} \to X l^- \bar{\nu}_l$ decay processes are equal whereas the $P \to X l^- \bar{\nu}_l$ and $\bar{P} \to X l^+ \nu_l$ semileptonic processes have vanishing decay amplitudes. Thus, the indirect CP asymmetry can be defined as

$$A_{\rm CP}^{\rm mixing} = \frac{\frac{d\Gamma}{dt}\left(\bar{P}(t) \to X l^+ \nu_l\right) - \frac{d\Gamma}{dt}\left(P(t) \to X l^- \bar{\nu}_l\right)}{\frac{d\Gamma}{dt}\left(\bar{P}(t) \to X l^+ \nu_l\right) + \frac{d\Gamma}{dt}\left(P(t) \to X l^- \bar{\nu}_l\right)} = \frac{1 - \left|q/p\right|^4}{1 + \left|q/p\right|^4}. \tag{1.70}$$

- **CP violation in the interference between mixing and decay**:

  As the name suggests, this type of CP violation arises due to the interference between the decay and neutral meson mixing and exists even if $|\bar{A}_{\bar{f}}/A_f| = 1,\ |q/p| = 1$. If there is a single final state f, to which both the P and $\bar{P}$ meson can decay, then the CP asymmetry is defined as

$$\begin{aligned} A_{\rm CP}(t,f) &= \frac{\frac{d\Gamma}{dt}\left(P(t) \to f\right) - \frac{d\Gamma}{dt}\left(\bar{P}(t) \to f\right)}{\frac{d\Gamma}{dt}\left(P(t) \to f\right) + \frac{d\Gamma}{dt}\left(\bar{P}(t) \to f\right)} \\ &= C_{\rm fcp}\cos(\Delta M_P t) - S_{\rm fcp}\sin(\Delta M_P t), \end{aligned} \tag{1.71}$$

  where

$$C_{\rm fcp} = \frac{1 - |\lambda_f|^2}{1 + |\lambda_f|^2}, \qquad S_{\rm fcp} = \frac{2{\rm Im}\lambda_f}{1 + |\lambda_f|^2}. \tag{1.72}$$

  Here $C_{\rm fcp}$ are the contribution from the direct CP violation and $S_{\rm fcp}$ describes the CP violation in the interference and mixing and is commonly known as mixing-induced CP violation.

  Eqn. (1.71) implies that even though the CP violation in decay is absent, i.e., $|\bar{A}_{\bar{f}}/A_f| = 1$ and there is also no CP violation in mixing ($|q/p| = 1$), still CP violation can occur through the interference between decay and mixing, if ${\rm Im}\lambda_f \neq 0$. Thus, Eqn. (1.71) reduces to

$$A_{\rm CP}(t,f) = -{\rm Im}\lambda_f \sin(\Delta M_P t). \tag{1.73}$$

1.6 Why do we need extension of the SM?

Though, SM is a well established and fascinating theoretical model of particle physics which has an ability to explain all the observed experimental data, but it fails to answer some of the open questions of particle physics. The limitations and the unanswered questions of the SM are:

- Why there are only three generations of fundamental particles in the SM ?
- The masses of 3rd generation quarks/leptons are greater than the quarks/leptons of second generation, which are again higher than the first generation particles.

There is no satisfactory answer to this puzzling nature, i.e., why there is mass hierarchy in the SM?

- In the SM, the masses of neutrinos are negligible and their is no oscillation between different flavors of neutrinos. However, various experiments have confirmed that neutrinos oscillate during propagation and they have non-zero mass. Here the question arises, why SM unable to accommodate the observed neutrino oscillation?

- SM does not contain any component for the fourth fundamental interaction of nature, i.e., the gravitational force.

- Though our universe constitute 26.8% of the dark matter (DM) and 68.3% dark energy (DE), the SM does not include any components of invisible sector.

These are the basic failures of the SM, which motivates every particle physicist to move forward and to look for NP beyond it.

In addition to these common limitations, SM once again fails to accommodate some of the observed angular observables of the rare semileptonic B decays. Many of the rare B decay observables have discrepancy at the level of $(3-4)\sigma$ between the SM results and the experimental data. Below, we have listed the recent important anomalies in the rare semileptonic decays of B meson.

Recent anomalies in rare semileptonic B decays

- The discrepancy of 2.6σ [39] is found in the observed lepton non-universality (LNU) parameter (R_K), in the $B^+ \to K^+ l^+ l^-$ processes.

- The observation of 3σ deviation in the decay rate [69] and the well known P_5' observable [70] of $\bar{B} \to \bar{K}^* l^+ l^-$ decay processes.

- Recently LHCb Collaboration has reported inconsistency between the SM and experimental results of R_{K^*} parameter at the level of 2.2σ (2.4σ) [40] in the $q^2 \in [0.045, 1.1]$ GeV^2 ($q^2 \in [1.1, 6.0]$ GeV^2) bin.

- Deviation of 1.9σ [41–45] and 3.3σ [45, 46] in the LNU parameters R_D and R_{D^*} respectively.

- 3.3σ [71] discrepancy in the measurement of the decay distribution of $B_s \to \phi\mu^+\mu^-$ modes in the high recoil limit.

- The experimental observation of lepton flavor violating decay processes [24] in the charged lepton and B sector such as $\mu^- \to e^-\gamma$, $\tau^- \to l^-\gamma$, $\tau^- \to 3\mu^-(e^-)$, $B_{s,d} \to l_i^\mp l_j^\pm$, $B^+ \to K^+(\pi^+) l_i^\mp l_j^\pm$ which are forbidden in the SM.

The occurrence of these anomalies may be due to the statistical fluctuation or due to the presence of NP beyond the SM. The experimental observed data on these physical observables strongly indicate the presence of either new theory or new particles. These anomalies motivate us to study rare semileptonic decay modes in a simplified theoretical framework with an additional leptoquark (LQ).

1.7 Thesis overview

In this chapter, we gave a brief introduction to the SM and to the physics of quark sector. After mentioning the failures of SM and the B decay anomalies in this chapter, we present a comprehensive discussion on the new hypothetical gauge boson, namely leptoquark in the next chapter. We mainly focus on the leptoquarks, which play an important role in resolving the anomalies associated with the rare semileptonic B meson decays. We also compute the constraints on leptoquark couplings from various rare exclusive/inclusive B decay processes in chapter 2. The rest of the chapters of this thesis provide a detailed analysis of above defined anomalies in the SM and in the leptoquark model. In chapter 3, we investigate the rare $\bar{B} \to \bar{K} l^+ l^-$ and $\bar{B} \to (\bar{K}^{(*)}, X_s)\nu\bar{\nu}$ processes in the $(3, 2, 7/6)$ scalar leptoquark model. Chapter 4 deals with a comparison study of the effect of $(3, 2, 7/6)$ and $(3, 2, 1/6)$ scalar leptoquark on various angular observables of $\bar{B} \to \bar{K}^* l^+ l^-$ processes in the full q^2 region. We perform a simultaneous study of R_K and $R_{D^{(*)}}$ anomalies with $(3, 3, 2/3)$ and $(3, 1, 2/3)$ vector leptoquark couplings in chapter 5. The lepton flavor violating B decay modes are explored in chapter 6 and chapter 7 summarizes our findings in the leptoquark model.

Chapter 2

Leptoquark Model

2.1 Leptoquark in a nutshell

The SM particle content does not have any boson with both color and electric charge quantum numbers, thus quarks and leptons are treated as two distinct fields in the SM. Nonetheless, the equal and opposite contribution of two sectors cause phenomenal cancellation of triangle anomalies of gauged currents in the quantum theory and fabricates the SM a renormalizable theory [72]. Though quarks and leptons belong to two different sectors of the SM, there exist several similarities between them. Both have three families with mixing between different generations and the electric charges are integer multiples of 1/3. The above spectacular symmetry indicates the existence of a new kind of particle beyond the SM, which connects quarks and leptons at the fundamental level. Consequently many extended SM theories such as $SU(5)$ grand unified theories (GUTs) [73–77], color $SU(4)$ Pati-Salam model [77–81], super-sting inspired models based on E_6 group [82], quark and lepton composite model [83] and technicolor model [84, 85] are proposed to describe the quark lepton interactions. All these theories predict the existence of a new hypothetical gauge boson, named as "**LEPTOQUARK**".

As the name suggests, leptoquark (LQ) provides the link between the quark and lepton sectors. They are hypothetical color-triplet elementary particles which have both the lepton (L) and baryon (B) quantum numbers. LQs may or may not conserve B and L quantum numbers. Based on the spin quantum number, they can be either scalar (spin = 0) or vector (spin = 1). The schematic diagram for $b \to q l l'$ processes mediated via scalar (left panel) and vector (right panel) LQs are presented in Fig. 2.1. As LQs connect up type ($Q = \pm 2/3$) or down type ($Q = \pm 1/3$) quarks with the charged ($Q = \pm 1$) or neutral ($Q = 0$) leptons, their feasible fractional electric charges are $Q = \pm 5/3,\ \pm 4/3,\ \pm 2/3,\ \pm 1/3$. Beyond the spin and charge, they are also distinguished from each other by their fermion no. ($|F| = 3B+L$), which can be either 2 or 0 depending on their couplings to fermion-fermion (lq) or fermion-antifermion ($l\bar{q}$) pairs. According to the couplings of LQs with different families of quarks and leptons, they are also divided into three types, namely first, second and third generation LQs. In the effective theories, the B and L number violating LQs are very heavy, at the level of GUT scale ($\sim \mathcal{O}(10^{15})$ GeV) and have both the LQ and diquark couplings, thus destabilize the proton. On the contrary, the LQ gauge bosons that conserve either B or L or both do not allow proton decay, and hence, they could be light enough ($\sim \mathcal{O}(10^2)$ GeV) to be observed in the current colliders.

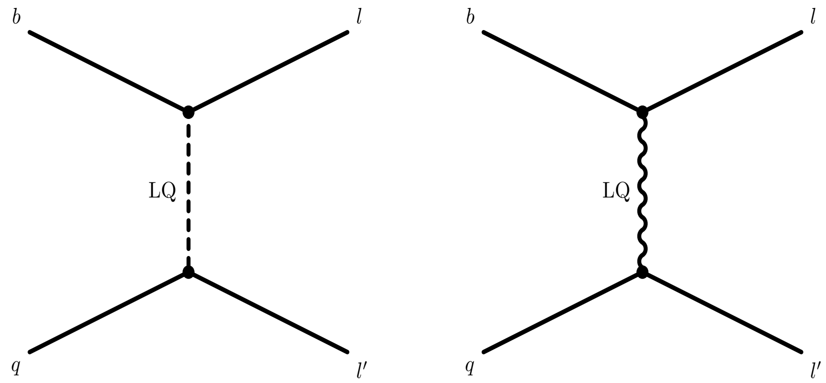

FIGURE 2.1: Feynman diagrams for semileptonic $b \to qll'$ processes mediated by the scalar (left panel) and vector (right panel) leptoquark.

Since the leptoquarks couple to quarks and leptons simultaneously, the light LQs could be useful to explain the recent anomalies in the B sector. Thus, one should have best knowledge about the couplings of the light LQs. In order to avoid the problematic massive GUT scale LQs in the NP models, the following constraints should be implemented on the LQs [86–88].

- The presence of diquark couplings should be avoided [73], since these couplings in combination with the genuine LQ couplings destabilize the proton.
- The strict bound on LQ couplings coming from the FCNC processes [77, 89, 90] can be eschewed by requiring that LQ couplings are diagonal, i.e., they interact only with the same generation of SM fermions (quarks and leptons). However, one couldn't foise diagonality on LQs which interact only to the left handed quarks [87, 88], as the CKM matrix rotation restricts simultaneous diagonalization of LQ interaction with the up and down type quarks [18, 22].
- The nonchiral LQs that couple to both the left and right-handed quarks have significant contributions to the leptonic pion decays and the decays of other pseudoscalar mesons[81, 87, 89, 91], which lead to stringent bounds on LQ couplings.

> To evade these strict bounds, chirality on LQ couplings are demanded. Chirality implies that LQs interact to specific chiral quark only, i.e, they interact to left-handed or right-handed quarks at a time but not to both.

From the above discussion we notice that, if the light LQs could couple chirally and diagonally with SM fermions and do not have any diquark couplings, then they could affect the low-energy physics.

The production of LQs in the proton-proton (pp) collisions are two types: single and pair productions. The scattering cross section for the single production of LQ depends on the Yukawa couplings whereas in the pair production, the cross section has dependance only on the LQ mass. Therefore, the single productions are model-dependent and the pair productions are independent of any models. Currently, the LHCb as well as the CMS and ATLAS Collaborations are profoundly looking for LQ pair production. They have obtained the mass bounds on all generation scalar LQs at 95% CL. The mass limit on the vector LQs are more stringent in comparison to the scalar LQs. The measured lower bound on the mass of first and second generations scalar LQs by the CDF, D0, CMS and ATLAS experiments are presented in Table 2.1. In this Table β represents the branching ratio of LQ $\to l^{\pm}q$ processes, whose value can be 0 , 0.5, or 1 [92]. The CMS Collaborations have set a limit on the mass of third generation LQs above 685 GeV [93], 740 GeV [94] and 450 GeV [95] for the case of $\mathrm{LQ}-t-\tau$, $\mathrm{LQ}-b-\tau$ and $\mathrm{LQ}-b-\nu_\tau$ channels, respectively. Similarly ATLAS experiments have excluded the mass of 3^{rd} generation LQs below 625 GeV [96] and 640 GeV [97] respectively for $\mathrm{LQ}-b-\nu_\tau$ and $\mathrm{LQ}-t-\nu_\tau$ interactions.

TABLE 2.1: The experimental lower bounds on the mass of first and second generation scalar leptoquarks at 95% CL [98].

Experiments	Limits on the scalar LQs mass	
	1st gen	2nd Gen
CDF	$>$ 236 GeV ($\beta = 1$) [99]	$>$ 226 GeV ($\beta = 1$) [100]
D0	$>$ 299 GeV ($\beta = 1$) [101]	$>$ 316 GeV ($\beta = 1$) [102]
CMS	$>$ 830 GeV ($\beta = 1$) [103] $>$ 640 GeV ($\beta = 0.5$) [103]	$>$ 1070 GeV ($\beta = 1$) [104] $>$ 785 GeV ($\beta = 0.5$) [104]
ATLAS	$>$ 1050 GeV ($\beta = 1$) [97] $>$ 900 GeV ($\beta = 0.5$)[97]	$>$ 1000 GeV ($\beta = 1$) [97] $>$ 850 GeV ($\beta = 0.5$) [97]

After getting an idea on the experimental mass limits of the scalar LQ bosons, some important questions may strike to our mind. These are (a) where do the relevant LQs come from? (b) what are the roles of LQs in the B meson anomalies? The existence of LQs at TeV scale are strongly motivated by various extended SM theories, in which both the quarks and leptons are treated on the equal basis. They are mainly found in Grand

Unified Theories [73–77] based on $SU(5)$ [73, 105] and $SO(10)$ [74, 106] gauge group, Pati-Salam color $SU(4)$ model [77–81], extended technicolor model [84, 85], super-sting inspired E_6 model [82], and composite models [83]. Though LQs fail to answer some important open questions like the dark matter content of the universe or the origin of the electroweak scale, they play a vital role to settle almost all the anomalies in the B sector (which we have already mentioned in chapter 1). In Ref. [107], the authors have investigated both the $R_{D^{(*)}}$ and R_K anomalies in the $(3, 2, 1/6)$ scalar LQ model. According to the Ref. [108], the extension of the SM with the $SU(2)_L$ singlet scalar LQ can accommodate the R_K through a loop correction and the $R_{D^{(*)}}$ via the tree level LQ contribution. The LFV decays in the B sector are analyzed in the context of LQ model in the literature [109–111]. There are many articles in the literature where the phenomenology of scalar LQs and their contributions to new physics are studied. The LQ model in the context of B meson anomalies has been investigated in the literature [90, 107–131], though the effect of scalar LQs in various observables associated with the $\bar{B} \to \bar{K}^{(*)} l^+ l^-$ processes has not been elaborately investigated.

2.2 Classification of leptoquarks

The light LQs are required to settle the flavor physics anomalies. Light LQs demand chirality, diagonality and vanishing diquark couplings. Besides this, LQs should have renormalizable interactions with the SM elementary particles and the interactions should be invariant under the $SU(3)_C \times SU(2)_L \times U(1)_Y$ SM gauge group [132, 133]. These requirements lead to 14 relevant LQs (7 scalars and 7 vectors) [134–136]. Of these, the LQs that couple only to the SM fermions are listed in Table 2.2 [132]. In this Table, we classify the LQs according to their fermion no. and spin. The scalar (vector) LQs are denoted by S_i (V_i), where the subscript i stands for the $SU(2)_L$ representation of LQ multiplet. The LQ states which have same $SU(2)_L$ representation and different Y are denoted by an extra tilde above the symbol of LQ state. Out of these possible LQ states, we only study $S_2(3, 2, 7/6)$, $\tilde{S}_2(3, 2, 1/6)$ scalar LQs and $V_3(3, 3, 2/3)$, $V_1(3, 1, 2/3)$ vector LQs to investigate the issues in B sector. The detailed discussion on these four LQ multiplets are presented in the subsection below.

2.2.1 Scalar leptoquark

There are two genuine scalar LQ multiplets $S_2(3, 2, 7/6)$ and $\tilde{S}_2(3, 2, 1/6)$ having fermion number zero. These LQs conserve baryon number and don't allow proton decay in the perturbation theory. This is the main reason of our interest in these LQs.

TABLE 2.2: List of pertinent leptoquarks which are invariant under the SM $SU(3)_C \times SU(2)_L \times U(1)_Y$ gauge group [113].

Leptoquark	Spin	$\lvert F\rvert$	$(SU(3)_C,\ SU(2)_L,\ U(1)_Y)$
S_1	0	2	$(\bar{3},\ 1,\ 1/3)$
$\tilde{S}_1$	0	2	$(\bar{3},\ 1,\ 4/3)$
S_2	0	0	$(3,\ 2,\ 7/6)$
$\tilde{S}_2$	0	0	$(3,\ 2,\ 1/6)$
S_3	0	2	$(\bar{3},\ 3,\ 1/3)$
V_1	1	0	$(3,\ 1,\ 2/3)$
$\tilde{V}_1$	1	0	$(3,\ 1,\ 5/3)$
V_2	1	2	$(\bar{3},\ 2,\ 5/6)$
$\tilde{V}_2$	1	2	$(\bar{3},\ 2,\ -1/6)$
V_3	1	0	$(3,\ 3,\ 2/3)$

$S_2(3, 2, 7/6)$

The Lagrangian describing the interaction of the scalar LQ doublet $S_2(3, 2, 7/6)$ with the quarks and charged leptons is given by [113, 120, 121, 132]

$$\mathcal{L} = -\lambda_{RL}^{ij}\ \bar{u}_R^i S_{2\alpha}^T \epsilon_{\alpha\beta} L_{\beta L}^j - \lambda_{LR}^{ij}\ \bar{e}_R^i S_{2\alpha}^\dagger Q_{\alpha L}^j + h.c.\ , \tag{2.1}$$

where $i, j = 1, 2, 3$ $(\alpha, \beta = 1, 2)$ are the generation $(SU(2)_L)$ indices, Q_L and L_L are the left-handed quark and lepton doublets, u_R and e_R are the right-handed up type quark and charged lepton singlets and $\epsilon = i\sigma_2$ is a 2×2 matrix. These multiplets can be represented more explicitly as

$$S_2 = \begin{pmatrix} S_2^{5/3} \\ S_2^{2/3} \end{pmatrix}, \quad Q_L = \begin{pmatrix} u_L \\ d_L \end{pmatrix}, \quad L_L = \begin{pmatrix} \nu_L \\ e_L \end{pmatrix}, \quad \text{and} \quad \epsilon = \begin{pmatrix} 0 & 1 \\ -1 & 0 \end{pmatrix}. \tag{2.2}$$

The superscripts of the components of LQ doublets denote the electric charge of the LQ components. The transition of weak basis to mass basis divides the Yukawa couplings to two part of couplings pertinent for the upper and lower doublet components. We use the basis where CKM and PMNS rotations are assigned to up type quarks and neutrinos, i.e., $u_L \to V_{\rm CKM} u_L$ and $\nu_L \to V_{\rm PMNS}\nu_L$. Here λ_{RL}^{ij} and λ_{LR}^{ij} are the LQ couplings in the mass basis of the down type quark and charged leptons.

Now expanding the $SU(2)_L$ indices, the interaction Lagrangian becomes

$$\begin{aligned} \mathcal{L} \ &= \ -\lambda_{RL}^{ij}\ \bar{u}_{\alpha R}^i S_{2\alpha}^{5/3} e_L^j + [\lambda_{RL} V_{\rm PMNS}]^{ij} u_{\alpha R}^i S_{2\alpha}^{2/3} \nu_L^j \\ &\quad -[\lambda_{LR} V_{\rm CKM}]^{ij}\ \bar{e}_R^i S_{2\alpha}^{5/3^\dagger} u_{\alpha L}^j - \lambda_{LR}^{ij}\ \bar{e}_R^i S_{2\alpha}^{2/3^\dagger} d_{\alpha L}^j + h.c.\ . \end{aligned} \tag{2.3}$$

Using the Fierz transformation, one can obtain from Eqn. (2.3), the contribution to the interaction Hamiltonian for the $b \to q_k l_i^+ l_i^-$ processes as

$$\mathcal{H}_{\rm LQ} \;=\; \frac{\lambda_{LR}^{i3}\lambda_{LR}^{ik*}}{8M^2_{S_2^{2/3}}}[\bar{q}\gamma^\mu(1-\gamma_5)b][\bar{l}\gamma_\mu(1+\gamma_5)l] \equiv \frac{\lambda_{LR}^{i3}\lambda_{LR}^{ik*}}{4M^2_{S_2^{2/3}}}\Big(\mathcal{O}_9+\mathcal{O}_{10}\Big). \tag{2.4}$$

One can thus write the LQ effective Hamiltonian (2.4) analogous to its SM counterpart (1.48, 1.49) as

$$\mathcal{H}_{LQ} = -\frac{G_F\alpha_{\rm em}}{\sqrt{2}\pi}V_{tb}V_{tq}^*(C_9^{\rm LQ}\mathcal{O}_9 + C_{10}^{\rm LQ}\mathcal{O}_{10})\;, \tag{2.5}$$

with the new Wilson coefficients as

$$C_9^{\rm LQ} = C_{10}^{\rm LQ} = -\frac{\pi}{2\sqrt{2}G_F\alpha_{\rm em}V_{tb}V_{tq}^*}\frac{\lambda_{LR}^{i3}\lambda_{LR}^{ik*}}{M^2_{S_2^{2/3}}}, \tag{2.6}$$

where k is the generation index of the down type quark flavor q.

$\tilde{S}_2(3, 2, 1/6)$

Similarly the interaction Lagrangian for the coupling of $\tilde{S}_2(3, 2, 1/6)$ LQ to the fermion bilinear can be expressed as [113, 120, 121, 132]

$$\mathcal{L} = -\lambda_{RL}^{ij}\;\bar{d}^{\,i}_{\alpha R}\tilde{S}^T_{2\alpha}\epsilon_{\alpha\beta}L^j_{\beta L} + h.c.\;, \tag{2.7}$$

where the $\tilde{S}_2$ LQ doublet in terms of its component is $\tilde{S}_2 = \Big(\tilde{S}_2^{2/3},\ \tilde{S}_2^{-1/3}\Big)^T$. Now expanding the terms in Eqn. (2.7), the interaction Lagrangian in terms of different LQ components is given by

$$\mathcal{L} = -\lambda_{RL}^{ij}\bar{d}^i_{\alpha R}\tilde{S}^{2/3}_{2\alpha}e^j_L + [\lambda_{RL}V_{\rm PMNS}\nu]^{ij}\bar{d}^i_{\alpha R}\tilde{S}^{-1/3}_{2\alpha}\nu^j_L\,, \tag{2.8}$$

After performing the Fierz transformation, the interaction Hamiltonian becomes

$$\mathcal{H}_{\rm LQ} \;=\; \frac{\lambda_{RL}^{ki}\lambda_{RL}^{3i\;*}}{8M^2_{\tilde{S}_2^{2/3}}}[\bar{q}\gamma^\mu(1+\gamma_5)b][\bar{l}\gamma_\mu(1+\gamma_5)l] \equiv \frac{\lambda_{RL}^{ki}\lambda_{RL}^{3i\;*}}{4M^2_{\tilde{S}_2^{2/3}}}\Big(\mathcal{O}_9'+\mathcal{O}_{10}'\Big). \tag{2.9}$$

where $\mathcal{O}_9'$ and $\mathcal{O}_{10}'$ are the four-fermion current-current operators obtained from $\mathcal{O}_{9,10}$ by making the replacement $L \leftrightarrow R$. Thus, due to the exchange of the LQ $\tilde{S}_2(3, 2, 1/6)$, one can obtain the new Wilson coefficients $C_9^{\prime\rm LQ}$ and $C_{10}^{\prime\rm LQ}$ associated with the $\mathcal{O}_9'$ and

$\mathcal{O}'_{10}$ operators of $b \to q_k l_i^+ l_i^-$ process as

$$C_9^{\prime \rm LQ} = -C_{10}^{\prime \rm LQ} = \frac{\pi}{2\sqrt{2}\ G_F \alpha_{\rm em} V_{tb} V_{tq}^*} \frac{\lambda_{RL}^{ki} \lambda_{RL}^{3i*}}{M^2_{\tilde{S}_2^{2/3}}} \,. \tag{2.10}$$

In addition to the $b \to q_k l_i^+ l_i^-$ processes, these LQs also contribute new Wilson coefficients to the semileptonic B decay processes with dineutrino in the final state, $b \to q_k \nu_i \bar{\nu}_i$. The effective Hamiltonian of $\tilde{S}_2$ LQ after applying the Fierz transformation is given by

$$\mathcal{H}_{\rm LQ}\left(b \to q_k \nu_i \bar{\nu}_i\right) = \frac{\lambda_{RL}^{ki} \lambda_{RL}^{3i*}}{4M^2_{\tilde{S}_2^{-1/3}}} (\bar{q}\gamma^\mu R b)(\bar{\nu}\gamma_\mu(1-\gamma_5)\nu) \,. \tag{2.11}$$

Now comparing the SM Hamiltonian (1.48, 1.49) with the Hamiltonian of LQ model (2.9), we obtain the $C_R^{\rm LQ}$ new Wilson coefficient as

$$C_R^{\rm LQ} = -\frac{\pi}{2\sqrt{2} G_F \alpha_{\rm em} V_{tb} V_{tq}^*} \frac{\lambda_{RL}^{ki} \lambda_{RL}^{3i*}}{M^2_{\tilde{S}_2^{-1/3}}} \,. \tag{2.12}$$

2.2.2 Vector leptoquark

$V_3(3, 3, 2/3)$

The interaction Lagrangian of isotriplet state $V_3(3,3,2/3)$ with fermions is [62, 120, 132]

$$\mathcal{L} = \lambda_{LL}^{ij}\, \overline{Q}^i_{\alpha L} \left(\tau \cdot V_{3\mu}\right)_{\alpha\beta} \gamma^\mu L^j_{\beta L} + h.c., \tag{2.13}$$

where $\mu = 0,1,2,3$ denotes the Lorentz indices. This baryon and lepton number conserving LQ allows only LL type coupling, thus chiral in nature. Now expanding all the $SU(2)_L$ indices, the Lagrangian can be written as

$$\begin{aligned} \mathcal{L} \;=\; & -\lambda_{LL}^{ij} \bar{d}^i{}_L \gamma^\mu V_{3\mu}^{2/3} e_L^j + [V_{\rm CKM}\lambda_{LL}]^{ij} \bar{u}_L^i \gamma^\mu V_{3\mu}^{2/3} \nu_L^j \\ & + \sqrt{2}[V_{\rm PMNS}\lambda_{LL}]_{ij} \bar{d}_L^i \gamma^\mu V_{3\mu}^{-1/3} \nu_L^j + \sqrt{2}[V_{CKM}\lambda_{LL}]_{ij} \bar{u}_L^i \gamma^\mu V_{3\mu}^{5/3} e_L^j + h.c.. \end{aligned} \tag{2.14}$$

Now using Fierz transformation and comparing with the SM effective Hamiltonian (1.48,1.49), we observe that it contributes new Wilson coefficients to the $b \to q_k l_i^+ l_i^-$ processes as

$$C_9^{\rm LQ} = -C_{10}^{\rm LQ} = \frac{\pi}{\sqrt{2} G_F V_{tb} V_{tq}^* \alpha_{\rm em}} \frac{\lambda_{LL}^{ki} \lambda_{LL}^{3i*}}{M^2_{V_3^{2/3}}} \,. \tag{2.15}$$

It should be noted from (2.14) that, V_3 vector LQ provides additional Wilson coefficient contribution to $b \to q_k \nu_i \bar{\nu}_i$ process, which is given by

$$C_L^{\rm LQ} = \frac{2\pi}{\sqrt{2} G_F \alpha_{\rm em} V_{tb} V_{tq}^*} \sum_{m,n=1}^{3} V_{m3} V_{n2}^* \frac{\lambda_{LL}^{ni} \lambda_{LL}^{mi*}}{M^2_{V_3^{-1/3}}}. \tag{2.16}$$

From Eq. (2.14), one can also notice that V_3 vector LQ gives additional contribution to the Wilson coefficients of $b \to c l \bar{\nu}_i$ processes as

$$C_{V_1}^l = -\frac{1}{2\sqrt{2} G_F V_{cb}} \sum_{i=1}^{3} V_{i3} \frac{\lambda_{LL}^{2i} \lambda_{LL}^{l3*}}{M^2_{V_3^{2/3}}}, \tag{2.17}$$

where V_{i3} denotes the CKM matrix element, $M_{V_3^{2/3}}$ is the mass of the LQ and the superscript denotes the charge of V_3.

$V_1(3, 1, 2/3)$

The Lagrangian for isosinglet state, V_1 is [62, 120, 132]

$$\mathcal{L} = \left(\lambda_{LL}^{ij} \, \overline{Q}^i_{\alpha L} \gamma^\mu L^j_{\alpha L} + \lambda_{RR}^{ij} \, \overline{d}^i_R \gamma^\mu \ell^j_R \right) V_{1\mu} + h.c., \tag{2.18}$$

which violates baryon number and has the coupling to both left and right-handed fermions. In the basis of mass eigenstates, this Lagrangian can be written as

$$\begin{aligned} \mathcal{L} \; = \; & [V_{\rm CKM} \lambda_{LL}]^{ij} \bar{u}^i_L \gamma^\mu V_{1\mu}^{2/3} \nu^j_L + \lambda_{LL}^{ij} \bar{d}^i_L \gamma^\mu V_{1\mu}^{2/3} e^j_L \\ & \lambda_{RR}^{ij} \bar{d}^i_R \gamma^\mu V_{1\mu}^{2/3} e^j_R + \lambda_{RR}^{ij} \bar{u}^i_R \gamma^\mu V_{1\mu}^{2/3} \nu^j_R + h.c.. \end{aligned} \tag{2.19}$$

In addition to $C_{9,10}$ Wilson coefficients, these nonchiral leptoquarks contribute scalar and pseudoscalar operators to the $b \to q_k l_i^+ l_i^-$ processes [120]

$$C_9^{\rm LQ} = -C_{10}^{\rm LQ} = \frac{\pi}{\sqrt{2} G_F V_{tb} V_{tq}^* \alpha_{\rm em}} \frac{\lambda_{LL}^{ki} \lambda_{LL}^{3i*}}{M^2_{V_1^{2/3}}}, \tag{2.20a}$$

$$C_9^{\prime\rm LQ} = C_{10}^{\prime\rm LQ} = \frac{\pi}{\sqrt{2} G_F V_{tb} V_{tq}^* \alpha_{\rm em}} \frac{\lambda_{RR}^{ki} \lambda_{RR}^{3i*}}{M^2_{V_1^{2/3}}}, \tag{2.20b}$$

$$-C_P^{\rm LQ} = C_S^{\rm LQ} = \frac{\sqrt{2}\pi}{G_F V_{tb} V_{tq}^* \alpha_{\rm em}} \frac{\lambda_{LL}^{ki} \lambda_{RR}^{3i*}}{M^2_{V_1^{2/3}}}, \tag{2.20c}$$

$$C_P^{\prime\rm LQ} = C_S^{\prime\rm LQ} = \frac{\sqrt{2}\pi}{G_F V_{tb} V_{tq}^* \alpha_{\rm em}} \frac{\lambda_{RR}^{ki} \lambda_{LL}^{3i*}}{M^2_{V_1^{2/3}}}. \tag{2.20d}$$

Furthermore, they also contribute additional Wilson coefficients to the $b \to c l \bar{\nu}_i$ process as [62, 132]

$$C^l_{V_1} = \frac{1}{2\sqrt{2} G_F V_{cb}} \sum_{i=1}^{3} V_{i3} \frac{\lambda^{2l}_{LL} \lambda^{i3*}_{LL}}{M^2_{V_1^{2/3}}}, \qquad C^l_{V_2} = 0, \tag{2.21a}$$

$$C^l_{S_1} = -\frac{1}{2\sqrt{2} G_F V_{cb}} \sum_{i=1}^{3} V_{i3} \frac{\lambda^{2l}_{LL} \lambda^{i3*}_{RR}}{M^2_{V_1^{2/3}}}. \tag{2.21b}$$

2.3 Bounds on scalar leptoquarks

After gathering the information about the NP contributions to the processes $b \to q l^+ l^-$ $(\nu\bar{\nu})$ and $(b \to c l \nu)$ in hand, we now proceed to constrain the NP parameter space using the recent measurement of various rare decay processes of B mesons such as $B_{s,d} \to l^+ l^-$, $\bar{B} \to X_s l^+ l^-$ and the $B^0_s - \bar{B}^0_s$ mixing data.

2.3.1 $B_{s,d} \to l^+ l^-$ processes

The rare leptonic decay processes $B_{s,d} \to l^+ l^-$, where $l = e, \mu, \tau$, mediated by the FCNC transition $b \to (s,d) l^+ l^-$ are strongly suppressed in the standard model as they occur at one loop level and also suffer from helicity suppression. These decay processes are very clean and the only non-perturbative quantity involved is the B meson decay constant, which can be reliably calculated using the non-perturbative methods such as QCD sum rules, lattice gauge theory etc. Therefore, they are considered as one of the most powerful tools to provide important constraints on models of new physics. In the SM, only C_{10} Wilson coefficient contributes to the decay amplitude.

Including scalar LQ contributions, the effective Hamiltonian of $B_q \to l^+ l^-$ processes is given by [137]

$$\mathcal{H}_{\rm eff} = \frac{G_F \alpha_{\rm em}}{\sqrt{2}\pi} V_{tb} V^*_{tq} \left[C^{\rm total}_{10} \mathcal{O}_{10} + C'^{\rm LQ}_{10} \mathcal{O}'_{10} \right], \tag{2.22}$$

where $q = d$ or s, $C^{\rm total}_{10} = C^{\rm SM}_{10} + C^{\rm LQ}_{10}$. The corresponding branching ratios for $B_q \to l^+ l^-$ process are given as

$${\rm BR}(B_q \to l^+ l^-) = \frac{G_F^2}{16\pi^3} \tau_{B_q} \alpha^2_{\rm em} f^2_{B_q} M_{B_q} m^2_l |V_{tb} V^*_{tq}|^2 \left| C^{\rm total}_{10} - C'^{\rm LQ}_{10} \right|^2 \sqrt{1 - \frac{4 m_l^2}{M^2_{B_q}}}. \tag{2.23}$$

However, as discussed in Ref. [137], the average time-integrated branching ratios $\overline{\rm BR}(B_q \to l^+ l^-)$ depend on the details of $B_q - \bar{B}_q$ mixing, which in the SM are related to the decay widths $\Gamma(B_q \to l^+l^-)$ by a very simple relation as $\overline{\mathrm{BR}}(B_q \to l^+l^-) = \Gamma(B_q \to l^+l^-)/\Gamma_H^q$, where Γ_H^q is the total width of the heavier mass eigenstate.

Including the corrections of $\mathcal{O}(\alpha_{\rm em})$ and $\mathcal{O}(\alpha_s^2)$, the updated branching ratios in the standard model are calculated in [138] as

$$\mathrm{BR}(B_s \to ee)^{\rm SM} = (8.54 \pm 0.55) \times 10^{-14}, \tag{2.24}$$
$$\mathrm{BR}(B_s \to \mu\mu)^{\rm SM} = (3.65 \pm 0.23) \times 10^{-9}, \tag{2.25}$$
$$\mathrm{BR}(B_s \to \tau\tau)^{\rm SM} = (7.73 \pm 0.49) \times 10^{-7}, \tag{2.26}$$
$$\mathrm{BR}(B_d \to ee)^{\rm SM} = (2.48 \pm 0.21) \times 10^{-15}, \tag{2.27}$$
$$\mathrm{BR}(B_d \to \mu\mu)^{\rm SM} = (1.06 \pm 0.09) \times 10^{-10}, \tag{2.28}$$
$$\mathrm{BR}(B_d \to \tau\tau)^{\rm SM} = (2.22 \pm 0.19) \times 10^{-8}. \tag{2.29}$$

The corresponding experimental branching ratios of these processes are [139–143]

$$\mathrm{BR}(B_s \to ee)^{\rm Expt} < 2.8 \times 10^{-7}, \tag{2.30}$$
$$\mathrm{BR}(B_s \to \mu\mu)^{\rm Expt} = (2.8^{+0.7}_{-0.6}) \times 10^{-9}, \tag{2.31}$$
$$\mathrm{BR}(B_s \to \tau\tau)^{\rm Expt} < 3.0 \times 10^{-3}, \tag{2.32}$$
$$\mathrm{BR}(B_d \to ee)^{\rm Expt} < 8.3 \times 10^{-8}, \tag{2.33}$$
$$\mathrm{BR}(B_d \to \mu\mu)^{\rm Expt} = (1.8 \pm 3.1) \times 10^{-10}, \tag{2.34}$$
$$\mathrm{BR}(B_d \to \tau\tau)^{\rm Expt} < 4.1 \times 10^{-3}. \tag{2.35}$$

The experimental branching ratio [141] of $B_{s,d} \to \mu^+\mu^-$ processes are more or less consistent with the latest SM prediction [138], but certainly they do not rule out the possibility of new physics as the experimental errors are still quite large.

Including the contributions arising from scalar LQ exchange, one can write the transition amplitude for these processes from Eqn. (2.22) as

$$\mathcal{M}(B_q^0 \to l^+l^-) = \langle l^+l^-|\mathcal{H}_{\rm eff}|B_q^0\rangle = -\frac{G_F}{\sqrt{2}\,\pi} V_{tb}V_{tq}^* \alpha_{\rm em} f_{B_q} M_{B_q} m_l C_{10}^{\rm SM} P, \tag{2.36}$$

where

$$P \equiv \frac{C_{10}^{\rm total} - C_{10}^{\prime \rm LQ}}{C_{10}^{\rm SM}} = 1 + \frac{C_{10}^{\rm LQ} - C_{10}^{\prime \rm LQ}}{C_{10}^{\rm SM}} = 1 + re^{i\phi^{\rm LQ}}\ , \tag{2.37}$$

with

$$re^{i\phi^{\rm LQ}} = (C_{10}^{\rm LQ} - C_{10}^{\prime \rm LQ})/C_{10}^{\rm SM}\ . \tag{2.38}$$

The expression r denotes the magnitude of the ratio of NP to SM contributions and $\phi^{\rm LQ}$ is the relative phase between them. As discussed in section 2.2, the exchange of the leptoquarks $S_2(3, 2, 7/6)$ and $\tilde{S}_2(3, 2, 1/6)$ give new additional contributions to the

Wilson coefficients $C_{10}^{\rm LQ}$ and $C_{10}^{\prime\rm LQ}$ respectively. Thus, the branching ratio in both the cases will be

$$\overline{\rm BR}(B_q \to l^+l^-) = \overline{\rm BR}(B_q \to l^+l^-)|_{\rm SM}(1 + r^2 - 2r\cos\phi^{\rm LQ})\ . \tag{2.39}$$

Using the theoretical and experimental branching ratios from (2.24) and (2.30), the constraints on the combination of LQ couplings can be obtained by requiring that each individual LQ contribution to the branching ratio does not exceed the experimental result. The allowed region in $r - \phi^{\rm LQ}$ plane which are compatible with the 1σ range of the experimental data are shown in Fig. 2.2 for $B_d \to \mu^+\mu^-$ (left panel) and for $B_s \to \mu^+\mu^-$ (right panel). From the figure one can see that for $B_d \to \mu^+\mu^-$ the allowed range of r and $\phi^{\rm LQ}$ as

$$0.5 \le r \le 1.3\ , \quad \text{for} \quad \big(0 \le \phi^{\rm LQ} \le \pi/2\big) \quad \text{or} \quad \big(3\pi/2 \le \phi^{\rm LQ} \le 2\pi\big)\ , \tag{2.40}$$

which can be translated to obtain the bounds for the leptoquark couplings using Eqns. (2.6), (2.10) and (2.38) as

$$1.5\times 10^{-9}\ {\rm GeV}^{-2} \le \frac{|\lambda^{32}\lambda^{12*}|}{M_S^2} \le 3.9\times 10^{-9}\ {\rm GeV}^{-2}\ , \tag{2.41}$$

with M_S as the LQ mass [1]. For the $B_s \to \mu^+\mu^-$ process for $0 \le r \le 0.1$ the entire range for $\phi^{\rm LQ}$ is allowed, i.e.,

$$0 \le r \le 0.1\ , \quad \text{for} \quad 0 \le \phi^{\rm LQ} \le 2\pi\ . \tag{2.42}$$

However, in our analysis we will use relatively mild constraint of

$$0 \le r \le 0.35\ , \quad \text{with} \quad \pi/2 \le \phi^{\rm LQ} \le 3\pi/2\ . \tag{2.43}$$

This gives the constraint on leptoquark couplings associated with $b \to s\mu^+\mu^-$ transition as

$$0 \le \frac{|\lambda^{32}\lambda^{22*}|}{M_S^2} \le 5\times 10^{-9}\ {\rm GeV}^{-2} \quad \text{for} \quad \pi/2 \le \phi^{\rm LQ} \le 3\pi/2\ . \tag{2.44}$$

For other leptonic decay channels i.e., $B_{s,d} \to e^+e^-,\ \tau^+\tau^-$ only the experimental upper limits exists [24, 98]. Using now the theoretical predictions for these branching ratios from [138], we obtain the constrain on the upper limits of the various combinations of LQ couplings as presented in Table 2.3. However, the constraints obtained from such processes are rather weak.

[1] For simplicity, we have not kept the subscripts on the LQ coupling parameters.

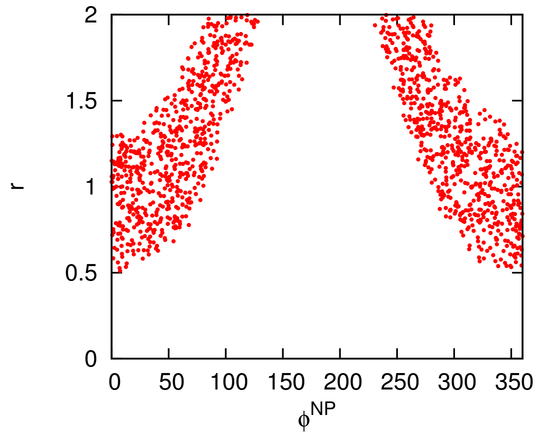

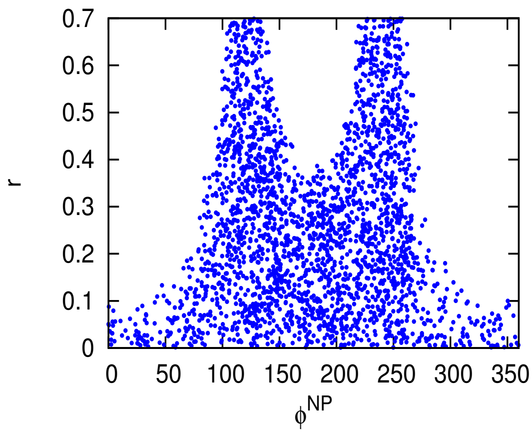

FIGURE 2.2: The allowed region in the $r - \phi^{\rm NP}$ parameters space obtained from the $\text{BR}(B_d \to \mu^+\mu^-)$ (left panel) and $\text{BR}(B_s \to \mu^+\mu^-)$ (right panel). Here $\phi^{\rm NP} = \phi^{\rm LQ}$.

TABLE 2.3: Constraints on the leptoquark couplings obtained from various leptonic $B_{s,d} \to l^+l^-$ decays.

Decay Process	Couplings involved	Upper bound of the couplings (in GeV^{-2})
$B_d \to e^\pm e^\mp$	$\frac{\vert\lambda^{31}\lambda^{11*}\vert}{M_S^2}$	$< 1.73 \times 10^{-5}$
$B_d \to \tau^\pm \tau^\mp$	$\frac{\vert\lambda^{33}\lambda^{13*}\vert}{M_S^2}$	$< 1.28 \times 10^{-6}$
$B_s \to e^\pm e^\mp$	$\frac{\vert\lambda^{31}\lambda^{21*}\vert}{M_S^2}$	$< 2.54 \times 10^{-5}$

2.3.2 $\bar{B} \to X_s l^+ l^-$ processes

For the analysis of semileptonic $b \to s l^+ l^-$ process, we need to know the values of the leptoquark couplings $\lambda^{3i}\lambda^{ki*}/M_S^2$, which can also be extracted from the inclusive decay rates $\bar{B} \to X_s l^+ l^-$. To obtain such constraints, we closely follow the procedure adopted in Ref. [123]. In this subsection, we discuss the constraint on LQ couplings from the branching ratio of inclusive $\bar{B} \to X_s l^+ l^-$ decay process mediated via $b \to s l^+ l^-$ transitions. The branching ratio for this process in the SM is given by [144]

$$\begin{aligned}\left.\frac{d\text{BR}}{ds_1}\right|_{\text{SM}} &= B_0 \frac{8}{3}(1-s_1)^2\sqrt{1-\frac{4t^2}{s_1}} \times \left[(2s_1+1)\left(\frac{2t^2}{s_1}+1\right)|C_9^{\text{eff}}|^2\right.\\ &+ \left(\frac{2(1-4s_1)t^2}{s_1}+(2s_1+1)\right)|C_{10}|^2 + 4\left(\frac{2}{s_1}+1\right)\left(\frac{2t^2}{s_1}+1\right)|C_7|^2\\ &+ \left. 12\left(\frac{2t^2}{s_1}+1\right)\text{Re}(C_7 C_9^{\text{eff}*})\right], \qquad (2.45)\end{aligned}$$

where $t = m_l/m_b^{pole}$, $s_1 = q^2/(m_b^{pole})^2$ and B_0 is the normalization constant related to $\mathrm{BR}(\bar{B} \to X_c e \bar{\nu}_e)$ process as

$$B_0 = \frac{3\alpha_{\rm em}^2 \mathrm{BR}(\bar{B} \to X_c e \bar{\nu}_e)}{32\pi^2 f(\hat{m}_c)\kappa(\hat{m}_c)} \frac{|V_{tb}V_{ts}^*|^2}{|V_{cb}|^2} \,. \tag{2.46}$$

Here $\hat{m}_c = m_c^{pole}/m_b^{pole}$ and the functions $f(\hat{m}_c)$ and $\kappa(\hat{m}_c)$ are defined in Refs. [123, 144]. For the numerical estimation, we use the values of the parameters as $\hat{m}_c = 0.29 \pm 0.02$ [145] and $\mathrm{BR}(\bar{B} \to X_c e \bar{\nu}_e) = (10.1 \pm 0.4)\%$ [98]. For the CKM matrix elements we use the Wolfenstein parameters with values $A = 0.814^{+0.023}_{-0.024}$, $\lambda = 0.22537 \pm 0.00061$, $\bar{\rho} = 0.117 \pm 0.021$ and $\bar{\eta} = 0.353 \pm 0.013$ [98]. The particle masses and the lifetime of B meson are taken from [98]. Now using these parameters, the branching ratios of $\bar{B} \to X_s l^+ l^-$ processes in the SM for the low $q^2 \in [1,6]$ GeV^2 region are found as

$$\mathrm{BR}(\bar{B} \to X_s e^+ e^-)|_{q^2 \in [1,6]\ \mathrm{GeV}^2} = (1.67 \pm 0.06) \times 10^{-6}, \tag{2.47}$$

$$\mathrm{BR}(\bar{B} \to X_s \mu^+ \mu^-)|_{q^2 \in [1,6]\ \mathrm{GeV}^2} = (1.6 \pm 0.61) \times 10^{-6}, \tag{2.48}$$

and the predicted branching ratios in the high q^2 (≥ 14.2 GeV^2) region are given as

$$\mathrm{BR}(\bar{B} \to X_s e^+ e^-)|_{q^2 \geq 14.2\ \mathrm{GeV}^2} = (3.9 \pm 0.15) \times 10^{-7}, \tag{2.49}$$

$$\mathrm{BR}(\bar{B} \to X_s \mu^+ \mu^-)|_{q^2 \geq 14.2\ \mathrm{GeV}^2} = (3.8 \pm 0.25) \times 10^{-7}, \tag{2.50}$$

$$\mathrm{BR}(\bar{B} \to X_s \tau^+ \tau^-)|_{q^2 \geq 14.2\ \mathrm{GeV}^2} = (1.78 \pm 0.29) \times 10^{-7}. \tag{2.51}$$

The corresponding experimental results for both low and high q^2 regions are given by [146]

$$\begin{aligned}
\mathrm{BR}(\bar{B} \to X_s e^+ e^-)^{\rm Expt} &= (1.93^{+0.47}_{-0.45}\,{}^{+0.21}_{-0.16} \pm 0.18) \times 10^{-6} \quad \text{For low } q^2, && (2.52)\\
&= (0.56^{+0.19}_{-0.18}\,{}^{+0.03}_{-0.03} \pm 0.00) \times 10^{-6} \quad \text{For high } q^2, && (2.53)\\
\mathrm{BR}(\bar{B} \to X_s \mu^+ \mu^-)^{\rm Expt} &= (0.66^{+0.82}_{-0.76}\,{}^{+0.30}_{-0.24} \pm 0.07) \times 10^{-6} \quad \text{For low } q^2, && (2.54)\\
&= (0.60^{+0.31}_{-0.29}\,{}^{+0.05}_{-0.04} \pm 0.00) \times 10^{-6} \quad \text{For high } q^2, && (2.55)
\end{aligned}$$

where the first uncertainties are statistical, the second experimental systematics, and the third model-dependent systematics. Since there is no experimental measurement for the branching ratio of $\bar{B} \to X_s \tau^+ \tau^-$ process, we consider the limit as $\sim 1\%$ in our analysis. Including the new physics contribution, the total branching ratio of $\bar{B} \to X_s l^+ l^-$ process is given by [123, 144]

$$\begin{aligned}
\left(\frac{d\mathrm{BR}}{ds_1}\right)_{\mathrm{Total}} &= \left(\frac{d\mathrm{BR}}{ds_1}\right)_{\mathrm{SM}} + B_0\Big[\frac{16}{3}(1-s_1)^2(1+2s_1)[\mathrm{Re}(C_9^{\mathrm{eff}}C_9^{\mathrm{LQ}^*} + \mathrm{Re}(C_{10}C_{10}^{\mathrm{LQ}^*}] \\
&+ \frac{8}{3}(1-s_1)^2(1+2s_1)\left[|C_9^{\mathrm{LQ}}|^2 + |C_{10}^{\mathrm{LQ}}|^2 + |C_9^{\prime\mathrm{LQ}}|^2 + |C_{10}^{\prime\mathrm{LQ}}|^2\right] \\
&+ 32(1-s_1)^2\ \mathrm{Re}(C_7C_{10}^{\mathrm{LQ}^*})\Big]\,, \qquad (2.56)
\end{aligned}$$

where $C_{9,10}^{(\prime)\mathrm{LQ}}$ are the new Wilson coefficients.

In Ref. [123], the constraint on the r and ϕ^{LQ} parameters from $\bar{B} \to X_s\mu^+\mu^-$ process is already discussed. According to Ref. [123], the bounds on r and ϕ^{LQ} parameters are given by [123]

$$0 \le r \le 0.36, \qquad 0 \le \phi^{\mathrm{LQ}} \le 2\pi. \qquad (2.57)$$

However, these constraints are more relaxed than those obtained from $B_s \to \mu^+\mu^-$.

In the left panel of Fig. 2.3, we show the allowed region in $C_{10}^{\mathrm{LQ}} - \phi^{\mathrm{LQ}}$ parameter space due to exchange of the leptoquark $S_2(3,2,7/6)$ for $b \to se^+e^-$ processes. The right panel depicts the allowed region in the $C_9^{\prime\mathrm{LQ}} - C_{10}^{\prime\mathrm{LQ}}$ space due to the exchange of the leptoquark $\tilde{S}_2(3,2,1/6)$, where the green (red) regions corresponds to high-q^2 (low-q^2) limits in both the panels. Thus, it can be noticed that the bounds coming from the high-q^2 measurements are rather weak. Considering the exchange of the $S_2(3,2,7/6)$ leptoquark as an example, we obtain the bound on C_{10}^{LQ} as $-2.0 \le C_{10}^{\mathrm{LQ}} \le 3.0$ for the entire range of ϕ^{LQ}, which gives the bound on r parameter associated with $b \to se^+e^-$ transition as

$$0 \le r \le 0.7\,. \qquad (2.58)$$

2.3.3 $B_s^0 - \bar{B}_s^0$ mixing

Now we will obtain the constraint on the LQ couplings from the mass difference between the B_s meson mass eigenstates (ΔM_s), which characterizes the $B_s - \bar{B}_s$ mixing phenomena. In the SM, $B_s - \bar{B}_s$ mixing proceeds to an excellent approximation through the box diagram with internal top quark and W boson exchange, and the effective Hamiltonian describing the $\Delta B = 2$ transition is given by [147]

$$\mathcal{H}_{\mathrm{eff}} = \frac{G_F^2}{16\pi^2}\ \lambda_t^2\ M_W^2 S_0(x_t)\eta_B(\bar{s}b)_{V-A}(\bar{s}b)_{V-A}\,, \qquad (2.59)$$

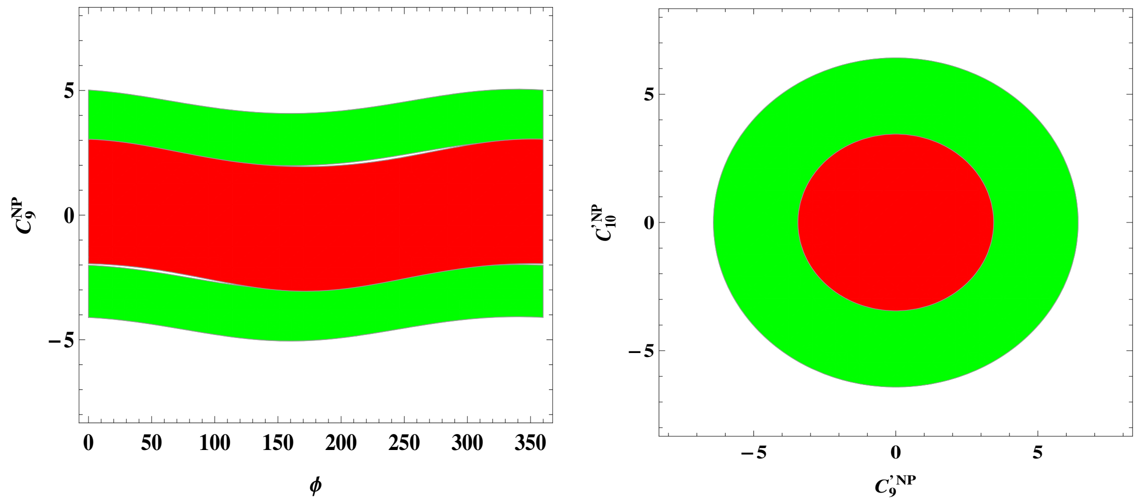

FIGURE 2.3: The allowed region in $C_{10}^{\rm NP} - \phi^{\rm NP}$ parameter space (left panel) and $C_9^{\prime\rm NP} - C_{10}^{\prime\rm NP}$ (right panel) obtained from BR($B \to X_s e^+ e^-$), where the green (red) region corresponds to high q^2 (low q^2) limits. Here $C_{9,10}^{(\prime)\rm NP} = C_{9,10}^{(\prime)\rm LQ}$ and $\phi^{\rm NP} = \phi^{\rm LQ}$.

where $\lambda_t = V_{tb}V_{ts}^*$, η_B is the QCD correction factor and $S_0(x_t)$ is the loop function

$$S_0(x_t) = \frac{4x_t - 11x_t^2 + x_t^3}{4(1-x_t)^2} - \frac{3}{2}\frac{\log x_t x_t^3}{(1-x_t)^3}\ , \tag{2.60}$$

with $x_t = m_t^2/M_W^2$. Thus, the $B_s - \bar{B}_s$ mixing amplitude in the SM can be written as

$$M_{12}^{\rm SM} = \frac{1}{2M_{B_s}} \langle \bar{B}_s | \mathcal{H}_{\rm eff} | B_s \rangle = \frac{G_F^2}{12\pi^2} M_W^2\ \lambda_t^2\ \eta_B\ \hat{B}_s f_{B_s}^2 M_{B_s} S_0(x_t)\ , \tag{2.61}$$

where the vacuum insertion method has been used to evaluate the matrix element

$$\langle \bar{B}_s | (\bar{s}\gamma^\mu(1-\gamma_5)b)(\bar{s}\gamma_\mu(1-\gamma_5)b) | B_s \rangle = \frac{8}{3}\hat{B}_s f_{B_s}^2 M_{B_s}^2\ . \tag{2.62}$$

The corresponding mass difference is related to the mixing amplitude through $\Delta M_s = 2|M_{12}|$. Now using the particle masses from [98], $\eta_B = 0.551$, the Bag parameter $\hat{B}_{B_s} = 1.320 \pm 0.017 \pm 0.030$, the decay constant $f_{B_s} = 225.6 \pm 1.1 \pm 5.4$ and the top quark mass $m_t = 165.95$ from [148], we obtain the value of ΔM_s in the SM as

$$\Delta M_s^{\rm SM} = (17.426 \pm 1.057)\ {\rm ps}^{-1}, \tag{2.63}$$

which is in good agreement with the experimental result [98]

$$\Delta M_s = 17.761 \pm 0.022\ {\rm ps}^{-1}. \tag{2.64}$$

However, the central value of the theoretical prediction deviates from the corresponding experimental value. The ratio of these two results yields

$$\Delta M_s/\Delta M_s^{\rm SM} = 1.019 \pm 0.062 \ , \tag{2.65}$$

which is consistent with 1, but it does not completely rule out the possibility of new physics in $B_s - \bar{B}_s$ mixing. The mixing amplitude receives an additional contribution

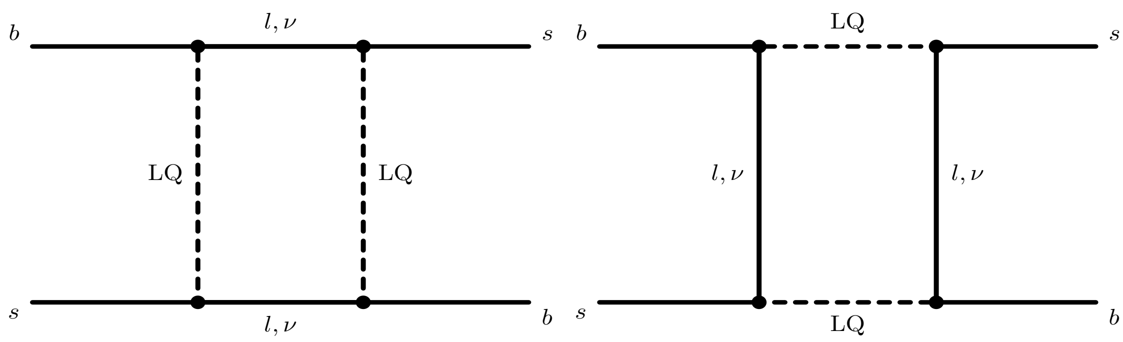

FIGURE 2.4: Box diagram for $B_s - \bar{B}_s$ mixing phenomenon in the leptoquark model.

due to the flow of LQs and charged leptons/neutrinos in the box diagram as shown in Fig. 2.4. For $S_2(3,2,7/6)$ LQ, there will be contribution coming only from charged leptons in the loop whereas for $\tilde{S}_2(3,2,1/6)$, both charged leptons and neutrinos will contribute to the mixing amplitude.

The effective Hamiltonian due to the leptoquark $S_2(3,2,7/6)$ and charged lepton in the loop is given by

$$\mathcal{H}_{\rm LQ} = \sum_{i=e,\mu,\tau} \frac{(\lambda_{LR}^{3i} \lambda_{LR}^{2i\,*})^2}{128\pi^2} \frac{1}{M_{S_2}^2} \ I\left(\frac{m_i^2}{M_{S_2}^2}\right) (\bar{b}\gamma^\mu L s)(\bar{b}\gamma_\mu L s) \ , \tag{2.66}$$

where the loop function $I(x)$ is given as

$$I(x) = \frac{1 - x^2 + 2x \log x}{(1-x)^2}, \tag{2.67}$$

which is always very close to $I(0) = 1$. For the $\tilde{S}_2(3,2,1/6)$ contribution there will be charged leptons as well as neutrinos in the loop, and the corresponding effective Hamiltonian becomes

$$\mathcal{H}_{\rm LQ} = \sum_{i=e,\mu,\tau} \frac{(\lambda_{RL}^{3i\,*} \lambda_{RL}^{2i})^2}{128\pi^2} \left[\frac{1}{M_{\tilde{S}_2}^2} \ I\left(\frac{m_i^2}{M_{\tilde{S}_2}^2}\right) + \frac{1}{M_{\tilde{S}_2}^2}\right] (\bar{b}\gamma^\mu R s)(\bar{b}\gamma_\mu R s) \ . \tag{2.68}$$

To obtain the constraints on the LQ coupling, we require that the individual LQ contribution to the mass difference does not exceed the 1σ range of the experimental value. Since we are interested in obtaining the bounds on λ^{32} and λ^{22} couplings, we consider the muon contribution to the mixing amplitude. Neglecting the mass of muon and using Eqn. (2.62), we obtain the contribution due to LQ exchange as

$$M_{12}^{\rm LQ} = \frac{(\lambda_{LR}^{32}\lambda_{LR}^{22\,*})^2}{384\pi^2 M_{S_2}^2}\eta_B \hat{B}_{B_s} f_{B_s}^2 M_{B_s}\,, \qquad \text{for } S_2(3,2,7/6), \tag{2.69}$$

$$M_{12}^{\rm LQ} = \frac{(\lambda_{RL}^{32\,*}\lambda_{RL}^{22})^2}{192\pi^2 M_{\tilde{S}_2}^2}\eta_B \hat{B}_{B_s} f_{B_s}^2 M_{B_s}\,, \qquad \text{for } \tilde{S}_2(3,2,1/6). \tag{2.70}$$

Thus, including both SM and LQ couplings, the total contribution to mass difference is given as

$$\begin{aligned}\Delta M_s &= \Delta M_s^{\rm SM}\Bigg|\Bigg[1+\frac{1}{16G_F^2 V_{tb}^2 V_{ts}^{*2} m_W^2 S_0(x_t)}\\ &\times\left(\frac{(\lambda_{LR}^{32}\lambda_{LR}^{22\,*})^2}{2M_{S_2}^2}+\frac{(\lambda_{RL}^{32\,*}\lambda_{RL}^{22})^2}{M_{\tilde{S}_2}^2}\right)\Bigg]\Bigg|\,.\end{aligned} \tag{2.71}$$

Now, varying the ratio of mass difference ($\Delta M_s/\Delta M_s^{\rm SM}$) within its 1σ allowed range (2.65), we obtain the constraint on $|\lambda^{32}\lambda^{22}/M_S|$ as shown in Fig. 2.5, where the left plot corresponds to the constraint on $S_2(3,2,7/6)$ and the right plot shows the constraint on $\tilde{S}_2(3,2,1/6)$ couplings. From the figure, the bounds on $|\lambda^{32}\lambda^{22}/M_S|$ for the entire allowed range of ϕ^{NP} are found to be

$$\begin{aligned}0 \le \left|\frac{\lambda_{LR}^{32}\lambda_{RL}^{22\,*}}{M_{S_2}}\right| &\le 7.5\times 10^{-5}\ {\rm GeV}^{-1}\,, \qquad \text{for } S_2(3,2,7/6),\\ 0 \le \left|\frac{\lambda_{RL}^{32\,*}\lambda_{RL}^{22}}{M_{\tilde{S}_2}}\right| &\le 5.0\times 10^{-5}\ {\rm GeV}^{-1}\,, \qquad \text{for } \tilde{S}_2(3,2,1/6).\end{aligned} \tag{2.72}$$

It should be noted that using the $B_s - \bar{B}_s$ mass difference, we obtained the bounds on $|\lambda^{32}\lambda^{22}|/M_S$, whereas using the $B_s \to \mu^+\mu^-$ and $\bar{B} \to X_s\mu^+\mu^-$ data, the bounds on $|\lambda^{32}\lambda^{22}|/M_S^2$ have been obtained. So to correlate these two results, we need to know the mass of the scalar leptoquark M_S. The upper limits on the LQs mass are discussed in section 2.1. Hence, if we scale the couplings obtained from the $B_s - \bar{B}_s$ mass difference for a benchmark leptoquark mass of 1 TeV, the bounds in Eq. (2.72) can be translated as

$$0 \leq \left| \frac{\lambda_{LR}^{32} \lambda_{LR}^{22\,*}}{M_{S_2}^2} \right| \leq 7.5 \times 10^{-8}\ \mathrm{GeV}^{-2}, \qquad \text{for } S_2(3,2,7/6),$$
$$0 \leq \left| \frac{\lambda_{RL}^{32\,*} \lambda_{RL}^{22}}{M_{\tilde{S}_2}^2} \right| \leq 5.0 \times 10^{-8}\ \mathrm{GeV}^{-2}, \qquad \text{for } \tilde{S}_2(3,2,1/6). \qquad (2.73)$$

Since these bounds are reasonably higher than those obtained from $B_s \to \mu^+\mu^-$ and $\bar{B} \to X_s\mu^+\mu^-$, we will use the bounds (2.43) as mentioned in the previous subsection, in our analysis.

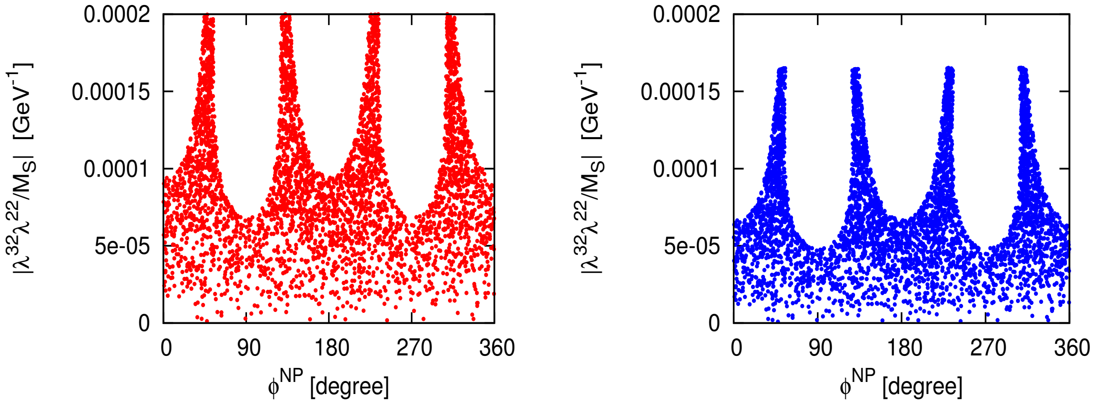

FIGURE 2.5: The allowed parameter space for the leptoquark couplings in the $|\lambda^{32}\lambda^{22}/M_S|$ vs. $\phi^{\rm NP} \sim \phi^{\rm LQ}$ plane obtained from the mass difference between B_s meson mass eigenstates (ΔM_s). The left panel corresponds to bounds on $S_2(3,2,7/6)$ and right panel is for $\tilde{S}_2(3,2,1/6)$ couplings.

2.4 Bounds on vector leptoquarks

In this section, we discuss the constraint on new Wilson coefficients which are obtained due to the exchange of $V_3(3,3,2/3)$ and $V_1(3,1,2/3)$ vector LQs. We compute the bounds on the vector LQ couplings by using various rare leptonic/semileptonic B and K decay modes such as $B_s \to l^+l^-$, $\bar{B} \to X_s l^+l^-$, $\bar{B} \to X_s\nu\bar{\nu}$, $B_u^+ \to l^+\nu_l$, $K_L \to l^+l^-$ as well as the LFV decay modes $\tau^- \to l^-\gamma$.

2.4.1 $B_{s,d} \to l^+ l^-$ processes

In the LQ model, the branching ratio of $B_q \to l^+ l^-$ process including the pseudo(scalar) Wilson coefficients is given by [137]

$$\begin{aligned} \mathrm{BR}(B_q \to l^+ l^-) &= \frac{G_F^2}{16\pi^3} \tau_{B_q} \alpha_{\rm em}^2 f_{B_q}^2 |C_{10}^{\rm SM}|^2 M_{B_q} m_l^2 |V_{tb} V_{tq}^*|^2 \sqrt{1 - \frac{4m_l^2}{M_{B_q}^2}} \\ &\quad \times \left(|P|^2 + |S|^2 \right), \end{aligned} \tag{2.74}$$

where P and S are defined as

$$\begin{aligned} P &\equiv \frac{C_{10}^{\rm SM} + C_{10}^{\rm LQ} - C_{10}^{\prime \rm LQ}}{C_{10}^{\rm SM}} + \frac{M_{B_q}^2}{2m_l} \frac{m_b}{m_b + m_q} \Big(\frac{C_P^{\rm LQ} - C_P^{\prime \rm LQ}}{C_{10}^{\rm SM}} \Big), \\ S &\equiv \sqrt{1 - \frac{4m_l^2}{M_{B_q}^2}} \frac{M_{B_q}^2}{2m_\mu} \frac{m_b}{m_b + m_q} \Big(\frac{C_S^{\rm LQ} - C_S^{\prime \rm LQ}}{C_{10}^{\rm SM}} \Big). \end{aligned} \tag{2.75}$$

Here $C_{10,S,P}^{(\prime)\rm LQ}$ are the new Wilson coefficients arising due to the exchange of vector LQ, which are negligible in the SM. Thus, $P = 1$ and $S = 0$ in the SM. The theoretical and experimental results are interconnected through the following relation [137]

$$\mathrm{BR}^{\rm th}(B_q \to l^+ l^-) = \left[\frac{1 - y_q^2}{1 + A_{\Delta\Gamma} y_q} \right] \mathrm{BR}^{\rm Expt}(B_q \to l^+ l^-), \tag{2.76}$$

where $y_q = \tau_{B_q} \Delta\Gamma_q / 2$ and $A_{\Delta\Gamma}$ is the mass eigenstate rate asymmetry. Now to compare the theory with the experiment we define their ratio as

$$R_q = \frac{\mathrm{BR}^{\rm th}(B_q \to l^+ l^-)}{\mathrm{BR}^{\rm SM}(B_q \to l^+ l^-)} = |P|^2 + |S|^2. \tag{2.77}$$

In our analysis, we compute the bound on vector LQ couplings for the two different cases: (a) LQ couplings are real, (b) LQ coupings are imaginary.

Case-I: Real leptoquark couplings

Here, we assume that the couplings coming from the vector LQ exchange are real. If we consider the LQ couplings as chiral, then only the $C_{10}^{\rm LQ}$ Wilson coefficient will give additional contributions. Now comparing the SM theoretical predicted values [138] with the corresponding experimental results [141] for the branching ratios of $B_q \to l^+ l^-$ processes, one can obtain the constraints on the new Wilson coefficients $C_{10}^{(\prime)\rm LQ}$ generated in the LQ model. The detailed formalism of the constraints on r and $\phi^{\rm LQ}$ parameters for scalar LQ has been discussed in the previous section. Using these bounds on the r and $\phi^{\rm LQ}$ parameters, one can envisage the rare leptonic/semileptonic B decay processes driven by vector LQ, if the masses of scalar and vector LQs are of same order, $M_{\rm LQ} = 1$ TeV. The upper bound on the product of the leptoquark couplings ($\lambda_{LL}^{ki}\lambda_{LL}^{3i*}$) from various two body leptonic $B_{s,d} \to l^+l^-$, $l = e, \mu, \tau$ decays are presented in Table 2.4.

TABLE 2.4: The allowed values of the product of vector leptoquark couplings obtained from the processes $B_{s,d} \to l^+l^-$.

Decay Process	Couplings involved	Upper bound of the couplings
$B_s \to e^\pm e^\mp$	$\lvert\lambda_{LL}^{21}\lambda_{LL}^{31\ *}\rvert$	< 11.8
$B_s \to \mu^\pm \mu^\mp$	$\lvert\lambda_{LL}^{22}\lambda_{LL}^{32\ *}\rvert$	$< 2.3 \times 10^{-3}$
$B_s \to \tau^\pm \tau^\mp$	$\lvert\lambda_{LL}^{23}\lambda_{LL}^{33\ *}\rvert$	< 0.4
$B_d \to e^\pm e^\mp$	$\lvert\lambda_{LL}^{11}\lambda_{LL}^{31\ *}\rvert$	< 8.0
$B_d \to \mu^\pm \mu^\mp$	$\lvert\lambda_{LL}^{12}\lambda_{LL}^{32\ *}\rvert$	$(0.7 - 1.81) \times 10^{-3}$
$B_d \to \tau^\pm \tau^\mp$	$\lvert\lambda_{LL}^{13}\lambda_{LL}^{33\ *}\rvert$	< 0.593

As seen from Eqn. (2.75), the scalar and pseudoscalar Wilson coefficients are dominated by the $M_{B_q}^2/m_l$ multiplication factor, therefore, the new physics contribution to the $C_{10}^{\rm LQ}$ Wilson coefficient can be neglected. In the presence of only $C_{S,P}^{(\prime)\rm LQ}$ Wilson coefficients, using Eqns. (2.94), (2.20c), (2.20d) and (2.77), the R_q parameter turns into

$$R_q = \frac{|C_S^{\rm LQ} - C_S^{\prime\rm LQ}|^2}{r_q^2} + \left|1 - \frac{|C_S^{\rm LQ} + C_S^{\prime\rm LQ}|}{r_q}\right|^2 \tag{2.78}$$

where

$$r_q = \frac{2m_l\,(m_b + m_q)\,C_{10}^{SM}}{M_{B_q}^2}. \tag{2.79}$$

Now comparing the theoretical and experimental branching ratios of $B_q \to l^+l^-$ decay modes, we estimate the allowed range of $C_S^{\rm LQ} \pm C_S^{\prime\rm LQ}$ coefficients. In the presence of only real pseudo(scalar) Wilson coefficients, Eqn. (2.78) will be a circle of radius $|r_q|\sqrt{R_q^{\rm Expt}}$ with center at $\left(C_S^{\rm LQ} + C_S^{\prime\rm LQ}, C_S^{\rm LQ} - C_S^{\prime\rm LQ}\right) = (r_q, 0)$. We show in Fig. 2.6, the allowed region in the $C_S^{\rm LQ} - C_S^{\prime\rm LQ}$, $C_S^{\rm LQ} + C_S^{\prime\rm LQ}$ plane, obtained from the $B_s \to e^+e^-$ (top left panel), $B_s \to \mu^+\mu^-$ (top right panel) and $B_s \to \tau^+\tau^-$ (bottom panel) processes. Analogously, the constraint on real Wilson coefficients acquired from $B_d \to e^+e^-$ (top left panel), $B_d \to \mu^+\mu^-$ (top right panel) and $B_d \to \tau^+\tau^-$ (bottom panel) decays are presented in Fig. 2.7. In Table 2.5, we report the constraint on the $C_S^{\rm LQ} \pm C_S^{\prime\rm LQ}$ real Wilson coefficients obtained from the experimental bound on the branching fractions of the processes $B_q \to l^+l^-$. Using the bounds on the real Wilson coefficients, one can obtain the constraints on the product of several LQ couplings using the Eqns. (2.20c, 2.20d).

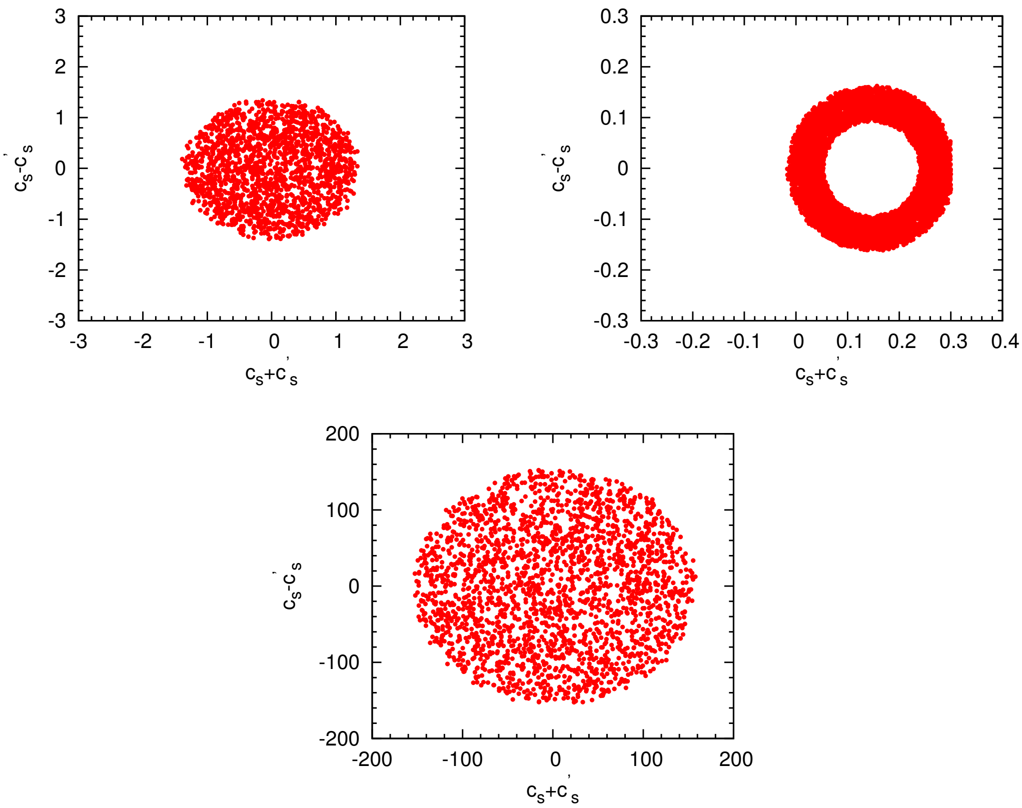

FIGURE 2.6: The allowed region for the $C_S \pm C_S'$ Wilson coefficient obtained from $B_s \to e^+e^-$ (top left panel), $B_s \to \mu^+\mu^-$ (top right panel) and $B_s \to \tau^+\tau^-$ (bottom panel) processes.

TABLE 2.5: The allowed values of the combinations of $C_S^{(\prime)\mathrm{LQ}}$ Wilson coefficients obtained from the processes $B_{s,d} \to l^+l^-$.

Decay Process	Bound on $C_S^{\mathrm{LQ}} + C_S^{\prime\mathrm{LQ}}$	Bound on $C_S^{\mathrm{LQ}} - C_S^{\prime\mathrm{LQ}}$
$B_s \to \mu^\pm\mu^\mp$	$0.0 \to 0.32$	$0.1 \to 0.18$
$B_s \to e^\pm e^\mp$	$-1.4 \to 1.4$	$-1.4 \to 1.4$
$B_s \to \tau^\pm\tau^\mp$	$-150 \to 150$	$-150 \to 150$
$B_d \to \mu^\pm\mu^\mp$	$-0.16 \to 0.44$	$0.2 \to 0.36$
$B_d \to e^\pm e^\mp$	$-4 \to 4$	$-4 \to 4$
$B_d \to \tau^\pm\tau^\mp$	$-1000 \to 1000$	$-1000 \to 1000$

Case-II: Imaginary leptoquark couplings

Here, we assume the leptoquark couplings as imaginary. Now comparing the theoretical value of branching ratio of $B_s \to l^+l^-$ processes from Eqn. (2.24) with the 1σ range of the experimental data (2.30), the allowed region of real and imaginary parts of the chiral LQ couplings are shown in Fig. 2.8, for $B_s \to e^+e^-$ (top left panel), $B_s \to \mu^+\mu^-$ (top right panel) and $B_s \to \tau^+\tau^-$ (bottom panel) processes. The constrained values of real and imaginary parts of LQ couplings are given in Table 2.6. Now considering only

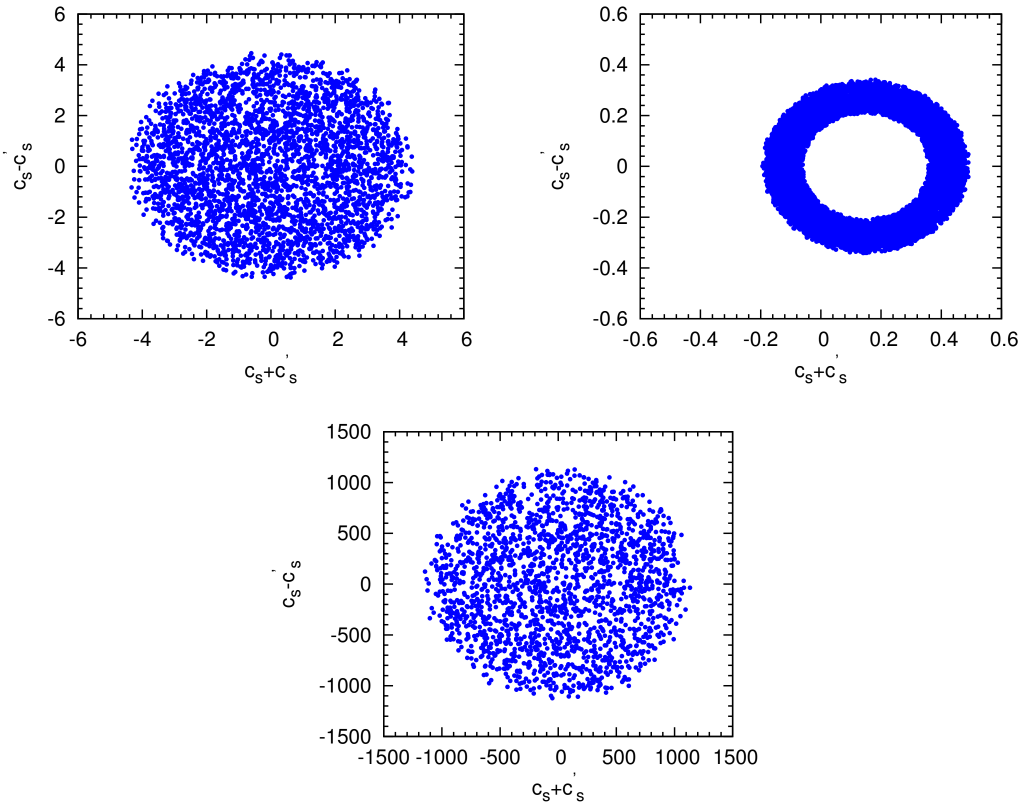

FIGURE 2.7: The allowed region for the $C_S \pm C'_S$ Wilson coefficient obtained from $B_d \to e^+e^-$ (top left panel), $B_d \to \mu^+\mu^-$ (top right panel) and $B_d \to \tau^+\tau^-$ (bottom panel) processes.

the $C_{S,P}^{(\prime)\rm LQ}$ new Wilson coefficients, the allowed region on real and imaginary parts of LQ couplings for $B_s \to e^+e^-$ (top left panel), $B_s \to \mu^+\mu^-$ (top right panel) and $B_s \to \tau^+\tau^-$ (bottom panel) processes are shown in Fig. 2.9 and the allowed range of LQ couplings are presented in Table 2.6.

TABLE 2.6: Constraints on the real and imaginary parts of the leptoquark couplings from $B_s \to l^+l^-$ processes, where $l = e, \mu, \tau$.

Leptoquark Couplings	Real part	Imaginary part
$\lambda_{LL}^{21}\lambda_{LL}^{31\,*}$	$-13.0 \to 13.0$	$-13 \to 13$
$\lambda_{LL}^{22}\lambda_{LL}^{32\,*}$	$-0.016 \to 0.0$	$-0.008 \to 0.008$
$\lambda_{LL}^{23}\lambda_{LL}^{33\,*}$	$-0.4 \to 0.4$	$-0.4 \to 0.4$
$\lambda_{LL}^{21}\lambda_{RR}^{31\,*}$	$(-0.8 \to 0.8) \times 10^{-3}$	$(-0.8 \to 0.8) \times 10^{-3}$
$\lambda_{LL}^{22}\lambda_{RR}^{32\,*}$	$-0.016 \times 10^{-2} \to 0.0$	$(-0.8 \to 0.8) \times 10^{-4}$
$\lambda_{LL}^{23}\lambda_{RR}^{33\,*}$	$-0.1 \to 0.1$	$-0.1 \to 0.1$

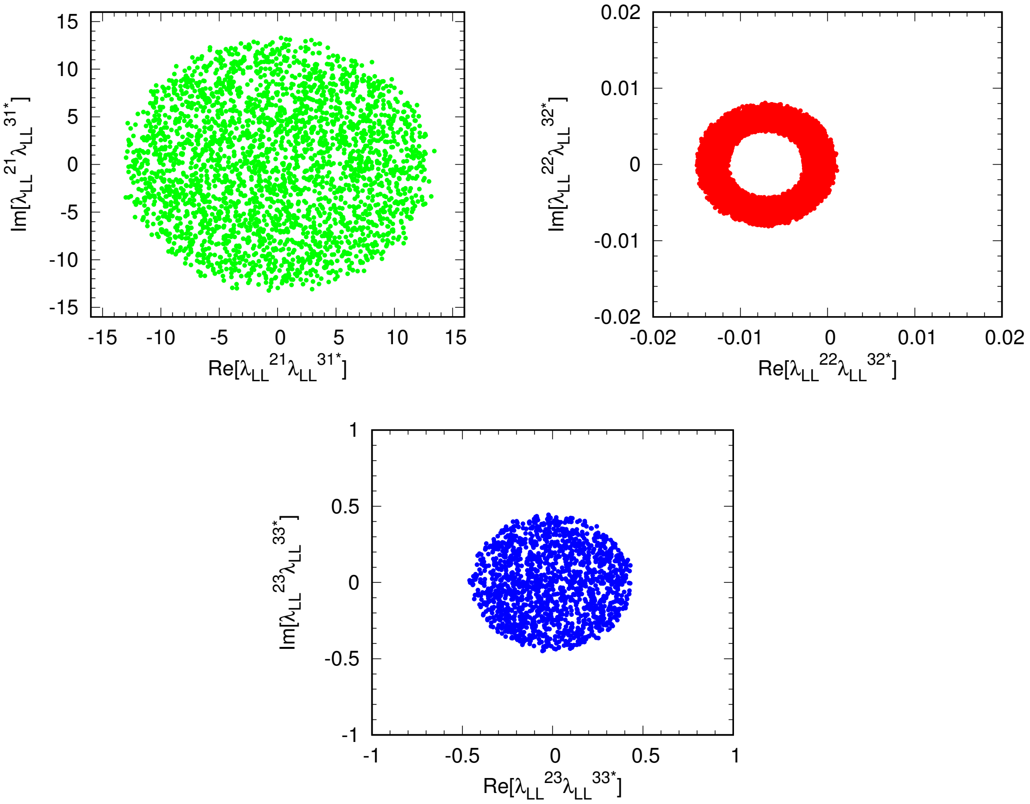

FIGURE 2.8: Constraints on the real and imaginary parts of the leptoquark couplings from $B_s \to e^+e^-$ (top left panel), $B_s \to \mu^+\mu^-$ (top right panel) and $B_s \to \tau^+\tau^-$ (bottom panel) processes in $V_3(3,3,2/3)$ leptoquark model.

2.4.2 $\bar{B} \to X_s l^+ l^-$ processes

The detailed expressions for the branching ratios of inclusive $\bar{B} \to X_s l^+ l^-$ processes are discussed in subsection 2.3.2. Therefore, in this subsection we will present our findings on LQ couplings from these processes. By comparing the theoretical and experimental branching ratios, we show the constraints on $V_3(3,3,2/3)$ LQ couplings from $\bar{B} \to X_s e^+e^-(\mu^+\mu^-)$ process for low q^2 (left panel) and high q^2 (right panel) in Fig. 2.10 (Fig. 2.11) respectively. Similarly in Fig. 2.12, we show the allowed region from $\bar{B} \to X_s \tau^+\tau^-$ process in high q^2 region. From these figures, the allowed range of real and imaginary parts of LQ parameter space in the low and high q^2 regime are presented in Table 2.7.

2.4.3 $\bar{B} \to X_s \nu\bar{\nu}$ process

The study of the processes involving $b \to s\nu\bar{\nu}$ transitions are quite important, as they are related to $b \to sl^+l^-$ processes by $SU(2)_L$ and are also very sensitive to the search for NP beyond the SM. The inclusive decay $\bar{B} \to X_s\nu\bar{\nu}$ is theoretically very clean,

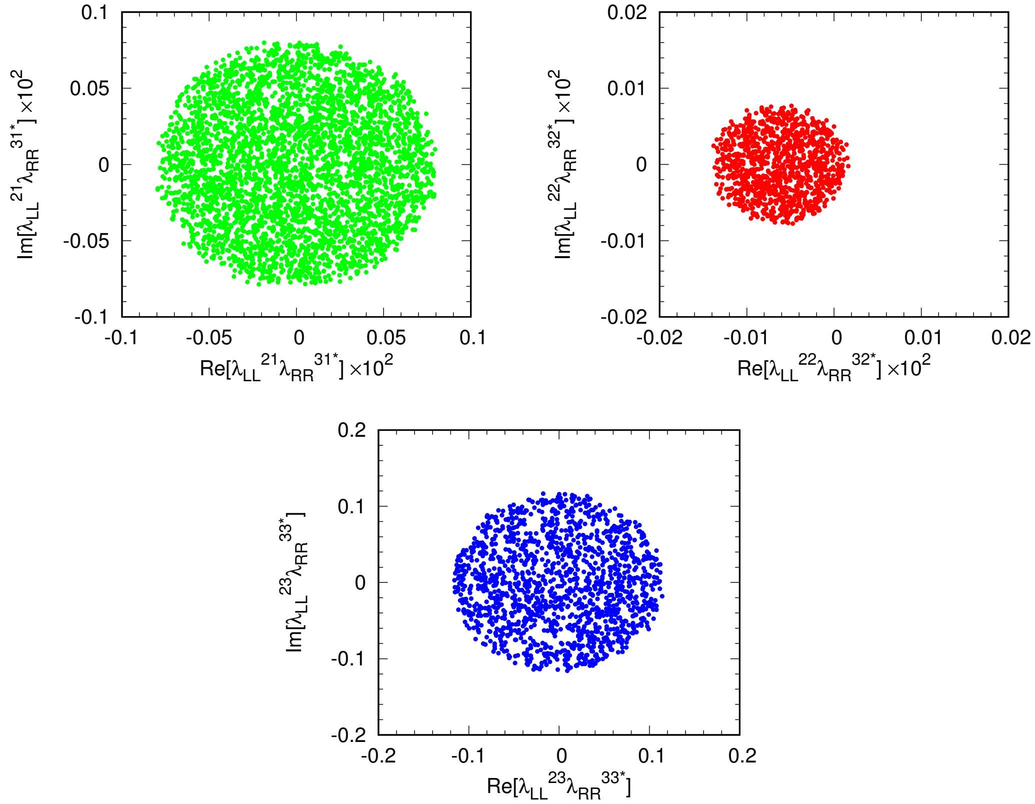

FIGURE 2.9: Constraints on the real and imaginary parts of the leptoquark couplings from $B_s \to e^+e^-$ (top left panel), $B_s \to \mu^+\mu^-$ (top right panel) and $B_s \to \tau^+\tau^-$ (bottom panel) processes in $V_1(3,1,2/3)$ leptoquark model.

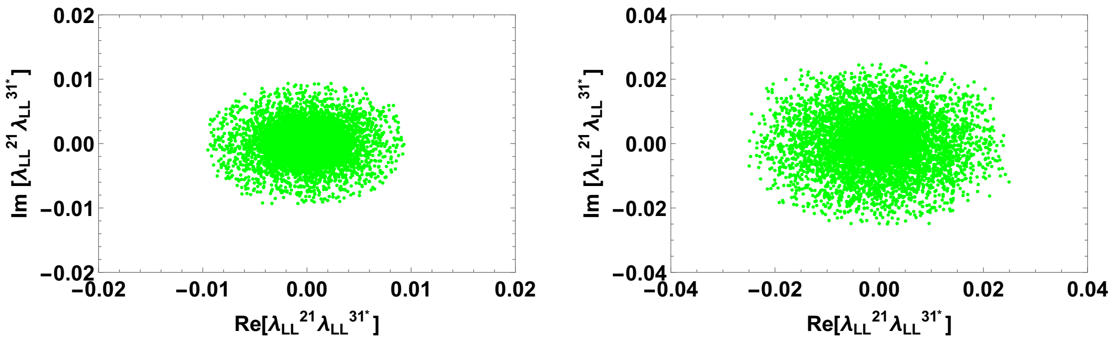

FIGURE 2.10: Constraints on the real and imaginary parts of the leptoquark couplings from $\bar{B} \to X_s e^+e^-$ process in low q^2 (left panel) and high q^2 region (right panel) in the $V_3(3,3,2/3)$ leptoquark model.

since both the perturbative and the non-perturbative corrections are small. Thus, these decays do not suffer from the form factor uncertainties.

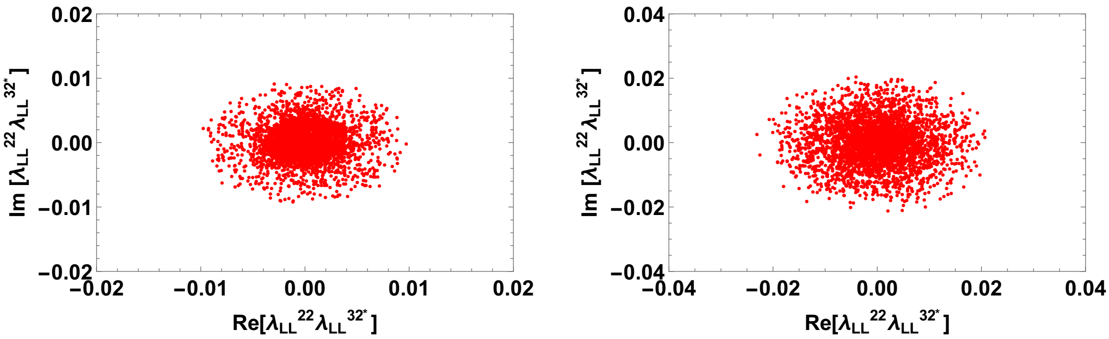

FIGURE 2.11: Constraints on the real and imaginary parts of the leptoquark couplings from $\bar{B} \to X_s \mu^+\mu^-$ process in low q^2 (left panel) and high q^2 region (right panel) in the $V_3(3,3,2/3)$ leptoquark model.

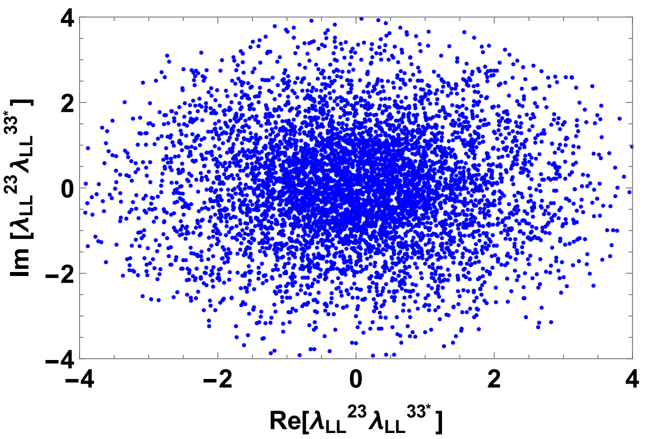

FIGURE 2.12: Constraints on the real and imaginary parts of the leptoquark couplings from $\bar{B} \to X_s \tau^+\tau^-$ process in the $V_3(3,3,2/3)$ leptoquark model.

TABLE 2.7: Constraints on the real and imaginary parts of the leptoquark coupling for low and high q^2 region from $\bar{B} \to X_s l^+ l^-$ process, where $l = e, \mu, \tau$.

q^2 bin	Leptoquark Couplings	Real part	Imaginary part
low q^2	$\lambda_{LL}^{21} \lambda_{LL}^{31\ *}$	$-0.01 \to 0.01$	$-0.01 \to 0.01$
	$\lambda_{LL}^{22} \lambda_{LL}^{32\ *}$	$-0.008 \to 0.008$	$-0.008 \to 0.008$
high q^2	$\lambda_{LL}^{21} \lambda_{RR}^{31\ *}$	$-0.022 \to 0.022$	$-0.022 \to 0.022$
	$\lambda_{LL}^{22} \lambda_{RR}^{32\ *}$	$-0.018 \to 0.018$	$-0.018 \to 0.018$
	$\lambda_{LL}^{23} \lambda_{RR}^{33\ *}$	$-3.8 \to 3.8$	$-3.8 \to 3.8$

The branching ratio of $\bar{B} \to X_s \nu\bar{\nu}$ process is [59]

$$\begin{aligned} \frac{d\Gamma}{ds_b} &= m_b^5 \frac{\alpha_{\rm em}^2 G_F^2}{128\pi^5} |V_{ts}^* V_{tb}|^2 \kappa(0) \left(|C_L^\nu|^2 + |C_R^\nu|^2\right) \lambda^{1/2}(1, \tilde{m}_s^2, s_b) \\ &\times \left[3 s_b (1 + \tilde{m}_s^2 - s_b - 4\tilde{m}_s \frac{\mathrm{Re}(C_L^\nu C_R^{\nu *})}{|C_L^\nu|^2 + |C_R^\nu|^2}) + \lambda(1, \tilde{m}_s^2, s_b)\right], \end{aligned} \tag{2.80}$$

where $\tilde{m}_s = m_s/m_b$, $s_b = s/m_b^2$ and $\kappa(0) = 0.83$ is the QCD correction to the $b \to s\nu\bar{\nu}$ matrix element [61, 149].

The $V_3(3,3,2/3)$ vector LQ has additional $C_L^{\rm LQ}$ coefficients contribution to the SM. In the presence of LQ, the total decay rate of $\bar{B} \to X_s\nu\bar{\nu}$ process can be obtained from (2.80) by replacing the Wilson coefficient, $C_L^\nu \to C_L^\nu + C_L^{\rm LQ}$. Using all the particle masses and the lifetime of B meson from [98], the branching ratio in the SM is given by

$$\mathrm{BR}(\bar{B} \to X_s\nu\bar{\nu}) = (2.74 \pm 0.16) \times 10^{-5}, \tag{2.81}$$

and the corresponding experimental upper limit, measured by the ALEPH collaboration is given by [150]

$$\mathrm{BR}(\bar{B} \to X_s\nu\bar{\nu})^{\rm Expt} < 6.4 \times 10^{-4}. \tag{2.82}$$

Now comparing the theoretical and experimental branching ratio, we show the constraints on $V_3(3,3,2/3)$ leptoquark couplings in Fig. 2.13. From the figure, the allowed ranges of real and imaginary parts of the couplings are found as

$$-0.02 \le \mathrm{Re}[\lambda_{LL}^{22}\lambda_{LL}^{32\,*}] \le 0.02, \qquad -0.02 \le \mathrm{Im}[\lambda_{LL}^{22}\lambda_{LL}^{32\,*}] \le 0.02. \tag{2.83}$$

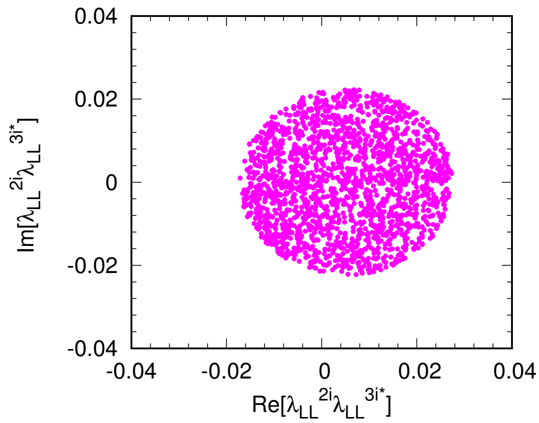

FIGURE 2.13: Constraints on the real and imaginary parts of the leptoquark couplings from $\bar{B} \to X_s\nu\bar{\nu}$ process in the $V_3(3,3,2/3)$ leptoquark model.

2.4.4 $B_u^+ \to l^+\nu_l$ processes

The rare leptonic $B_u^+ \to l^+\nu_l$ decay modes, where $l = e, \mu, \tau$ mediated by $b \to ul\nu$ transitions can provide significant constraints on models of new physics. Neglecting the electromagnetic radiative corrections, the branching ratio of the $B_u^+ \to l^+\nu_l$ processes in the $V_{1,3}$ leptoquark model is given by [151],

$$\begin{aligned} \mathrm{BR}(B_u^+ \to l^+\nu_l) &= \frac{G_F^2 M_{B_u} m_l^2}{8\pi}\Big(1-\frac{m_l^2}{M_{B_u}^2}\Big)^2 f_{B_u}^2 \left|V_{ub}\right|^2 \tau_{B^+} \\ &\quad \times \Big| (1+C_{V_1}-C_{V_2}) + \frac{M_{B_u}^2}{m_l(m_b+m_u)} C_{S_1}\Big|^2, \end{aligned} \tag{2.84}$$

where $C_{V_{1,2}}$ and C_{S_1} Wilson coefficients arise due to $V_{1,3}$ leptoquark exchange and is negligible in the SM. Using the particle masses and life time of B_u^+ meson from [98], the decay constants $f_{B_{u,d}} = 190.5(4.2)$ MeV [152] and $|V_{ub}| = 4.13(49) \times 10^{-3}$ [98], the branching ratios in the SM are found to be

$$\begin{aligned} \mathrm{BR}(B_u^+ \to e^+\nu_e)^{\mathrm{SM}} &= (8.9 \pm 0.23) \times 10^{-12}, \\ \mathrm{BR}(B_u^+ \to \mu^+\nu_\mu)^{\mathrm{SM}} &= (3.83 \pm 0.1) \times 10^{-7}, \\ \mathrm{BR}(B_u^+ \to \tau^+\nu_\tau)^{\mathrm{SM}} &= (8.48 \pm 0.28) \times 10^{-5}, \end{aligned} \tag{2.85}$$

and the corresponding averaged experimental values are [98]

$$\begin{aligned} \mathrm{BR}(B_u^+ \to e^+\nu_e)^{\mathrm{Expt}} &< 9.8 \times 10^{-7}, \\ \mathrm{BR}(B_u^+ \to \mu^+\nu_\mu)^{\mathrm{Expt}} &< 1.0 \times 10^{-6}, \\ \mathrm{BR}(B_u^+ \to \tau^+\nu_\tau)^{\mathrm{Expt}} &= (1.14 \pm 0.27) \times 10^{-4}. \end{aligned} \tag{2.86}$$

If we apply chirality on LQ, then only C_{V_1} Wilson coefficient will contribute to the branching ratios. Now comparing the theoretical (2.85) and experimental (2.86) values, the allowed region of real and imaginary parts of LQ couplings from $B_u^+ \to e^+\nu_e$ (top left panel), $B_u^+ \to \mu^+\nu_\mu$ (top right panel) and $B_u^+ \to \tau^+\nu_\tau$ (bottom panel) processes are shown in Fig. 2.14 and the constrained values are given in Table 2.8. From (2.84), it should be noted that the contribution of C_{S_1} Wilson coefficient is enhanced by the factor $M_{B_u}^2/m_l$, so we will neglect the NP in C_{V_1} for simplicity. Then the branching ratio is only sensitive to the C_{S_1} Wilson coefficient. In Fig. 2.15, we show the constraint on $V_1(3,1,2/3)$ LQ couplings from $B_u^+ \to e^+\nu_e$ (top left panel), $B_u^+ \to \mu^+\nu_\mu$ (top right panel) and $B_u^+ \to \tau^+\nu_\tau$ (bottom panel) processes and the allowed ranges are given in Table 2.8.

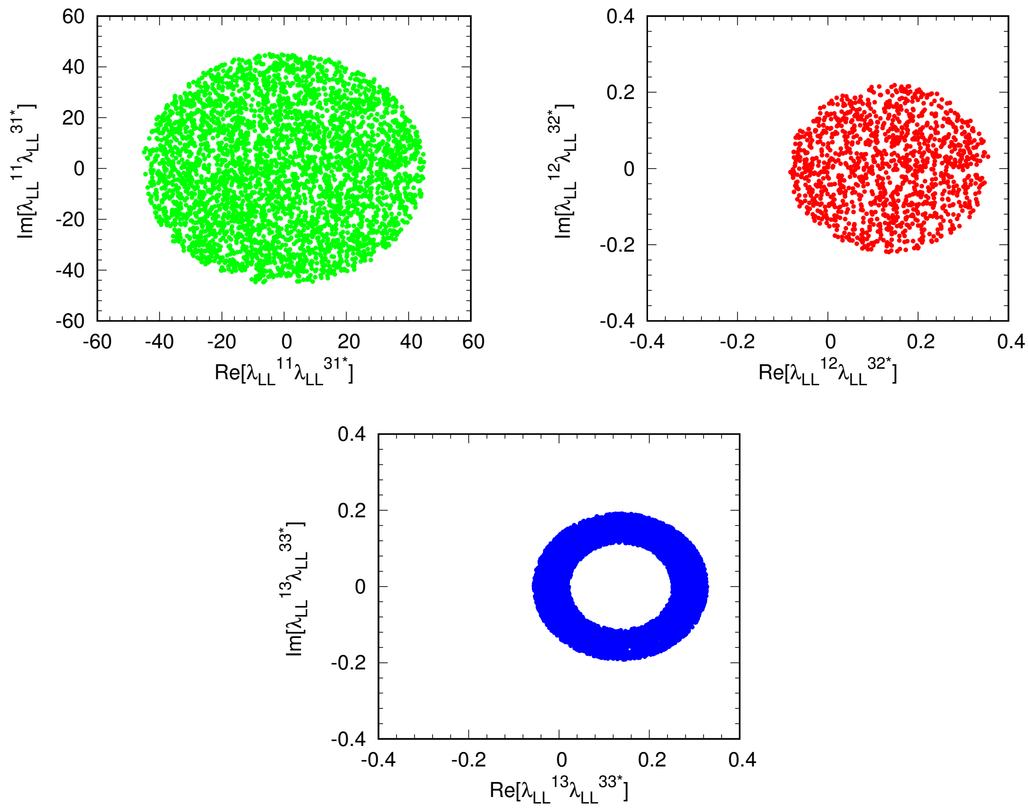

FIGURE 2.14: Constraints on the real and imaginary parts of the leptoquark couplings from $B_u^+ \to e^+\nu_e$ (top left panel), $B_u^+ \to \mu^+\nu_\mu$ (top right panel) and $B_u^+ \to \tau^+\nu_\tau$ (bottom panel) processes in $V_3(3,3,2/3)$ leptoquark model.

TABLE 2.8: Constraint on real and imaginary part of the leptoquark couplings from $B_u^+ \to l^+\nu_l$ processes, where $l = e, \mu, \tau$

Leptoquark Couplings	Real part	Imaginary Part
$\lambda_{LL}^{11}\lambda_{LL}^{31\ *}$	$-40.0 \to 40.0$	$-40.0 \to 40.0$
$\lambda_{LL}^{12}\lambda_{LL}^{32\ *}$	$-0.08 \to 0.32$	$-0.2 \to 0.2$
$\lambda_{LL}^{13}\lambda_{LL}^{33\ *}$	$0.24 \to 0.32$	$-0.2 \to 0.2$
$\lambda_{LL}^{11}\lambda_{RR}^{31\ *}$	$-0.002 \to 0.002$	$-0.002 \to 0.002$
$\lambda_{LL}^{12}\lambda_{RR}^{32\ *}$	$-0.0008 \to 0.0032$	$-0.002 \to 0.002$
$\lambda_{LL}^{13}\lambda_{RR}^{33\ *}$	$-0.034 \to 0.046$	$-0.028 \to 0.028$

2.4.5 $K_L \to \mu^+\mu^-(e^+e^-)$ processes

In the SM, the effective Hamiltonian describing the quark level transition $s \to d\mu^+\mu^-$ is given by [153]

$$\mathcal{H}_{\rm eff} = \frac{G_F}{\sqrt{2}}\frac{\alpha_{\rm em}}{2\pi\sin^2\theta_W}\left(\lambda_c Y_{NL} + \lambda_t Y(x_t)\right)\left(\bar{s}\gamma^\mu(1-\gamma_5)d\right)\left(\bar{\mu}\gamma_\mu(1-\gamma_5)\mu\right), \quad (2.87)$$

$$= \frac{G_F}{\sqrt{2}}\frac{\alpha_{\rm em}}{2\pi}\lambda_u C_{\rm SM}^K\left(\bar{s}\gamma^\mu(1-\gamma_5)d\right)\left(\bar{\mu}\gamma_\mu(1-\gamma_5)\mu\right), \quad (2.88)$$

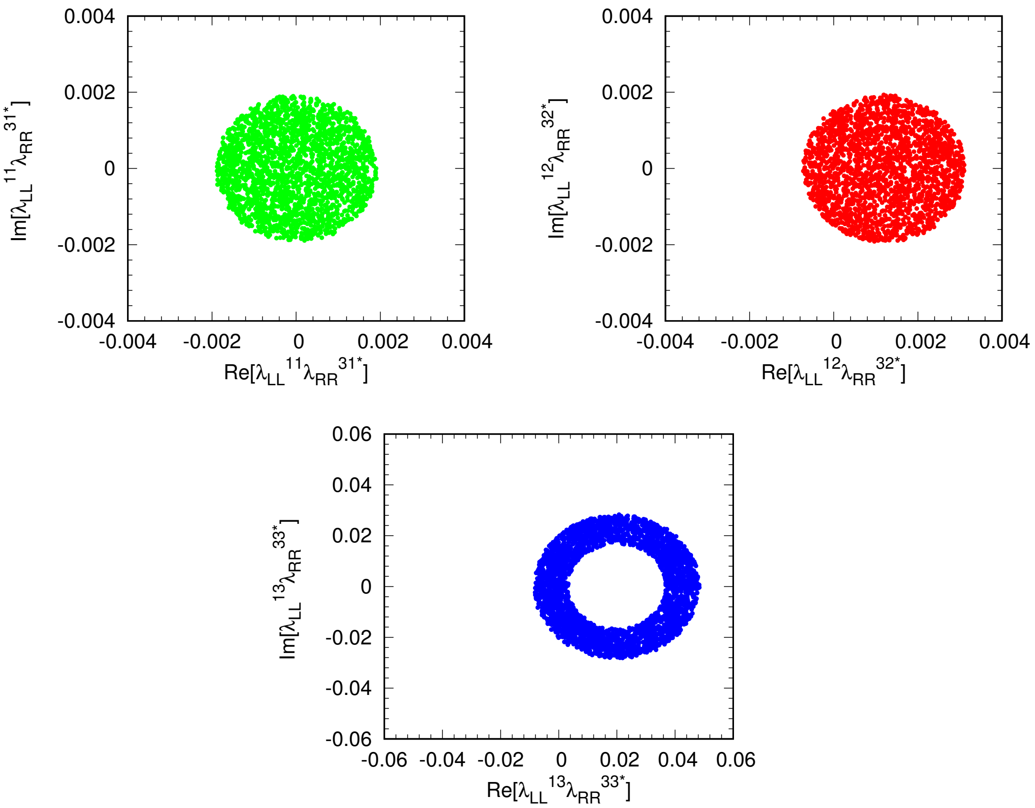

FIGURE 2.15: Constraints on the real and imaginary parts of the leptoquark couplings from $B_u^+ \to e^+\nu_e$ (top left panel), $B_u^+ \to \mu^+\nu_\mu$ (top right panel) and $B_u^+ \to \tau^+\nu_\tau$ (bottom panel) processes in $V_1(3,1,2/3)$ leptoquark model.

where $\lambda_i = V_{id}V_{is}^*$ and $x_t = m_t^2/M_W^2$. Here the SM Wilson coefficient $C_{\rm SM}^K$ is given by

$$C_{\rm SM}^K = \frac{\lambda_c Y_{NL} + \lambda_t Y(x_t)}{\sin^2\theta_W \lambda_u}. \tag{2.89}$$

The functions Y_{NL} and $Y(x_t)$ [60, 61] are the contributions from the charm and top quark, respectively. At next-to-leading order (NLO), the expression for $Y(x_t)$ function is given by

$$Y(x_t) = \eta_Y \frac{x_t}{8}\left(\frac{4-x_t}{1-x_t} + \frac{3x_t}{(1-x_t)^2}\ln x_t\right). \tag{2.90}$$

The estimated branching ratio of the short distance (SD) part of the $K_L \to \mu^+\mu^-$ process is ${\rm BR}(K_L \to \mu^+\mu^-)|_{\rm SD} < 2.5 \times 10^{-9}$ [154]. The branching ratio for the SD part of $K_L \to \mu^+\mu^-$ process in the SM is given by

$${\rm BR}(K_L \to \mu^+\mu^-)|_{\rm SD} = \tau_{K_L}\frac{G_F^2}{2\pi}|\lambda_u|^2\sqrt{1-\frac{4m_\mu^2}{M_K^2}}\, f_K^2 M_K m_\mu^2 \left|C_{\rm SM}^K\right|^2. \tag{2.91}$$

The total branching fraction of the leptonic $K_L \to \mu^+\mu^-$ process in the $V_3(3,3,2/3)$ vector LQ model is given by

$$\mathrm{BR}(K_L \to \mu^+\mu^-) = \frac{G_F^2}{8\pi^3}\tau_{K_L}\alpha_{\rm em}^2 f_K^2 M_K m_\mu^2 |\lambda_u|^2 \sqrt{1-\frac{4m_\mu^2}{M_K^2}} \times \left|C_{\rm SM}^K + \frac{C_{10}^{\rm LQ}}{2}\right|^2, \quad (2.92)$$

and in the $V_1(3,1,2/3)$ vector LQ model,

$$\begin{aligned}\mathrm{BR}(K_L \to \mu^+\mu^-) &= \frac{G_F^2}{8\pi^3}\tau_{K_L}\alpha_{\rm em}^2 f_K^2 M_K m_\mu^2 |\lambda_u|^2 \left|C_{\rm SM}^K\right|^2 \sqrt{1-\frac{4m_\mu^2}{M_K^2}} \\ &\times \left(|P_K|^2 + |S_K|^2\right), \end{aligned} \quad (2.93)$$

where P_K and S_K are defined as

$$\begin{aligned} P_K &\equiv \frac{C_{\rm SM}^K + C_{10}^{\rm LQ} - C_{10}^{\prime\rm LQ}}{C_{\rm SM}^K} + \frac{M_K^2}{2m_\mu}\Big(\frac{m_s}{m_s+m_d}\Big)\Big(\frac{C_P^{\rm LQ} - C_P^{\prime\rm LQ}}{C_{\rm SM}^K}\Big), \\ S_K &\equiv \sqrt{1-\frac{4m_\mu^2}{M_K^2}}\frac{M_K^2}{2m_\mu}\Big(\frac{m_s}{m_s+m_d}\Big)\Big(\frac{C_S^{\rm LQ} - C_S^{\prime\rm LQ}}{C_{\rm SM}^K}\Big). \end{aligned} \quad (2.94)$$

Here the additional coefficients $C_i^{(\prime)\rm LQ}$, where $i = 10, S, P$ arise due to the vector LQ exchange's between the external fermion particles. These new coefficients are related to the LQ couplings through the relations below.

$$C_{10}^{\rm LQ} = -\frac{\pi}{G_F\alpha_{\rm em}\lambda_u}\frac{\mathrm{Re}[\lambda_{LL}^{12}\lambda_{LL}^{22\;*}]}{M^2_{V_1^{2/3}}}, \quad (2.95a)$$

$$C_{10}^{\prime\rm LQ} = -\frac{\pi}{G_F\alpha_{\rm em}\lambda_u}\frac{\mathrm{Re}[\lambda_{RR}^{12}\lambda_{RR}^{22\;*}]}{M^2_{V_1^{2/3}}}, \quad (2.95b)$$

$$C_S^{\rm LQ} = -C_P^{\rm LQ} = \frac{\pi}{2G_F\alpha_{\rm em}\lambda_u}\frac{\mathrm{Re}[\lambda_{LL}^{12}\lambda_{RR}^{22\;*}]}{M^2_{V_1^{2/3}}}, \quad (2.95c)$$

$$C_S^{\prime\rm LQ} = C_P^{\prime\rm LQ} = \frac{\pi}{2G_F\alpha_{\rm em}\lambda_u}\frac{\mathrm{Re}[\lambda_{RR}^{12}\lambda_{LL}^{22\;*}]}{M^2_{V_1^{2/3}}}. \quad (2.95d)$$

The present experimental limits on the branching ratios of the dileptonic decays of the B meson are [98]

$$\begin{aligned} &\mathrm{BR}(K_L \to e^+e^-)^{\rm Expt} = 9^{+6}_{-4} \times 10^{-12}, \\ &\mathrm{BR}(K_L \to \mu^+\mu^-)^{\rm Expt} = (6.84 \pm 0.11) \times 10^{-9}. \end{aligned} \quad (2.96)$$

If we impose chirality on the scalar leptoquarks, i.e., they couple to either left handed or right handed quarks, but not to both, then the $C_{S,P}^{(\prime)\rm LQ}$ Wilson coefficients will vanish and we get only the additional contribution of the $C_{10}^{(\prime)\rm LQ}$ Wilson coefficients to the SM.

Now comparing the theoretical and experimental branching ratios of $K_L \to \mu^+\mu^-(e^+e^-)$ decays, the allowed ranges of the vector LQ couplings for $M_{\rm LQ} = 1$ TeV are given by

$$1.3 \times 10^{-3} \ \leq \ {\rm Re}[\lambda_{LL}^{11} \lambda_{LL}^{21\,*}] \ \leq \ 2.35 \times 10^{-3}, \tag{2.97}$$
$$1.4 \times 10^{-4} \ \leq \ {\rm Re}[\lambda_{LL}^{12} \lambda_{LL}^{22\,*}] \ \leq \ 1.5 \times 10^{-4}. \tag{2.98}$$

Since the scalar and pseudoscalar coefficients are dominated by an additional multiplication factor, one can neglect the new physics contribution to the Wilson coefficient C_{10}. In Fig. 2.16, we show the allowed region in the $(C_S^{\rm LQ} \pm C_S^{\prime {\rm LQ}})$ plane, obtained from the $K_L \to e^+e^-$ (left panel) and $K_L \to \mu^+\mu^-$ (right panel) processes. From the figure one can see that for $K_L \to e^+e^-$ the allowed range of the LQ couplings are

$$-2 \times 10^{-4} \ \leq \ C_S^{\rm LQ} + C_S^{\prime {\rm LQ}} \ \leq \ 2 \times 10^{-4}, \tag{2.99}$$
$$1.25 \times 10^{-4} \ \leq \ C_S^{\rm LQ} - C_S^{\prime {\rm LQ}} \ \leq \ 2 \times 10^{-4}, \tag{2.100}$$

and for $K_L \to \mu^+\mu^-$ process

$$-6 \times 10^{-3} \ \leq C_S^{\rm LQ} + C_S^{\prime {\rm LQ}} \ \leq \ 3 \times 10^{-3}, \tag{2.101}$$
$$5 \times 10^{-5} \ \leq \ C_S^{\rm LQ} - C_S^{\prime {\rm LQ}} \ \leq \ 5.6 \times 10^{-3}. \tag{2.102}$$

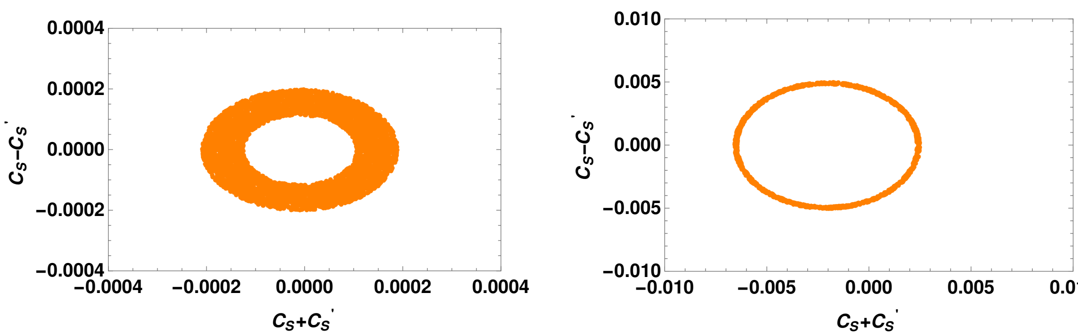

FIGURE 2.16: The allowed region of $C_S^{\rm LQ} \pm C_S^{\prime {\rm LQ}}$ Wilson coefficients from $K_L \to e^+e^-$ (left panel) and $K_L \to \mu^+\mu^-$ (right panel) processes.

2.4.6 $\tau^- \to \mu^-\gamma$ process

The constraints on the vector LQ parameter spaces from the $\tau^- \to l^-\gamma$, where $l = \mu, e$ decay modes are calculated in this subsection. The study of these radiative charged LFV processes provide hints for new physics beyond the SM. The $\tau^- \to l^-\gamma$ decay modes in scalar LQ model have been investigated in the literature [155–157]. In the Ref. [158], the authors have given the general loop formulas for the radiative decay modes. In the vector LQ model, the effective Hamiltonian responsible for $\tau^- \to \mu^-\gamma$ decay is given by

$$\mathcal{H}_{\rm eff} = e\Bigg(C_L\bar{\mu}_R\sigma^{\mu\nu}F_{\mu\nu}\tau_L + C_R\bar{\mu}_L\sigma^{\mu\nu}F_{\mu\nu}\tau_R\Bigg), \tag{2.103}$$

where the $C_{L,R}$ Wilson coefficients are expressed as

$$\begin{aligned} C_L \ &= \ \frac{N_c}{16\pi^2 M^2_{V_1^{2/3}}}\Bigg(-\frac{1}{3}\Bigg[\lambda^{33}_{LL}\lambda^{32\,*}_{LL}f_2(x_b) + \lambda^{33}_{RR}\lambda^{32\,*}_{RR}f_1(x_b) \\ &\qquad + \lambda^{33}_{LL}\lambda^{32\,*}_{RR}f_3(x_b) + \lambda^{33}_{RR}\lambda^{32\,*}_{LL}f_4(x_b)\Bigg] \\ &\quad + \frac{2}{3}\Bigg[\lambda^{33}_{LL}\lambda^{32\,*}_{LL}\bar{f}_2(x_b) + \lambda^{33}_{RR}\lambda^{32\,*}_{RR}\bar{f}_1(x_b) \\ &\qquad + \lambda^{33}_{LL}\lambda^{32\,*}_{RR}f_3(x_b) + \lambda^{33}_{RR}\lambda^{32\,*}_{LL}f_4(x_b)\Bigg]\Bigg) \\ &+ \frac{N_c}{16\pi^2 M^2_{V_3^{2/3}}}\lambda^{33}_{LL}\lambda^{32\,*}_{LL}\Bigg[-\frac{1}{6}f_2^{(3)}(x_b) + \frac{1}{3}\bar{f}_2^{\,(3)}(x_b)\Bigg], \end{aligned} \tag{2.104}$$

$$\begin{aligned} C_R \ &= \ \frac{N_c}{16\pi^2 M^2_{V_1^{2/3}}}\Bigg(-\frac{1}{3}\Bigg[\lambda^{33}_{LL}\lambda^{32\,*}_{LL}f_1(x_b) + \lambda^{33}_{RR}\lambda^{32\,*}_{RR}f_2(x_b) \\ &\qquad \lambda^{33}_{LL}\lambda^{32\,*}_{RR}f_4(x_b) + \lambda^{33}_{RR}\lambda^{32\,*}_{LL}f_3(x_b)\Bigg] \\ &\quad + \frac{2}{3}\Bigg[\lambda^{33}_{LL}\lambda^{32\,*}_{LL}\bar{f}_1(x_b) + \lambda^{33}_{RR}\lambda^{32\,*}_{RR}\bar{f}_2(x_b) \\ &\qquad \lambda^{33}_{LL}\lambda^{32\,*}_{RR}\bar{f}_4(x_b) + \lambda^{33}_{RR}\lambda^{32\,*}_{LL}\bar{f}_3(x_b)\Bigg]\Bigg) \\ &+ \frac{N_c}{16\pi^2 M^2_{V_3^{2/3}}}\lambda^{33}_{LL}\lambda^{32\,*}_{LL}\Bigg[-\frac{1}{6}f_1^{(3)}(x_b) + \frac{1}{3}\bar{f}_1^{\,(3)}(x_b)\Bigg]. \end{aligned} \tag{2.105}$$

Here $N_c = 3$ is the color factor, $x_b = m_b^2/M^2_{V_1^{2/3}}$ and the loop functions are given as [158]

$$f_1(x_b) = m_\tau \left[\frac{-5x_b^3 + 9x_b^2 - 30x_b + 8}{12(x_b-1)^3} + \frac{3x_b^2 \ln x_b}{2(x_b-1)^4}\right], \tag{2.106a}$$

$$f_2(x_b) = m_\mu \left[\frac{-5x_b^3 + 9x_b^2 - 30x_b + 8}{12(x_b-1)^3} + \frac{3x_b^2 \ln x_b}{2(x_b-1)^4}\right], \tag{2.106b}$$

$$f_3(x_b) = m_b \left[\frac{x_b^2 + x_b + 4}{2(x_b-1)^2} - \frac{3x_b \ln x_b}{(x_b-1)^3}\right], \tag{2.106c}$$

$$f_4(x_b) = -\frac{m_\tau m_\mu m_b}{m^2_{V_1^{2/3}}} \left[\frac{-2x_b^2 + 7x_b - 11}{6(x_b-1)^3} + \frac{\ln x_b}{(x_b-1)^4}\right], \tag{2.106d}$$

$$\bar{f}_1(x_b) = m_\tau \left[\frac{-4x_b^3 + 45x_b^2 - 33x_b + 10}{12(x_b-1)^3} - \frac{3x_b^3 \ln x_b}{2(x_b-1)^4}\right], \tag{2.106e}$$

$$\bar{f}_2(x_b) = m_\mu \left[\frac{-4x_b^3 + 45x_b^2 - 33x_b + 10}{12(x_b-1)^3} - \frac{3x_b^3 \ln x_b}{2(x_b-1)^4}\right], \tag{2.106f}$$

$$\bar{f}_3(x_b) = m_b \left[\frac{x_b^2 - 11x_b + 4}{2(x_b-1)^2} + \frac{3x_b^2 \ln x_b}{(x_b-1)^3}\right], \tag{2.106g}$$

$$\bar{f}_4(x_b) = \frac{m_\tau m_\mu m_b}{m^2_{V_1^{2/3}}} \left[\frac{x_b^2 - 5x_b - 6 - 6x_b(1+x_b)\ln x_b}{6(x_b-1)^3} + \frac{x_b^3 \ln x_b}{(x_b-1)^4}\right]. \tag{2.106h}$$

The branching fraction of $\tau^- \to \mu^-\gamma$ process in the vector LQ model is given by

$$\mathrm{BR}(\tau^- \to \mu^-\gamma) = \frac{\tau_\tau \left(m_\tau^2 - m_\mu^2\right)^3}{16\pi m_\tau^3} \Big[|C_L|^2 + |C_R|^2\Big]. \tag{2.107}$$

Using this expression, one can also analyze various charged LFV radiative processes like, $\tau^- \to e^-\gamma$ and $\mu^- \to e^-\gamma$ by incorporating the appropriate input parameters and LQ couplings. The present experimental limits on the branching ratios of radiative decays of τ lepton, $\tau^- \to \mu^-(e^-)\gamma$ are given by [98]

$$\begin{aligned} &\mathrm{BR}(\tau^- \to \mu^-\gamma)^{\mathrm{Expt}} < 4.4 \times 10^{-8}, \\ &\mathrm{BR}(\tau^- \to e^-\gamma)^{\mathrm{Expt}} < 3.3 \times 10^{-8}. \end{aligned} \tag{2.108}$$

For numerical evaluation, we take the particle masses and the lifetime of the τ lepton from [98]. Now comparing Eqn. (2.107) with the present experimental upper limit, the constraints on $\lambda_{LL}^{3i}\lambda_{LL}^{3j\,*}$ ($\lambda_{RR}^{3i}\lambda_{RR}^{3j\,*}$) leptoquark couplings from $\tau^- \to e^-\gamma$ (left panel) and $\tau^- \to \mu^-\gamma$ (right panel) decay processes are presented in Fig. 2.17. The allowed region of the $\lambda_{LL}^{3i}\lambda_{RR}^{3j\,*}$ ($\lambda_{RR}^{3i}\lambda_{LL}^{3j\,*}$) leptoquark couplings are shown in Fig. 2.18, for $\tau^- \to e^-\gamma$ (left panel) and $\tau^- \to \mu^-\gamma$ (right panel) processes. The predicted integrated values of the bounds on the product of vector LQ couplings are presented in Table 2.9.

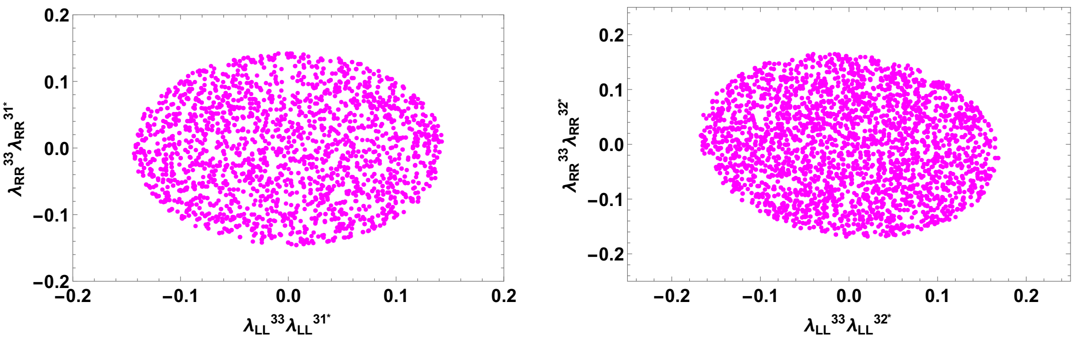

FIGURE 2.17: The constraint on $\lambda_{LL}^{33}\lambda_{LL}^{31}{}^*$ and $\lambda_{RR}^{33}\lambda_{RR}^{32}{}^*$ leptoquark couplings from $\tau^- \to e^-\gamma$ (left panel) and $\tau^- \to \mu^-\gamma$ (right panel) processes.

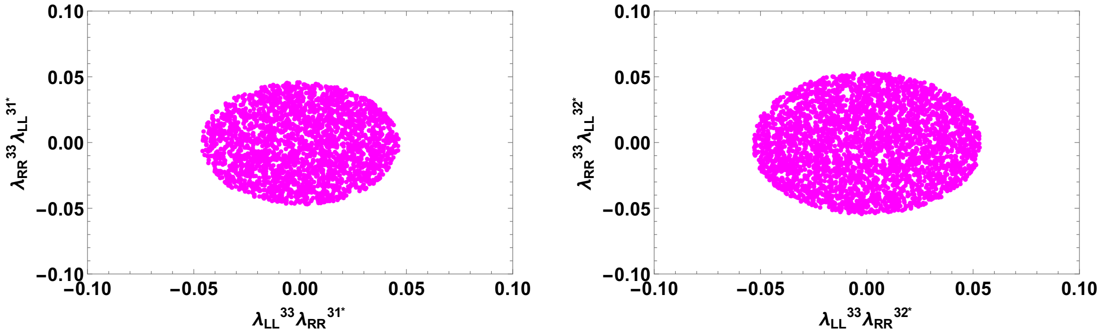

FIGURE 2.18: The constraint on $\lambda_{LL}^{33}\lambda_{RR}^{31}{}^*$ and $\lambda_{RR}^{33}\lambda_{LL}^{32}{}^*$ leptoquark couplings from $\tau^- \to e^-\gamma$ (left panel) and $\tau^- \to \mu^-\gamma$ (right panel) processes.

TABLE 2.9: Bounds on the product of vector leptoquark couplings obtained from $\tau^- \to l^-\gamma$ processes. Here $i = 1$ (2) for e (μ).

Couplings involved	$\tau^- \to e^-\gamma$ process	$\tau^- \to \mu^-\gamma$ process
$\lambda_{LL}^{33}\lambda_{LL}^{3i}{}^*$	$-0.14 \to 0.14$	$-0.16 \to 0.16$
$\lambda_{RR}^{33}\lambda_{RR}^{3i}{}^*$	$-0.14 \to 0.14$	$-0.16 \to 0.16$
$\lambda_{LL}^{33}\lambda_{RR}^{3i}{}^*$	$-0.04 \to 0.04$	$-0.05 \to 0.05$
$\lambda_{RR}^{33}\lambda_{LL}^{3i}{}^*$	$-0.04 \to 0.04$	$-0.05 \to 0.05$

2.5 Chapter summary

Leptoquarks are unique speculative gauge bosons which interact with both quark and lepton simultaneously. In recent times, they draw the attention of many particle physicist due to their unique behavior. Because of their interesting behavior, they could be the potential candidates to solve the anomalies in the flavor physics. In our work, we have investigated the phenomenology of light leptoquarks which could be seen in the current running experiments. The light leptoquarks couple chirally and diagonally with the SM fermions so that the strict bounds from FCNC processes can be avoided. Furthermore, these leptoquarks have vanishing diquark coupling, thus, they don't allow proton decay. Out of 10 possible leptoquark states, we have considered $S_2(3,2,7/6)$ and $\tilde{S}_2(3,2,1/6)$ scalar (spin=0) leptoquarks and $V_1(3,1,2/3)$ and $V_3(3,3,2/3)$ vector (spin=1) leptoquarks in our analysis, which are invariant under the SM gauge group $SU(3)_C \times SU(2)_L \times U(1)_Y$. The bound on scalar leptoquark couplings are obtained by using the branching ratios of $B_{s,d} \to l^+l^-$, $\bar{B} \to X_s l^+l^-$ processes and the experimental data on $B_s^0 - \bar{B}_s^0$ oscillation. The vector leptoquark couplings are constrained by using various leptonic/semileptonic B (K) decay processes such as $B_s \to l^+l^-$, $\bar{B} \to X_s l^+l^-$, $B_u^+ \to l^+\nu_l$, $K_L \to l^+l^-$ and $\tau^- \to l^-\gamma$. At present, LHCb, CMS and ATLAS experiments are dedicately looking for the signature of leptoquarks. These experiments have put the upper limit on different generations of leptoquarks masses. If experiments will succeed to discover leptoquarks, then it will definitely open a new era in the high energy physics.

Chapter 3

An analysis of rare semileptonic $\bar{B} \to \bar{K} l^+ l^-$ and $\bar{B} \to (\bar{K}^{(*)}, X_s) \nu \bar{\nu}$ processes with scalar leptoquark

Recently the LHCb experiments, as well as the B factories have studied various promising channels involving the $b \to s$ flavor changing neutral current interactions. The particularly important decay channels are the rare semileptonic decays $\bar{B} \to \bar{K} l^+ l^- (\nu\bar{\nu})$. In the SM, FCNC transitions occur via either one loop penguin or box diagrams. Since these processes involve only electroweak loop diagrams, the possibility of the presence of new particles inside the loop is more. In addition, these processes also strongly suffer from both helicity and GIM suppression, hence, they are very rare in the SM. However, they can occur at tree level in various extensions of the model and are considered to be ideal testing ground to look for new physics. In this chapter, we would like to investigate the $\bar{B} \to \bar{K} l^+ l^- (\nu\bar{\nu})$ decay processes in the scalar LQ model. Due to the presence of charmonium resonance in the intermediate q^2 region around $q^2 \sim (m_{\psi}^2,\ m_{\psi'}^2)$, the theoretical prediction of various observables of $\bar{B} \to \bar{K} l l$ processes in this region is very difficult. Therefore, these processes are generally studied in the high and low recoil limits. However, the analysis of semileptonic B decay processes with a neutrino pair $(\nu\bar{\nu})$ in the final state can be performed in the full q^2 region without any such of difficulty. The SM does not have any intermediate bosons which can decay to dineutrino, thus, there is no long distance QCD contribution to the $\bar{B} \to (\bar{K}^{(*)}, X_s) \nu\bar{\nu}$ processes.

3.1 $\bar{B} \to \bar{K} l^+ l^-$ processes

In this section, we consider the semileptonic decay processes $\bar{B} \to \bar{K} l^+ l^-$, which are mediated by the quark level transition $b \to s l^+ l^-$ and hence, they constitute a suitable tool to look for new physics. In this chapter, we will study these processes in the large recoil region ($1 \le q^2 \le 6$ GeV^2) in order to be well below the radiative tail of the charmonium resonances, using the QCD factorization (QCDf) approach [58, 159, 160]. Though the experimental measurement on most of the physical observables of $\bar{B} \to \bar{K} l^+ l^-$ processes are in accordance with the SM results, still some observables have appreciable deviations. LHCb has measured the branching ratio of $B^+ \to K^+ \mu^+ \mu^-$ process in the large recoil region, the updated result is [69]

$$\text{BR}\left(B^+ \to K^+ \mu^+ \mu^-\right)^{\text{Expt}} = (1.19 \pm 0.03 \pm 0.06) \times 10^{-7}, \tag{3.1}$$

slightly lower than the SM predicted values [161–163]

$$\text{BR}\left(B^+ \to K^+ \mu^+ \mu^-\right)^{\text{SM}} = \left(1.75^{+0.60}_{-0.29}\right) \times 10^{-7}. \tag{3.2}$$

However, the branching ratio of $B^+ \to K^+ e^+ e^-$ process [98]

$$\text{BR}\left(B^+ \to K^+ e^+ e^-\right)^{\text{Expt}} = (5.5 \pm 0.7) \times 10^{-7}, \tag{3.3}$$

is in good agreement with the SM prediction, though the error is large.

All the charged leptons in the SM behave equally except the heirachy in their masses. The electroweak interactions of all the three families of leptons with the vector gauge bosons are alike, which is called lepton universality. In this formalism, the branching ratio of $B^+ \to K^+ l^+ l^-$ processes, where $l = \mu, e$ should be equal. Hence, the ratio of the branching fractions of these two decays [164]

$$R_K = \frac{\text{BR}\left(B^+ \to K^+ \mu^+ \mu^-\right)}{\text{BR}\left(B^+ \to K^+ e^+ e^-\right)}, \tag{3.4}$$

is a measure of lepton universality. The experimental measured value of R_K in the dilepton invariant mass squared bin $(1 < q^2 < 6)$ GeV^2 is [39]

$$R_K^{\text{Expt}}|_{q^2 \in [1,6]\ \text{GeV}^2} = 0.745^{+0.090}_{-0.074} \pm 0.036. \tag{3.5}$$

Combining the statistical and systematic uncertainties in quadrature, this observation corresponds to a 2.6σ deviation from its SM prediction $R_K^{\text{SM}} = 1.0003 \pm 0.0001$ [164], where corrections of order α_s and $(1/m_b)$ are included. In contrast to the anomaly in the rare decay $\bar{B} \to \bar{K}^* \mu^+\mu^-$, which is affected by unknown power corrections, the ratio R_K is theoretically clean and this might be a sign of lepton flavor non-universal physics.

Besides the above anomalies, another promising observable for NP search is isospin asymmetry, which is defined as the difference of decay rate of neutral (B^0) and charged (B^+) decays of B meson to a K meson and dileptons. Mathematically,

$$A_I = \frac{d\Gamma(B^0 \to K^0\mu^+\mu^-) - d\Gamma(B^+ \to K^+\mu^+\mu^-)}{d\Gamma(B^0 \to K^0\mu^+\mu^-) + d\Gamma(B^+ \to K^+\mu^+\mu^-)}. \tag{3.6}$$

This asymmetry arises due to the emission of a photon from the spectator quark. The decay rates of these processes are directly proportional to the charge of corresponding spectator quark. The u and d are respectively the spectator quarks of $B^+ \to K^+\mu^+\mu^-$ and $B^0 \to K^0\mu^+\mu^-$ decay processes. Since u and d are interconnected by the $SU(2)_L$ symmetry, so isospin symmetry is expected for this process. However, due to the difference in the charge of up and down quark, the value of A_I deviate from zero in the negative direction. The measurement of isospin asymmetry in $B \to K\mu^+\mu^-$ process by LHCb experiment [165] with a 1 fb^{-1} data set gave a negative deviation from zero at the level of 4σ taking into account the entire q^2-spectrum. The isospin asymmetry in $B \to Kll$ is expected to be vanishingly small in the SM and hence, the measured asymmetry provides another smoking gun signal for new physics. However, the current data on isospin symmetry is consistent with the SM prediction. The observation of above anomalies provide the indirect hint for the presence of NP, thus motivate us to study these processes in the LQ model.

The semileptonic $b \to sll$ decay modes have only contribution from $\mathcal{O}_{7,9,10}$ operators. The brief discussion on the required effective Hamiltonian and operators for semileptonic decay processes in the SM are presented in chapter 1. Semileptonic decay modes have both lepton and quark parts. The theoretical computation of leptonic part is very trivial. Whereas the hadronic part includes the form factors ($F_{0,1,T}$), which have QCD corrections, thus, need to be computed using any non-perturbative methods. The hadronic matrix elements can be computed by using the form factor relation (1.53). In the large recoil region, the energy of the kaon (E_K) is large compared to the typical size of hadronic binding energies (Λ_{QCD}) and the dilepton invariant mass squared q^2 is low. As a consequence, in this region the virtual photon exchange between the hadronic part and the dilepton pair, as well as the hard gluon scattering can be treated in an expansion in $1/E_K$ [164], using either QCD factorization [58, 160] or soft collinear effective theory [166–168]. At leading order in the $1/E_K$ expansion, all the form factors $F_{0,1,T}(q^2)$ can be related to a single form factor $F_1(q^2)$. Within the QCDf approach, including subleading corrections, the other form factors can be written as [164]

$$\begin{aligned}
\frac{F_0}{F_1} &= \frac{2E_K}{M_B}\left[1 + \mathcal{O}(\alpha_s) + \mathcal{O}\left(\frac{q^2}{M_B^2}\sqrt{\frac{\Lambda_{QCD}}{E_K}}\right)\right], \\
\frac{F_T}{F_1} &= \frac{M_B + M_K}{M_B}\left[1 + \mathcal{O}(\alpha_s) + \mathcal{O}\left(\sqrt{\frac{\Lambda_{QCD}}{E_K}}\right)\right], \qquad (3.7)
\end{aligned}$$

where M_K is the mass of K meson. Thus, only one soft form factor $F_1(q^2)$ appears in the $B \to K$ transition amplitude due to the symmetry relations in the large energy limit of QCD [159, 169]. The transition amplitude for the process $B \to K l^+ l^-$ can be written as [164]

$$\begin{aligned}
\mathcal{M}\left(\bar{B}(p_B) \to K(p_K)\bar{l}l\right) &= i\frac{G_F \alpha_{\rm em}}{\sqrt{2}\pi} V_{tb} V_{ts}^* F_1(q^2) \\
&\quad \left[F_V p_B^\mu (\bar{l}\gamma_\mu l) + F_A p_B^\mu (\bar{l}\gamma_\mu \gamma_5 l) + F_P (\bar{l}\gamma_5 l)\right], \qquad (3.8)
\end{aligned}$$

where the coefficients F_i, $i = V, A, P$ are defined as

$$\begin{aligned}
F_V &= C_9^{\rm eff} + \frac{2m_b M_B}{q^2} C_7^{\rm eff}, \\
F_A &= C_{10}^{\rm SM}, \\
F_P &= m_l C_{10}^{\rm SM}\Big[\frac{M_B^2 - M_K^2}{q^2}\Big(\frac{F_0(q^2)}{F_1(q^2)} - 1\Big) - 1\Big]. \qquad (3.9)
\end{aligned}$$

Here m_l is the charged lepton mass and the b quark mass is denoted by m_b. p_B and p_K are respectively the momenta of B and K mesons and $q^2 = (p_B - p_K)^2$ is the momentum transfer between the initial and final particles. The $C_{7,9}^{\rm eff}$ and $C_{10}^{\rm SM}$ are the SM Wilson coefficients which are calculated at the next-to-next-leading order (NNLO) by matching the full theory to the effective theory at the electroweak scale and, subsequently solving the renormalization group equation to run them down to the b-quark mass scale. More explicitly, $C_9^{\rm eff} = C_9^{\rm SM} + Y(q^2)$, where the function $Y(q^2)$ denotes the perturbative part coming from the one loop matrix elements of the four quark operators and is given in Ref. [160].

With Eqn. (3.8), the double differential decay rate with respect to q^2 and $\cos\theta$ for the lepton flavor l is given as [164]

$$\frac{d^2\Gamma_l}{dq^2 d\cos\theta} = a_l(q^2) + b_l(q^2)\cos\theta + c_l(q^2)\cos^2\theta\,, \qquad (3.10)$$

where the $a_l(q^2),\ b_l(q^2),$ and $c_l(q^2)$ functions in terms of the F_i coefficients are given as

$$\begin{aligned} a_l(q^2) &= \Gamma_0 \sqrt{\lambda\left(M_B^2, M_K^2, q^2\right)} \beta_l F_1^2 \Big[q^2 |F_P|^2 + \frac{\lambda\left(M_B^2, M_K^2, q^2\right)}{4} (|F_A|^2 + |F_V|^2) \\ &+ 2m_l (M_B^2 - M_K^2 + q^2) \mathrm{Re}(F_P F_A^*) + 4m_l^2 M_B^2 |F_A|^2 \Big] , \\ b_l(q^2) &= 0, \\ c_l(q^2) &= -\Gamma_0 \sqrt{\lambda\left(M_B^2, M_K^2, q^2\right)} \beta_l^3 F_1^2 \frac{\lambda\left(M_B^2, M_K^2, q^2\right)}{4} \left(|F_A|^2 + |F_V|^2\right), \end{aligned} \tag{3.11}$$

with

$$\Gamma_0 = \frac{G_F^2 \alpha_{\rm em}^2 |V_{tb} V_{ts}^*|^2}{2^9 \pi^5 M_B^3} , \qquad \beta_l = \sqrt{1 - 4m_l^2/q^2} , \tag{3.12}$$

and

$$\lambda\left(M_B^2, M_K^2, q^2\right) = M_B^4 + M_K^4 + q^4 - 2(M_B^2 M_K^2 + M_B^2 q^2 + M_K^2 q^2). \tag{3.13}$$

The kinematic region of the physical parameters in these processes are given by

$$4m_l^2 \le q^2 \le (M_B - M_K)^2 , \qquad -1 \le \cos\theta \le 1. \tag{3.14}$$

The forward-backward asymmetry is an another useful physical observables to probe NP, which is defined as

$$\begin{aligned} A_{FB}(q^2) &= \left[\int_0^1 d\cos\theta \frac{d^2\Gamma}{dq^2 d\cos\theta} - \int_{-1}^0 d\cos\theta \frac{d^2\Gamma}{dq^2 d\cos\theta} \right] \Big/ \frac{d\Gamma}{dq^2} \\ &= \frac{b_l(q^2)}{a_l(q^2) + c_l(q^2)/3}. \end{aligned} \tag{3.15}$$

The $b_l(q^2)$ function is directly proportional to the $C_{S,P}^{(\prime)},\ C_{T,T_5}$ Wilson coefficients, thus the forward-backward asymmetry is zero in the SM. Since the $S_2(3, 2, 7/6)$ scalar LQ does not provide any pseudo(scalar) coefficients, so it doesn't affect the forward-backward asymmetry parameter.

One can also study a unique parameter called as the flat term

$$F_H^l(q^2) = \frac{a_l(q^2) + c_l(q^2)}{a_l(q^2) + c_l(q^2)/3}, \tag{3.16}$$

where the hadronic uncertainties are reduced due to cancellation between the numerator and denominator. It should be noted that the lepton mass suppression of $(a_l + c_l)$ follows as $(F_H^l)^{\rm SM} \propto m_l^2$, hence, it vanishes in the limit $m_l \to 0$.

With these formulae at hand, we now proceed for numerical estimation. To make predictions for SM observables, or to extract information about potentially new short distance physics, one should require the knowledge of associated hadronic form factors. For this purpose we use value of the form factors $F_1(q^2)$ calculated in the light cone sum rule approach [170], where the q^2 dependence is given by simple fits as

$$F_1(q^2) = \frac{r_1}{1 - q^2/m_{\rm fit}^2} + \frac{r_2}{\left(1 - q^2/m_{\rm fit}^2\right)^2}, \tag{3.17}$$

and the values of the parameters used are taken from [170]. For low recoil limit, we use the following parametrization for the q^2 dependence of form factors $F_{0,1,T}(q^2)$ [162, 171]

$$F_i(q^2) = \frac{F_i(0)}{1 - q^2/m_{res,i}^2}\left[1 + b_1^i\Big(z(q^2) - z(0) + \frac{1}{2}\left(z^2(q^2) - z^2(0)\right)\Big)\right], \tag{3.18}$$

with

$$z(q^2) = \frac{\sqrt{\tau_+ - q^2} - \sqrt{\tau_+ - \tau_0}}{\sqrt{\tau_+ - q^2} + \sqrt{\tau_+ - \tau_0}}, \tag{3.19}$$

and

$$\tau_0 = \sqrt{\tau_+}\left(\sqrt{\tau_+} - \sqrt{\tau_+ - \tau_-}\right), \qquad \tau_\pm = \left(M_B + M_K\right)^2. \tag{3.20}$$

The values of $F_i(0)$ and b_1^i are taken from [162]. The particle masses, lifetime of B meson, and the decay constants are taken from [98], and the values of the SM Wilson coefficients C_i's used in this analysis are listed in Table 3.1 [172]. For the CKM matrix elements we use the Wolfenstein parametrization with the values $A = 0.814^{+0.023}_{-0.024}$, $\lambda = 0.22537 \pm 0.00061$, $\bar{\rho} = 0.117 \pm 0.021$ and $\bar{\eta} = 0.353 \pm 0.013$ [98]. The values of the quark masses used in our analysis are as follows. The b-quark mass used in $\mathcal{T}_P$ and F_V is the potential subtracted (PS) mass $m_{\rm PS}(\mu_f)$ at the factorization scale $\mu_f \sim \sqrt{\Lambda_{QCD} m_b}$ and is denoted by m_b. The function $Y(q^2)$ is evaluated by using the pole mass m_b^{pole}, and its relation to the PS mass is given as $m_b^{pole} = m_b^{PS}(\mu_f) + 4\alpha_s \mu_f/3\pi$. The quark masses (in GeV) used are m_b=4.6, m_c=1.4, and the fine structure coupling constant $\alpha_{\rm em} = 1/130$.

TABLE 3.1: The SM Wilson coefficients evaluated at the scale $\mu = 4.6$ GeV [172].

C_1	C_2	C_3	C_4	C_5	C_6
-0.3001	1.008	-0.0047	-0.0827	0.0003	0.0009
$C_7^{\rm eff}$	$C_8^{\rm eff}$	C_9	C_{10}		
-0.2969	-0.1642	4.2607	-4.2453		

In the LQ model, these processes will receive additional contributions arising from the

LQ exchange and hence, the Wilson coefficients $C_{9,10}$ will receive additional contributions $C_{9,10}^{\rm LQ}$ as well as new Wilson coefficients $C_{9,10}^{\prime \rm LQ}$ associated with the chirally flipped operators $\mathcal{O}_{9,10}^{\prime}$ will also be present, as already discussed in chapter 2. Mathematically,

$$C_9^{\rm total} = C_9^{\rm eff} + C_9^{\rm LQ} + C_9^{\prime \rm LQ}, \quad C_{10}^{\rm total} = C_{10}^{\rm SM} + C_{10}^{\rm LQ} + C_{10}^{\prime \rm LQ}. \tag{3.21}$$

In section 2.3 of chapter 2, we already discuss the bounds on these new Wilson coefficients obtained from the constraint on r (2.43) which has been extracted from the experimental results on $\text{BR}(B_s \to \mu^+\mu^-)$, $\text{BR}(\bar{B} \to X_s \mu^+\mu^-)$ and $B_s^0 - \bar{B}_s^0$ mixing. Thus, for the LQs S_2 and $\tilde{S}_2$, we obtain the value of $r \lesssim 0.35$ for $\pi/2 \le \phi^{\rm LQ} \le 3\pi/2$, which can be translated with Eqns. (2.38) and (2.43) to give the value of the new Wilson coefficients as

$$\begin{aligned} |C_9^{\rm LQ}| = |C_{10}^{\rm LQ}| \le |r\ C_{10}^{\rm SM}| \qquad & \text{for } S_2(3,2,7/6), \\ |C_9^{\prime\ \rm LQ}| = |C_{10}^{\prime\ \rm LQ}| \le |r\ C_{10}^{\rm SM}| \qquad & \text{for } \tilde{S}_2(3,2,1/6)\ . \end{aligned} \tag{3.22}$$

Since both $B_s \to l^+l^-$ and $\bar{B} \to \bar{K} l^+ l^-$ processes are mediated by $b \to sll$ quark level transitions, these constraints can be used to analyze various angular observables of $\bar{B} \to \bar{K} l^+ l^-$ processes. Using these values, we show the variation of differential branching ratios of $B^0 \to K^0 \mu^+\mu^-$ and $B^+ \to K^+\mu^+\mu^-$ processes with low q^2 in the left and right panel of Fig. 3.1. In this figure, the $S_2(3,2,7/6)$ LQ contributions are shown in red color bands, the blue dashed lines are for the SM. Here the red bands are obtained by using the upper bound of r parameter ($r = 0.35$) and varying the phase in the $\pi/2 \le \phi^{\rm LQ} \le 3\pi/2$ range. For $r = 0$ (lower bound), there is no contribution from LQ and the branching ratio will consistent with the SM. The bin-wise experimental values are shown in black in $B \to K\mu\mu$ process. We observe that our prediction on branching fractions are slightly larger than the experimental data. For the calculation of the $B^+ \to K^+ e^+ e^-$, we have used the constraint on the LQ couplings obtained from $\bar{B} \to X_s e^+ e^-$ inclusive decay rate. In the $q^2 \in [1,6]$ GeV^2 regime, the integrated values of the branching ratios of $B \to K\mu^+\mu^-(e^+e^-)$ processes are given in Table 3.2.

For $B \to K\tau\tau$ processes we use the limits on the LQ couplings extracted from $B_s \to \tau^+\tau^-$ processes. With these input parameters, the differential branching ratios for $\bar{B} \to \bar{K} e^+ e^-$ (top left panel), $\bar{B} \to \bar{K}\mu^+\mu^-$ (top right panel) and $\bar{B} \to \bar{K}\tau^+\tau^-$ (bottom panel) processes with respect to high $q^2 \ge 14.18$ GeV^2, both in the SM and in the S_2 leptoquark model are shown in Fig. 3.2 and corresponding numerical values are presented in Table 3.2. The gray bands in these plots correspond to the uncertainties arising in the SM due to the uncertainties associated with the CKM matrix elements and the hadronic form factors. Since the LQ couplings are more tightly constrained in $b \to s\mu\mu$ transitions, the deviations of the branching ratios in the LQ model from the corresponding SM values

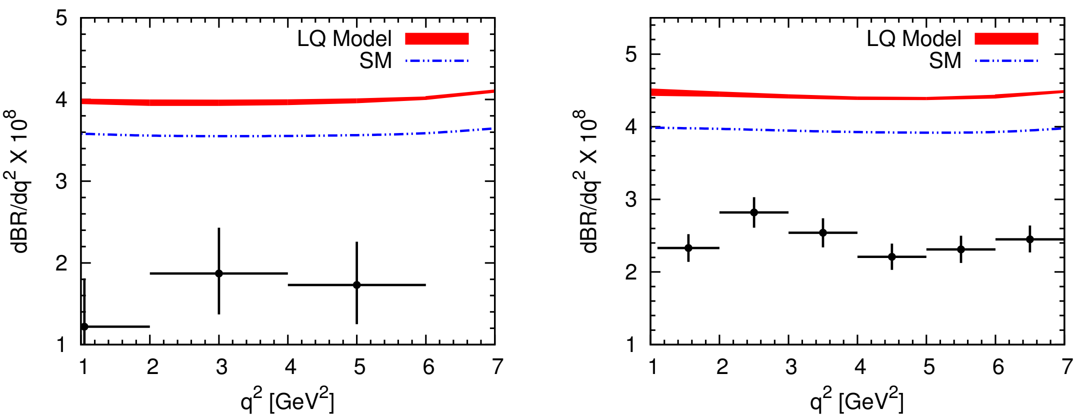

FIGURE 3.1: The branching ratios of $B^0 \to K^0 \mu^+\mu^-$ (left panel) and $B^+ \to K^+\mu^+\mu^-$ (right panel) processes in the high recoil limit. Here the blue dotted lines stand for the SM and the red bands represent the contributions from LQ. The binwise 1σ experimental data are shown by black plots.

are found to be small. For $B \to Kee$ and $B \to K\tau\tau$ these deviations are found to be significantly large. The integrated branching ratio for $B^0 \to K^0\mu^+\mu^-$ process in the range $q^2 \in [15, 22]$ GeV^2 has been measured by the LHCb Collaboration [69] and is given as

$$\mathrm{BR}\left(B^0 \to K^0\mu^+\mu^-\right) = (6.7 \pm 1.1 \pm 0.4) \times 10^{-8}. \tag{3.23}$$

Our predicted integrated value of the branching ratio of $B^0 \to K^0\mu^+\mu^-$ process in the $q^2 \in [15, 22]$ GeV^2 region is

$$\begin{aligned}
\mathrm{BR}\left(B^0 \to K^0\mu^+\mu^-\right) &= (8.35 \pm 0.5) \times 10^{-8}, \qquad \mathrm{SM} && (3.24)\\
&= (8.34 - 9.26) \times 10^{-8}, \qquad S_2(3, 2, 7/6)\ \mathrm{LQ}. && (3.25)
\end{aligned}$$

The predicted values of the branching ratios are slightly higher than the central measured value but consistent with its 1σ range.

The q^2 variation of the isospin asymmetry parameter of $B \to K\mu\mu$ process in the $q^2 \in [1, 6]$ GeV^2 regime is presented in Fig. 3.3 and the numerical value is given in Table 3.2. The plots in Fig. 3.4 explain the violation of lepton universality in $B^+ \to K^+l^+l^-$ process. Here the left panel represents the variation of $R_K(q^2)$ ratio in the low q^2 region and the right panel is for the low recoil limit. Table 3.2 contains the q^2 integrated values of lepton universality parameter. We found that in the scalar LQ model the lepton universality parameter deviates remarkably from the SM in both the regions and the experimental value can be accommodated. Our results confirm the violation of lepton universality in this process. The flat term for $B \to Ke^+e^-$ process has been found to be negligibly small ($F_H^e \sim \mathcal{O}(10^{-7})$) due to tiny electron mass. For the $B \to K\mu\mu$ process,

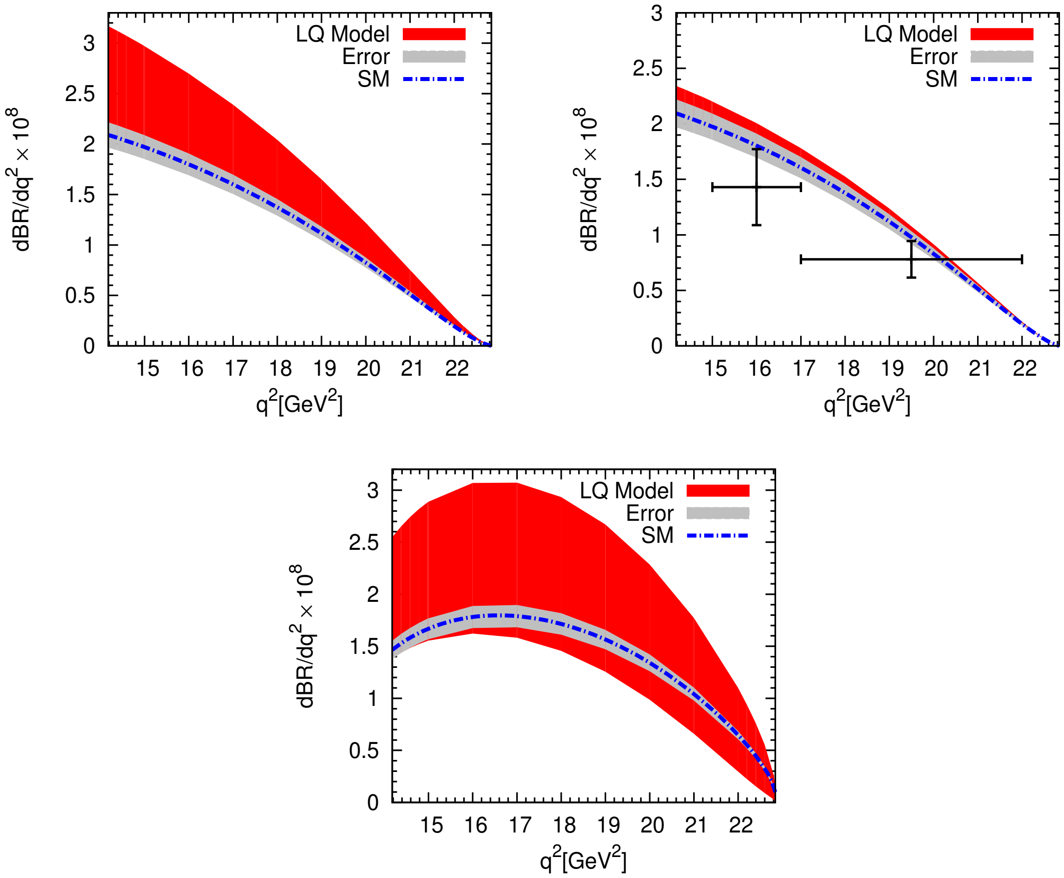

FIGURE 3.2: The branching ratios of $\bar{B} \to \bar{K}^0 e^+ e^-$ (top left panel), $\bar{B} \to \bar{K}\mu^+\mu^-$ (top right panel) and $\bar{B} \to \bar{K}\tau^+\tau^-$ (bottom panel) processes versus q^2 in the low recoil limit.

the flat term has also no deviation from the SM even in the presence of LQ. However, the process having tau lepton in the final state has significant deviation from the SM

$$\begin{aligned} &F_H^\mu|_{\rm SM} = 7.5 \times 10^{-3}, \quad F_H^\mu|_{\rm LQ} = (7.4 - 7.55) \times 10^{-3}, \\ &F_H^\tau|_{\rm SM} = 0.89, \qquad\qquad F_H^\tau|_{\rm LQ} = 0.8 \to 1.38. \end{aligned} \tag{3.26}$$

3.2 $\bar{B} \to \bar{K}^{(*)}\nu\bar{\nu}$ processes

The rare semileptonic $\bar{B} \to \bar{K}^{(*)}\nu\bar{\nu}$ processes driven by the $b \to s\nu\bar{\nu}$ transitions are studied in this section. Since these processes are related with $\bar{B} \to \bar{K}^{(*)}\mu\mu$ processes by $SU(2)_L$ symmetry, the analysis of these processes in the context of some NP models are very much crucial. The upper limit on the branching ratios of exclusive decay processes, $\bar{B} \to \bar{K}^{(*)}\nu\bar{\nu}$ are measured by the LHCb Collaborations. The experimental information

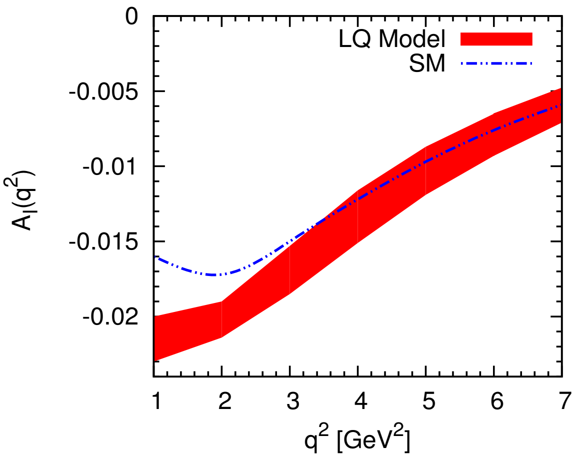

FIGURE 3.3: The plot for isospin asymmetry of $B \to K\mu\mu$ process versus low q^2 in the scalar leptoquark model.

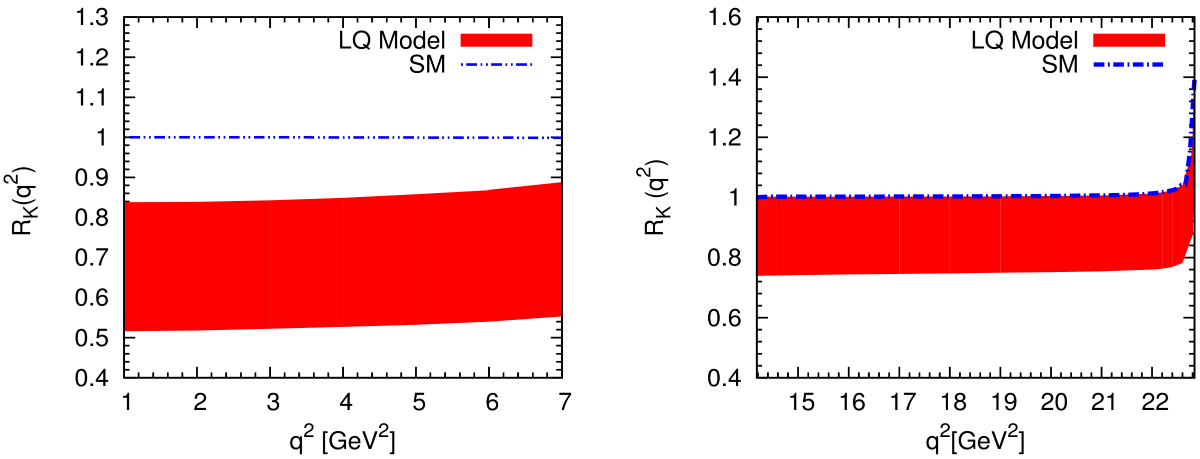

FIGURE 3.4: The variation of R_K ratio with respect to low q^2 (left panel) and high q^2 (right panel) in the S_2 LQ model.

about this exclusive decay process can be described by the double differential decay distribution. In order to compute the decay rate, we must have the idea about the matrix element of the effective Hamiltonian (1.50) between the initial B meson and the final particles. The differential decay rate of these processes with respect to the kinematic parameter s_B, where $s_B = q^2/M_B^2$ can be obtained by using Eqns. (1.50), (1.53) and (1.55). From Eqns. (2.11, 2.12), one can see that $\tilde{S}_2(3, 2, 1/6)$ scalar LQ has coupling with the down type quarks and neutral leptons, thus can contribute nonzero C_R coupling to the SM. Including the LQ contributions, the total decay rate of $\bar{B} \to \bar{K}\nu\bar{\nu}$ process is given by [173]

$$\frac{d\Gamma\left(\bar{B} \to \bar{K}\nu\bar{\nu}\right)}{ds_B} = \frac{G_F^2 \alpha_{\rm em}^2}{256\pi^5} |V_{ts}^* V_{tb}|^2 M_B^5 \lambda^{3/2}(s_B, \tilde{M}_K^2, 1) |F_1(s_B)|^2 \left| C_L^\nu + C_R^{\rm LQ} \right|^2, \quad (3.27)$$

TABLE 3.2: Our predicted numerical values of the branching ratios, isospin asymmetry and the lepton universality parameter in both the high and low recoil limit in the $(3, 2, 7/6)$ scalar leptoquark model.

q^2 bin	Observables	SM Predictions	Values in LQ model
low q^2	$\text{BR}(B^+ \to K^+ e^+ e^-)$	1.82×10^{-7}	$(2.3 - 3.7) \times 10^{-7}$
	$\text{BR}(B^+ \to K^+ \mu^+ \mu^-)$	1.99×10^{-7}	$(2.2 - 2.3) \times 10^{-7}$
	$\text{BR}(\bar{B}^0 \to \bar{K}^0 \mu^+ \mu^-)$	1.82×10^{-7}	$(2.04 - 2.16) \times 10^{-7}$
	$\langle A_I \rangle$	-0.03	$-0.036 \to -0.024$
	$\langle R_K \rangle$	1.09	$0.62 - 0.96$
high q^2	$\text{BR}(\bar{B} \to \bar{K}^0 e^+ e^-)$	(1.005 ± 0.06)	$(1.004 - 1.5)$
	$\text{BR}(\bar{B}^0 \to \bar{K}^0 \mu^+ \mu^-)$	(1.01 ± 0.06)	$(1.01 - 1.12)$
	$\langle R_K \rangle$	1.0035	$0.75 - 1.00$

where $\tilde{M}_i = M_i/M_B$. Since, one can use any generation of neutrino to probe NP, the decay rate has been multiplied with an extra factor 3 due to the sum over all neutrino flavors. In contrast to $\bar{B} \to \bar{K} l^+ l^-$ process, which has dominant charmonium resonance background from $\bar{B} \to \bar{K}(J/\psi) \to K l^+ l^-$, there are no such analogous long-distance QCD contributions in this case as there are no intermediate states which can decay into two neutrinos. For the $b \to s\nu\bar{\nu}$ LQ couplings, we use the values as we used for $b \to s\mu\mu$ as these two processes are related by $SU(2)_L$ symmetry. The numerical values of $B \to K$ form factor evaluated in the LCSR are taken from [170]. Now using all the necessary input parameters from [98], the plot for the branching ratio of $\bar{B} \to \bar{K}\nu\bar{\nu}$ process is given in the left panel of Fig. 3.5. Here the branching ratio deviate remarkabley due to the addition of LQ couplings. The predicted numerical value is given in Table 3.3, which is well below the measured experimental upper limit [98].

Due to the non-detection of the two neutrinos, experimentally we can't distinguish between the transverse polarization of K^* meson, so the decay rate will be the addition of both longitudinal and transverse polarizations. The double differential decay rate of $\bar{B} \to \bar{K}^* \nu\bar{\nu}$ process with respect to s_B and $\cos\theta$ is given by [59, 174]

$$\frac{d^2\Gamma\left(\bar{B} \to \bar{K}^* \nu\bar{\nu}\right)}{ds_B d\cos\theta} = \frac{3}{4}\frac{d\Gamma_T}{ds_B}\sin^2\theta + \frac{3}{2}\frac{d\Gamma_L}{ds_B}\cos^2\theta, \tag{3.28}$$

where

$$\frac{d\Gamma_L}{ds_B} = 3M_B^2|A_0|^2, \qquad \frac{d\Gamma_T}{ds_B} = 3M_B^2(|A_\perp|^2 + |A_\parallel|^2), \tag{3.29}$$

are respectively the longitudinal and transverse decay rate of this process and the transversity amplitudes $(A_{\perp,\parallel,0})$ in terms of form factors and Wilson coefficients are defined as

$$A_\perp(s_B) = 2N\sqrt{2}\sqrt{\lambda(1, \tilde{M}^2_{K^*}, s_B)}\left(C^\nu_L + C^{\rm LQ}_R\right)\frac{V(s_B)}{1+\tilde{M}_{K^*}}, \tag{3.30}$$

$$A_\parallel(s_B) = -2N\sqrt{2}\left(1+\tilde{M}_{K^*}\right)\left(C^\nu_L - C^{\rm LQ}_R\right)A_1(s_B), \tag{3.31}$$

$$\begin{aligned} A_0(s_B) = & -\frac{N}{\tilde{M}_{K^*}\sqrt{s_B}}\left(C^\nu_L - C^{\rm LQ}_R\right)\Bigg[\left(1-\tilde{M}^2_{K^*}-s_B\right)\left(1+\tilde{M}_{K^*}\right)A_1(s_B) \\ & -\lambda(1, \tilde{M}^2_{K^*}, s_B)\frac{A_2(s_B)}{1+\tilde{M}_{K^*}}\Bigg], \end{aligned} \tag{3.32}$$

with

$$N = V_{tb}V^*_{ts}\sqrt{\frac{G_F^2\alpha^2_{\rm em}M_B^3 s_B \lambda^{1/2}(1, \tilde{M}^2_{K^*}, s_B)}{3\times 2^{10}\pi^5}}. \tag{3.33}$$

The K^* meson longitudinal and transverse polarization fraction is given as [59]

$$F_{L,T} = \frac{d\Gamma_{L,T}/ds_B}{d\Gamma/ds_B}. \tag{3.34}$$

Using the $F_{L,T}$ observables, one can also define a new useful observables know as K^* polarization factor as

$$\alpha_{K^*} = \frac{2F_L}{F_T} - 1. \tag{3.35}$$

The transverse asymmetry parameters are given as [175, 176]

$$A^{(1)}_T = \frac{-2{\rm Re}(A_\perp A^*_\parallel)}{|A_\perp|^2 + |A_\parallel|^2}, \qquad A^{(2)}_T = \frac{|A_\perp|^2 - |A_\parallel|^2}{|A_\perp|^2 + |A_\parallel|^2}. \tag{3.36}$$

However, one can not extract $A^{(1)}_T$ from the full angular distribution of $\bar{B} \to \bar{K}^*\nu\bar{\nu}$, as it is not invariant under the symmetry of the distribution function and requires measurement of the neutrino polarization. So it can not be measured experimentally at B factories or in LHCb. The transverse asymmetry $A^{(2)}_T$ is theoretically clean and could be measurable in Belle II.

For numerical evaluation we use the q^2 dependence of the $B \to K^*$ form factors $V(q^2),\ A_1(q_2),\ A_2(q^2)$ from [177, 178]. The variation of the branching ratio of $\bar{B} \to \bar{K}^*\nu\bar{\nu}$ with respect to the neutrino invariant mass, s_B is shown in the right panel of Fig. 3.5. Fig. 3.6 contains the longitudinal and transverse polarizations of K^* verses s_B. The polarization factor and the transverse asymmetry variation with respect to s_B in the full region are shown in Fig. 3.7. Although there is certain deviation found between the SM and LQ model predictions for the branching fraction, but no such noticeable deviations found between the SM and LQ predictions for the longitudinal/transverse polarizations, transverse asymmetry parameters $A_T^{(2)}$. The predicted integrated values of branching ratio and the experimental upper limit over the range $s_B \in [0, 0.69]$ are presented in Table 3.3.

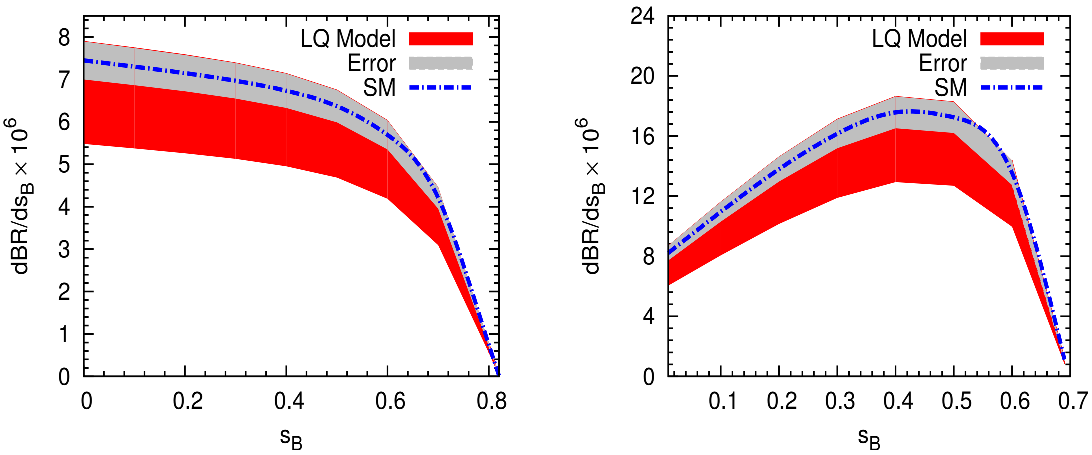

FIGURE 3.5: The branching ratio of $\bar{B} \to \bar{K}\nu\bar{\nu}$ (left panel) and $\bar{B} \to \bar{K}^*\nu\bar{\nu}$ (right panel) with respect to s_B in the scalar LQ model.

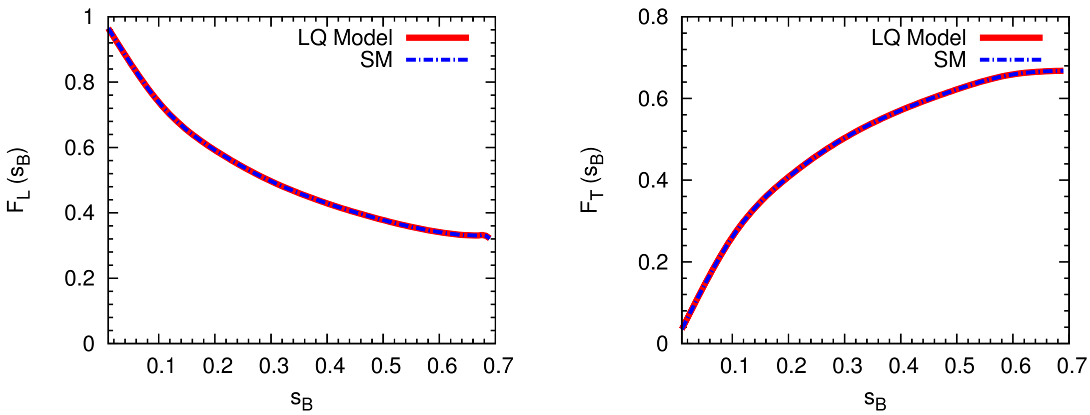

FIGURE 3.6: The variation of longitudinal (left panel) and transverse (right panel) polarization of K^* with s_B.

3.2.1 $\bar{B} \to X_s\nu\bar{\nu}$ process

The inclusive decay $B \to X_s\nu\bar{\nu}$ is dominated by the Z-exchange and can be searched through the large missing energy associated with the two neutrinos. This decay mode is theoretically very clean, since both the perturbative α_s and the non-perturbative corrections are small. So these decays do not suffer from the form factor uncertainties and thus, are very sensitive to the search for new physics beyond the SM. The decay

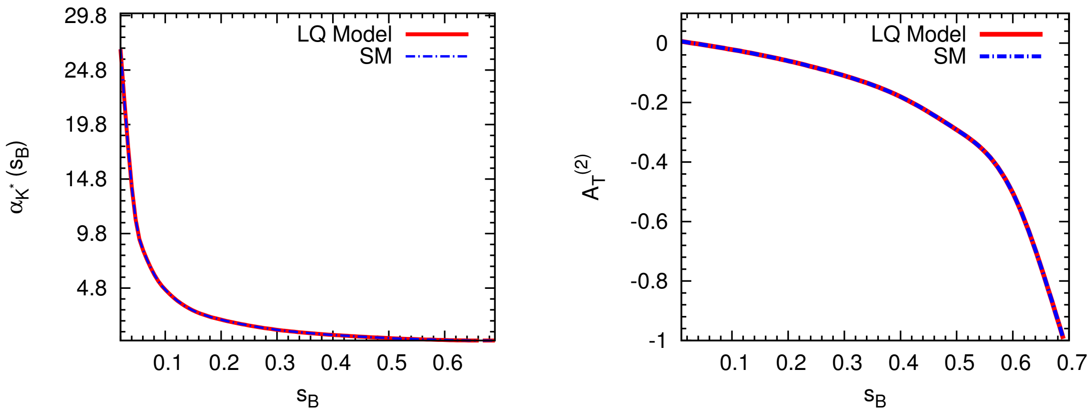

FIGURE 3.7: The variation of K^* polarization factor (left panel) and the transverse asymmetry (right panel) with respect to s_B.

rate of the inclusive decay mode is calculated in terms of b and other light quarks. The decay distribution with respect to $s_b = s/m_b^2$ can be written as [59]

$$\begin{aligned} \frac{d\Gamma\left(\bar{B} \to X_s \nu\bar{\nu}\right)}{ds_b} &= \frac{\alpha_{\rm em}^2 G_F^2 m_b^5}{128\pi^5}|V_{ts}^* V_{tb}|^2 \kappa(0)(|C_L^\nu|^2 + |C_R^{\rm LQ}|^2)\lambda^{1/2}(1, \tilde{m}_s^2, s_b) \\ &\times \left[3s_b(1 + \tilde{m}_s^2 - s_b - 4\tilde{m}_s \frac{{\rm Re}(C_L^\nu C_R^{\rm LQ*})}{|C_L^\nu|^2 + |C_R^{\rm LQ}|^2}) + \lambda(1, \tilde{m}_s^2, s_b)\right]. \quad (3.37) \end{aligned}$$

Here $\tilde{m}_i = m_i/m_s$, m_s is the mass of the strange quark and $\kappa(0) = 0.83$ is the QCD correction to the hadronic matrix element [149, 179]. In Fig. 3.8, we show the variation of the branching ratio of $\bar{B} \to X_s\nu\bar{\nu}$ with respect to s_b and the integrated branching ratio values over the range $s_b \in [0, 0.96]$ both in the SM and in the leptoquark model are presented in Table 3.3.

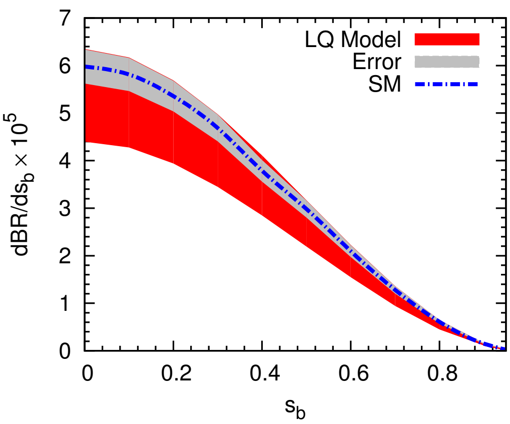

FIGURE 3.8: The plots for the branching ratio of $B \to X_s\nu\bar{\nu}$ against s_b.

To search more NP in the semileptonic process, where B decays to a meson and two final state neutrino, we define the following ratios as [173],

$$R_K^\nu = \frac{\mathrm{BR}(\bar{B} \to \bar{K}\nu\bar{\nu})}{\mathrm{BR}(\bar{B} \to X_s\nu\bar{\nu})}, \qquad R_{K^*}^\nu = \frac{\mathrm{BR}(\bar{B} \to \bar{K}^*\nu\bar{\nu})}{\mathrm{BR}(\bar{B} \to X_s\nu\bar{\nu})}. \tag{3.38}$$

Fig. 3.9 contains the plots for the R_K^ν (left panel) and $R_{K^*}^\nu$ (right panel) ratios against s_B in the full kinematically allowed region and the corresponding numerical values are given in Table 3.3. From this figures, we observe that the deviation of LQ results from the SM is negligible.

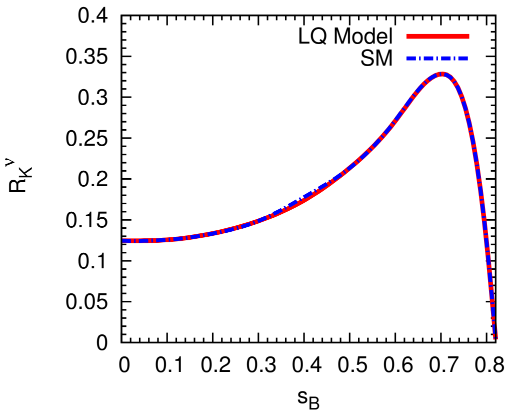

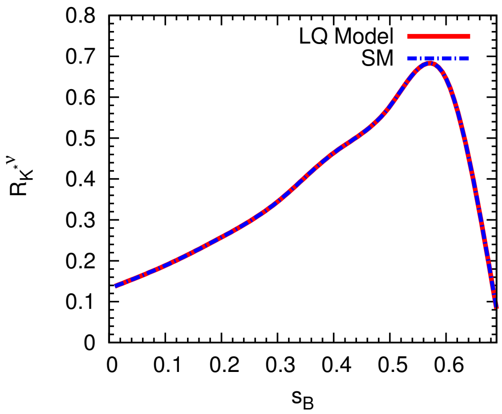

FIGURE 3.9: The R_K^ν (left panel) and $R_{K^*}^\nu$ (right panel) parameters versus s_B.

TABLE 3.3: Our predicted numerical values of the branching ratios and $R_{K^{(*)}}^\nu$ parameters of $B \to (K^{(*)}, X_s)\nu\bar{\nu}$ processes in both the SM and $\tilde{S}_2$ LQ model.

Observables	SM prediction	Values in $\tilde{S}_2$ LQ model	Expt. value [24, 98]
$\mathrm{BR}(B_d^0 \to K^0\nu\bar{\nu})$	$(4.9 \pm 0.29) \times 10^{-6}$	$(3.6 - 5.2) \times 10^{-6}$	$< 4.9 \times 10^{-5}$
$\mathrm{BR}(B_d^0 \to K^*\nu\bar{\nu})$	$(9.54 \pm 0.57) \times 10^{-6}$	$(7.02 - 10.13) \times 10^{-6}$	$< 5.5 \times 10^{-5}$
$\mathrm{BR}(B \to X_s\nu\bar{\nu})$	$(2.98 \pm 0.18) \times 10^{-5}$	$(2.2 - 3.17) \times 10^{-5}$	$\cdots$
$\langle R_K^\nu \rangle$	0.164	(0.163 – 0.164)	$\cdots$
$\langle R_{K^*}^\nu \rangle$	0.32	0.32	$\cdots$

3.3 Chapter summary

The flavor changing neutral current $b \to s$ processes occur only through one loop diagrams in the SM and are also highly suppressed by several mechanisms. We have investigated the rare $\bar{B} \to \bar{K} l^+ l^- (\nu\bar{\nu})$ processes in the full q^2 regimes in the framework of $(3, 2, 7/6)$ scalar leptoquark model. The constraints on the new couplings are taken from the branching ratios of $B_s \to l^+ l^-$ and $\bar{B} \to X_s l^+ l^-$ processes and $B_s \to \bar{B}_s$

oscillation data. We then estimated the branching ratios, isospin asymmetry and lepton non-universality parameters of $\bar{B} \to \bar{K} l^+ l^-$ decay modes in both the high and low recoil limit. We observed that due to the effect of leptoquarks, the theoretical results on branching ratios deviate from the SM values. Leptoquark model explained the R_K ratio very well. We have also analyzed the $\bar{B} \to (\bar{K}^{(*)}, X_s) \nu \bar{\nu}$ processes with the scalar leptoquark couplings. We have computed the branching ratios and various asymmetries associated with these processes. The branching ratios deviate significantly from the SM and are found to be well below the experimental upper bounds.

Chapter 4

Probing new physics in rare semileptonic $\bar{B} \to \bar{K}^* ll$ decay modes

This chapter is based on the semileptonic decay mode $\bar{B} \to \bar{K}^*(\to K\pi)\mu^+\mu^-$, which is quite an interesting channel, as the measurement of four-body angular distribution provides a large number of observables which can be used to probe and discriminate different scenarios of NP. Theoretical predictions for such observables are particularly precise and free from hadronic uncertainties in the low range of dimuon invariant mass squared q^2, i.e., $1 < q^2 < 6$ GeV^2. While the observed forward-backward asymmetry is systematically below the SM prediction, the zero-crossing point is consistent with it. The measured decay rate of $\bar{B} \to \bar{K}^*\mu^+\mu^-$ process has about 3σ deviation [69] from its SM prediction. Also there are a few deviations from the SM expectations have been observed by LHCb experiment in the angular observables. Specifically, the largest discrepancy of 3.7σ encountered in the observable P_5' [70] in the bin $q^2 \in [4.3, 8.68]$ is quite captivating. Another interesting observable to look for the evidence of new physics is the isospin asymmetry distribution, which is measured by the LHCb experiment in the entire q^2 spectrum [180]. The leading uncertainties due to the $\bar{B} \to \bar{K}^*$ form factor are expected to cancel in this asymmetry.

The angular distributions of $\bar{B} \to \bar{K}^* l^+ l^-$ processes with the dilepton invariant mass have been studied by various experiments such as BaBar, Belle, CDF, and LHCb. All these experiments cover the full kinematical dilepton mass region, i.e. $4m_l^2 \leqslant q^2 \leqslant (M_B - M_{K^*})^2$, leaving the regions around $q^2 \sim m_{J/\psi}^2$ and $m_{\psi'}^2$. In general, the kinematically allowed region can be classified into three regions, and different theoretical approaches are usually adopted to study the properties of various observables. In the region of large hadron recoil, i.e. for $q^2 \leqslant m^2_{J/\psi}$, the kaon is very energetic and the physical observables can be computed using QCD factorization approach. The intermediate values of q^2, i.e., 7 GeV$^2 \leqslant q^2 \leqslant$ 14 GeV^2, fall into the narrow resonance region, and appropriate cuts are employed to remove the dominant charmonium resonance $(\bar{c}c) = J/\psi, \psi'$ backgrounds from $\bar{B} \to \bar{K}^* (\bar{c}c) \to \bar{K}^* l^+ l^-$. The larger dilepton invariant mass region, i.e., $q^2 \geqslant 14$ GeV^2, corresponds to the low recoil limit, and in this region the kaon energy is around a GeV or less. Here soft collinear effective theory and QCD factorization approaches are not justified properly and become invalid near the zero-recoil point $q^2 \sim q^2_{\rm max} = (M_B - M_{K^*})^2$. At low recoil, the heavy-to-light decays can be studied by an operator product expansion in $1/Q$ where $Q = \left(m_b, \sqrt{q^2}\right)$, i.e., $\sqrt{q^2}$ is of the order of the mass of the b quark, m_b [181–183]. The combination of operator product expansion with the heavy quark effective theory and the use of improved Isgur-Wise form factor relations [181, 184] allows us to obtain the $\bar{B} \to \bar{K}^* l^+ l^-$ matrix element expansion in the strong coupling and in power corrections suppressed by the heavy quark mass, in low recoil.

Though phenomenologically the rare semileptonic $b \to s l^+ l^-$ decays have been studied in the framework of scalar leptoquark, the effect of scalar LQs in various observables associated with $\bar{B} \to \bar{K}^* \mu^+ \mu^-$ process is not yet explicitly studied. In this work, using the scalar LQ model, we would like to investigate the $\bar{B} \to \bar{K}^* l^+ l^-$ processes, which contain quite a large number of clean observables in the full kinematics except for the intermediate q^2 region. In particular, we are interested in looking for the effect of the $S_2(3, 2, 7/6)$ and $\tilde{S}_2(3, 2, 1/6)$ scalar LQs on some of the observables such as dilepton mass spectra, lepton-angle distribution, and various asymmetries like forward-backward asymmetry and isospin asymmetry. We would like to see how the scalar LQs affect these observables and whether it would be possible to differentiate between these two scalar LQ models from some of these observables.

4.1 Analysis of $\bar{B} \to \bar{K}^* l^+ l^-$ processes

Here we will consider the decay modes $\bar{B} \to \bar{K}^* l^+ l^-$. At the quark level, these processes proceed through the FCNC transition $b \to s l^+ l^-$, which occurs only through loops in the SM, and hence they are quite suitable to look for new physics. Moreover, the dileptons present in these processes allow one to formulate several useful observables which can serve as a testing ground to decipher the presence of new physics.

The transition amplitude for these processes can be obtained using the effective Hamiltonian presented in Eqn. (1.48, 1.49). The matrix elements of the various hadronic currents between the initial B meson and the final K^* vector meson can be parametrized in terms of seven form factors by means of a narrow width approximation. The amplitude for the process $\bar{B} \to \bar{K}^*(\to K\pi)l^+l^-$ can be represented by seven transversity amplitudes, $A^{L,R}_{\perp,\|,0}$ and A_t. The relevant form factors [65, 185, 186] are given in Eqn. (1.55). The explicit form of these amplitudes (up to corrections $\mathcal{O}(\alpha_s)$) are presented in section A.2 (A.3) of Appendix A for low q^2 (high q^2) region.

Assuming $\bar{K}^{*0} \to K^-\pi^+$ to be on the mass shell, the full angular distribution of the decay $\bar{B} \to \bar{K}^{*0}\,(\to K^-\pi^+)\,l^+l^-$ can be described by four independent kinematic variables; the lepton-pair invariant mass; and the three angles θ_{K^*}, θ_l and ϕ. The differential decay distribution in terms of three variables can be written as [175, 187, 188]

$$\frac{d^4\Gamma}{dq^2\ d\cos\theta_l\ d\cos\theta_{K^*}\ d\phi} = \frac{9}{32\pi} J\left(q^2, \theta_l, \theta_{K^*}, \phi\right)\ , \tag{4.1}$$

where the lepton spins have been summed over. Here q^2 is the dilepton invariant mass squared, θ_l is the angle between the negatively charged lepton and the $\bar{B}$ in the dilepton frame, θ_{K^*} is the angle between K^- and $\bar{B}$ in the $K^-\pi^+$ center-of-mass system, and ϕ is given by the angle between the normals of the $K^-\pi^+$ and the dilepton (l^+l^-) planes. The full kinematically allowed physical region in the phase space is given by

$$4m_l^2 \leqslant q^2 \leqslant (M_B - M_{K^*})^2\,, \quad -1 \leqslant \cos\theta_l \leqslant 1, \quad -1 \leqslant \cos\theta_{K^*} \leqslant 1, \quad 0 \leqslant \phi \leqslant 2\pi, \tag{4.2}$$

where M_{K^*} is the mass of K^* meson. More explicitly, the dependence of the decay distribution on the three angles can be written as

$$\begin{aligned} J\left(q^2, \theta_l, \theta_{K^*}, \phi\right) &= J_1^s \sin^2\theta_{K^*} + J_1^c \cos^2\theta_{K^*} + \left(J_2^s \sin^2\theta_{K^*} + J_2^c \cos^2\theta_{K^*}\right)\cos 2\theta_l \\ &+ J_3 \sin^2\theta_{K^*} \sin^2\theta_l \cos 2\phi + J_4 \sin 2\theta_{K^*} \sin 2\theta_l \cos\phi + J_5 \sin 2\theta_{K^*} \sin\theta_l \cos\phi \\ &+ (J_6^s \sin^2\theta_{K^*} + J_6^c \cos^2\theta_{K^*})\cos\theta_l + J_7 \sin 2\theta_{K^*} \sin\theta_l \sin\phi \\ &+ J_8 \sin 2\theta_{K^*} \sin 2\theta_l \sin\phi + J_9 \sin^2\theta_{K^*} \sin^2\theta_l \sin 2\phi\ , \end{aligned} \tag{4.3}$$

where the coefficients $J_i^{(a)} = J_i^{(a)}\left(q^2\right)$ for $i = 1, ..., 9$ and $a = s, c$ are functions of the dilepton mass, and are expressed in terms of the transversity amplitudes A_0, $A_\|$, $A_\perp$, and A_t, as given in section A.1 of Appendix A.

The dilepton invariant mass spectrum for $\bar{B} \to \bar{K}^* l^+l^-$ decay after integration over all angles [187] is given by

$$\frac{d\Gamma}{dq^2} = \frac{3}{4}\left(J_1 - \frac{J_2}{3}\right), \tag{4.4}$$

where $J_i = 2J_i^s + J_i^c$. Beside the decay rate, this process provides many interesting observables to look for NP, which are discussed below.

- The zero crossing of forward-backward asymmetry A_{FB}, which can be obtained after integrating the 4-differential distribution over ϕ and θ_{K^*} angles and is defined as [187]

$$A_{FB}\left(q^2\right) = -\frac{3}{8}\frac{J_6}{d\Gamma/dq^2} \ . \tag{4.5}$$

- The longitudinal and transverse polarization fractions of the K^* meson can be defined in terms of the transversity amplitudes as

$$F_L(q^2) = \frac{|A_0|^2}{|A_0|^2 + |A_\parallel|^2 + |A_\perp|^2} \ , \qquad F_T(q^2) = \frac{|A_\parallel|^2 + |A_\perp|^2}{|A_0|^2 + |A_\parallel|^2 + |A_\perp|^2} \ , \tag{4.6}$$

and in terms of the angular coefficients J_i's, these observables can be expressed as [189]

$$F_L\left(q^2\right) = \frac{3J_1^c - J_2^c}{4d\Gamma/dq^2} \ , \qquad F_T\left(q^2\right) = 1 - F_L(q^2) \, , \tag{4.7}$$

so that one can define the ratio of the K^* polarization fraction α_{K^*} as [190]

$$\alpha_{K^*}\left(q^2\right) = \frac{2F_L}{F_T} - 1 = \frac{-J_2}{2J_2^s} \ . \tag{4.8}$$

- The transverse asymmetries are given as [190]

$$\begin{aligned}
A_T^{(1)}(q^2) &= \frac{-2\mathrm{Re}\left(A_\parallel A_\perp^*\right)}{|A_\perp|^2 + |A_\parallel|^2}, \qquad A_T^{(2)}\left(q^2\right) = \frac{J_3}{2J_2^s}, \\
A_T^{(3)}\left(q^2\right) &= \left(\frac{4\left(J_4\right)^2 + \beta_l^2\left(J_7\right)^2}{-2J_2^c\left(2J_2^s + J_3\right)}\right)^{1/2}, \quad A_T^{(4)}\left(q^2\right) = \left(\frac{4\left(J_8\right)^2 + \beta_l^2\left(J_5\right)^2}{4\left(J_4\right)^2 + \beta_l^2\left(J_7\right)^2}\right)^{1/2}, \\
A_T^{(5)}\left(q^2\right) &= \frac{|A_\perp^L A_\parallel^{R*} + A_\parallel^L A_\perp^{R*}|}{|A_\perp|^2 + |A_\parallel|^2}, \qquad A_{\mathrm{Im}}\left(q^2\right) = \frac{J_9}{d\Gamma/dq^2}.
\end{aligned} \tag{4.9}$$

- Another set of interesting observables are the six form-factor-independent (FFI) observables [191], which are given by

$$\begin{aligned}
P_1\left(q^2\right) &= \frac{J_3}{2J_2^s} \ , \qquad P_2\left(q^2\right) = \beta_l\frac{J_6^s}{8J_2^s} \ , \qquad P_3\left(q^2\right) = -\frac{J_9}{4J_2^s} \ , \\
P_4\left(q^2\right) &= \frac{\sqrt{2}J_4}{\sqrt{-J_2^c\left(2J_2^s - J_3\right)}} \ , \qquad P_5\left(q^2\right) = \frac{\beta_l J_5}{\sqrt{-2J_2^c\left(2J_2^s + J_3\right)}} \ , \\
P_6\left(q^2\right) &= -\frac{\beta_l J_7}{\sqrt{-2J_2^c\left(2J_2^s - J_3\right)}} \ .
\end{aligned} \tag{4.10}$$

- Also useful are a slightly modified set of clean observables $P'_{4,5,6}$ which are related to $P_{4,5,6}$ through the relations [192]

$$P'_4 \equiv P_4\sqrt{1-P_1} = \frac{J_4}{\sqrt{-J_2^c J_2^s}} \,,$$
$$P'_5 \equiv P_5\sqrt{1+P_1} = \frac{J_5}{2\sqrt{-J_2^c J_2^s}} \,,$$
$$P'_6 \equiv P_6\sqrt{1-P_1} = \frac{-J_7}{2\sqrt{-J_2^c J_2^s}} \,. \tag{4.11}$$

- Another interesting observable is the isospin asymmetry distribution, which has been recently measured by LHCb experiment with a 3 fb^{-1} data set [69]. This asymmetry arises due to the non-factorizable part, where a photon is radiated from the spectator quark in annihilation and spectator scattering. The CP-averaged isospin asymmetry is defined as [193, 194]

$$\frac{dA_I}{dq^2} = \frac{d\Gamma\left[\bar{B}^0 \to \bar{K}^{*0} l^+ l^-\right]/dq^2 - d\Gamma\left[B^+ \to K^{*+} l^+ l^-\right]/dq^2}{d\Gamma\left[\bar{B}^0 \to \bar{K}^{*0} l^+ l^-\right]/dq^2 + d\Gamma\left[B^+ \to K^{*+} l^+ l^-\right]/dq^2} \,. \tag{4.12}$$

Including longitudinal photon polarizations appearing for $q^2 \neq 0$, the isospin asymmetry distribution in the QCD factorization scheme is given by

$$A_I\left(q^2\right) = \mathrm{Re}\left(b_d^{\perp}\left(q^2\right) - b_u^{\perp}\left(q^2\right)\right) \frac{|C_9^{(0)\perp}\left(q^2\right)|^2}{|C_{10}\left(\mu_b\right)|^2 + |C_9^{(0)\perp}\left(q^2\right)|^2} \times \frac{F\left(q^2\right)}{G\left(q^2\right)}, \tag{4.13}$$

with

$$F\left(q^2\right) = 1 + \frac{1}{4}\frac{E_{K^*}^2 M_B^2}{q^2 M_{K^*}^2}\frac{\xi_{\parallel}^2\left(q^2\right)}{\xi_{\perp}^2\left(q^2\right)}\frac{\mathrm{Re}\left(b_d^{\parallel}\left(q^2\right) - b_u^{\parallel}\left(q^2\right)\right)}{\mathrm{Re}\left(b_d^{\perp}\left(q^2\right) - b_u^{\perp}\left(q^2\right)\right)}\frac{|C_9^{(0)\parallel}\left(q^2\right)|^2}{|C_9^{(0)\perp}\left(q^2\right)|^2}, \tag{4.14}$$
$$G\left(q^2\right) = 1 + \frac{1}{4}\frac{E_{K^*}^2 M_B^2}{q^2 M_{K^*}^2}\frac{\xi_{\parallel}^2\left(q^2\right)}{\xi_{\perp}^2\left(q^2\right)}\frac{|C_9^{(0)\parallel}\left(q^2\right)|^2 + |C_{10}\left(\mu_b\right)|^2}{|C_9^{(0)\perp}\left(q^2\right)|^2 + |C_{10}\left(\mu_b\right)|^2} \,, \tag{4.15}$$

where the generalized standard model Wilson coefficients are

$$C_9^{(0)\perp}\left(q^2\right) = C_9\left(\mu_b\right) + Y\left(q^2\right) + \frac{2m_b M_B}{q^2}C_7^{\mathrm{eff}}\left(\mu_b\right), \tag{4.16}$$
$$C_9^{(0)\parallel}\left(q^2\right) = C_9\left(\mu_b\right) + Y\left(q^2\right) + \frac{2m_b}{M_B}C_7^{\mathrm{eff}}\left(\mu_b\right). \tag{4.17}$$

The b_q^a, $(a = \perp, \parallel)$ terms appearing in the above equations are given as

$$\begin{aligned} b_q^{\perp}\left(q^2\right) &= \frac{24\pi^2 M_B f_B e_q}{q^2 \xi_{\perp}\left(q^2\right) C_9^{(0)\perp}\left(q^2\right)} \left(\frac{f_{K^*}^{\perp}}{m_b} K_1^{\perp}\left(q^2\right) + \frac{f_{K^*} M_{K^*}}{6\lambda_{B,+}\left(q^2\right) M_B} \frac{K_2^{\perp}\left(q^2\right)}{1 - q^2/M_B^2} \right), \\ b_q^{\parallel}\left(q^2\right) &= \frac{24\pi^2 f_B e_q M_{K^*}}{M_B E_{K^*} \xi_{\parallel}\left(q^2\right) C_9^{(0)\parallel}\left(q^2\right)} \left(\frac{f_{K^*}}{3\lambda_{B,-}\left(q^2\right)} K_1^{\parallel}\left(q^2\right) \right), \end{aligned} \tag{4.18}$$

where the expressions for the terms $K_{1,2}^a$ are presented in the section A.4 of Appendix A.

4.1.1 Numerical analysis in the large recoil

After getting familiar with the different observables, we now proceed to study these observables in the large recoil limit. For that we need to know the associated form factors for the $\bar{B} \to \bar{K}^* l^+ l^-$ process. In the heavy quark limit, the QCDf form factors obey symmetry relations, and at leading order in the $1/E$ expansion, they can be expressed in terms of two universal soft non-perturbative form factors, $\xi_\perp$ and $\xi_\parallel$. In order to calculate the universal form factors we use the QCDf scheme [58, 187], where they are expressed as

$$\xi_\perp(E_{K^*}) = \frac{M_B}{M_B + M_{K^*}} V(q^2)\ , \quad \xi_\parallel(E_{K^*}) = \frac{M_B + M_{K^*}}{M_B} A_1(q^2) - \frac{M_B - M_{K^*}}{M_B} A_2(q^2). \tag{4.19}$$

The q^2 dependence of the form factors $V,\ A_1,\ A_2$ can be parameterized as

$$\begin{aligned} V\left(q^2\right) &= \frac{r_1}{1 - q^2/m_R^2} + \frac{r_2}{1 - q^2/m_{\rm fit}^2}\ , \\ A_1\left(q^2\right) &= \frac{r_2}{1 - q^2/m_{\rm fit}^2}\ , \\ A_2\left(q^2\right) &= \frac{r_1}{1 - q^2/m_{\rm fit}^2} + \frac{r_2}{\left(1 - q^2/m_{\rm fit}^2\right)^2}\ . \end{aligned} \tag{4.20}$$

The values of the parameters involved in the calculation of form factors are taken from [178]. The T_i formfactors are related to the universal form factors $\xi_{\perp,\parallel}$ as

$$T_1(q^2) = \xi_\perp(E_{K^*})\ , \quad T_2(q^2) = \frac{2E_{K^*}}{M_B} \xi_\perp(E_{K^*})\ , \quad T_3(q^2) = \xi_\perp(E_{K^*}) - \xi_\parallel(E_{K^*}). \tag{4.21}$$

After getting sufficient knowledge about the different observables and the associated form factors for $\bar{B} \to \bar{K}^* l^+ l^-$ processes in the high recoil limit, we now proceed for numerical estimation. The masses of particles and the lifetime of B meson are taken from [98]. For the LQ couplings we use a representative value for the parameter r as $r = 0.3$ and vary the associated phase between $\pi/2 \le \phi^{\rm LQ} \le 3\pi/2$. Furthermore, we will

TABLE 4.1: Summary of the values of various input parameters.

$\alpha_{\rm em}$	1/137	$a_{1,\perp}$	0.10
$\alpha_s(M_z)$	0.1184	$a_{2,\perp}$	0.13
$m_{b,ps}$	4.6 GeV	$a_{1,\parallel}$	0.10
$m_{c,pole}$	1.4 GeV	$a_{2,\parallel}$	0.09
$f_{K^*,\perp}$	0.185 GeV	λ	0.22537±0.0006
$f_{K^*,\parallel}$	0.220 GeV	A	$0.814^{+0.023}_{-0.024}$
f_B	0.2 GeV	$\bar{\rho}$	0.117 ± 0.021
		$\bar{\eta}$	0.353 ± 0.013

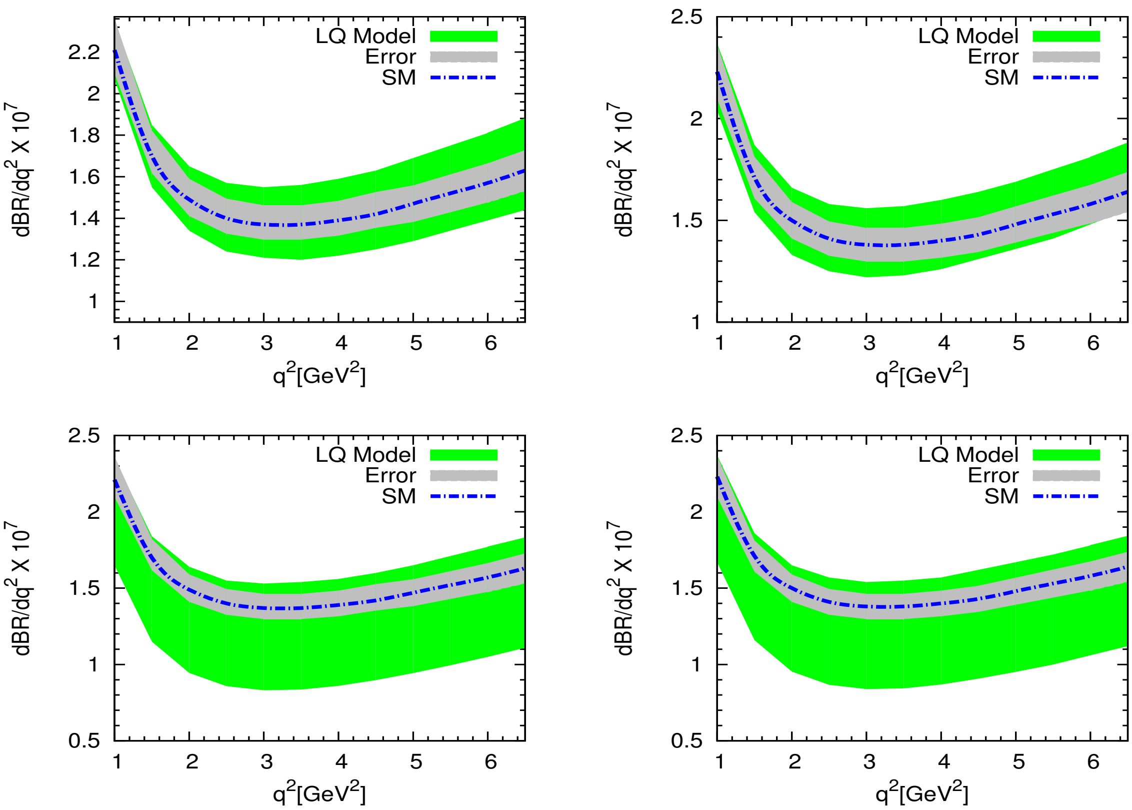

FIGURE 4.1: The variation of branching ratios of $\bar{B} \to \bar{K}^* \mu^+\mu^-$ (left panel) and $\bar{B} \to \bar{K}^* e^+e^-$ (right panel) with low q^2 in the standard model and in leptoquark model. The green bands are due to the leptoquark contributions and the gray bands represent the theoretical uncertainties from the input parameters in the SM. The plots in the top panel are for $S_2(3,2,7/6)$ and those in the bottom panel are for $\tilde{S}_2(3,2,1/6)$.

present most of the the results only for $S_2(3,2,7/6)$ LQ and only a few representative plots for $\tilde{S}_2(3,2,1/6)$. The values of quark masses and all the input parameters used in our analysis are listed in Table 4.1.

In Fig. 4.1, we show the variation of the branching ratios for $\bar{B} \to \bar{K}^* \mu^+\mu^-$ (left panel) and $\bar{B} \to \bar{K}^* e^+e^-$ (right panel) in the low q^2 region. The plots in the top panel are for $S_2(3,2,7/6)$ and those in the bottom panel are for $\tilde{S}_2(3,2,1/6)$. The variation of the

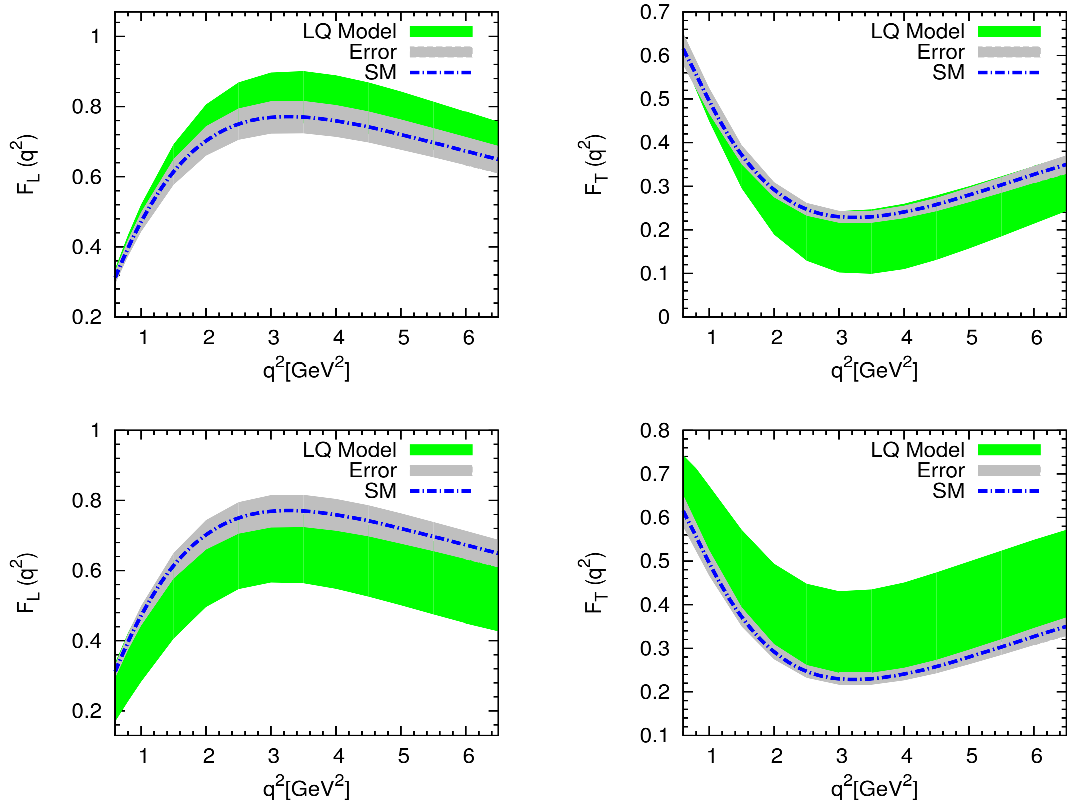

FIGURE 4.2: Variation of longitudinal and transverse K^* polarization fractions in the low q^2 region. The plots in the top panel are for $S_2(3,2,7/6)$ and those in the bottom panel are for $\tilde{S}_2(3,2,1/6)$.

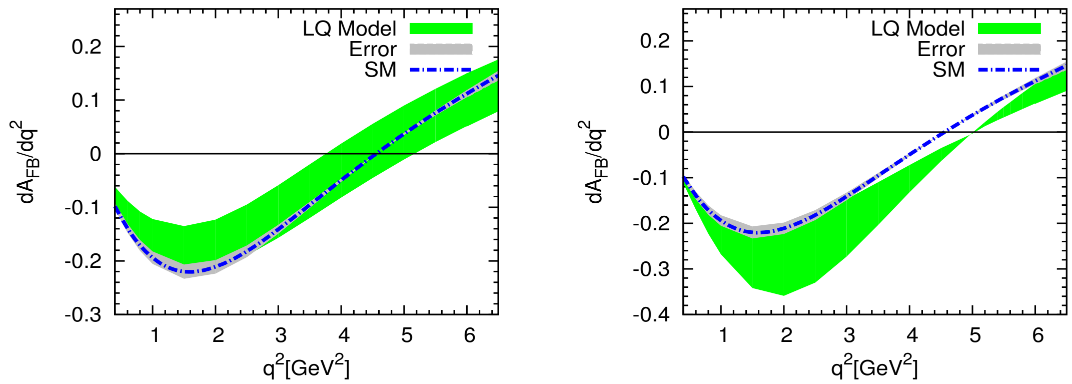

FIGURE 4.3: The variation of forward backward asymmetry for $S_2(3,2,7/6)$ (left panel) and for $\tilde{S}_2(3,2,1/6)$ (right panel) with q^2.

longitudinal and transverse polarization fractions of K^* has been shown in Fig. 4.2 and that of forward-backward asymmetry in Fig. 4.3. From these figures, one can see that the effect of the LQs $S_2(3,2,7/6)$ and $\tilde{S}_2(3,2,1/6)$ are quite different, and one can easily differentiate between these two models from the measured values of the K^* polarization fractions $F_L(q^2)$ and $F_T(q^2)$. The transverse asymmetry parameters $A_T^{(3)}$, $A_T^{(4)}$, $A_{\rm Im}$ and the K^* polarization factor α_{K^*} variations with q^2 are presented in Fig. 4.4 and 4.5. The

TABLE 4.2: The predicted values for the integrated branching ratio, forward-backward asymmetry, isospin asymmetry and the polarization fractions in the range $q^2 \in [1, 6]$ GeV^2 for the $\bar{B} \to \bar{K}^* \mu^+ \mu^-$ process.

Observables	SM prediction	Values in LQ model $S_2(3, 2, 7/6)$	Values in LQ model $\tilde{S}_2(3, 2, 1/6)$
$\text{BR}(\bar{B} \to \bar{K}^* \mu^+ \mu^-)$	$(7.738 \pm 0.464) \times 10^{-7}$	$(6.88 \to 8.73) \times 10^{-7}$	$(4.8 \to 8.3) \times 10^{-7}$
$\text{BR}(\bar{B} \to \bar{K}^* e^+ e^-)$	$(7.742 \pm 0.465) \times 10^{-7}$	$(7.03 \to 8.73) \times 10^{-7}$	$(4.85 \to 8.38) \times 10^{-7}$
$\langle A_{FB} \rangle$	$-(0.09 \pm 0.005)$	$-0.11 \to 0.004$	$-0.185 \to -0.08$
$\langle A_I \rangle$	$-(0.03 \pm 0.002)$	$-0.06 \to -0.04$	$-0.02 \to -0.01$
$\langle F_L \rangle$	0.71 ± 0.043	$0.7 \to 0.8$	$0.5 \to 0.7$
$\langle F_T \rangle$	0.29 ± 0.017	$0.2 \to 0.3$	$0.3 \to 0.5$

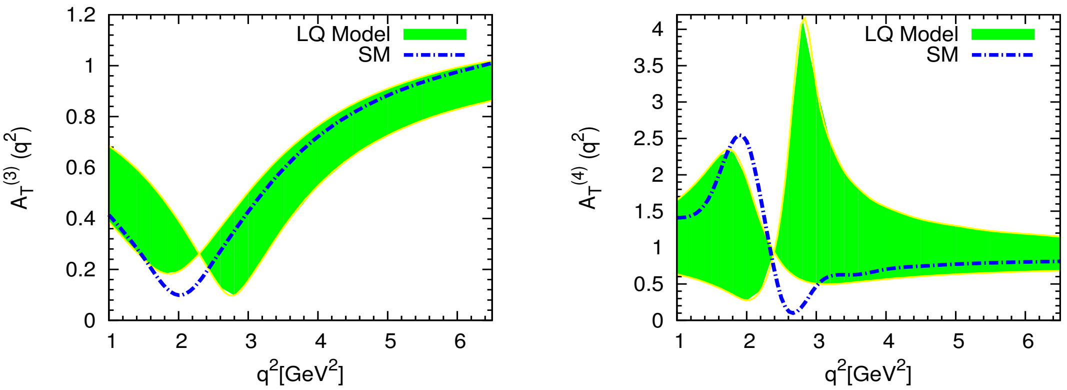

FIGURE 4.4: The variation of transverse asymmetry parameters $A_T^{(3)}$ (left panel), and $A_T^{(4)}$ (right panel) with q^2 in high recoil for $S_2(3, 2, 7/6)$.

variation of form-factor-independent observables as a function of dimuon invariant mass squared have been shown in Fig. 4.6. The total branching ratios and the asymmetries integrated over the range $q^2 \in [1, 6]$ GeV^2 are presented in Table 4.2, and the allowed range of transverse asymmetry and the FFI observables are given in Table 4.3. It should be noted that in the LQ model these observables deviate significantly from their SM predictions. The variation of isospin asymmetry distribution with respect to dimuon invariant mass squared in the $S_2(3, 2, 7/6)$ (left panel) and $\tilde{S}_2(3, 2, 1/6)$ (right panel) scalar LQ model are given in Fig. 4.7. Table 4.2 contains the allowed range of isospin asymmetries.

4.1.2 Numerical analysis in the low recoil

At low recoil, the exclusive $\bar{B} \to \bar{K}^* l^+ l^-$ decays depend on the improved form factor relations and an operator product expansion in $1/Q$. The OPE controls the non-perturbative contributions from four-quark operators and is important for the charm

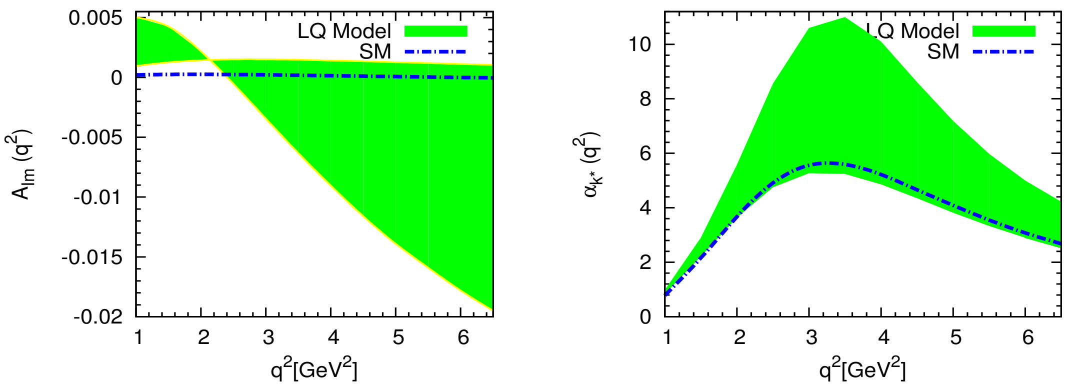

FIGURE 4.5: The variation of transverse asymmetry parameters $A_{\rm Im}$ (left panel) and the K^* polarization factor (right panel) with q^2 in high recoil for $S_2(3, 2, 7/6)$.

TABLE 4.3: The predicted integrated values of the FFI observables and the CP violating observables in the range $q^2 \in [1, 6]$ GeV^2 for the $\bar{B} \to \bar{K}^* \mu^+\mu^-$ process.

Observables	SM prediction	Values in LQ model $S_2(3, 2, 7/6)$	Values in LQ model $\tilde{S}_2(3, 2, 1/6)$
$\langle P_1 \rangle$	-0.044 ± 0.003	$-0.037 \to -0.046$	$-0.017 \to 0.14$
$\langle P_2 \rangle$	0.203 ± 0.012	$0.08 \to 0.23$	$0.19 \to 0.21$
$\langle P_3 \rangle$	$-(6.0 \pm 0.4) \times 10^{-4}$	$-(9.4 \to 1.8) \times 10^{-3}$	$-0.014 \to 0.08$
$\langle P_4 \rangle$	0.395 ± 0.024	$0.294 \to 0.45$	$0.24 \to 0.52$
$\langle P_5 \rangle$	-0.204 ± 0.012	$-0.42 \to -0.13$	$-0.39 \to -0.13$
$\langle P_6 \rangle$	-0.0075 ± 0.0005	$-0.07 \to 0.08$	$0.079 \to 0.112$
$\langle A_T^{(3)} \rangle$	0.55 ± 0.033	$0.56 \to 0.6$	$0.37 \to 0.6$
$\langle A_T^{(4)} \rangle$	0.87 ± 0.05	$0.82 \to 0.94$	$0.99 \to 1.5$
$\langle A_{\rm Im} \rangle$	$(1.7 \pm 0.1) \times 10^{-4}$	$(2.0 \to 5.3) \times 10^{-4}$	$-0.023 \to 0.005$
$\langle \alpha_{K^*} \rangle$	3.73 ± 0.22	$3.6 \to 5.6$	$1.8 \to 3.6$

quark, whose operators enter without any suppression from CKM matrix elements and small Wilson coefficients. The QCD operator identity for the massless strange quark ($m_s = 0$) is [181, 195]

$$i\partial^\nu \left(\bar{s} i \sigma_{\mu\nu} b\right) = -m_b \left(\bar{s}\gamma_\mu b\right) + i\partial_\mu \left(\bar{s} b\right) - 2\left(\bar{s} i \overleftarrow{D}_\mu b\right) , \tag{4.22}$$

which allows us to extract the relation between the form factors T_1 and V and the matrix elements of the current $\bar{s} i \overleftarrow{D}_\mu b$. The improved Isgur-Wise relations to leading order in $1/m_b$ including radiative corrections are

$$T_1\left(q^2\right) = \kappa V\left(q^2\right) \ , \quad T_2\left(q^2\right) = \kappa A_1\left(q^2\right) \ , \quad T_3\left(q^2\right) = \kappa A_2\left(q^2\right) \frac{M_B^2}{q^2} \ , \tag{4.23}$$

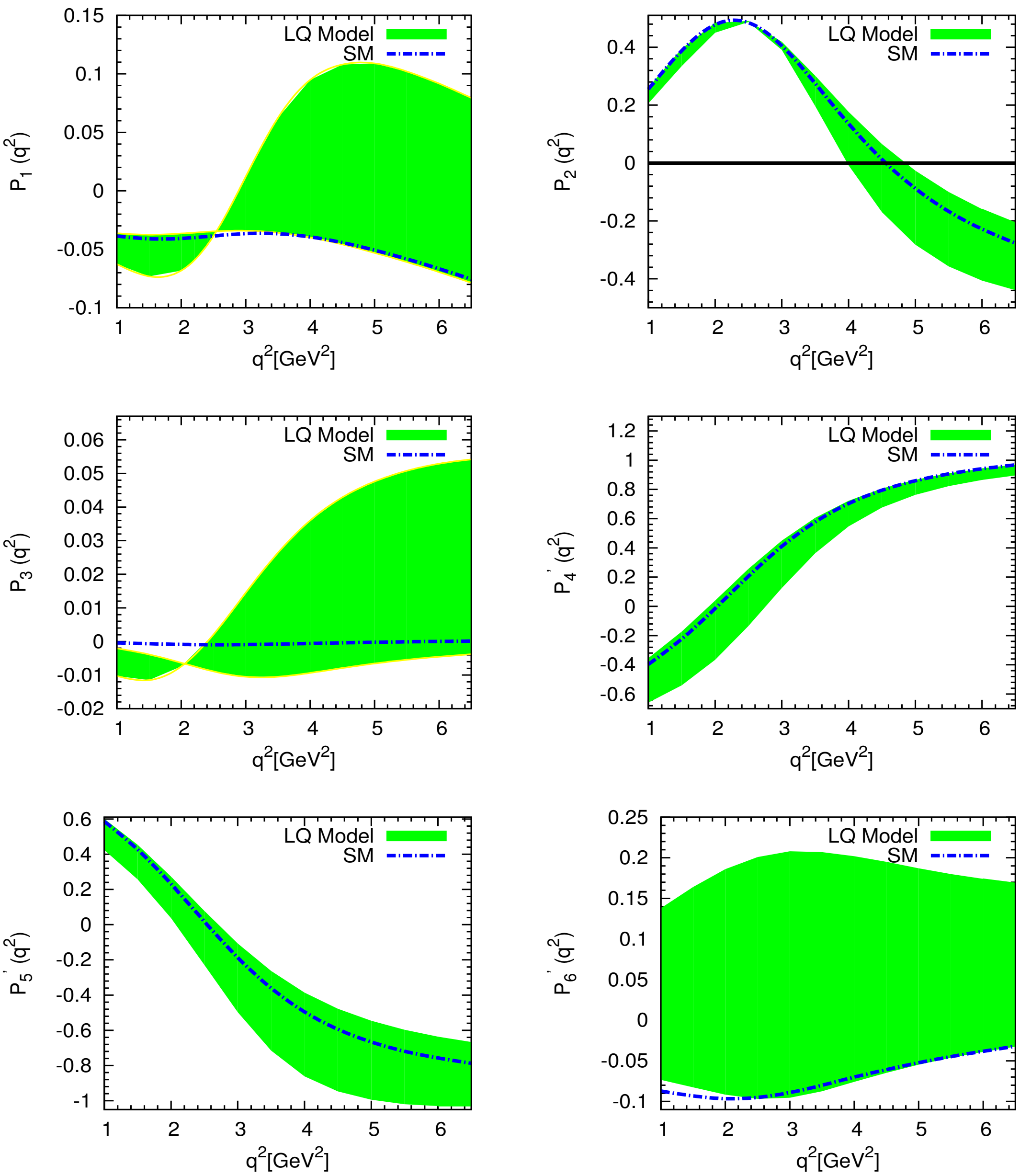

FIGURE 4.6: The variation of the observables $P_{1,2,3}$ and $P'_{4,5,6}$ with q^2 for $S_2(3,2,7/6)$ leptoquark.

where

$$\kappa = \left(1 + \frac{2D_0^{(\nu)}(\mu)}{C_0^{(\nu)}(\mu)}\right) \frac{m_b(\mu)}{M_B} , \tag{4.24}$$

and at $\mu = m_b$ including $\mathcal{O}(\alpha_s)$ corrections, it reads $\kappa = 1 + \mathcal{O}(\alpha_s^2)$.

We have shown the variation of the branching ratio for $\bar{B} \to \bar{K}^* \mu^+ \mu^-$ (left panel) and $\bar{B} \to \bar{K}^* e^+ e^-$ (right panel) with q^2 in Fig. 4.8. In the low-recoil region, the variation of forward-backward asymmetry (left panel) and isospin asymmetry (right panel) with

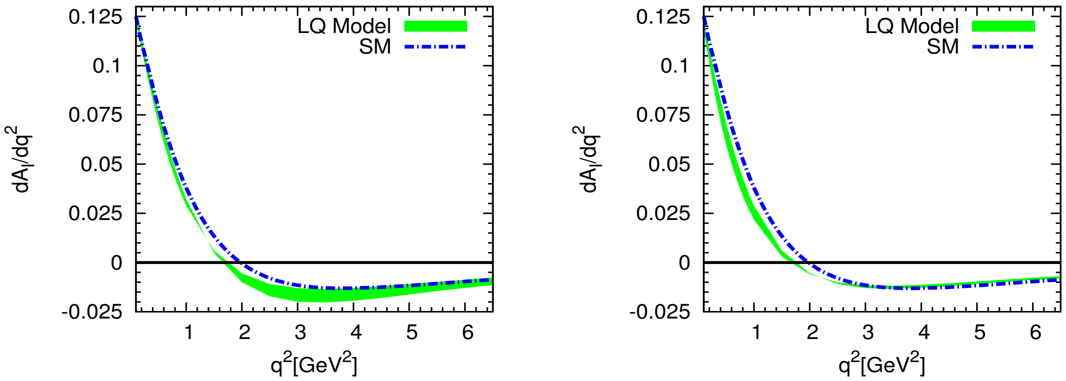

FIGURE 4.7: The variation of isospin asymmetry for $S_2(3, 2, 7/6)$ (left panel) and for $\tilde{S}_2(3, 2, 1/6)$ (right panel) with q^2.

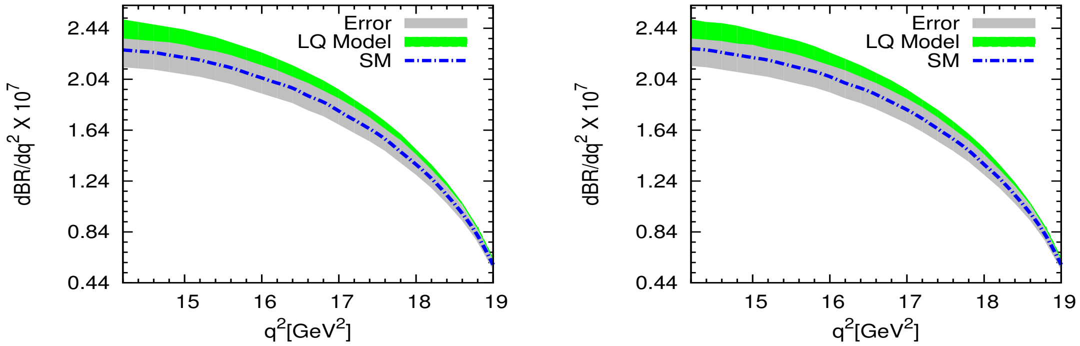

FIGURE 4.8: The variation of branching ratio for $\bar{B} \to \bar{K}^* l^+ l^-$ with high q^2 for $S_2(3, 2, 7/6)$ leptoquark.

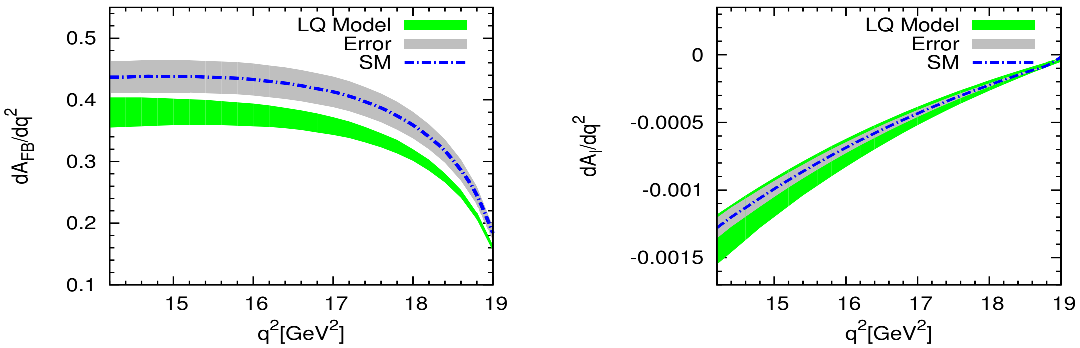

FIGURE 4.9: The variation of forward-backward asymmetry (left panel) and isospin asymmetry (right panel) with high q^2 for $S_2(3, 2, 7/6)$ leptoquark.

respect to q^2 are shown in Fig. 4.9. In the low recoil limit, the longitudinal and transverse polarizations of K^* meson in the presence of LQ model are consistence with the SM results. The plots for $F_L(q^2)$ (left panel) and $F_T(q^2)$ (right panel) are shown in Fig. 4.10. Fig. 4.11 shows the variation of P_2 (left panel) and A_T^4 (right panel) with respect to dimuon invariant mass squared. Table 4.4 contains the integrated values of

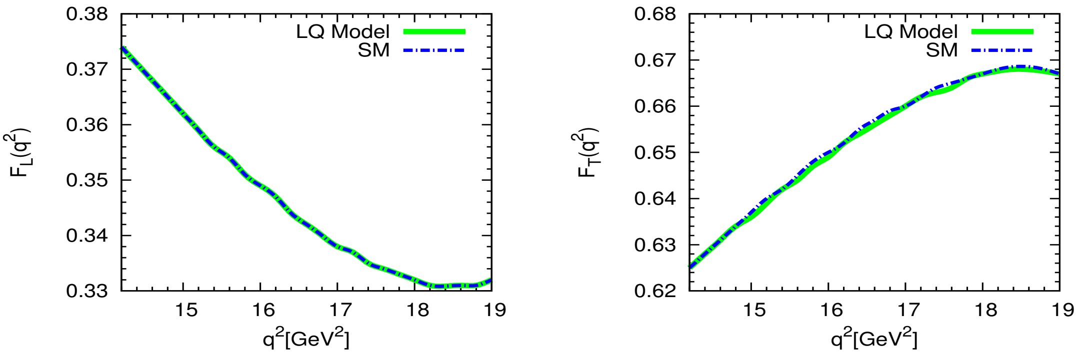

FIGURE 4.10: The variation of longitudinal (left panel) and transverse (right panel) polarization fraction with high q^2 for $S_2(3, 2, 7/6)$.

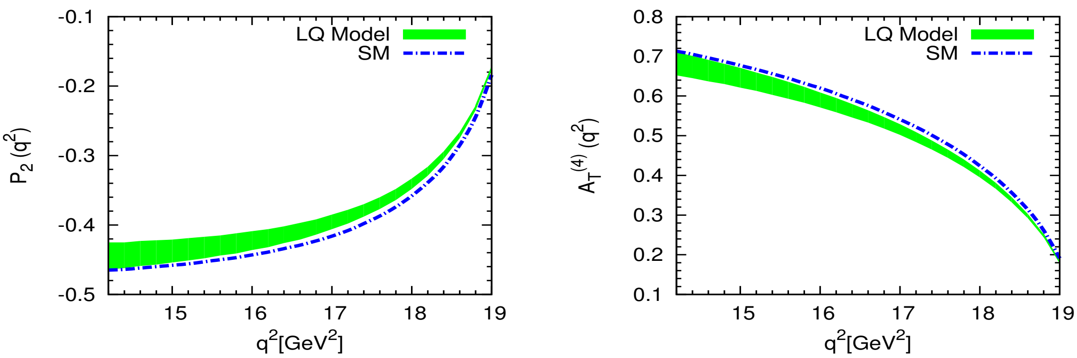

FIGURE 4.11: Variation of the observables P_2 (left panel), and $A_T^{(4)}$ (right panel) for $S_2(3, 2, 7/6)$ leptoquark.

TABLE 4.4: The predicted values for the integrated branching ratio and other parameters in the range $q^2 \in [14.2, 19]$ GeV^2 for the $\bar{B} \to \bar{K}^* l^+ l^-$ processes.

Observables	SM prediction	Values in LQ model $S_2(3, 2, 7/6)$
BR($B \to K^* \mu^+ \mu^-$)	$(8.5 \pm 0.51) \times 10^{-7}$	$(8.93 \to 9.31) \times 10^{-7}$
BR($B \to K^* e^+ e^-$)	$(8.52 \pm 0.511) \times 10^{-7}$	$(8.92 \to 9.32) \times 10^{-7}$
$\langle A_{FB} \rangle$	0.4	$0.34 \to 0.38$
$\langle A_I \rangle$	$-(2.75 \pm 0.17) \times 10^{-3}$	$(-3.3 \to 2.5) \times 10^{-3}$
$\langle P_2 \rangle$	-0.42	$-0.41 \to -0.38$
$\langle A_T^{(4)} \rangle$	0.57	$0.53 \to 0.58$
$\langle F_L \rangle$	0.35	0.35
$\langle F_T \rangle$	0.65	$0.65 \to 0.66$

branching ratio, forward-backward asymmetry, and isospin asymmetry in the low recoil, i.e. $q^2 \in [14.2, 19]$ GeV^2. It should be noted from these figures that at high q^2, there is no significant deviation between the SM results and the LQ predictions.

4.2 Chapter summary

We have studied the rare semileptonic decays $\bar{B} \to \bar{K}^* l^+ l^-$ using the simple renormalizable leptoquark model, in which a single scalar leptoquark is added to the standard model with the requirement that proton decay would not be induced in perturbation theory. The leptoquark parameter space is constrained using the recent measurement on $B_s \to \mu^+ \mu^-$. Using such constrained parameters we estimated the branching ratios, isospin and forward-backward asymmetries for $\bar{B} \to \bar{K}^* l^+ l^-$ processes in the full physical region except for the intermediate region of q^2. The CP violating observables and the form-factor-independent observables have also been studied in the leptoquark model. It is found that in these models, there could be significant deviation in these observables in high-recoil but comparatively less in low-recoil regimes. We found that the time-integrated values of some of the asymmetry parameters have deviated significantly from their corresponding SM values.

Chapter 5

Simultaneous study of R_K and $R_{D^{(*)}}$ anomalies in the vector leptoquark model

This chapter deals with the analysis of semileptonic decays of B meson mediated through flavor changing charged current $b \to c l \bar{\nu}_l$ and neutral current $b \to s l^+ l^-$ transitions in the vector leptoquark model. The $b \to c l \bar{\nu}_l$ processes occur at tree level with $W^\pm$ gauge boson as the propagator. The study of the nuclear beta decay has set the $V - A$ current structure of the weak interaction, which describes various charged current interactions in all the generation of quarks and leptons to a high precision. However, the recently measured experimental data indicate that the processes involving the third generation of fermions in both the initial and final states are comparably less precise than the first two generations. The couplings of the third generation fermions to the electroweak gauge sector is comparatively stronger due to their larger masses and thus, sensitive to new physics, which could modify the $V - A$ structure of the SM. In this context, the study of $\bar{B} \to \bar{D}^{(*)} \tau \bar{\nu}_l$ charge current processes, involving the quark level transition $b \to c$ are captivating. Recently, BaBar [41, 42] and Belle [43, 44] have measured the ratio of branching fractions of $\bar{B} \to \bar{D} \tau \bar{\nu}_\tau$ over $\bar{B} \to \bar{D} l \bar{\nu}_l$, where $l = e$, μ and the current experimental average [45] is

$$R_D = \frac{\mathrm{BR}\left(\bar{B} \to \bar{D} \tau \bar{\nu}_\tau\right)}{\mathrm{BR}\left(\bar{B} \to \bar{D} l \bar{\nu}_l\right)} = 0.397 \pm 0.040 \pm 0.028, \tag{5.1}$$

which has a 1.9σ deviation from its SM result $R_D^{\mathrm{SM}} = 0.300 \pm 0.008$ [196]. In addition, both the B factories and LHCb [46] have reported a 3.3σ discrepancy [45] in the measurement of R_{D^*}

$$R_{D^*} = \frac{\mathrm{BR}\left(\bar{B} \to \bar{D}^* \tau \bar{\nu}_\tau\right)}{\mathrm{BR}\left(\bar{B} \to \bar{D}^* l \bar{\nu}_l\right)} = 0.316 \pm 0.016 \pm 0.010, \tag{5.2}$$

from its SM prediction $R_{D^*}^{\mathrm{SM}} = 0.252 \pm 0.003$ [116, 197]. These observations may considered as the smoking gun signals for the violation of lepton flavor universality (LFU). The dominant theoretical uncertainties are reduced in these observables, as the hadronic uncertainties cancel out to a large extent in these ratios. The branching ratio of the semileptonic $b \to c l \bar{\nu}_l$ process can be computed precisely due to the light mass of leptons in the final state, thus, the deviation in $R_{D^{(*)}}$ could be from new physics affecting $\bar{B} \to \bar{D}^{(*)} \tau \bar{\nu}_\tau$ processes. Since these decays occur at the tree level in the SM, new physics models with a mass of the new particles near the TeV scale would be required to explain the $R_{D^{(*)}}$ anomalies. The branching ratios of $\bar{B} \to \bar{D}^{(*)} \tau \bar{\nu}_\tau$ processes and the associated $R_{D^{(*)}}$ anomalies have been investigated in the literature both in the SM as well as in various new physics models [62, 108, 110, 112, 116, 117, 119, 151, 198–216].

Recently, LHCb collaboration has measured analogous lepton flavor universality violating parameters, $R_{K^{(*)}}$, in the $\bar{B} \to \bar{K}^{(*)} l^+ l^-$ processes, which is defined as the ratio of $\bar{B} \to \bar{K}^{(*)} \mu^+ \mu^-$ to $\bar{B} \to \bar{K}^{(*)} e^+ e^-$ process

$$R_{K^{(*)}} = \frac{\mathrm{BR}(\bar{\mathrm{B}} \to \bar{\mathrm{K}}^{(*)} \mu^+ \mu^-)}{\mathrm{BR}(\bar{\mathrm{B}} \to \bar{\mathrm{K}}^{(*)} \mathrm{e}^+ \mathrm{e}^-)} \,. \tag{5.3}$$

In chapter 3, we have already presented an elaborate discussion on the R_K ratio. The LHCb experiment has also reported a discrepancy of 2.2σ [40] in the R_{K^*} ratio in the $q^2 \in [0.045, 1.1]$ GeV^2 bin

$$R_{K^*}^{\mathrm{LHCb}} = 0.660^{+0.110}_{-0.070} \pm 0.024, \tag{5.4}$$

from the SM prediction $R_{K^*}^{\mathrm{SM}} = 0.92 \pm 0.02$ [217] and discrepancy of 2.4σ [40] has reported in $q^2 \in [1.1, 6]$ GeV^2 region between the experimental value [40]

$$R_{K^*}^{\mathrm{LHCb}} = 0.685^{+0.113}_{-0.069} \pm 0.047, \tag{5.5}$$

and the SM prediction $R_{K^*}^{\mathrm{SM}} = 1.00 \pm 0.01$ [217].

In most of the studies in the literature, the authors have discussed either R_K or $R_D^{(*)}$ anomaly, but not both on the same footing. In Ref. [107], both the $R_{D^{(*)}}$ and R_K anomalies have been investigated in the $(3, 2, 1/6)$ scalar LQ model. According to the scenario presented in [108], the extension of the SM with the $SU(2)_L$ singlet scalar LQ can accommodate the R_K through a loop correction and the $R_{D^{(*)}}$ via the tree level LQ contribution. However, in Ref. [111], it has been argued that a simultaneous explanation of the R_K and $R_{D^{(*)}}$ is not realistic and would imply serious phenomenological problems elsewhere. In this chapter, we would like to focus on both the anomalies $R_{D^{(*)}}$ and R_K as well as some other observables in the $b \to c l \bar{\nu}$ decay processes.

5.1 $\bar{B} \to \bar{D}^{(*)} l \bar{\nu}_l$ process

In this section, we discuss the theoretical framework to compute the branching ratios and other physical observables in $\bar{B} \to \bar{D}^{(*)} l \bar{\nu}_l$ processes. The hadronic matrix elements between the initial B meson and final D meson can be parametrized in terms of the form factors $F_{0,1,T}(q^2)$ as discussed in Eqn. (1.53) of chapter 1. The expression for $F_{1,0,T}(q^2)$ form factors in terms of heavy quark effective theory form factors $(h_{\pm,T}(q^2))$ [62, 213] are given in section B.1 of Appendix B. Using Eqn. (1.53), the differential decay rate of $\bar{B} \to \bar{D} \tau \bar{\nu}_l$ process with respect to q^2 is given by [62, 213]

$$\begin{aligned}
\frac{d\Gamma\left(\bar{B} \to D\tau\bar{\nu}_l\right)}{dq^2} &= \frac{G_F^2 |V_{cb}|^2}{192\pi^3 M_B^3} q^2 \sqrt{\lambda_D\left(q^2\right)} \Big(1 - \frac{m_\tau^2}{q^2}\Big)^2 \\
&\times \left[\left|\delta_{l\tau} + C_{V_1}^l\right|^2 \left(\Big(1 + \frac{m_\tau^2}{2q^2}\Big) {H_{V,0}^s}^2 + \frac{3}{2} \frac{m_\tau^2}{q^2} {H_{V,t}^s}^2 \right) \right. \\
&+ \left. \frac{3}{2} \left|C_{S_1}^l\right|^2 {H_S^s}^2 + 3\mathrm{Re}\left[\left(\delta_{l\tau} + C_{V_1}^l\right) C_{S_1}^{l*} \right] \frac{m_\tau}{\sqrt{q^2}} H_S^s H_{V,t}^s \right], \qquad (5.6)
\end{aligned}$$

where $\lambda_D\left(q^2\right) = \left[(M_B - M_D)^2 - q^2\right]\left[(M_B + M_D)^2 - q^2\right]$ and the hadronic amplitudes $(H_{V,(0,t)}^s$ and $H_S^s)$ are given in Appendix B.

The differential decay distribution of $\bar{B} \to \bar{D}^* \tau \nu_l$ with respect to q^2 is given as [62, 213]

$$\begin{aligned}
\frac{d\Gamma\left(\bar{B} \to D^*\tau\bar{\nu}_l\right)}{dq^2} &= \frac{G_F^2 |V_{cb}|^2}{192\pi^3 M_B^3} q^2 \sqrt{\lambda_{D^*}\left(q^2\right)} \Big(1 - \frac{m_\tau^2}{q^2}\Big)^2 \\
&\times \left[\left|\delta_{l\tau} + C_{V_1}^l\right|^2 \left(\Big(1 + \frac{m_\tau^2}{2q^2}\Big) \left(H_{V,+}^2 + H_{V,-}^2 + H_{V,0}^2\right) + \frac{3}{2} \frac{m_\tau^2}{q^2} H_{V,t}^2 \right) \right. \\
&+ \left. \frac{3}{2} \left|C_{S_1}^l\right|^2 H_S^2 + 3\mathrm{Re}\left[\left(\delta_{l\tau} + C_{V_1}^l\right) C_{S_1}^{l*} \right] \frac{m_\tau}{\sqrt{q^2}} H_S H_{V,t} \right], \qquad (5.7)
\end{aligned}$$

where $H_{V,\pm}$, $H_{V,0}$, $H_{V,t}$ and H_S are the hadronic amplitudes described in section B.2 of Appendix B.

Another interesting observable, i.e., the lepton non-universality parameter, is the ratio of branching fractions of $\bar{B} \to \bar{D}^{(*)} \tau \bar{\nu}_\tau$ to $\bar{B} \to \bar{D}^{(*)} l \bar{\nu}_l$ processes, defined as [62, 108, 119, 151, 213]

$$R_{D^{(*)}} = \frac{\mathrm{BR}\left(\bar{B} \to \bar{D}^{(*)}\tau\bar{\nu}_l\right)}{\mathrm{BR}\left(\bar{B} \to \bar{D}^{(*)}l\bar{\nu}_l\right)}, \tag{5.8}$$

which probes the lepton flavor dependent term in and beyond the SM. Similarly, in the $b \to sl^+l^-$ transition, the lepton non-universality parameter is given by [218]

$$R_{K^{(*)}} = \frac{\mathrm{BR}\left(\bar{B} \to \bar{K}^{(*)}\mu^+\mu^-\right)}{\mathrm{BR}\left(\bar{B} \to \bar{K}^{(*)}e^+e^-\right)}. \tag{5.9}$$

Besides the branching ratios and lepton non-universality parameters, the following interesting observables could be sensitive to new physics.

- The τ forward-backward asymmetry in the $\bar{B} \to \bar{D}^{(*)}\tau\bar{\nu}_l$ process is defined as [62, 151]

$$A_{FB}(q^2) = \frac{b_\theta(q^2)}{d\Gamma/dq^2}, \tag{5.10}$$

  where θ is the angle between the direction of the charged lepton and the $D^{(*)}$ meson in the $\tau\bar{\nu}$ rest frame. The expression for $b_\theta(q^2)$ can be found in [62].

- τ polarization parameter is defined as [62]

$$P_\tau(q^2) = \frac{d\Gamma(\lambda_\tau = 1/2)/dq^2 - d\Gamma(\lambda_\tau = -1/2)/dq^2}{d\Gamma(\lambda_\tau = 1/2)/dq^2 + d\Gamma(\lambda_\tau = -1/2)/dq^2}, \tag{5.11}$$

  where the decay distribution $d\Gamma(\lambda_\tau = \pm 1/2)/dq^2$ is given in section B.3 of Appendix B.

- The longitudinal and transverse polarization of D^* can be defined as [151]

$$F^{D^*}_{L,T}(q^2) = \frac{d\Gamma_{L,T}\left(\bar{B} \to \bar{D}^*\tau\bar{\nu}\right)/dq^2}{d\Gamma\left(\bar{B} \to \bar{D}^*\tau\bar{\nu}\right)/dq^2}, \tag{5.12}$$

  where the subscripts L, and T denote the longitudinal and transverse components, respectively, and $d\Gamma_T/dq^2 = d\Gamma_+/dq^2 + d\Gamma_-/dq^2$. The complete expression for $d\Gamma_\pm/dq^2$ is presented in Appendix B.

- Analogous to R_{D^*}, one can also define the ratio of the longitudinal and transverse D^* polarization distribution of $\bar{B} \to \bar{D}^*\tau\bar{\nu}_l$ to the corresponding $\bar{B} \to \bar{D}^*l\bar{\nu}_l$ process as [151]

$$R^{D^*}_{L,T}(q^2) = \frac{d\Gamma_{L,T}\left(\bar{B} \to \bar{D}^*\tau\bar{\nu}\right)/dq^2}{d\Gamma_{L,T}\left(\bar{B} \to \bar{D}^*l\bar{\nu}\right)/dq^2}. \tag{5.13}$$

5.2 Numerical analysis

After getting familiar with the expressions for branching ratios and different physical observables of $\bar{B} \to \bar{D}^{(*)} l \bar{\nu}_l$ processes, we now proceed for a numerical estimation. All the particle masses and the life time of a B meson are taken from [24] and the CKM matrix element $|V_{cb}| = 0.0424(9)$ [219]. We use the numerical values of form factors from [62, 213]. To avoid rapid proton decay, we consider the $V_1(3,1,2/3)$ and $V_3(3,3,2/3)$ vector LQs which do not couple to diquark and therefore conserve baryon and lepton numbers. Chapter 2 contains a detailed discussion on these leptoquarks. Since the LQ couplings associated with both $b \to s l_i^+ l_i^-$ and $b \to c l_i \nu_i$ processes are same, one can use the constraint on new parameters obtained from $B_s \to l^+ l^-$, $\bar{B} \to X_s l^+ l^-$ and $B_u^+ \to l^+ \nu_l$ to envisage the $b \to c l \nu_l$ decay modes. Now using the constrained leptoquark parameter space as discussed in section 2.4 of chapter 2 and the Eqns. (2.17, 2.21a, 2.21b), we calculate bound on the new Wilson coefficients $C_{V_1} (C_{S_1})$. If we apply chirality on vector LQs, then C_{V_1} is the only additional Wilson coefficient to the SM. As the constraint on C_{V_1} is found to be same for both $V_{1,3}$ leptoquark, (with only a sign difference), we present the effects of only a V_3 leptoquark in our analysis.

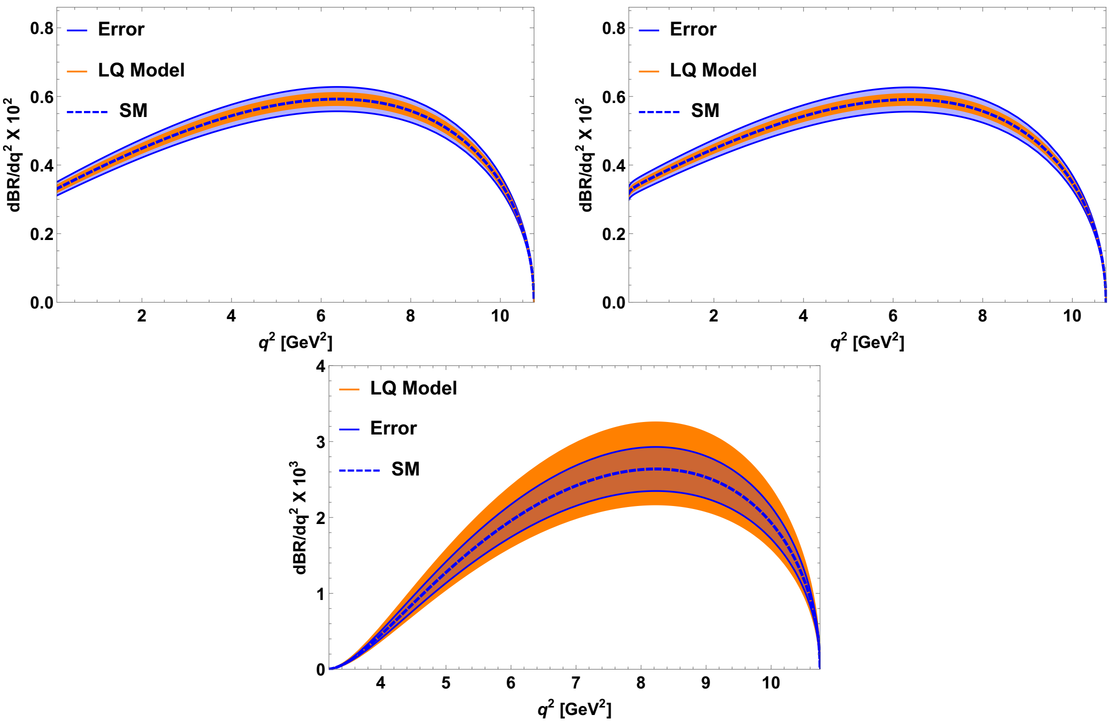

FIGURE 5.1: The variation of branching ratios of $\bar{B} \to \bar{D} e \bar{\nu}_e$ (top left panel), $\bar{B} \to \bar{D} \mu \bar{\nu}_\mu$ (top right panel) and $\bar{B} \to \bar{D} \tau \bar{\nu}_\tau$ (bottom panel) processes with respect to q^2 in the leptoquark model. Here, darker blue dashed lines are for the SM and orange bands represent the leptoquark model. The lighter blue bands stand for the theoretical uncertainties that arise due to the input parameters in the SM.

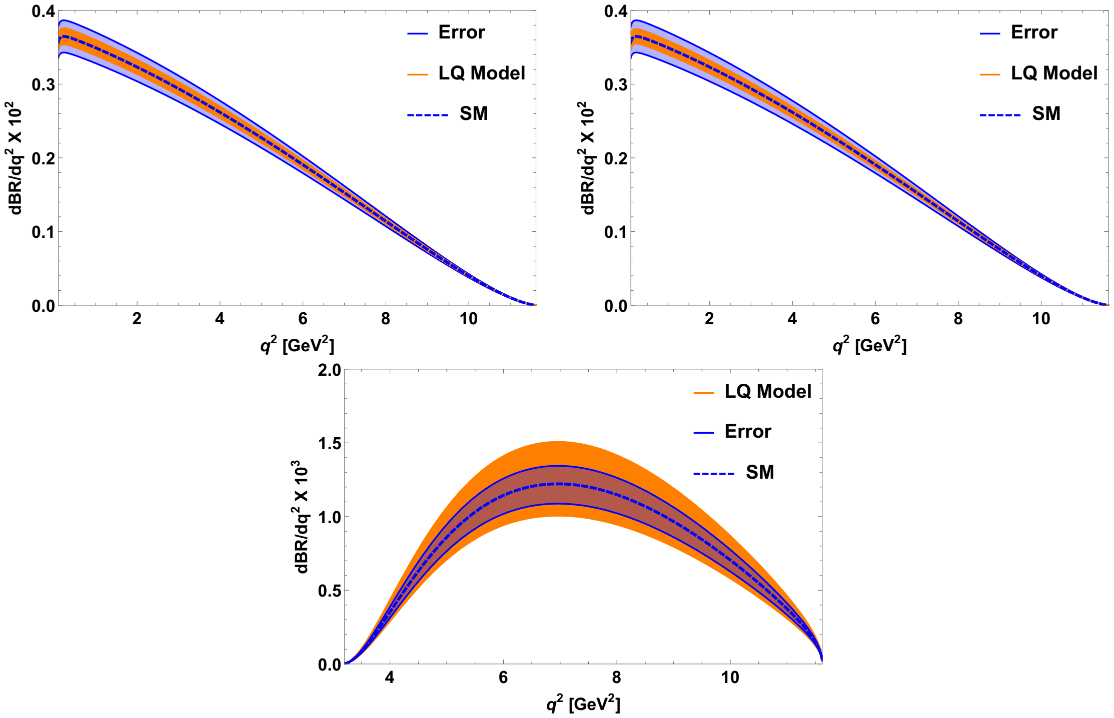

FIGURE 5.2: The variation of branching ratios of $\bar{B} \to \bar{D}^* e\bar{\nu}_e$ (top left panel), $\bar{B} \to \bar{D}^* \mu\bar{\nu}_\mu$ (top right panel) and $\bar{B} \to \bar{D}^* \tau\bar{\nu}_\tau$ (bottom panel) processes with respect to q^2 in the leptoquark model.

We show in Fig. 5.1, the branching ratio of $\bar{B} \to \bar{D} e\bar{\nu}_e$ (top left panel), $\bar{B} \to \bar{D}\mu\bar{\nu}_\mu$ (top right panel), and $\bar{B} \to \bar{D}\tau\bar{\nu}_\tau$ processes (bottom panel) with respect to q^2 in the V_3 vector LQ model. Here, darker blue dashed lines represent the SM contribution, and the orange bands are due to new physics contribution from the LQ model. The lighter blue bands correspond to the uncertainties arising in the SM due to the uncertainties associated with the CKM matrix elements and the hadronic form factors. Similarly, the q^2 variation of branching ratio of $\bar{B} \to \bar{D}^* e\bar{\nu}_e$ (top left panel), $\bar{B} \to \bar{D}^* \mu\bar{\nu}_\mu$ (top right panel) and $\bar{B} \to \bar{D}^* \tau\bar{\nu}_\tau$ (bottom panel) processes in the LQ model are presented in Fig. 5.2. The branching ratios of the $\bar{B} \to \bar{D}^{(*)} \tau\bar{\nu}_l$ process has a significant deviation from its SM value whereas the deviation in the $\bar{B} \to \bar{D}^{(*)} l\bar{\nu}_l$ process is negligible. The integrated values of branching ratios of these processes in the SM and LQ model are given in Table 5.1. In Fig. 5.3, we present the plot for the D^* polarization distributions in $\bar{B} \to \bar{D}^* l\nu_l$. The left panel of the figure is for $R_L^{D^*}$ and right panel for $R_T^{D^*}$. The predicted numerical values are given in Table 5.1. Since the LQ contribution does not affect some observables like forward-backward asymmetry, τ polarization and $F_{L,T}^{D^*}(q^2)$, we do not provide the corresponding results.

In Fig. 5.4, we show the variation of lepton non-universality parameters, $R_D(q^2)$ (left panel) and $R_{D^*}(q^2)$ (right panel) with respect to q^2, and the corresponding numerical values are presented in Table 5.2. Now using the constraints on the real and imaginary

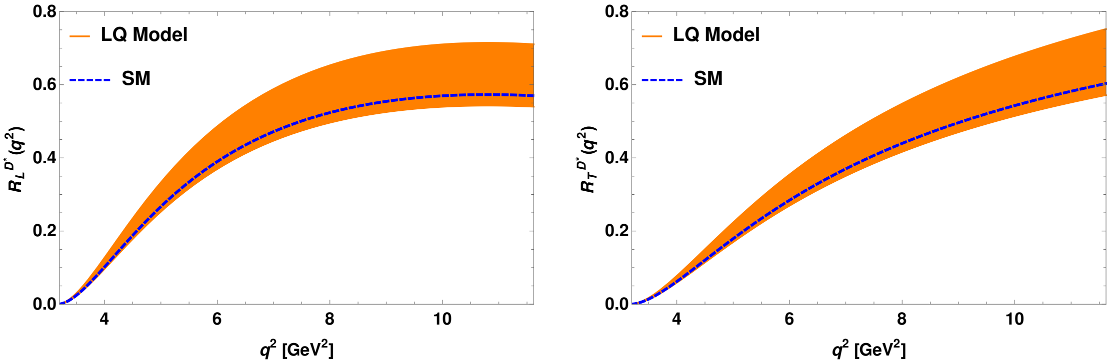

FIGURE 5.3: The plot for $R_L^{D^*}$ (left panel) and $R_T^{D^*}$ (right panel) in the leptoquark model

TABLE 5.1: The predicted values of branching ratios, forward-backward asymmetries, τ and D^* polarizations of $\bar{B} \to \bar{D}^{(*)}\tau\bar{\nu}_l$ processes in the vector leptoquark model.

Observables	SM Predictions	Values in LQ Model
$\mathrm{BR}(\bar{B} \to \bar{D} l \bar{\nu}_l)$	$(2.18 \pm 0.13) \times 10^{-2}$	$(2.13 - 2.25) \times 10^{-2}$
$\mathrm{BR}(\bar{B} \to \bar{D} \tau \bar{\nu}_l)$	$(6.75 \pm 0.08) \times 10^{-3}$	$(2.48 - 8.2) \times 10^{-3}$
$\mathrm{BR}(\bar{B} \to \bar{D}^* l \bar{\nu}_l)$	$(5.18 \pm 0.31) \times 10^{-2}$	$(5.04 - 5.32) \times 10^{-2}$
$\mathrm{BR}(\bar{B} \to \bar{D}^* \tau \bar{\nu}_l)$	$(1.33 \pm 0.14) \times 10^{-2}$	$(1.3 - 1.6) \times 10^{-2}$
$R_L^{D^*}$	0.227	$0.215 - 0.283$
$R_T^{D^*}$	0.29	$0.274 - 0.36$

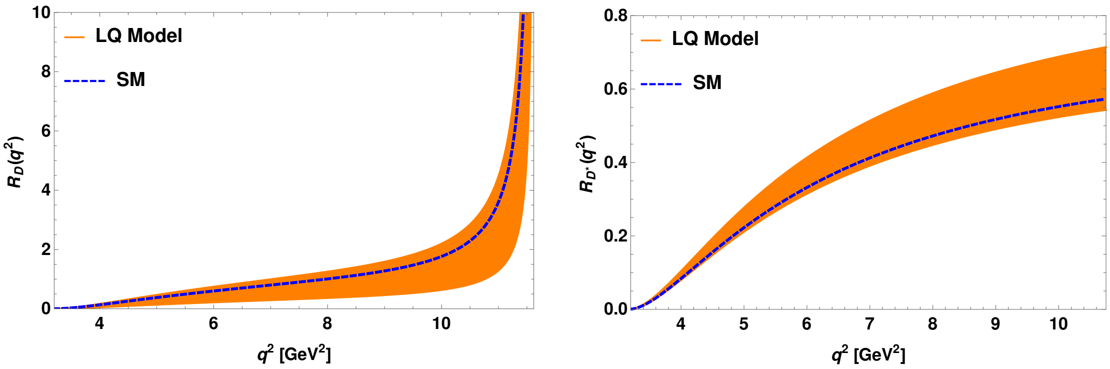

FIGURE 5.4: The q^2 variation of lepton non-universality $R_D(q^2)$ (left panel) and $R_{D^*}(q^2)$ (right panel) in leptoquark model.

part of the LQ couplings as given in Tables 2.6, 2.7 and 2.8, and the Eqns. (2.15, 2.20a, 2.20b, 2.20c, 2.20d), we compute the constraint on the new $C_{9,10,S,P}^{(\prime)\mathrm{LQ}}$ Wilson coefficients. Using the constrained parameters, the plot for $R_K^{\mu e}(q^2)$ in low q^2 (left panel) and in high q^2 (right panel) are presented in Fig. 5.5. Fig. 5.6 shows the $R_{K^*}^{\mu e}(q^2)$ anomaly plots in low q^2 (left panel) and high q^2 (right panel) in the LQ model. The predicted numerical values of lepton non-universality ($R_{K^{(*)}}$) are given in Table 5.2. From Table 5.2, one can see that, the predicted values of lepton non-universality parameters in the LQ model have significant deviation from the SM and are within the 1σ range of experimental

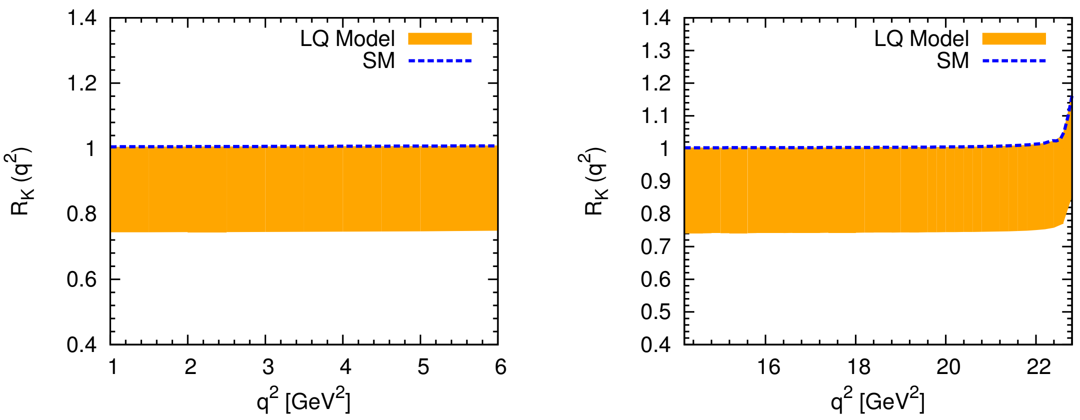

FIGURE 5.5: The plot for $R_K^{\mu e}(q^2)$ in low q^2 (left panel) and high q^2 (right panel) in the leptoquark model.

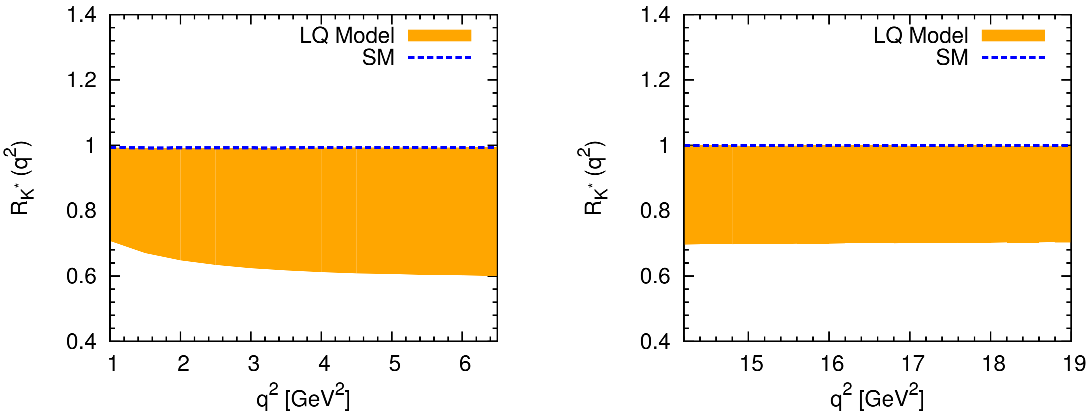

FIGURE 5.6: The plot for $R_{K^*}^{\mu e}(q^2)$ in low q^2 (left panel) and high q^2 (right panel) in the leptoquark model.

limit. We observe that the addition of the new vector LQ can explain both the $R_{D^{(*)}}$ and $R_{K^{(*)}}$ anomalies very well.

TABLE 5.2: The predicted values of $R_{D^{(*)}}$ and $R_{K^{(*)}}$ in the vector leptoquark model.

Observables	SM Predictions	Values in LQ Model	Experimental Limit
R_D	0.31	$0.11 - 0.386$	$0.397 \pm 0.040 \pm 0.028$
R_{D^*}	0.26	$0.243 - 0.32$	$0.316 \pm 0.016 \pm 0.010$
${R_K}^{\mu e}_{q^2\in[1,6]}$	1.006	$0.75 - 1.006$	$0.745^{+0.090}_{-0.074} \pm 0.036$
${R_K}^{\mu e}_{q^2\geq 14.18}$	1.004	$0.74 - 1.004$	$\cdots$
${R_{K^*}}^{\mu e}_{q^2\in[1,6]}$	0.996	$0.725 - 0.996$	$\cdots$
${R_{K^*}}^{\mu e}_{q^2\geq 14.18}$	0.999	$0.816 - 0.999$	$\cdots$

5.3 Chapter summary

To summarize, we considered the vector leptoquark model to explain the anomalies observed in the semileptonic $\bar{B} \to \bar{D}^{(*)}\tau\bar{\nu}_l$ decay processes in light of the recent B factories result, especially the deviation of $R_{D^{(*)}}$ observables from the SM predictions. There are two relevant vector leptoquark ($V_{1,3}$) states which conserve baryon and lepton numbers and can simultaneously explain the processes mediated by quark level transitions $b \to cl\bar{\nu}_l$ and $b \to sl^+l^-$. Using the constrained leptoquark couplings obtained from the branching ratios of $B_s \to l^+l^-$, $\bar{B} \to X_s l^+l^-(\nu\bar{\nu})$ and $B_u^+ \to l^+\nu_l$ processes, where l is any charged lepton, we estimated the branching ratios, forward-backward asymmetries, lepton non-universality, τ and D^* polarization parameters in the $\bar{B} \to \bar{D}^{(*)}l\bar{\nu}_l$ processes. We looked into the lepton non-universality parameters in both $\bar{B} \to \bar{D}^{(*)}l\bar{\nu}_l$ and $\bar{B} \to \bar{K}^{(*)}l^+l^-$ processes and found that both the $R_{K^{(*)}}$ and $R_{D^{(*)}}$ anomalies could be explained by $V_{1,3}$ vector leptoquarks. The observation of these processes at LHCb and Belle II in near future could manifest NP beyond the SM.

Chapter 6

Rare lepton flavor violating decay processes of B meson with vector leptoquark couplings

This chapter comprises the rare lepton flavor violating decay processes of B meson. The observation of neutrino oscillation has provided unambiguous evidence for lepton number violation in the neutral lepton sector, even though the individual lepton number is conserved in the SM of the electroweak interaction. The observation of the neutrino masses and mixing and the violation of family lepton number could in principle allow FCNC transitions in the charged lepton and B sector as well, such as $l_i \to l_j \gamma$, $l_i \to l_j l_k \bar{l}_k$, $B_s \to l_i^\mp l_j^\pm$ and $B \to K^{(*)} l_i^\mp l_j^\pm$ etc. It is interesting to see if these branching ratios could be enhanced in some new physics model which could simultaneously explain the observed anomalies. LHCb has already reported violation of lepton universality in the $B \to K l^+ l^-$ process having deviation from the SM by 2.6σ, which in turn hints at the possibility of observing lepton flavor violating decays as well. As pointed out in Ref. [220], a possible explanation for the observed LHCb anomaly on R_K, i.e., the lepton non-universality parameter, is due to a 25% deficit in the muon channel, which indicates that LFV effects could be larger for muons than for electrons. In recent times, the CMS Collaboration [221] has reported 2.6σ discrepancy in the branching ratio of lepton flavor violating $h \to \tau\mu$ decay $\text{BR}(h \to \tau\mu)|^{\text{Expt}} = 0.84^{+0.39}_{-0.37}$, from the SM value. In the SM, there are no intermediate states which can decay into two leptons belonging to different generations. Therefore, LFV decays have no long distance QCD contributions and no dominant charmonium resonance background like the $\bar{B} \to \bar{K}^{(*)} l^+ l^-$ processes and hence, the background suppression for these channels would be relatively low. The LFV decays in the charged lepton sector have been studied in various new physics models in the literature [109–111, 222–225]. Even though there is no direct experimental evidence for such processes, there exist severe constraints on some of these LFV modes [24]. The experimental observation of lepton flavor violating decays would provide unambiguous signal of new physics beyond the SM.

To understand the origin of the current anomalies observed at LHCb experiment in a particular theoretical framework, we extend the SM by adding a single vector LQ. The baryon number conserving LQs avoid proton decay and could be light enough to be seen in the current experiments. Thus, in this work, we consider the singlet $(3, 1, 2/3)$ and triplet $(3, 3, 2/3)$ vector LQs, which are invariant under the SM $SU(3)_C \times SU(2)_L \times U(1)_Y$ gauge group and conserve both the baryon and lepton numbers. In addition to the (axial)vector operators, these LQs also provide the (pseudo)scalar operators to the SM. In this chapter, we are interested to investigate the LFV B meson decays such as $B^+ \to K^+(\pi^+) l_i^- l_j^+$ processes in the vector LQ model. These decay processes are extremely rare in the SM as they are either two loop suppressed or proceed through box diagrams with the presence of tiny neutrino masses in the loop. However, in the leptoquark model, they can occur at the tree level and, hence, can give an observable signature in the LHCb experiment. Fig. 6.1 depicts the tree level Feynman diagram for the LFV processes $b \to q_k l_i^- l_j^+$ mediated by the vector LQ, where LQ can couple to a quark and a lepton simultaneously. In this figure, i, j denote the lepton family numbers and k represent the quark family.

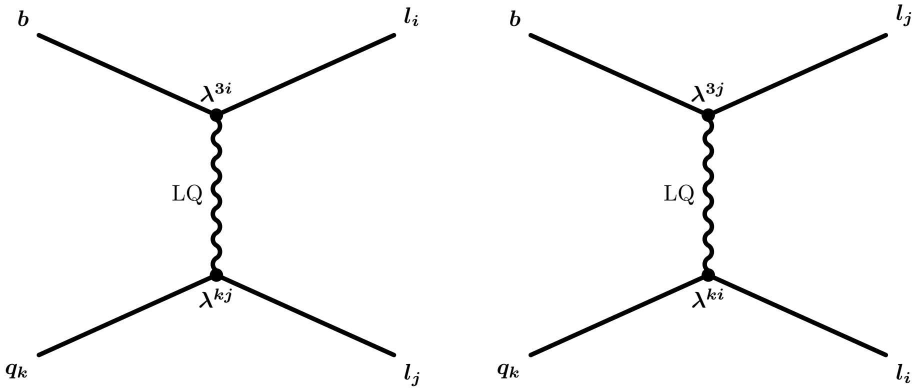

FIGURE 6.1: Feynman diagrams for lepton flavor violating $b \to q_k l_i^- l_j^+$ process (left panel) and $b \to q_k l_i^+ l_j^-$ (right panel) mediated by vector leptoquark, where $l = e, \mu, \tau$.

6.1 The effective Hamiltonian for $b \to q l_i^- l_j^+$ decays

This section presents the effective Hamiltonian mediating the rare semileptonic lepton flavor violating decays, $b \to q l_i^- l_j^+$, where $q = s, d$. We will emphasize mainly on the effective Hamiltonian of $b \to s l_i^- l_j^+$ process as one can obtain the Hamiltonian for the

$b \to d l_i^- l_j^+$ transition by incorporating clear-cut replacements in $b \to s$ Hamiltonian. In the SM, the effective Hamiltonian for $b \to s l_i^- l_j^+$ $(l = e, \mu, \tau)$ process is given by [56, 57]

$$\begin{aligned} \mathcal{H}_{\text{eff}}^{\text{SM}} &= -\frac{4G_F}{\sqrt{2}} V_{ts}^* V_{tb} \Big[\sum_{i=1}^{6} C_i(\mu) \mathcal{O}_i(\mu) + C_7^{\text{SM}} \frac{e}{16\pi^2} \left[\bar{s}\sigma_{\mu\nu}(m_s L + m_b R) b\right] F^{\mu\nu} \\ &\quad + C_9^{\text{SM}} \frac{\alpha_{\text{em}}}{4\pi} (\bar{s}\gamma^\mu L b) L_{ij}^\mu + C_{10}^{\text{SM}} \frac{\alpha_{\text{em}}}{4\pi} (\bar{s}\gamma^\mu L b) L_{ij}^{5\mu} \Big], \end{aligned} \tag{6.1}$$

where $L_{ij}^\mu = \bar{l}_i \gamma_\mu l_j$ and $L_{ij}^{5\mu} = \bar{l}_i \gamma_\mu \gamma_5 l_j$. Here, $C_{7,9,10}^{\text{SM}}$ are the SM Wilson coefficients for $i = j$ and for $i \neq j$ these coefficients will vanish.

The total effective Hamiltonian for processes involving $b \to s l_i^- l_j^+$ transition, in the presence of new physics operators with all the possible Lorentz structure, can be expressed as

$$\mathcal{H}_{\text{eff}}\left(b \to s l_i^- l_j^+\right) = \mathcal{H}_{\text{eff}}^{\text{SM}} + \mathcal{H}_{\text{eff}}^{\text{VA}} + \mathcal{H}_{\text{eff}}^{\text{SP}} + \mathcal{H}_{\text{eff}}^{T}, \tag{6.2}$$

where $\mathcal{H}_{\text{eff}}^{\text{SM}}$ is the SM effective Hamiltonian as given in Eqn. (6.1), and the NP contributions are given as

$$\begin{aligned} \mathcal{H}_{\text{eff}}^{\text{VA}} &= -N_F \Big[C_9 (\bar{s}\gamma^\mu L b) L_{ij}^\mu + C_{10} (\bar{s}\gamma^\mu L b) L_{ij}^{5\mu} + C_9' (\bar{s}\gamma^\mu R b) L_{ij}^\mu \\ &\quad + C_{10}' (\bar{s}\gamma^\mu R b) L_{ij}^{5\mu} \Big], \end{aligned} \tag{6.3}$$

$$\mathcal{H}_{\text{eff}}^{\text{SP}} = -N_F \Big[C_S (\bar{s} R b) L_{ij} + C_P (\bar{s} R b) L_{ij}^5 + C_S' (\bar{s} L b) L_{ij} + C_P' (\bar{s} L b) L_{ij}^5 \Big], \tag{6.4}$$

$$\mathcal{H}_{\text{eff}}^{T} = -N_F \Big[2C_T (\bar{s}\sigma_{\mu\nu} b) L_{ij}^{\mu\nu} + i 2 C_{T5} (\bar{s}\sigma_{\mu\nu} b) L_{ij}^{\mu\nu 5} \Big], \tag{6.5}$$

where $N_F = (G_F \alpha_{\text{em}} V_{tb} V_{ts}^*)/\sqrt{2}\pi$, $L_{ij}^5 = \bar{l}_i \gamma_5 l_j$, and $L_{ij}^{\mu\nu 5} = 2i \bar{l}_i \sigma^{\mu\nu} \gamma_5 l_j$. Here we use $\sigma^{\mu\nu}\gamma_5 = -\frac{i}{2}\epsilon^{\mu\nu\alpha\beta}\sigma_{\alpha\beta}$ to calculate $L_{ij}^{\mu\nu 5}$. The contributions from the primed operators, C_i', where $i = 9, 10, S, P$ as well as the scalar, pseudoscalar and tensor operators are absent in the SM and arise only in scenarios beyond the standard model.

6.2 $\bar{B} \to \bar{K}(\bar{\pi}) l_i l_j$ processes

Here, we will discuss the lepton flavor violating semileptonic B meson decays to pseudoscalar mesons K and π, which are mediated by the $b \to q l_i^- l_j^+$ quark level transition. As discussed earlier, these processes occur at tree level due to the exchange of vector LQ. The relevant kinematical variables describing the three-body decays are the invariant mass squared of the lepton pair q^2 and the polar angle θ_l. The differential decay distribution for the process $\bar{B} \to \bar{K} l_i l_j$ with respect to q^2 and $\cos\theta_l$ can be written as

$$\frac{d^2\Gamma}{dq^2 d\cos\theta_l} = \frac{G_F^2 \alpha_{\rm em}^2 \beta_{ij} \sqrt{\lambda} |V_{tb} V_{ts}^*|^2}{2^{12}\pi^5 M_B^3} \sum_{i=1}^{12} I_i\left(\cos\theta_l\right), \tag{6.6}$$

where $\lambda = \lambda\left(M_B^2, M_K^2, q^2\right)$ and $\beta_{ij} = \sqrt{\left(1 - \frac{(m_i+m_j)^2}{q^2}\right)\left(1 - \frac{(m_i-m_j)^2}{q^2}\right)}$. The twelve angular coefficients $I_i(\cos\theta_l)$ appearing in the angular distribution depend on the couplings, kinematic variables, form factors and the polar angle θ_l, which are defined as

$$\begin{aligned}
I_1 &= 2\Bigg[\left(1 - \frac{(m_i - m_j)^2}{q^2}\right)\left(q^2 - \left(q^2 - (m_i + m_j)^2\right)\cos^2\theta_l\right)|H_V^0|^2 \\
&\quad + 4k\frac{(m_i^2 - m_j^2)}{\sqrt{q^2}}{\rm Re}\left[H_V^0 H_V^{t^*}\right]\cos\theta_l + \frac{(m_i - m_j)^2}{q^2}\left(q^2 - (m_i + m_j)^2\right)|H_V^t|^2\Bigg], && (6.7a)\\
I_2 &= 2\Bigg[\left(1 - \frac{(m_i + m_j)^2}{q^2}\right)\left(q^2 - \left(q^2 - (m_i - m_j)^2\right)\cos^2\theta_l\right)|H_A^0|^2 \\
&\quad + 4k\frac{(m_i^2 - m_j^2)}{\sqrt{q^2}}{\rm Re}\left[H_A^0 H_A^{t^*}\right]\cos\theta_l + \frac{(m_i + m_j)^2}{q^2}\left(q^2 - (m_i - m_j)^2\right)|H_A^t|^2\Bigg], && (6.7b)\\
I_3 &= 2\left(q^2 - (m_i + m_j)^2\right)|H_S|^2, && (6.7c)\\
I_4 &= 2\left(q^2 - (m_i - m_j)^2\right)|H_P|^2, && (6.7d)\\
I_5 &= 8\left(1 - \frac{(m_i - m_j)^2}{q^2}\right)\left[(m_i + m_j)^2 + \left(q^2 - (m_i + m_j)^2\right)\cos^2\theta_l\right]|H_T^{0t}|^2, && (6.7e)\\
I_6 &= 32\left(1 - \frac{(m_i + m_j)^2}{q^2}\right)\left[(m_i - m_j)^2 + \left(q^2 - (m_i - m_j)^2\right)\cos^2\theta_l\right]|H_{TE}^{0t}|^2, && (6.7f)\\
I_7 &= 4{\rm Re}\Big[2k\left(m_i + m_j\right)H_V^0 H_S^*\cos\theta_l \\
&\quad + \frac{(m_i - m_j)}{\sqrt{q^2}}\left(q^2 - (m_i + m_j)^2\right)H_V^t H_S^*\Big], && (6.7g)\\
I_8 &= 4{\rm Re}\Big[2k\left(m_i - m_j\right)H_A^0 H_P^*\cos\theta_l \\
&\quad + \frac{(m_i + m_j)}{\sqrt{q^2}}\left(q^2 - (m_i - m_j)^2\right)H_A^t H_P^*\Big], && (6.7h)\\
I_9 &= -8{\rm Re}\Big[2k\left(m_i - m_j\right)H_V^t H_T^{0t^*}\cos\theta_l \\
&\quad + \frac{(m_i + m_j)}{\sqrt{q^2}}\left(q^2 - (m_i - m_j)^2\right)H_V^0 H_T^{0t^*}\Big], && (6.7i)\\
I_{10} &= 16{\rm Re}\Big[2k\left(m_i + m_j\right)H_A^t H_{TE}^{0t^*}\cos\theta_l \\
&\quad + \frac{(m_i - m_j)}{\sqrt{q^2}}\left(q^2 - (m_i + m_j)^2\right)H_0^t H_{TE}^{0t^*}\Big], && (6.7j)\\
I_{11} &= -16k\sqrt{q^2}{\rm Re}[H_S H_T^{0t^*}]\cos\theta_l, && (6.7k)\\
I_{12} &= 32k\sqrt{q^2}{\rm Re}[H_P H_{TE}^{0t^*}]\cos\theta_l, && (6.7l)
\end{aligned}$$

where $k = (\beta_{ij}\sqrt{q^2})/2$ is the lepton momentum. Here, H_i $(i = V, A, P, T, TE)$ are the helicity amplitudes, given as

$$H_V^0 = \sqrt{\frac{\lambda}{q^2}}\Big[\left(C_9^{\rm SM} + C_9 + C_9'\right) F_1(q^2) + 2C_7^{\rm SM} m_b \frac{F_T}{M_B + M_K}\Big], \tag{6.8a}$$

$$H_V^t = \frac{M_B^2 - M_K^2}{\sqrt{q^2}}\left(C_9^{\rm SM} + C_9 + C_9'\right) F_0(q^2), \tag{6.8b}$$

$$H_A^0 = \sqrt{\frac{\lambda}{q^2}}\left(C_{10}^{\rm SM} + C_{10} + C_{10}'\right) F_1(q^2), \tag{6.8c}$$

$$H_A^t = \frac{M_B^2 - M_K^2}{\sqrt{q^2}}\left(C_{10}^{\rm SM} + C_{10} + C_{10}'\right) F_0(q^2), \tag{6.8d}$$

$$H_S = \frac{M_B^2 - M_K^2}{m_b}\left(C_S + C_S'\right) F_0\left(q^2\right), \tag{6.8e}$$

$$H_P = \frac{M_B^2 - M_K^2}{m_b}\left(C_P + C_P'\right) F_0\left(q^2\right), \tag{6.8f}$$

$$H_T^{0t} = -2C_T \frac{\sqrt{\lambda}}{M_B + M_K} F_T(q^2), \tag{6.8g}$$

$$H_{T5}^{0t} = -2C_{T5} \frac{\sqrt{\lambda}}{M_B + M_K} F_T(q^2). \tag{6.8h}$$

If we integrate out the angle θ_l in Eqn. (6.6) in its kinematically accessible physical range, we will get the differential decay rate for $\bar{B} \to \bar{K} l_i l_j$ process with respect to the dilepton mass squared q^2, which is given by

$$\frac{d\Gamma}{dq^2} = \frac{G_F^2 \alpha_{\rm em}^2 \beta_{ij} \sqrt{\lambda} |V_{tb} V_{ts}^*|^2}{2^{12} \pi^5 M_B^3} \sum_{i=1}^{10} J_i, \tag{6.9}$$

where the expression for coefficients $J_i = \int_{-1}^{1} I_i\left(\cos\theta_l\right) d\cos\theta_l$ are given as

$$\begin{aligned}
J_1 &= 4\Bigg[\left(1-\frac{(m_i-m_j)^2}{q^2}\right)\frac{1}{3}\left(2q^2+(m_i+m_j)^2\right)|H_V^0|^2 \\
&\quad +\frac{(m_i-m_j)^2}{q^2}\left(q^2-(m_i+m_j)^2\right)|H_V^t|^2\Bigg], && (6.10)\\
J_2 &= 4\Bigg[\left(1-\frac{(m_i+m_j)^2}{q^2}\right)\frac{1}{3}\left(2q^2+(m_i-m_j)^2\right)|H_A^0|^2 \\
&\quad +\frac{(m_i+m_j)^2}{q^2}\left(q^2-(m_i-m_j)^2\right)|H_A^t|^2\Bigg], && (6.11)\\
J_3 &= 4\left(q^2-(m_i+m_j)^2\right)|H_S|^2, && (6.12)\\
J_4 &= 4\left(q^2-(m_i-m_j)^2\right)|H_P|^2, && (6.13)\\
J_5 &= 16\left(1-\frac{(m_i-m_j)^2}{q^2}\right)\frac{1}{3}\left(2\left(m_i+m_j\right)^2+q^2\right)|H_T^{0t}|^2, && (6.14)\\
J_6 &= 64\left(1-\frac{(m_i+m_j)^2}{q^2}\right)\frac{1}{3}\left(2\left(m_i-m_j\right)^2+q^2\right)|H_{TE}^{0t}|^2, && (6.15)\\
J_7 &= 8\frac{(m_i-m_j)}{\sqrt{q^2}}\left(q^2-(m_i+m_j)^2\right)\mathrm{Re}[H_V^t H_S^*], && (6.16)\\
J_8 &= 8\frac{(m_i+m_j)}{\sqrt{q^2}}\left(q^2-(m_i-m_j)^2\right)\mathrm{Re}[H_A^t H_P^*], && (6.17)\\
J_9 &= -16\frac{(m_i+m_j)}{\sqrt{q^2}}\left(q^2-(m_i-m_j)^2\right)\mathrm{Re}[H_V^0 H_T^{0t^*}], && (6.18)\\
J_{10} &= 32\frac{(m_i-m_j)}{\sqrt{q^2}}\left(q^2-(m_i+m_j)^2\right)\mathrm{Re}[H_0^t H_{TE}^{0t^*}]. && (6.19)
\end{aligned}$$

Here the coefficients $J_{11} = J_{12} = 0$. Another interesting observable is the zero-crossing of the forward-backward asymmetry, wherein the position of the zero value of the forward-backward asymmetry parameter (A_{FB}) is very useful to look for the NP signal. The lepton forward-backward asymmetry parameter is obtained by integrating over $\cos\theta_l$ in Eqn. (6.6). After integration, we obtain

$$A_{FB}(q^2) = \frac{X}{\sum_{i=1}^{10} J_i}, \qquad (6.20)$$

where the numerator X is defined as

$$\begin{aligned}
X &= 8k\mathrm{Re}\Big[\frac{\left(m_i^2-m_j^2\right)}{\sqrt{q^2}}\left(H_V^0 H_V^{t*}+H_A^0 H_A^{t*}\right)+\left(m_i+m_j\right)\left(H_V^0 H_S^*+4H_A^t H_{TE}^{0t^*}\right) \\
&+ \left(m_i-m_j\right)\left(H_A^0 H_P^*-2H_V^t H_T^{0t^*}\right)-2\sqrt{q^2}\left(H_S^0 H_T^{0t^*}-2H_P H_{TE}^{0t^*}\right)\Big]. \qquad (6.21)
\end{aligned}$$

Recently LHCb has observed 2.6σ discrepancy from the SM prediction in the measurement of the ratio of the branching fractions of the $B^+ \to K^+ l^+ l^-$ decays into dimuons over dielectrons in the dilepton invariant mass bin $(1 \le q^2 \le 6)$ GeV^2. Analogously, we would like to see whether it would be possible to observe the lepton non-universality effects in semileptonic LFV decays. Therefore, we define the following parameters as the ratios of branching fractions of several LFV processes as

$$R_{Kl}^{\mu e} = \frac{\text{BR}\left(B^+ \to K^+\mu^- e^+\right)}{\text{BR}\left(B^+ \to K^+ l^+ l^-\right)}, \tag{6.22}$$

$$R_{Kl}^{\tau e} = \frac{\text{BR}\left(B^+ \to K^+\tau^- e^+\right)}{\text{BR}\left(B^+ \to K^+ l^+ l^-\right)}, \tag{6.23}$$

$$R_{Kl}^{\tau \mu} = \frac{\text{BR}\left(B^+ \to K^+\tau^- \mu^+\right)}{\text{BR}\left(B^+ \to K^+ l^+ l^-\right)}, \tag{6.24}$$

$$R_{K}^{\mu \mu} = \frac{\text{BR}\left(B^+ \to K^+\mu^+ \mu^-\right)}{\text{BR}\left(B^+ \to K^+ e^+ e^-\right)}, \tag{6.25}$$

$$R_{Kl}^{\tau \tau} = \frac{\text{BR}\left(B^+ \to K^+\tau^+ \tau^-\right)}{\text{BR}\left(B^+ \to K^+ l^+ l^-\right)}, \tag{6.26}$$

where $l = \mu, e$. Similarly, one can obtain the branching ratios and other physical observables in $B \to \pi l_i^- l_j^+$ processes by incorporating the appropriate CKM matrix elements, form factors and the NP effective couplings. The ratio of branching ratios of $B^+ \to \pi^+\mu^+\mu^-$ and $B^+ \to K^+\mu^+\mu^-$ has recently been measured by LHCb experiments [226] as

$$\frac{\text{BR}(B^+ \to \pi^+\mu^+\mu^-)}{\text{BR}(B^+ \to K^+\mu^+\mu^-)} = 0.053 \pm 0.014(\text{stat}) \pm 0.001 \text{ (syst)}. \tag{6.27}$$

Analogously, one can also define the ratio of branching fractions of $B^+ \to \pi^+ l_i^- l_j^+$ and $B^+ \to K^+ l_i^- l_j^+$ LFV processes as

$$R_+^{l_i l_j} = \frac{\text{BR}\left(B^+ \to \pi^+ l_i^- l_j^+\right)}{\text{BR}\left(B^+ \to K^+ l_i^- l_j^+\right)}. \tag{6.28}$$

6.3 Numerical analysis

After obtaining the expression for the branching ratio and various observables of the $B^+ \to K^+(\pi^+) l_i^- l_j^+$ processes, we will proceed for numerical estimations. The LFV B meson decays have no contributions from SM Wilson coefficients. Including the contributions from the vector LQ, the modified helicity amplitudes are given as

$$H_V^{0\text{LQ}} = \sqrt{\frac{\lambda}{q^2}} \left(C_9^{\text{LQ}} + C_9^{\prime\text{LQ}} \right) F_1(q^2), \tag{6.29a}$$

$$H_V^{t\text{LQ}} = \frac{M_B^2 - M_K^2}{\sqrt{q^2}} \left(C_9^{\text{LQ}} + C_9^{\prime\text{LQ}} \right) F_0(q^2), \tag{6.29b}$$

$$H_A^{0\text{LQ}} = \sqrt{\frac{\lambda}{q^2}} \left(C_{10}^{\text{LQ}} + C_{10}^{\prime\text{LQ}} \right) F_1(q^2), \tag{6.29c}$$

$$H_A^{t\text{LQ}} = \frac{M_B^2 - M_K^2}{\sqrt{q^2}} \left(C_{10}^{\text{LQ}} + C_{10}^{\prime\text{LQ}} \right) F_0(q^2), \tag{6.29d}$$

$$H_S^{\text{LQ}} = \frac{M_B^2 - M_K^2}{m_b} \left(C_S^{\text{LQ}} + C_S^{\prime\text{LQ}} \right) F_0(q^2), \tag{6.29e}$$

$$H_P^{\text{LQ}} = \frac{M_B^2 - M_K^2}{m_b} \left(C_P^{\text{LQ}} + C_P^{\prime\text{LQ}} \right) F_0(q^2). \tag{6.29f}$$

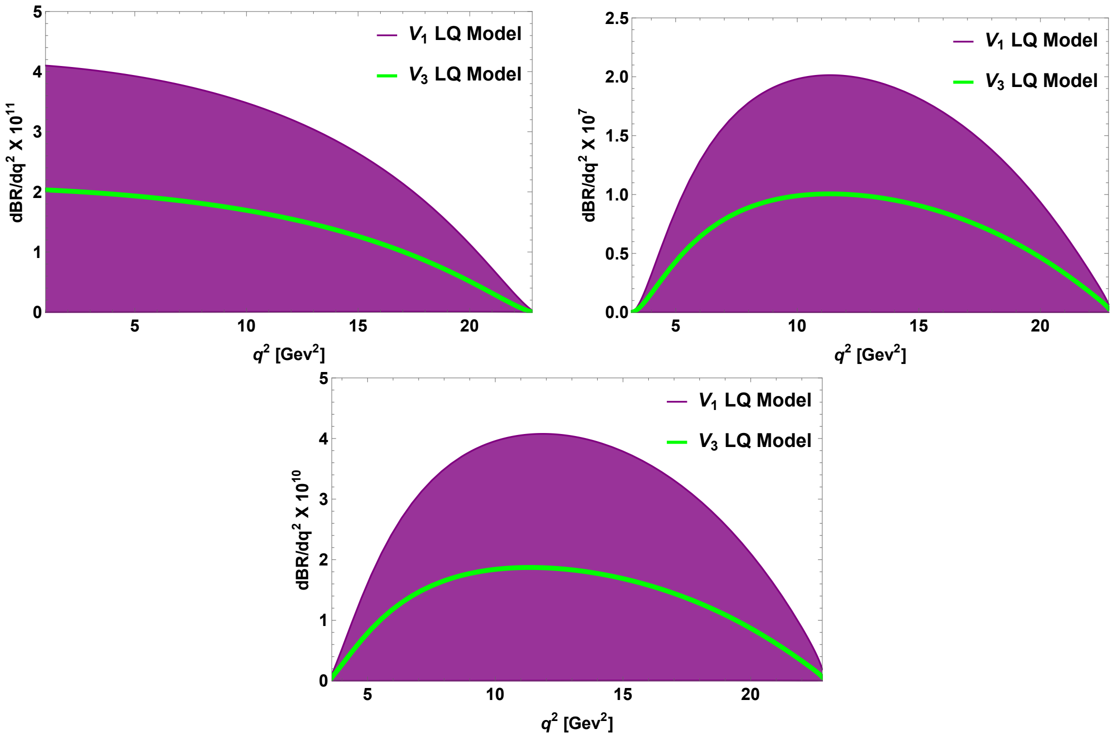

FIGURE 6.2: The variation of branching ratios of $B^+ \to K^+\mu^-e^+$ (top left panel), $B^+ \to K^+\tau^-e^+$ (top right panel) and $B^+ \to K^+\tau^-\mu^+$ (bottom panel) processes with respect to q^2 in the $V_{1,3}$ vector leptoquark model. In each plot, the purple band represents the $V_1(3,1,2/3)$ vector leptoquark contribution and the green solid line is for the $V_3(3,3,2/3)$ leptoquark model.

The particle masses and life times of the B_q mesons are taken from [98]. The form factors ($F_{0,1,T}$) for the kaon and pion are taken from [227] and [228], respectively. For the analysis of these LFV processes, we consider the LQ couplings as real. In order to compute the required LQ couplings, we use the values of the couplings extracted from $B_{s,d} \to l^+l^-$, as given in Table 2.4 and 2.5. Although the bounds obtained from $K_L \to$

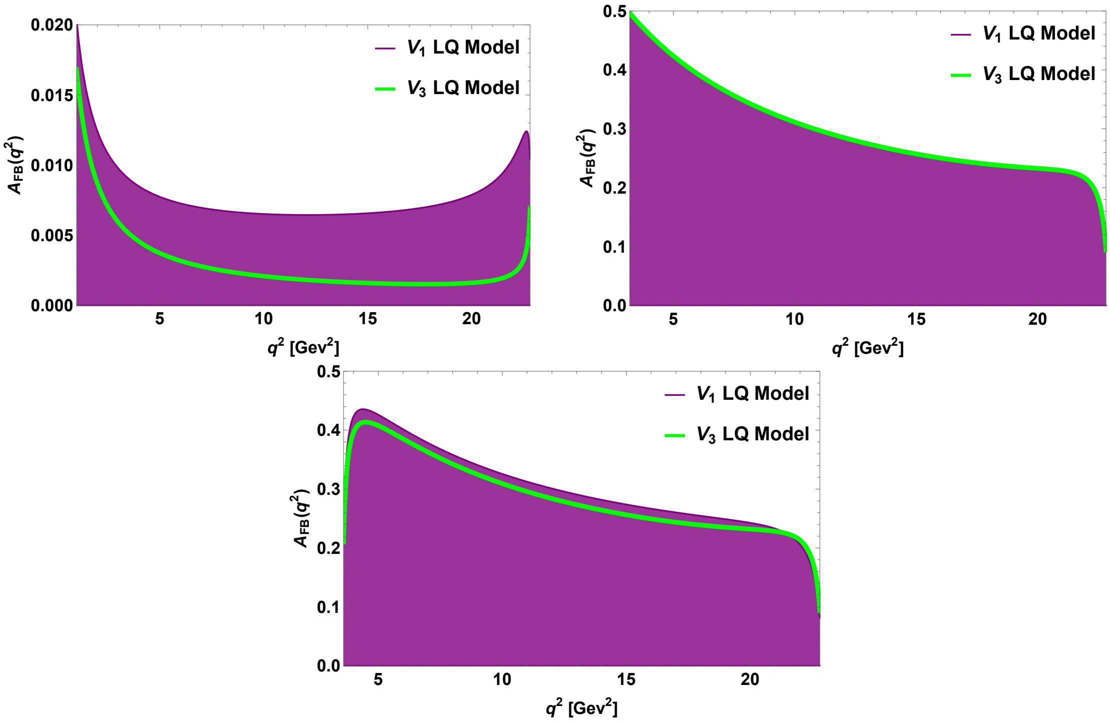

FIGURE 6.3: The forward-backward asymmetry variation of $B^+ \to K^+\mu^-e^+$ (top left panel), $B^+ \to K^+\tau^-e^+$ (top right panel) and $B^+ \to K^+\tau^-\mu^+$ (bottom panel) processes with respect to q^2 for $V_{1,3}$ vector leptoquark exchange.

l^+l^- processes (2.98) are little stronger than the bounds obtained from $B_{s,d} \to l^+l^-$, only the Real part of the couplings can be constrained there. The bounds obtained from $\tau^- \to l^-\gamma$ processes are comparatively weak. Therefore, for numerical estimation in the leptoquark model, we use the constrained leptoquark couplings obtained from the process $B_s \to l^+l^-$ as given in Table 2.4 and 2.5 and assume that the coupling between different generation of quarks and leptons follow the simple scaling law, i.e., $(\lambda_{LL(RR)})_{ij} = (m_i/m_j)^{1/2}(\lambda_{LL(RR)})_{ii}$ with $j > i$. As discussed in [131, 229, 230], such pattern of ansatz can explain the decay widths of radiative LFV decay $\mu \to e\gamma$. Now using such ansatz, we compute the branching ratios, forward-backward asymmetry and lepton non-universality parameters for $\bar{B} \to \bar{K}(\bar{\pi})l_i^-l_j^+$ decays. We show in Fig. 6.2, the variation of the differential branching ratios of the $B^+ \to K^+\mu^-e^+$ (top left panel), $B^+ \to K^+\tau^-e^+$ (top right panel) and $B^+ \to K^+\tau^-\mu^+$ (bottom panel) processes with respect to q^2 in the full physical region for both $V_{1,3}$ vector leptoquark exchange. Here the purple bands and green solid lines represent the allowed range of the branching ratio of semileptonic LFV decays $B^+ \to K^+l_i^-l_j^+$ induced by the V_1 and V_3 vector leptoquark, respectively. The predicted branching ratios of $B^+ \to K^+l_i^-l_j^+$ LFV decays in respective physical range in both the LQ model and their corresponding experimental upper limits are presented in Table 6.1. In Fig. 6.3, the variation of forward-backward asymmetry for $B^+ \to K^+\mu^-e^+$ (top left panel), $B^+ \to K^+\tau^-e^+$ (top right panel) and $B^+ \to K^+\tau^-\mu^+$

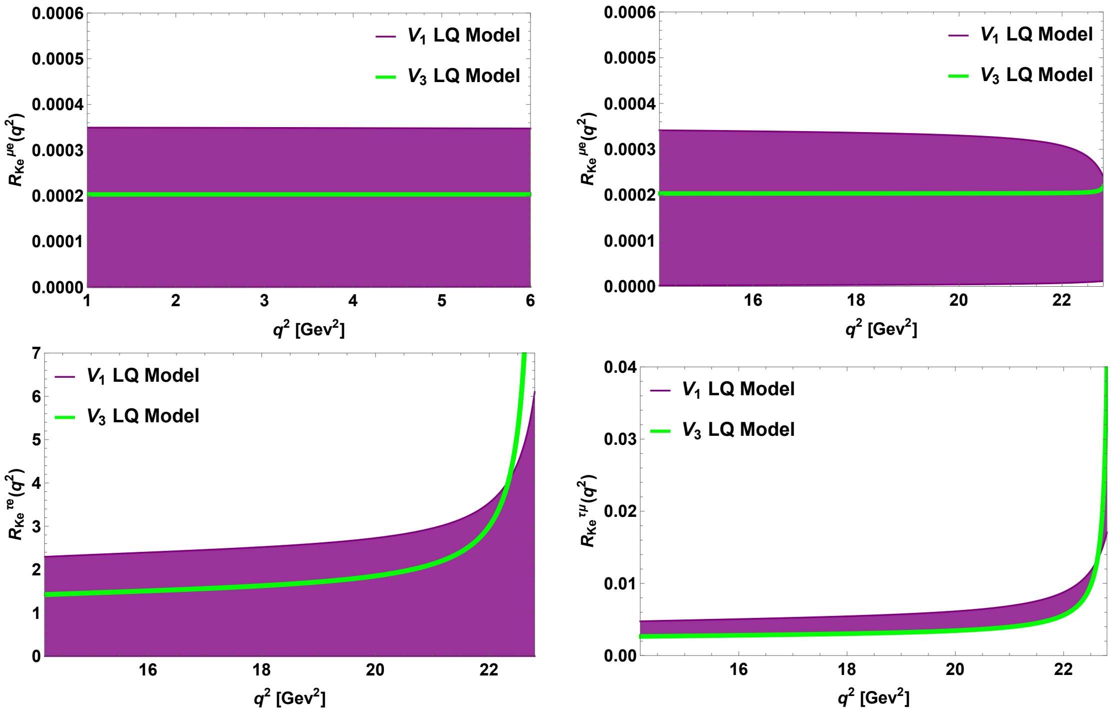

FIGURE 6.4: The variation of lepton universality violating parameters, $R_{Ke}^{\mu e}$ (top right panel), $R_{Ke}^{\tau e}$ (bottom left panel) and $R_{Ke}^{\tau\mu}$ (bottom right panel) in the low recoil limit for $V_{1,3}$ vector LQ exchange. Here $R_{Ke}^{\mu e}$ (top left panel) shows the non-universality in low $q^2 \in [1, 6]$ region.

(bottom panel) mode are depicted with respect to q^2 both in the V_1 and V_3 vector LQ model and the corresponding integrated values are presented in Table 6.2.

The variation of lepton non-universality parameters, $R_{Ke}^{\mu e}$ (top right panel), $R_{Ke}^{\tau e}$ (bottom left panel) and $R_{Ke}^{\tau\mu}$ (bottom right panel) in their respective q^2 region are presented in Fig. 6.4. In Fig. 6.5, we show the q^2 the variation of $R_{K\mu}^{\mu e}$ (top right panel), $R_{K\mu}^{\tau e}$ (bottom left panel) and $R_{K\mu}^{\tau\mu}$ (bottom right panel) in the $V_{1,3}$ leptoquark model. Also, we show the low q^2 behavior of $R_{Ke}^{\mu e}$ and $R_{K\mu}^{\mu e}$ parameters in the range $1 \le q^2 \le 6$ GeV^2 in the top left panel of Fig. 6.4 and Fig. 6.5, respectively. The integrated values these ratios such as $R_K^{l_i l_j}$ $R_{Ke}^{l_i l_j}$, $R_{K\mu}^{l_i l_j}$ are presented in Table 6.2. The variation of $R_K^{\mu\mu}$ parameter with respect to low q^2 (left panel) and high q^2 (right panel) are shown in Fig. 6.6 and the predicted values of this ratio are presented in Table 6.2. In these plots, the SM contributions are represented by solid red lines and the corresponding integrated values are given by

$$R_K^{\mu\mu}|^{\rm SM}_{q^2\in[1,6]} = 1.001, \quad R_K^{\mu\mu}|^{\rm SM}_{q^2\ge 14.18} = 1.003, \quad R_{Ke}^{\tau\tau}|^{\rm SM} = 1.144, \quad R_{K\mu}^{\tau\tau}|^{\rm SM} = 1.14. \tag{6.30}$$

Similarly, we have estimated branching ratios of the $B^+ \to \pi^+ l_i^- l_j^+$ processes. Fig. 6.7 shows the differential branching ratios of the $B^+ \to \pi^+\mu^- e^+$ (top left panel), $B^+ \to \pi^+\tau^- e^+$ (top right panel) and $B^+ \to \pi^+\tau^-\mu^+$ (bottom panel) processes with respect

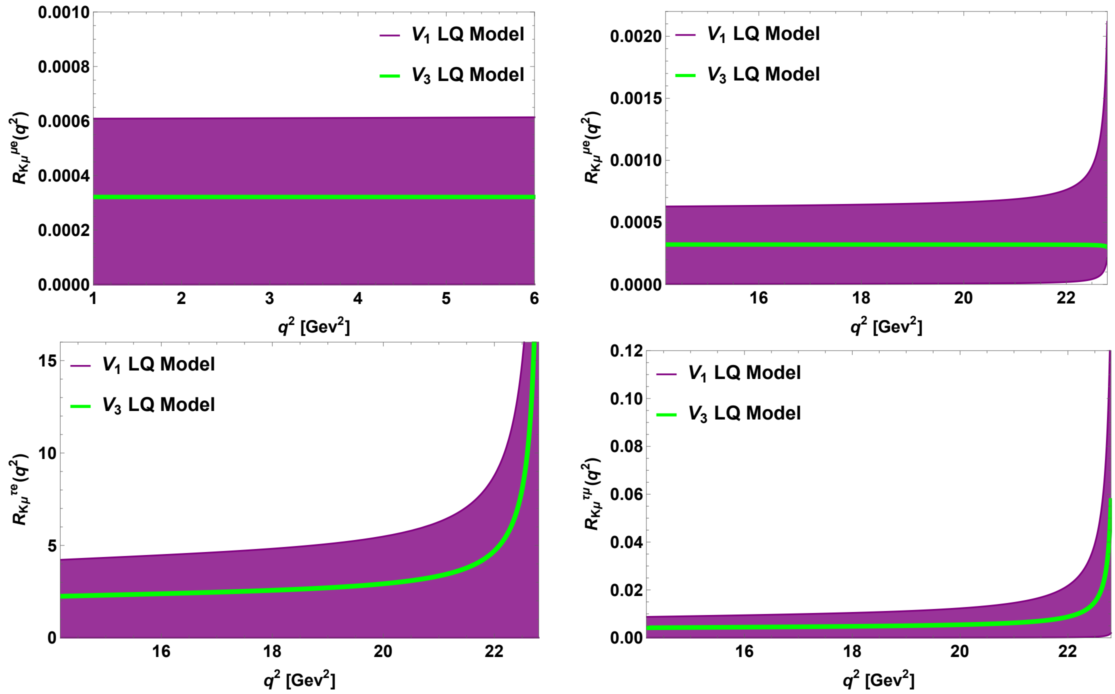

FIGURE 6.5: The variation of lepton universality violating parameters, $R_{K\mu}^{\mu e}$ (top right panel), $R_{K\mu}^{\tau e}$ (bottom left panel) and $R_{K\mu}^{\tau\mu}$ (bottom right panel) in the low recoil limit for $V_{1,3}$ vector LQ exchange. Here $R_{K\mu}^{\mu e}$ (top left panel) shows the non-universality in low $q^2 \in [1, 6]$ region.

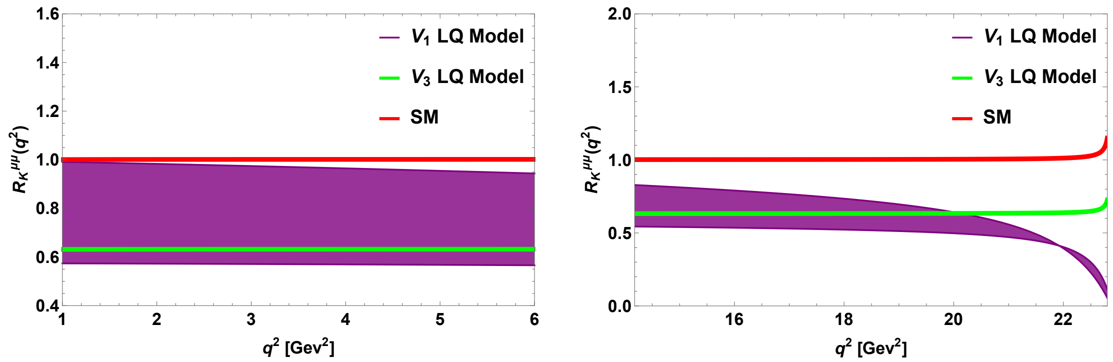

FIGURE 6.6: The variation of lepton non-universality parameter $R_K^{\mu\mu}$ for low $q^2 \in [1, 6]$ (left panel) and high q^2 (right panel) regimes.

to dilepton invariant mass squared. The integrated branching ratios these processes in the range $(m_i + m_j)^2$ to $(M_B - M_\pi)^2$ are presented in Table 6.1. The variation of forward-backward asymmetries of $B^+ \to \pi^+\mu^-e^+$ (top left panel), $B^+ \to \pi^+\tau^-e^+$ (top right panel) and $B^+ \to \pi^+\tau^-\mu^+$ (bottom panel) decays for $V_{1,3}$ vector LQ exchange are shown in Fig. 6.8. In Fig. 6.9, we show the lepton non-universality factors $R_{\pi\mu}^{\mu e}$ (top right panel), $R_{\pi\mu}^{\tau e}$ (bottom left panel) and $R_{\pi\mu}^{\tau\mu}$ (bottom right panel) variation with high q^2. Also, we present the low q^2 behavior of $R_{\pi\mu}^{\mu e}$ (top left panel) observable in the range $1 \le q^2 \le 6$ GeV^2 in the top left panel of Fig. 6.9. The integrated forward-backward asymmetries and lepton non-universality factors for the $B^+ \to \pi^+ l_i^- l_j^+$ processes over

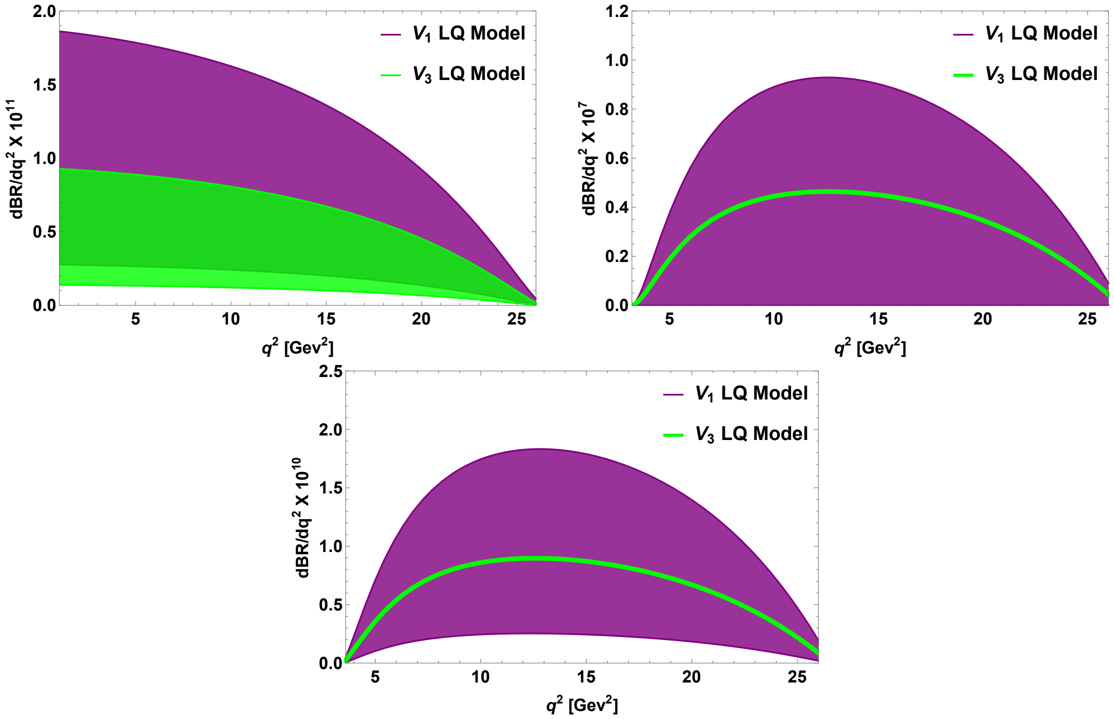

FIGURE 6.7: The variation of branching ratios of $B^+ \to \pi^+\mu^-e^+$ (top left panel), $B^+ \to \pi^+\tau^-e^+$ (top right panel) and $B^+ \to \pi^+\tau^-\mu^+$ (bottom panel) processes with respect to q^2 in the $V_{1,3}$ vector leptoquark model.

TABLE 6.1: The predicted branching ratios of $B^+ \to K^+(\pi^+)l_i^- l_j^+$ lepton flavor violating decays, where $l = e, \mu, \tau$ in the vector leptoquark $V_{1,3}$ model.

Decay process	Values in V_1 LQ model	Values in V_3 LQ model	Expt. upper limit [98]
$B^+ \to K^+\mu^-e^+$	$(0.009 - 6.16) \times 10^{-10}$	$< 2.98 \times 10^{-10}$	$< 9.1 \times 10^{-8}$
$B^+ \to K^+\tau^-e^+$	$(0.118 - 1.882) \times 10^{-10}$	$< 7.12 \times 10^{-11}$	$< 4.3 \times 10^{-5}$
$B^+ \to K^+\tau^-\mu^+$	$(0.0064 - 5.58) \times 10^{-9}$	$< 2.52 \times 10^{-9}$	$< 4.5 \times 10^{-5}$
$B^+ \to \pi^+\mu^-e^+$	$(0.48 - 3.23) \times 10^{-10}$	$< 1.6 \times 10^{-10}$	$< 6.4 \times 10^{-3}$
$B^+ \to \pi^+\tau^-e^+$	$5.23 \times 10^{-12} - 1.51 \times 10^{-6}$	$< 7.55 \times 10^{-7}$	$< 7.4 \times 10^{-5}$
$B^+ \to \pi^+\tau^-\mu^+$	$(0.41 - 2.99) \times 10^{-9}$	$< 1.46 \times 10^{-9}$	$< 6.2 \times 10^{-5}$

their respective physical q^2 range are given in Table 6.3. Table 6.3 also contains the numerical values of $R_\pi^{\mu\mu}$ parameter in both the V_1 and V_3 vector LQ model. In the SM, the predicted values of lepton universality violating factors of $B^+ \to \pi^+l^+l^-$ processes are given by

$$R_\pi^{\mu\mu}|_{q^2\in[1,6]} = 1.001, \qquad R_\pi^{\mu\mu}|_{q^2\geq 14.18} = 1.003, \qquad R_{\pi e}^{\tau\tau} = 1.149, \qquad R_{\pi\mu}^{\tau\tau} = 1.146. \quad (6.31)$$

TABLE 6.2: The predicted integrated values of the forward-backward asymmetries and lepton non-universality parameters with respect to their respective q^2 range for the $B^+ \to K^+ l_i^- l_j^+$ process in the SM and the $V_{1,3}$ vector leptoquark model. This also contains the numerical values of $R_K^{\mu\mu}$, $R_{Ke}^{l_i l_j}$, $R_{K\mu}^{l_i l_j}$ observables in high recoil limit.

Observables	Values in V_1 LQ model	Values in V_3 LQ model
$\langle A_{FB}^{K\mu e} \rangle$	7.65×10^{-3}	2.82×10^{-3}
$\langle A_{FB}^{K\tau e} \rangle$	0.285	0.285
$\langle A_{FB}^{K\tau\mu} \rangle$	$(0.039 - 0.105) \times 10^{-3}$	4.8×10^{-3}
$\langle R_{Ke}^{\mu e} \rangle\vert_{q^2\in[1,6]}$	$(0.0038 - 3.5) \times 10^{-4}$	2.03×10^{-4}
$\langle R_{Ke}^{\mu e} \rangle$	$(0.033 - 3.36) \times 10^{-4}$	2.04×10^{-4}
$\langle R_{Ke}^{\tau e} \rangle$	$0.526 \times 10^{-4} - 2.52$	1.63
$\langle R_{Ke}^{\tau\mu} \rangle$	$(0.285 - 5.45) \times 10^{-3}$	3.04×10^{-3}
$\langle R_{K\mu}^{\mu e} \rangle\vert_{q^2\in[1,6]}$	$(0.0039 - 6.1) \times 10^{-4}$	3.2×10^{-4}
$\langle R_{K\mu}^{\mu e} \rangle$	$(0.0454 - 6.44) \times 10^{-4}$	3.3×10^{-4}
$\langle R_{K\mu}^{\tau e} \rangle$	$0.72 \times 10^{-4} - 4.83$	2.58
$\langle R_{K\mu}^{\tau\mu} \rangle$	$(0.039 - 0.1) \times 10^{-3}$	4.8×10^{-3}
$\langle R_K^{\mu\mu} \rangle\vert_{q^2\in[1,6]}$	$0.57 - 0.9688$	0.63
$\langle R_K^{\mu\mu} \rangle$	$0.521 - 0.73$	0.64

In the $V_{1,3}$ vector LQ model, the estimated numerical values of $R_+^{l_i l_j}$ parameters are

$$R_+^{\mu e}|_{V_1 LQ} = 0.525 - 53.34, \qquad R_+^{\mu e}|_{V_3 LQ} = 0.536, \tag{6.32}$$

$$R_+^{\tau\mu}|_{V_1 LQ} = 0.536 - 64.1, \qquad R_+^{\tau\mu}|_{V_3 LQ} = 0.578, \tag{6.33}$$

$$R_+^{\tau e}|_{V_1 LQ} = 0.443 - 0.56, \qquad R_+^{\tau e}|_{V_3 LQ} = 0.56. \tag{6.34}$$

6.4 $(g-2)_\mu$

The muon anomalous magnetic moment has discrepancy of $\sim 3\sigma$ [231] from the corresponding SM prediction. The experimental value of a_μ is given as [231]

$$a_\mu^{\rm Expt} = 116592080(63) \times 10^{-11}, \tag{6.35}$$

which when compared to the SM value [232]

$$a_\mu^{\rm SM} = 116591785(61) \times 10^{-11}, \tag{6.36}$$

has the discrepancy

$$\Delta a_\mu = a_\mu^{\rm Expt} - a_\mu^{\rm SM} = (295 \pm 88) \times 10^{-11}. \tag{6.37}$$

TABLE 6.3: The predicted integrated values of the forward-backward asymmetries and lepton non-universality parameters with respect to their respective q^2 range for the $B^+ \to \pi^+ l_i^- l_j^+$ process in the SM and the $V_{1,3}$ vector leptoquark model. This also contains the numerical values of $R_K^{\mu\mu}$, $R_{\pi e}^{l_i l_j}$, $R_{\pi\mu}^{l_i l_j}$ observables in high recoil limit.

Observables	Values in V_1 LQ model	Values in V_3 LQ model
$\langle A_{FB}^{\pi\mu e}\rangle$	$(0.432 - 4.42)\times 10^{-3}$	2.4×10^{-3}
$\langle A_{FB}^{\pi\tau e}\rangle$	0.2632	0.263
$\langle A_{FB}^{\pi\tau\mu}\rangle$	$0.263 - 0.271$	0.26
$\langle R_{\pi}^{\mu\mu}\rangle\vert_{q^2\in[1,6]}$	$1.084\times 10^{-7} - 1.95$	1.655×10^{-7}
$\langle R_{\pi}^{\mu\mu}\rangle$	$1.09\times 10^{-7} - 0.6$	1.66×10^{-7}
$\langle R_{\pi e}^{\mu e}\rangle\vert_{q^2\in[1,6]}$	$2.48\times 10^{-10} - 1.8\times 10^{-3}$	2.46×10^{-10}
$\langle R_{\pi e}^{\mu e}\rangle$	$2.5\times 10^{-10} - 5.5\times 10^{-4}$	2.47×10^{-10}
$\langle R_{\pi e}^{\tau e}\rangle$	$(0.0187 - 1.53)\times 10^{-4}$	1.86×10^{-6}
$\langle R_{\pi e}^{\tau\mu}\rangle$	$3.75\times 10^{-9} - 7.33\times 10^{-3}$	3.6×10^{-9}
$\langle R_{\pi\mu}^{\mu e}\rangle\vert_{q^2\in[1,6]}$	$(1.8 - 2.29)\times 10^{-3}$	1.492×10^{-3}
$\langle R_{\pi\mu}^{\mu e}\rangle$	$(0.932 - 2.3)\times 10^{-3}$	1.49×10^{-3}
$\langle R_{\pi\mu}^{\tau e}\rangle$	$2.57\times 10^{-4} - 17.14$	11.23
$\langle R_{\pi\mu}^{\tau\mu}\rangle$	$0.0123 - 0.073$	0.07

The absolute magnitude of the discrepancy is small and can be accommodate by adding the new physics contributions. In the $V_{1,3}$ vector LQ model, a_μ is given by

$$\begin{aligned}\Delta a_\mu &= -2N_c m_\mu \Bigg[\lambda_{LL}^{32}\lambda_{RR}^{32\,*}\Big(-\frac{1}{3}\left(f_3(x_b)+f_4(x_b)\right)+\frac{2}{3}\left(\bar{f}_3(x_b)+\bar{f}_4(x_b)\right)\Big) \\ &\quad + \Big(|\lambda_{LL}^{32}|^2+|\lambda_{RR}^{32}|^2\Big)\Big(-\frac{1}{3}f_1(x_b)+\frac{2}{3}\bar{f}_1(x_b)\Big)\Bigg] \\ &\quad -2N_c m_\mu\Big(|\lambda_{LL}^{32}|^2+|\lambda_{RR}^{32}|^2\Big)\Big(-\frac{1}{6}f_1(x_b)+\frac{1}{3}\bar{f}_1(x_b)\Big), \end{aligned} \tag{6.38}$$

where the loop functions are given in section 2.4.6. Now using the constrained LQ couplings from $\tau^- \to \mu^-\gamma$ process (discussed in chapter 2) with the scaling law as discussed in the above section, Δa_μ in the LQ model is found as

$$2.38\times 10^{-9} \le \Delta a_\mu \le 2.95\times 10^{-9}, \tag{6.39}$$

which is within its 1σ range.

6.5 Chapter summary

To summarize, we have studied the rare lepton flavor violating semileptonic B meson decays in the vector leptoquark model in this work. These decays are extremely rare

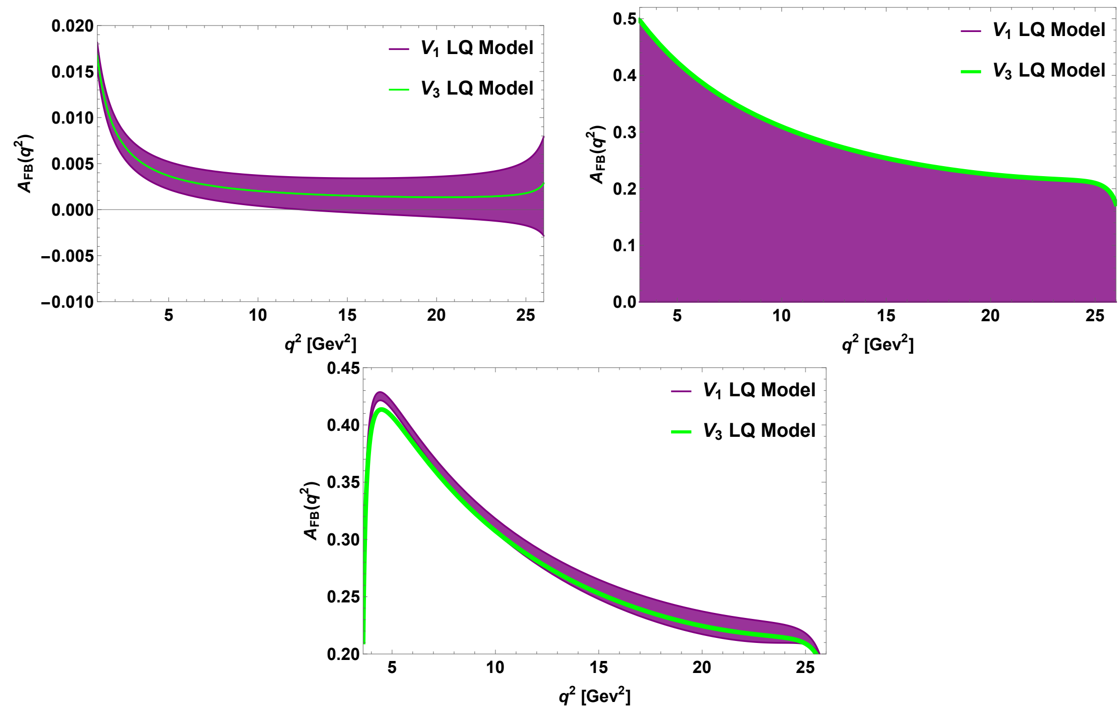

FIGURE 6.8: The forward-backward asymmetry variation of $B^+ \to \pi^+\mu^-e^+$ (top left panel), $B^+ \to \pi^+\tau^-e^+$ (top right panel) and $B^+ \to \pi^+\tau^-\mu^+$ (bottom panel) processes with respect to q^2 for $V_{1,3}$ vector leptoquark exchange.

in the SM as they occur at loop level. They are further suppressed due to tiny neutrino masses in one of the loop. However, in the vector leptoquark model, these decays can occur at the tree level as the leptoquark couples to quark and lepton simultaneously thereby mediating the LFV processes at tree level. We consider $(3, 3, 2/3)$ and $(3, 1, 2/3)$ vector leptoquarks which do not have baryon number violation in perturbation theory, forbid proton decay and could be light enough to be accessible in accelerator searches. The leptoquark parameter space is constrained using the recently measured branching ratios of $B_{s,d} \to l^+l^-$, $K_L \to l^+l^-$ and $\tau^- \to l^-\gamma$ processes and using such constrained parameters, we estimated the branching ratios and forward-backward asymmetries of $B^+ \to K^+l_i^-l_j^+$ and $B^+ \to \pi^+l_i^-l_j^+$ processes. We studied the ratios of various combinations of LFV decays like $R^{l_il_j}_{K(\pi)e}$, $R^{l_il_j}_{K(\pi)\mu}$ and $R^{l_il_j}_{+}$ parameters, in order to check the presence of lepton non-universality. We also study the effect of vector leptoquark on the muon $g-2$ anomaly. We found that our predicted values are within the present experimental limits, the observation of which in the LHCb experiment or upcoming Belle II experiments would provide an unambiguous signal of new physics.

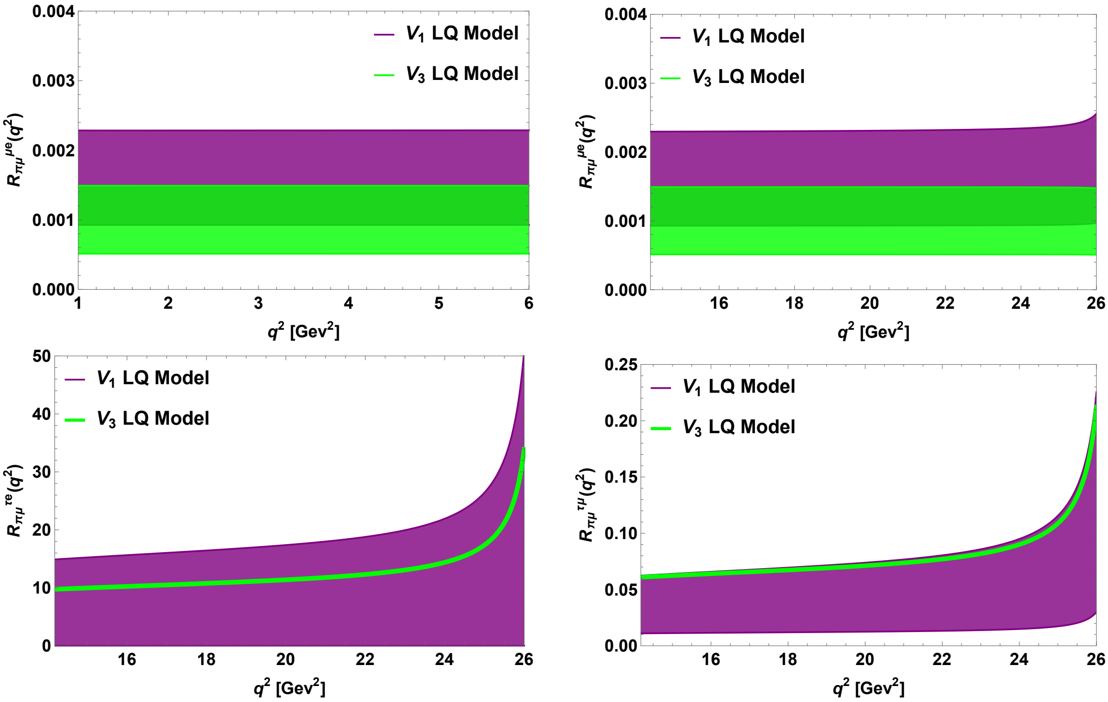

FIGURE 6.9: Same as Fig. 6.5 for $B^+ \to \pi^+ l_i^- l_j^+$ processes.

Chapter 7

Summary and Conclusion

This chapter summarizes our research work presented in this thesis, which is mainly focused on the phenomenological study of the rare semileptonic B meson decays. Chapter 1, starts with a brief introduction to the SM, its particle content and the number of of free parameters, origin of CP violation in the SM etc. We then discussed about the CKM mechanism and its role in explaining the CP violation in K and B meson systems. After discussing the theoretical tools for the investigation of rare semileptonic decays of B meson, we concluded the chapter by mentioning about the recent anomalies observed in the B meson decay processes.

In spite of the precise illustration of the fundamental particles and their interactions, SM fails to elucidate some of the imperative questions of particle physics such as the baryon asymmetry of the universe, non-zero neutrino mass, dark matter and dark energy components, etc. These limitations point towards the necessity of new physics beyond the SM. In recent times, the search of new physics in B meson decays is an world wide effort. Many dedicated experiments are committed in achieving the goal of this grand challenge. Though the experimental results on many physical observables are consistent with the SM predictions, some of them have $(2-4)\sigma$ discrepancy. To resolve these issues in B meson, we need to go beyond the SM framework. In this context, we have chosen the leptoquark model, where the SM is extended by inclusion of an additional hypothetical leptoquark boson. The discussion on leptoquark model and the constraints on the leptoquark parameter space from the B-sector are presented in chapter 2. Leptoquarks have the ability to couple with both quark and lepton simultaneously, hence they have both the baryon and lepton quantum numbers. Though experimental efforts are going on for the search of leptoquark signature for many years, but till now there is no definitive result except the indirect limit on leptoquark masses. Leptoquark with spin 0 (1) is known as scalar (vector) leptoquark. To evade the fast proton decay, we have considered $(3, 2, 7/6)$, $(3, 2, 1/6)$ scalar leptoquarks and $(3, 3, 2/3)$, $(3, 1, 2/3)$ vector leptoquarks which conserve both the baryon and lepton number and are invariant under the SM gauge group $SU(3)_C \times SU(2)_L \times U(1)_Y$. The new Wilson coefficients are obtained by comparing the leptoquark Hamiltonian with the SM Hamiltonian. We found that the $C_{9,10}^{(\prime)\,\rm LQ}$ new Wilson coefficients arise due to the scalar leptoquark exchange, whereas the vector leptoquarks provide additional (pseudo)scalar coefficients contributions to the SM. We have constrained the product of scalar leptoquark couplings by using the measured branching ratios of $B_s \to l^+l^-$, $\bar{B} \to X_s l^+l^-$ processes and the $B_s - \bar{B}_s$ oscillation data. The bounds on the vector leptoquark couplings are acquired by the $B_s \to l^+l^-$, $\bar{B} \to X_s l^+l^-$, $B_u^+ \to l^+\nu_l$, $K_L \to l^+l^-$ and $\tau^- \to l^-\gamma$ processes. It's quite difficult to compute bound on the vectorial and scalar couplings simultaneously from $B_s \to l^+l^-$ and $B_u^+ \to l^+\nu_l$ processes. Therefore, we have assumed the vector leptoquark as chiral and constrain the $C_{9,10}^{(\prime)\rm LQ}$ Wilson coefficients. In the branching ratios of these processes, the $C_{9,10}^{(\prime)\rm LQ}$ couplings are suppressed by a factor M_B^2/m_l, thus can be neglected. Then one can obtain the bound on $C_{S,P}^{(\prime)\rm LQ}$ couplings. These bounds on new Wilson coefficients can be used to scrutinize the issues in the $\bar{B} \to \bar{K}^{(*)} l^+l^-(\nu\bar{\nu})$, $\bar{B} \to \bar{D}^{(*)} l \bar{\nu}_l$ processes.

Chapter 3 is based on the anomalies in flavor changing neutral current $\bar{B} \to \bar{K} l^+l^-$ $(\nu\bar{\nu})$ decay processes in the context of scalar leptoquark. Here we have studied the $\bar{B} \to \bar{K} l^+l^-$ processes in both the high and low recoil limit except the intermediate region around $q^2 \to m_{J/\psi}^2$, and $m_{\psi'}^2$ in order to overcome the dominant charmonium resonance backgrounds from $B \to K(\bar{c}c) \to K l^+l^-$. The branching ratios and isospin asymmetries of $\bar{B} \to \bar{K} l^+l^-$ processes had $(3-4)\sigma$ discrepancy from the SM predictions (at present, almost consistent with the SM). Another important observation in these processes is the 2.6 deviation in the lepton universality ratio (R_K), which is the branching fractions of $B \to K\mu^+\mu^-$ to $B \to K e^+e^-$ processes. This is the first concrete evidence of the violation of lepton universality in the semileptonic B decays. Since the leptoquark couplings associated with $B_s \to l^+l^-$ and $\bar{B} \to \bar{K} l^+l^-$ processes are same, the constraint on new couplings coming from the $B_s \to l^+l^-$ processes can be used to resolve the above anomalies. We then estimate the branching ratios, CP asymmetry parameters and isospin asymmetry using the $(3, 2, 7/6)$ leptoquark model. We found that the observed lepton universality violation parameter can be accommodated in this model. We also presented the analysis of the $\bar{B} \to \bar{K}^{(*)}\nu\bar{\nu}$ decay processes in both the $(3, 2, 7/6)$ and $(3, 2, 1/6)$ leptoquark model. Unlike the $\bar{B} \to \bar{K} l^+l^-$ processes, these processes don't have large long-distance QCD contribution, thus could be studied in the full q^2 regions. We computed the branching ratios and lepton non-universality parameters in this processes . We found that the branching ratio deviates significantly due to the addition of leptoquark couplings.

In chapter 4, we have discussed the angular distribution of $\bar{B} \to \bar{K}^* l^+ l^-$ decay processes in the full q^2 regimes except the intermediate region to remove the dominant $\bar{c}c$ resonance contribution from $\bar{B} \to \bar{K}^*(J/\psi, \psi') \to \bar{K}^* l^+ l^-$. Among all the semileptonic decay processes of B mesons, the measurement of angular distribution of these processes (as they involve four particles in the final state) provide various observables to look for new physics. Recently, LHCb has reported 3σ deviation in the measurement of the form-factor-independent P_5' observable and the decay rate of this process. In addition, the observed forward-backward asymmetry is systematically below the corresponding SM prediction, though the zero crossing point is consistent with it. The isospin asymmetry is also measured by the LHCb experiment in the full q^2 regions, which can be used to explore the NP. Moreover, the LHCb Collaboration has reported many other deviations from the SM expectations in the angular observables. Using the obtained bounds on the leptoquark coupling, we investigated the $\bar{B} \to \bar{K}^* l^+ l^-$ processes. We have performed a comparison study of both the relevant $(3, 2, 7/6)$ and $(3, 2, 1/6)$ leptoquark in this work. We computed the branching ratios, isospin asymmetry, forward-backward asymmetries in the full q^2 regimes in both the leptoquark models. We found that the branching ratios have a significant deviation from the SM and can accommodate the experimental values. In the high recoil limit, we found a slight shift in the zero-crossing of the forward-backward asymmetry towards right however, it does not give any significant deviation in the high q^2 regions. The leptoquark model didn't provide much deviation in the isospin asymmetry in the full q^2 region. We have also computed the form factor independent observables, $P_i^{(\prime)}$ where $i = 1, 2, ..., 6$ in the leptoquark model, which gives significant deviation from the SM in the low q^2 regions. We notice that the leptoquark model can explain the famous P_5' observables. However, all the FFI observables and other CP asymmetry observables have no much deviation in the low recoil limit. The interesting point in this work is that both the scalar leptoquark is able to explain all the anomalies, though $(3, 2, 7/6)$ leptoquark gives comparatively significant deviation than $(3, 2, 1/6)$ leptoquark.

In chapter 5, we have discussed the $\bar{B} \to \bar{D}^{(*)} l \nu_l$ processes mediated by the flavor changing charged current $b \to c l \nu_l$ transitions. Due to the $R_{D^{(*)}}$ anomalies, these processes are at the center of attraction in recent times. The LHCb as well as BaBar and Belle experiments have reported 1.9σ (3.3σ) deviation in the measurement of R_D (R_{D^*}) anomaly from the corresponding SM results. We have investigated these processes in the $(3, 3, 2/3)$ and $(3, 1, 2/3)$ vector leptoquark model. The isotriplet $(3, 3, 2/3)$ leptoquark provides only the C_{V_1} Wilson coefficient, while the isosinglet $(3, 1, 2/3)$ leptoquark has both the vectorial (C_{V_1}) and scalar (C_{S_1}) Wilson coefficients. We constrain the real and imaginary parts of the leptoquark couplings by using the branching ratios of $B_s \to l^+ l^-$, $\bar{B} \to X_s l^+ l^-$ and $B_u^+ \to l^+ \nu_l$ processes. These bounds on the product of leptoquark couplings can be used to study $\bar{B} \to \bar{D}^{(*)} l \nu_l$ processes since the leptoquark couplings are same in both the processes. We then compute the branching ratios, forward-backward asymmetries, tau polarization asymmetries of $\bar{B} \to \bar{D}^{(*)} l \nu_l$ processes, where l is any charged lepton. We found a significant deviation in the branching ratio of $\bar{B} \to \bar{D}^{(*)} \tau \nu_l$ process in comparison with the processes with muon or electron in the final state. However, we didn't find any satisfactory deviation in the forward-backward asymmetry,τ polarization, longitudinal and transverse polarization asymmetries of $\bar{B} \to \bar{D}^{(*)} l \nu_l$ processes. The main aim of this work was to corroborate the lepton non-universality parameters. In the $(3, 3, 2/3)$ vector leptoquark model, we have presented the $R_{D^{(*)}}$ and $R_{K^{(*)}}$ lepton non-universality parameters in both the high and low q^2 regions. We found that all the non-universality parameters have sufficient deviations from the SM and can accommodate the experimental results. We observed that the addition of one isotriplet $(3, 3, 2/3)$ vector leptoquark is able to explain all the $R_{D^{(*)}}$ and $R_{K^{(*)}}$ anomalies simultaneously.

Chapter 6 devoted to the study of lepton flavor violating decay processes of B meson. The observation of neutrino oscillation in various experiments has confirmed the violation of lepton flavor in the neutral lepton sector, which implies that there could also be lepton flavor violating decays in the charged sector. The predicted branching ratios of lepton flavor violating B decays are negligible in the SM since these processes are mediated either via loop diagram or via box diagram. But these processes could occur at tree level in the leptoquark model. The bounds on vector leptoquark parameters are taken from $B_s \to l^+ l^-$, $K_L \to l^+ l^-$ and $\tau^- \to l^- \gamma$ processes. For the bound on other required couplings, we have assumed that all the generations of LQ couplings follow the simple scaling law, i.e., $(\lambda_{LL(RR)})_{ij} = (m_i/m_j)^{1/2} (\lambda_{LL(RR)})_{ii}$ with $j > i$. We have computed the branching ratios of semileptonic $B \to K^{(*)} l_i^{\mp} l_j^{\pm}$, $B_s \to \phi l_i^{\mp} l_j^{\pm}$ and $B \to \rho l_i^{\mp} l_j^{\pm}$ decay processes in the vector leptoquark model. Our predicted branching ratios are sizable and well below the experimental bounds.

In conclusion, the investigation of rare B meson decays provide new rooms to explore new physics beyond the standard model. We have shown that most of the observed anomalies in the rare semileptonic decays of B meson could be explained in the context of leptoquark model. The confirmation of these anomalies in the experiment will be the strong indirect evidence of the presence of leptoquark.

Appendix A

$\bar{B} \to \bar{K}^* ll$ processes

A.1 J_i coefficients

In terms of the transversity amplitudes A_0, $A_\parallel$, $A_\perp$, and A_t the J_i coefficients can be expressed as [177, 188]

$$
\begin{aligned}
J_1^s &= \frac{(2+\beta_l^2)}{4}\left[|A_\perp^L|^2 + |A_\parallel^L|^2 + (L \to R)\right] + \frac{4m_l^2}{q^2}\mathrm{Re}\left(A_\perp^L A_\perp^{R^*} + A_\parallel^L A_\parallel^{R^*}\right), && \text{(A.1)}\\
J_1^c &= |A_0^L|^2 + |A_0^R|^2 + \frac{4m_l^2}{q^2}\left[|A_t|^2 + 2\mathrm{Re}\left(A_0^L A_0^{R^*}\right)\right] + \beta_l^2|A_S|^2, && \text{(A.2)}\\
J_2^s &= \frac{\beta_l^2}{4}\left[|A_\perp^L|^2 + |A_\parallel^L|^2 + (L \to R)\right], && \text{(A.3)}\\
J_2^c &= -\beta_l^2\left[|A_0^L|^2 + (L \to R)\right], && \text{(A.4)}\\
J_3 &= \frac{1}{2}\beta_l^2\left[|A_\perp^L|^2 - |A_\parallel^L|^2 + (L \to R)\right], && \text{(A.5)}\\
J_4 &= \frac{1}{\sqrt{2}}\beta_l^2\left[\mathrm{Re}\left(A_0^L A_\parallel^{L^*}\right) + (L \to R)\right], && \text{(A.6)}\\
J_5 &= \sqrt{2}\beta_l\left[\mathrm{Re}\left(A_0^L A_\perp^{L^*}\right) - (L \to R) - \frac{m_l}{\sqrt{q^2}}\mathrm{Re}\left(A_\parallel^L A_S^* + A_\parallel^R A_S^*\right)\right], && \text{(A.7)}\\
J_6^s &= 2\beta_l\left[\mathrm{Re}\left(A_\parallel^L A_\perp^{L^*}\right) - (L \to R)\right], && \text{(A.8)}\\
J_6^c &= 4\beta_l\frac{m_l}{\sqrt{q^2}}\mathrm{Re}\left[A_0^L A_S^* + (L \to R)\right], && \text{(A.9)}\\
J_7 &= \sqrt{2}\beta_l\left[\mathrm{Im}\left(A_0^L A_\parallel^{L^*}\right) - (L \to R) + \frac{m_l}{\sqrt{q^2}}\mathrm{Im}\left(A_\perp^L A_S^* + A_\perp^R A_S^*\right)\right], && \text{(A.10)}\\
J_8 &= \frac{1}{\sqrt{2}}\beta_l^2\left[\mathrm{Im}\left(A_0^L A_\perp^{L^*}\right) + (L \to R)\right], && \text{(A.11)}\\
J_9 &= \beta_l^2\left[\mathrm{Im}\left(A_\parallel^{L^*} A_\perp^L\right) + (L \to R)\right], && \text{(A.12)}
\end{aligned}
$$

where

$$A_i A_j^* = A_i^L\left(q^2\right) A_j^{*L}\left(q^2\right) + A_i^R\left(q^2\right) A_j^{*R}\left(q^2\right) \qquad (i, j = 0, \|, \perp)\,, \tag{A.13}$$

in shorthand notation.

A.2 Transversity amplitudes at NLO in the large-recoil limit

In the large recoil limit, the transversity amplitudes at next-to-leading order (NLO) within QCDf can be given as [177, 187]

$$\begin{aligned}
A_\perp^{L,R} &= N_H \sqrt{2\lambda}\left[\left((C_9 + C_9^{\rm LQ} + C_9^{\prime\rm LQ}) \mp (C_{10} + C_{10}^{\rm LQ} + C_{10}^{\prime\rm LQ}\right)\frac{V\left(q^2\right)}{M_B + M_{K^*}} + \frac{2m_b}{q^2}\mathcal{T}_\perp^+\right], \\
A_\|^{L,R} &= -N_H\sqrt{2}\left(M_B^2 - M_{K^*}^2\right)\left[\left((C_9 + C_9^{\rm LQ} - C_9^{\prime\rm LQ}) \mp (C_{10} + C_{10}^{\rm LQ} - C_{10}^{\prime\rm LQ})\right)\frac{A_1\left(q^2\right)}{M_B - M_{K^*}}\right. \\
&\qquad \left. + \frac{4m_b}{M_B}\frac{E_{K^*}}{q^2}\mathcal{T}_\perp^-\right], \\
A_0^{L,R} &= -\frac{N_H}{2M_{K^*}\sqrt{q^2}}\left[\left((C_9 + C_9^{\rm LQ} - C_9^{\prime\rm LQ}) \mp (C_{10} + C_{10}^{\rm LQ} - C_{10}^{\prime\rm LQ})\right)\right. \\
&\times \left[\left(M_B^2 - M_{K^*}^2 - q^2\right)\left(M_B + M_{K^*}\right) A_1\left(q^2\right) - \lambda\frac{A_2\left(q^2\right)}{M_B + M_{K^*}}\right] \\
&+ \left. 2m_b\left[\frac{2E_{K^*}}{M_B}\left(M_B^2 + 3M_{K^*}^2 - q^2\right)\mathcal{T}_\perp^- - \frac{\lambda}{M_B^2 - M_{K^*}^2}\left(\mathcal{T}_\perp^- + \mathcal{T}_\|^-\right)\right]\right], \\
A_t &= \frac{2N_H}{\sqrt{q^2}}\frac{E_{K^*}}{M_{K^*}}\frac{\xi_\|}{\Delta_\|}\sqrt{\lambda}\left(C_{10} + C_{10}^{\rm LQ} - C_{10}^{\prime\rm LQ}\right)\,, \qquad A_S = 0\,,
\end{aligned} \tag{A.14}$$

where $C_{9,10}^{\rm LQ}$ and $C_{9,10}^{\prime\rm LQ}$ are the new Wilson coefficients arising due to leptoquark exchange and $E_K^* = \left(M_B^2 + M_{K^*}^2 - q^2\right)/2M_B$ is the energy of the kaon in the B meson rest frame. The normalization constant N_H is given as

$$N_H = \left[\frac{G_F^2\alpha_{\rm em}^2}{3\times 2^{10}\pi^5 M_B}|V_{tb}V_{ts}^*|^2\hat{s}\sqrt{\lambda}\beta_l\right]^{1/2}\,, \tag{A.15}$$

where $\hat{s} = q^2/M_B^2$ and

$$\lambda = \lambda\left(M_B^2, M_{K^*}^2, q^2\right) = M_B^4 + M_{K^*}^4 + q^4 - 2\left(M_B^2 M_{K^*}^2 + M_{K^*}^2 q^2 + M_B^2 q^2\right). \tag{A.16}$$

The transversity amplitude A_t contains $\Delta_{\|}$ and is negligible for a massless lepton. It contributes only for $m_l \neq 0$. The detailed expression for the function $\mathcal{T}_a\,(a = \perp, \|)$ at NLO in the QCDf framework is given in Appendix A.4.

A.3 Transversity amplitudes in the low-recoil limit

The transversity amplitudes to leading order in $1/m_b$ at low recoil are given as

$$\begin{aligned} A_{\perp}^{L,R} &= i\left[\left((C_9^{\rm eff} + C_9^{\rm LQ} + C_9^{\prime\rm LQ}) \mp (C_{10} + C_{10}^{\rm LQ} + C_{10}^{\prime\rm LQ})\right) + \kappa\frac{2\hat{m}_b}{\hat{s}}C_7^{\rm eff}\right] f_{\perp}\,, \\ A_{\|}^{L,R} &= -i\left[\left((C_9^{\rm eff} + C_9^{\rm LQ} - C_9^{\prime\rm LQ}) \mp (C_{10} + C_{10}^{\rm LQ} - C_{10}^{\prime\rm LQ})\right) + \kappa\frac{2\hat{m}_b}{\hat{s}}C_7^{\rm eff}\right] f_{\|}\,, \\ A_{0}^{L,R} &= -i\left[\left((C_9^{\rm eff} + C_9^{\rm LQ} - C_9^{\prime\rm LQ}) \mp (C_{10} + C_{10}^{\rm LQ} - C_{10}^{\prime\rm LQ})\right) + \kappa\frac{2\hat{m}_b}{\hat{s}}C_7^{\rm eff}\right] f_{0}\,, \end{aligned} \tag{A.17}$$

where the form factors read

$$f_{\perp} = N_L M_B \frac{\sqrt{2\hat{\lambda}}}{1+\hat{M}_{K^*}} V, \qquad f_{\|} = N_L M_B \sqrt{2}\left(1+\hat{M}_{K^*}\right) A_1, \tag{A.18}$$

$$f_0 = N_L M_B \frac{\left(1-\hat{s}-\hat{M}_{K^*}^2\right)\left(1+\hat{M}_{K^*}\right)^2 A_1 - \hat{\lambda} A_2}{2\hat{M}_{K^*}\left(1+\hat{M}_{K^*}\right)\sqrt{\hat{s}}}\,, \tag{A.19}$$

and the normalization factor is $N_L = \left[\left(G_F^2 \alpha_{\rm em}^2 |\lambda_t|^2 M_B \hat{s}\sqrt{\hat{\lambda}}\right)/\left(3\times 2^{10}\pi^5\right)\right]^{1/2}$. Here the dimensionless variables are $\hat{m}_i = m_i/M_B$ and $\hat{\lambda} = \lambda\left(1, \hat{s}, \hat{M}_{K^*}^2\right)$ and the effective coefficients including the four-quark and gluon dipole operators are given by [161]

$$\begin{aligned} C_7^{\rm eff} &= C_7 - \frac{1}{3}\left[C_3 + \frac{4}{3}C_4 + 20C_5 + \frac{80}{3}C_6\right] + \frac{\alpha_s}{4\pi}\left[\left(C_1 - 6C_2\right)A(q^2) - C_8 F_8^{(7)}(q^2)\right]\,, \\ C_9^{\rm eff} &= C_9 + h\left(0,q^2\right)\left[\frac{4}{3}C_1 + C_2 + \frac{11}{2}C_3 - \frac{2}{3}C_4 + 52C_5 - \frac{32}{3}C_6\right] \\ &- \frac{1}{2}h\left(m_b,q^2\right)\left[7C_3 + \frac{4}{3}C_4 + 76C_5 + \frac{64}{3}C_6\right] + \frac{4}{3}\left[C_3 + \frac{16}{3}C_5 + \frac{16}{9}C_6\right] \\ &+ \frac{\alpha_s}{4\pi}\left[C_1\left(B(q^2) + 4C(q^2)\right) - 3C_2\left(2B\left(q^2\right) - C\left(q^2\right)\right) - C_8 F_8^{(9)}\left(q^2\right)\right] \\ &+ 8\frac{m_c^2}{q^2}\left[\left(\frac{4}{9}C_1 + \frac{1}{3}C_2\right)(1+\lambda_u) + 2C_3 + 20C_5\right]\,. \end{aligned} \tag{A.20}$$

These include the CKM suppression and the QCD matching corrections at next-to-leading order proportional to $\lambda_u = (V_{ub}V_{us}^*)/(V_{tb}V_{ts}^*)$, which corresponds to the small amount of CP violation in the SM.

A.4 $\mathcal{T}_a^{\pm}$ calculation

The $B \to K^*$ matrix elements in large recoil limit depend on four independent functions $\mathcal{T}_a^{\pm}$ corresponding to a transversely ($a = \perp$) and longitudinally ($a = \|$) polarized K^* and next-to-leading order is given by [160]

$$\mathcal{T}_a = \xi_a C_a + \frac{\pi^2}{N_c} \frac{f_B f_{K^*,a}}{M_B} \Xi_a \sum_{\pm} \int \frac{d\omega}{\omega} \Phi_{B,\pm}(\omega) \int_0^1 du \Phi_{K^*,a}(u) \mathcal{T}_{a,\pm}(u,\omega) \ , \quad \text{(A.21)}$$

where $\Xi_\perp \equiv 1$, $\Xi_\| \equiv M_{K^*}/E_{K^*}$ and the factorization scale $\mu_f = \sqrt{m_b \Lambda_{QCD}}$.

The coefficient functions C_a and $\mathcal{T}_{a,\pm}$ can be written as

$$C_a = C_a^{(0)} + \frac{\alpha_s(\mu_b) C_F}{4\pi} C_a^{(1)} \ , \quad \text{(A.22)}$$

$$\mathcal{T}_{a,\pm} = \mathcal{T}_{a,\pm}^{(0)}(u,\omega) + \frac{\alpha_s(\mu_f) C_F}{4\pi} \mathcal{T}_{a,\pm}^{(1)}(u,\omega) \ . \quad \text{(A.23)}$$

The form factor terms $C_a^{(0)}$ at leading order are

$$C_\perp^{(0)} = C_7^{\text{eff}} + \frac{q^2}{2m_b M_B} Y\left(q^2\right) \ , \quad C_\|^{(0)} = -C_7^{\text{eff}} - \frac{M_B}{2m_b} Y\left(q^2\right) \ . \quad \text{(A.24)}$$

The coefficients $C_a^{(1)}$ at next-to-leading order can be divided into a factorizable and a non-factorizable part as,

$$C_a^{(1)} = C_a^{(f)} + C_a^{(nf)}. \quad \text{(A.25)}$$

At NLO, the factorizable correction reads

$$C_\perp^{(f)} = C_7^{\text{eff}} \left(\ln \frac{m_b^2}{\mu^2} - L + \Delta M \right) \ , \quad C_\|^{(f)} = -C_7^{\text{eff}} \left(\ln \frac{m_b^2}{\mu^2} + 2L + \Delta M \right) \ , \quad \text{(A.26)}$$

and the non-factorizable corrections for heavy to light transitions are

$$\begin{aligned} C_F C_\perp^{(nf)} &= -\bar{C}_2 F_2^{(7)} - C_8^{\text{eff}} F_8^{(7)} - \frac{q^2}{2m_b M_B} \left[\bar{C}_2 F_2^{(9)} + 2\bar{C}_1 \left(F_1^{(9)} + \frac{1}{6} F_2^{(9)} \right) + C_8^{\text{eff}} F_8^{(9)} \right], \\ C_F C_\|^{(nf)} &= \bar{C}_2 F_2^{(7)} + C_8^{\text{eff}} F_8^{(7)} + \frac{M_B}{2m_b} \left[\bar{C}_2 F_2^{(9)} + 2\bar{C}_1 \left(F_1^{(9)} + \frac{1}{6} F_2^{(9)} \right) + C_8^{\text{eff}} F_8^{(9)} \right], \quad \text{(A.27)} \end{aligned}$$

where L and ΔM have been given in Ref. [160]. At leading order the hard-spectator scattering term $\mathcal{T}_{a,\pm}^{(0)}(u,\omega)$ from weak annihilation diagram is given as

$$\mathcal{T}_{\perp,+}^{(0)}(u,\omega) = \mathcal{T}_{\perp,-}^{(0)}(u,\omega) = \mathcal{T}_{\|,+}^{(0)}(u,\omega) = 0 \ , \quad \text{(A.28)}$$

$$\mathcal{T}_{\|,-}^{(0)}(u,\omega) = -e_q \frac{M_B \omega}{M_B \omega - q^2 - i\epsilon} \frac{4M_B}{m_b} \left(\bar{C}_3 + 3\bar{C}_4\right) \ . \quad \text{(A.29)}$$

The hard scattering functions $\mathcal{T}_a^{(1)}$ at next to leading order contain a factorisable as well as non-factorizable part:

$$\mathcal{T}_a^{(1)} = \mathcal{T}_a^{(f)} + \mathcal{T}_a^{(nf)}. \tag{A.30}$$

Including $\mathcal{O}(\alpha_s)$ corrections, the factorizable term for the hard scattering functions $\mathcal{T}_{a,\pm}^{(1)}$ are given by

$$\mathcal{T}_{\perp,+}^{(f)}(u,\omega) = C_7^{\text{eff}} \frac{2M_B}{\bar{u}E_{K^*}} = \frac{\mathcal{T}_{\parallel,+}^{(f)}(u,\omega)}{2} \, , \quad \mathcal{T}_{\perp,-}^{(f)}(u,\omega) = \mathcal{T}_{\parallel,-}^{(f)}(u,\omega) = 0 \, , \tag{A.31}$$

and the non-factorizable correction can be computed by solving the matrix elements of four-quark operators and the chromomagnetic dipole operator

$$\begin{aligned}
\mathcal{T}_{\perp,+}^{(nf)}(u,\omega) &= -\frac{4e_d C_8^{\text{eff}}}{u + \bar{u}q^2/M_B^2} + \frac{M_B}{2m_b}[e_u t_\perp(u,m_c)\left(\bar{C}_2 + \bar{C}_4 - \bar{C}_6\right) \\
&+ e_d t_\perp(u,m_b)\left(\bar{C}_3 + \bar{C}_4 - \bar{C}_6 - 4m_b/M_B\bar{C}_5\right) + e_d t_\perp(u,0)\bar{C}_3] \, , && \text{(A.32)} \\
\mathcal{T}_{\perp,-}^{(nf)}(u,\omega) &= 0 \, , && \text{(A.33)} \\
\mathcal{T}_{\parallel,+}^{(nf)}(u,\omega) &= \frac{M_B}{m_b}[e_u t_\parallel(u,m_c)\left(\bar{C}_2 + \bar{C}_4 - \bar{C}_6\right) \\
&+ e_d t_\parallel(u,m_b)\left(\bar{C}_3 + \bar{C}_4 - \bar{C}_6\right) + e_d t_\parallel(u,0)\bar{C}_3] \, , && \text{(A.34)} \\
\mathcal{T}_{\parallel,-}^{(nf)}(u,\omega) &= e_q \frac{M_B\omega}{M_B\omega - q^2 - i\epsilon}\Bigg[\frac{8C_8^{\text{eff}}}{\bar{u} + uq^2/M_B^2} \\
&+ \frac{6M_B}{m_b}\Bigg(h\left(\bar{u}M_B^2 + uq^2, m_c\right)\left(\bar{C}_2 + \bar{C}_4 + \bar{C}_6\right) \\
&+ h\left(\bar{u}M_B^2 + uq^2, m_b^{\text{pole}}\right)\left(\bar{C}_3 + \bar{C}_4 + \bar{C}_6\right) \\
&+ h\left(\bar{u}M_B^2 + uq^2, 0\right)\left(\bar{C}_3 + 3\bar{C}_4 + 3\bar{C}_6\right) - \frac{8}{27}\left(\bar{C}_3 - \bar{C}_5 - 15\bar{C}_6\right)\Bigg)\Bigg] . && \text{(A.35)}
\end{aligned}$$

The $t_a(u,m_q)$ functions are given by

$$\begin{aligned}
t_\perp(u,m_q) &= \frac{2M_B}{\bar{u}E_{K^*}} I_1(m_q) + \frac{q^2}{\bar{u}^2 E_{K^*}^2}\left(B_0\left(\bar{u}M_B^2 + uq^2, m_q\right) - B_0\left(q^2, m_q\right)\right) , \\
t_\parallel(u,m_q) &= \frac{2M_B}{\bar{u}E_{K^*}} I_1(m_q) + \frac{\bar{u}M_B^2 + uq^2}{\bar{u}^2 E_{K^*}^2}\left(B_0\left(\bar{u}M_B^2 + uq^2, m_q\right) - B_0\left(q^2, m_q\right)\right) , && \text{(A.36)}
\end{aligned}$$

where B_0 and I_1 are

$$B_0\left(q^2, m_q\right) = -2\sqrt{4m_q^2/q^2 - 1}\,\arctan\frac{1}{\sqrt{4m_q^2/q^2 - 1}} \, , \tag{A.37}$$

$$I_1(m_q) = 1 + \frac{2m_q^2}{\bar{u}\left(M_B^2 - q^2\right)}\left[L_1(x_+) + L_1(x_-) - L_1(y_+) - L_1(y_-)\right] \, , \tag{A.38}$$

and

$$x_\pm = \frac{1}{2} \pm \left(\frac{1}{4} - \frac{m_q^2}{\bar{u}M_B^2 + uq^2}\right)^{1/2}, \qquad y_\pm = \frac{1}{2} \pm \left(\frac{1}{4} - \frac{m_q^2}{q^2}\right)^{1/2}, \quad \text{(A.39)}$$

$$L_1(x) = \ln\frac{x-1}{x}\ln(1-x) - \frac{\pi^2}{6} + Li_2\left(\frac{x}{x-1}\right). \quad \text{(A.40)}$$

A.5 Functions involved in the isospin asymmetry parameter

The function $K_1^{\parallel}$ receives an annihilation contribution to leading order, and the functions $K_{1,2}^{\perp}$ appear at subleading order of the Λ_h/m_B expansion. The meson-photon transition form factors and their role in the annihilation contribution to B meson decays has been given by the function with superscript (a). Here only transverse polarization contributes, and there are no contributions from C_5 and C_6. The functions $K_{1,2}^{(b)}$ contain the decay amplitude from the diagram of hard-spectator interactions involving the gluonic penguin operator $\mathcal{O}_8$, and the contributions of the hard-spectator interaction diagrams involving the operator $\mathcal{O}_{1-6}$ have been included in $K_{1,2}^{(b)}$. The functions $K_1^{\parallel}$ and $K_{1,2}^{\perp}$ defined via b_q^a are given as [194]

$$K_1^{\perp}\left(q^2\right) = K_1^{\perp(a)}\left(q^2\right) + K_1^{\perp(b)}\left(q^2\right) + K_1^{\perp(c)}\left(q^2\right), \quad \text{(A.41)}$$

with

$$\begin{aligned}
K_1^{\perp(a)}\left(q^2\right) &= -\left(\bar{C}_6(\mu_h) + \frac{\bar{C}_5(\mu_h)}{N_c}\right)F_\perp(\hat{s}), \qquad F_\perp(\hat{s}) = \frac{1}{3}\int_0^1 du\frac{\phi_{K^*}^{\perp}(u)}{\bar{u}+u\hat{s}}, \\
K_1^{\perp(b)}\left(q^2\right) &= C_8^{\text{eff}}(\mu_h)\frac{m_b}{M_B}\frac{C_F}{N_c}\frac{\alpha_s(\mu_h)}{4\pi}X_\perp(\hat{s}), \quad X_\perp(\hat{s}) = F_\perp(\hat{s}) + \frac{1}{3}\int_0^1 du\frac{\phi_{K^*}^{\perp}(u)}{(\bar{u}+u\hat{s})^2}, \\
K_1^{\perp(c)}\left(q^2\right) &= \frac{C_F}{N_c}\frac{\alpha_s(\mu_h)}{4\pi}\frac{2}{3}\int_0^1 du\frac{\phi_{K^*}^{\perp}(u)}{\bar{u}+u\hat{s}}F_V\left(\bar{u}M_B^2 + uq^2\right) \quad \text{(A.42)}
\end{aligned}$$

and

$$K_2^{\perp}\left(q^2\right) = K_2^{\perp(a)}\left(q^2\right) + K_2^{\perp(b)}\left(q^2\right) + K_2^{\perp(c)}\left(q^2\right), \quad \text{(A.43)}$$

with

$$
\begin{aligned}
K_2^{\perp(a)}\left(q^2\right) &= -\frac{\lambda_u}{\lambda_t}\left(\frac{\bar{C}_1}{3}\left(\mu_h\right)+\bar{C}_2\left(\mu_h\right)\right)\delta_{qu}+\left(\bar{C}_4\left(\mu_h\right)+\frac{\bar{C}_3\left(\mu_h\right)}{3}\right)\ , \\
K_2^{\perp(b)}\left(q^2\right) &= \mathcal{O}\left(\frac{\Lambda_h}{M_B}\right)\ , \\
K_2^{\perp(c)}\left(q^2\right) &= -\frac{C_F}{N_c}\frac{\alpha_s\left(\mu_h\right)}{4\pi}\frac{1}{2}\int_0^1 du\left(g_\perp^{(\nu)}\left(u\right)-\frac{g_\perp^{'(a)}\left(u\right)}{4}\right)F_V\left(\bar{u}M_B^2+uq^2\right)
\end{aligned}
\tag{A.44}
$$

For the parallel case in Eqn. (61),

$$
K_1^{\parallel}\left(q^2\right)=K_1^{\parallel(a)}\left(q^2\right)+K_1^{\parallel(b)}\left(q^2\right)+K_1^{\parallel(c)}\left(q^2\right)\ , \tag{A.45}
$$

with

$$
\begin{aligned}
K_1^{\parallel(a)}\left(q^2\right) &= K_2^{\perp(a)}\left(q^2\right), \\
K_1^{\parallel(b)}\left(q^2\right) &= -C_8^{\text{eff}}\left(\mu_h\right)\frac{m_b}{M_B}\frac{C_F}{N_c}\frac{\alpha_s\left(\mu_h\right)}{4\pi}F_\parallel\left(\hat{s}\right), \qquad F_\parallel\left(\hat{s}\right)=2\int_0^1 du\frac{\phi_\parallel\left(u\right)}{\bar{u}+u\hat{s}}, \\
K_1^{\parallel(c)}\left(q^2\right) &= -\frac{C_F}{N_c}\frac{\alpha_s\left(\mu_h\right)}{4\pi}2\int_0^1 du\phi_\parallel\left(u\right)F_V\left(\bar{u}M_B^2+uq^2\right)\ .
\end{aligned}
\tag{A.46}
$$

The vector form factor $F_V(q^2)$ can be found in [194].

Appendix B

$\bar{B} \to \bar{D}^{(*)} l \bar{\nu}_l$ processes

B.1 $\bar{B} \to \bar{D} \tau \bar{\nu}_l$ form factors

The nonzero hadronic amplitudes for $B \to D\tau\bar{\nu}_l$ process are

$$\begin{aligned}
H^s_{V,0}(q^2) \equiv H^s_{V_{1,0}}(q^2) \equiv H^s_{V_{2,0}}(q^2) &= \sqrt{\frac{\lambda_D\left(q^2\right)}{q^2}} F_1\left(q^2\right), \\
H^s_{V,t}(q^2) \equiv H^s_{V_{1,t}}(q^2) \equiv H^s_{V_{2,t}}(q^2) &= \frac{M_B^2 - M_D^2}{\sqrt{q^2}} F_0\left(q^2\right), \\
H^s_S(q^2) \equiv H^s_{S_1}(q^2) = H^s_{S_2}(q^2) &\simeq \frac{M_B^2 - M_D^2}{m_b - m_c} F_0\left(q^2\right),
\end{aligned} \tag{B.1}$$

where the form factors $F_{0,1}$ are defined as

$$\begin{aligned}
F_1(q^2) &= \frac{1}{2\sqrt{M_B M_D}} \left[(M_B + M_D)\, h_+\left(\omega(q^2)\right) - (M_B - M_D)\, h_-\left(\omega(q^2)\right) \right], \\
F_0(q^2) &= \frac{1}{2\sqrt{M_B M_D}} \left[\frac{(M_B + M_D)^2 - q^2}{M_B + M_D} h_+\left(\omega(q^2)\right) \right. \\
&\qquad \left. - \frac{(M_B - M_D)^2 - q^2}{M_B - M_D} h_-\left(\omega(q^2)\right) \right].
\end{aligned} \tag{B.2}$$

Here $h_\pm\left(\omega(q^2)\right)$ are the HQET form factors taken from the Ref. [62, 233].

B.2 $B \to \bar{D}^* \tau \bar{\nu}_l$ form factors

The hadronic amplitude for $B \to D^* l \bar{\nu}$ process are

$$\begin{aligned}
H_{V,\pm}(q^2) &\equiv H^{\pm}_{V_1,\pm}(q^2) = -H^{\mp}_{V_2,\mp}(q^2) = (M_B + M_{D^*})\, A_1(q^2) \mp \frac{\sqrt{\lambda_{D^*}(q^2)}}{M_B + M_{D^*}} V(q^2), \\
H_{V,0}(q^2) &\equiv H^{0}_{V_1,0}(q^2) = -H^{0}_{V_2,0}(q^2) = \frac{M_B + M_{D^*}}{2M_{D^*}\sqrt{q^2}} \Big[-\left(M_B^2 - M_{D^*}^2 - q^2\right) A_1(q^2) \\
&\qquad + \frac{\lambda_{D^*}(q^2)}{(M_B + M_{D^*})^2} A_2(q^2) \Big], \\
H_{V,t}(q^2) &\equiv H^{0}_{V_1,t}(q^2) = -H^{0}_{V_2,t}(q^2) = -\sqrt{\frac{\lambda_{D^*}(q^2)}{q^2}} A_0(q^2), \\
H_S(q^2) &\equiv H^{0}_{S_1}(q^2) = -H^{0}_{S_2}(q^2) \simeq -\frac{\sqrt{\lambda_{D^*}(q^2)}}{m_b + m_c} A_0(q^2), \qquad \text{(B.3)}
\end{aligned}$$

where the form factors are defined as

$$\begin{aligned}
V(q^2) &= \frac{M_B + M_{D^*}}{2\sqrt{M_B M_{D^*}}} h_V\left(\omega(q^2)\right), \\
A_1(q^2) &= \frac{(M_B + M_{D^*})^2 - q^2}{2\sqrt{M_B M_{D^*}}(M_B + M_{D^*})} h_{A_1}\left(\omega(q^2)\right), \\
A_2(q^2) &= \frac{M_B + M_{D^*}}{2\sqrt{M_B M_{D^*}}} \Big[h_{A_3}\left(\omega(q^2)\right) + \frac{M_{D^*}}{M_B} h_{A_2}\left(\omega(q^2)\right) \Big], \\
A_0(q^2) &= \frac{1}{2\sqrt{M_B M_{D^*}}} \Big[\frac{(M_B + M_{D^*})^2 - q^2}{2M_{D^*}} h_{A_1}\left(\omega(q^2)\right) \\
&- \frac{M_B^2 - M_{D^*}^2 + q^2}{2M_B} h_{A_2}\left(\omega(q^2)\right) - \frac{M_B^2 - M_{D^*}^2 - q^2}{2M_{D^*}} h_{A_3}\left(\omega(q^2)\right) \Big]. \qquad \text{(B.4)}
\end{aligned}$$

The complete expression for HQET form factors $h_i, i = V, A_{1,2,3}$ are given in [62, 233].

B.3 τ and D^* polarizations

For a fixed polarization of τ, the decay distribution of $B \to D \tau \bar{\nu}_l$ process with respect to q^2 are given as [62].

$$\begin{aligned}
\frac{d\Gamma^{\lambda_\tau = 1/2}\left(\bar{B} \to D \tau \bar{\nu}_l\right)}{dq^2} &= \frac{G_F^2 |V_{cb}|^2}{192 \pi^3 M_B^3} q^2 \sqrt{\lambda_D(q^2)} \Big(1 - \frac{m_\tau^2}{q^2}\Big)^2 \times \\
&\Big[\frac{1}{2} \Big| \delta_{l\tau} + C^l_{V_1} \Big|^2 \frac{m_\tau^2}{q^2} \left({H^s_{V,0}}^2 + 3 {H^s_{V,t}}^2 \right) + \frac{3}{2} \Big| C^l_{S_1} \Big|^2 {H^s_S}^2 \\
&+ 3\mathrm{Re}\Big[\left(\delta_{l\tau} + C^l_{V_1}\right) {C^l_{S_1}}^* \frac{m_\tau}{\sqrt{q^2}} H^s_S H^s_{V,t} \Big], \qquad \text{(B.5)}
\end{aligned}$$

$$\frac{d\Gamma^{\lambda_\tau=-1/2}\left(\bar{B} \to D\tau\bar{\nu}_l\right)}{dq^2} = \frac{G_F^2|V_{cb}|^2}{192\pi^3 M_B^3} q^2 \sqrt{\lambda_D(q^2)}\Big(1-\frac{m_\tau^2}{q^2}\Big)^2 \Big|\delta_{l\tau}+C_{V_1}^l\Big|^2 {H_{V,0}^s}^2, \quad \text{(B.6)}$$

and for $B \to D^* \tau \bar{\nu}_l$ process

$$\begin{aligned} \frac{d\Gamma^{\lambda_\tau=1/2}\left(\bar{B} \to D^*\tau\bar{\nu}_l\right)}{dq^2} &= \frac{G_F^2|V_{cb}|^2}{192\pi^3 M_B^3} q^2 \sqrt{\lambda_{D^*}(q^2)}\Big(1-\frac{m_\tau^2}{q^2}\Big)^2 \times \\ &\Bigg[\frac{1}{2}\Big|\delta_{l\tau}+C_{V_1}^l\Big|^2 \frac{m_\tau^2}{q^2}\left(H_{V,+}^2+H_{V,-}^2+H_{V,0}^2+3H_{V,t}^2\right) \\ &+\frac{3}{2}\Big|C_{S_1}^l\Big|^2 {H_S}^2 + 3\mathrm{Re}\Big[\left(\delta_{l\tau}+C_{V_1}^l\right){C_{S_1}^l}^* \frac{m_\tau}{\sqrt{q^2}} H_S H_{V,t}\Bigg], \quad \text{(B.7)} \end{aligned}$$

$$\begin{aligned} \frac{d\Gamma^{\lambda_\tau=-1/2}\left(\bar{B} \to D^*\tau\bar{\nu}_l\right)}{dq^2} &= \frac{G_F^2|V_{cb}|^2}{192\pi^3 M_B^3} q^2 \sqrt{\lambda_{D^*}(q^2)}\Big(1-\frac{m_\tau^2}{q^2}\Big)^2 \\ &\times\Bigg[\Big|\delta_{l\tau}+C_{V_1}^l\Big|^2\left(H_{V,+}^2+H_{V,-}^2+H_{V,0}^2\right)\Bigg]. \quad \text{(B.8)} \end{aligned}$$

The q^2 distributions of $B \to D^* \tau \bar{\nu}_l$ process for a given polarization of D^* are given as

$$\begin{aligned} \frac{d\Gamma^{\lambda_{D^*}=\pm1}\left(\bar{B} \to D^*\tau\bar{\nu}_l\right)}{dq^2} &= \frac{G_F^2|V_{cb}|^2}{192\pi^3 M_B^3} q^2 \sqrt{\lambda_{D^*}(q^2)}\Big(1-\frac{m_\tau^2}{q^2}\Big)^2 \\ &\times\Bigg[\Big(1+\frac{m_\tau^2}{2q^2}\Big)\Big|\delta_{l\tau}+C_{V_1}^l\Big|^2 H_{V,\pm}^2\Bigg], \quad \text{(B.9)} \end{aligned}$$

$$\begin{aligned} \frac{d\Gamma^{\lambda_{D^*}=0}\left(\bar{B} \to D^*\tau\bar{\nu}_l\right)}{dq^2} &= \frac{G_F^2|V_{cb}|^2}{192\pi^3 M_B^3} q^2 \sqrt{\lambda_{D^*}(q^2)}\Big(1-\frac{m_\tau^2}{q^2}\Big)^2 \times \\ &\Bigg[\Big|\delta_{l\tau}+C_{V_1}^l\Big|^2\Big[\Big(1+\frac{m_\tau^2}{2q^2}\Big)H_{V,0}^2+\frac{3}{2}\frac{m_\tau^2}{q^2}H_{V,t}^2\Big]+\frac{3}{2}\Big|C_{S_1}^l\Big|^2 H_S^2 \\ &+3\mathrm{Re}\Big[\left(\delta_{l\tau}+C_{V_1}^l\right){C_{S_1}^l}^* \frac{m_\tau}{\sqrt{q^2}} H_S H_{V,t}\Bigg]. \quad \text{(B.10)} \end{aligned}$$

Bibliography

[1] S. L. Glashow, "*Partial Symmetries of Weak Interactions*," Nucl. Phys. **22** (1961) 579–588.

[2] A. Salam, "*Weak and Electromagnetic Interactions*," in *Elementary particle theory*, N. Svartholm, ed., pp. 367–377. Almquist & Wiksell.

[3] S. Weinberg, "*A Model of Leptons*," Phys. Rev. Lett. **19** (1967) 1264–1266.

[4] F. Englert and R. Brout, "*Broken Symmetry and the Mass of Gauge Vector Mesons*," Phys. Rev. Lett. **13** (1964) 321–323.

[5] P. W. Higgs, "*Broken symmetries, massless particles and gauge fields*," Phys. Lett. **12** (1964) 132–133.

[6] P. W. Higgs, "*Broken Symmetries and the Masses of Gauge Bosons*," Phys. Rev. Lett. **13** (1964) 508–509.

[7] G. S. Guralnik, C. R. Hagen, and T. W. B. Kibble, "*Global Conservation Laws and Massless Particles*," Phys. Rev. Lett. **13** (1964) 585–587.

[8] **ATLAS**, G. Aad *et al.*, "*Observation of a new particle in the search for the Standard Model Higgs boson with the ATLAS detector at the LHC*," Phys. Lett. **B716** (2012) 1–29, `arXiv:1207.7214`.

[9] **CMS**, S. Chatrchyan *et al.*, "*Observation of a new boson at a mass of 125 GeV with the CMS experiment at the LHC*," Phys. Lett. **B716** (2012) 30–61, `arXiv:1207.7235`.

[10] Y. Nir, "*CP violation: A New era*," in *Heavy flavor physics: Theory and experimental results in heavy quark physics and CP violation. Proceedings, 55th Scottish Universities Summer School in Physics, SUSSP 2001, St. Andrews, UK, August 7-23, 2001*, pp. 147–200. 2001. `arXiv:hep-ph/0109090`.

[11] Y. Nir, "*CP violation in and beyond the standard model*," in *Proceedings, 27th SLAC Summer Institute on Particle Physics: CP Violation in and Beyond the*

Standard Model (SSI 99): Stanford, USA, July 7-16, 1999, pp. 165–243. 1999. arXiv:hep-ph/9911321. http://www-public.slac.stanford.edu/sciDoc/docMeta.aspx?slacPubNumber=slac-r-719.

[12] Y. Grossman, "*Introduction to flavor physics*," in *Flavianet School on Flavour Physics Karlsruhe, Germany, September 7-18, 2009*, pp. 111–144. 2014. arXiv:1006.3534. https://inspirehep.net/record/858514/files/arXiv:1006.3534.pdf. [,73(2014)].

[13] A. J. Buras, "*Weak Hamiltonian, CP violation and rare decays*," in *Probing the standard model of particle interactions. Proceedings, Summer School in Theoretical Physics, NATO Advanced Study Institute, 68th session, Les Houches, France, July 28-September 5, 1997. Pt. 1, 2*, pp. 281–539. 1998. arXiv:hep-ph/9806471.

[14] P. H. Frampton, *GAUGE FIELD THEORIES*. 1987.

[15] R. E. Marshak, *Conceptual foundations of modern particle physics*. 1993.

[16] A. D. Sakharov, "*Violation of CP Invariance, c Asymmetry, and Baryon Asymmetry of the Universe*," Pisma Zh. Eksp. Teor. Fiz. **5** (1967) 32–35. [Usp. Fiz. Nauk161,61(1991)].

[17] A. D. Sakharov, "*Baryonic Asymmetry of the Universe*," Sov. Phys. JETP **49** (1979) 594–599. [Zh. Eksp. Teor. Fiz.76,1172(1979)].

[18] N. Cabibbo, "*Unitary Symmetry and Leptonic Decays*," Phys. Rev. Lett. **10** (1963) 531–533. [,648(1963)].

[19] G. Buchalla, "*Kaon and charm physics: Theory*," in *Flavor physics for the millennium. Proceedings, Theoretical Advanced Study Institute in elementary particle physics, TASI 2000, Boulder, USA, June 4-30, 2000*, pp. 143–205. 2001. arXiv:hep-ph/0103166. http://weblib.cern.ch/abstract?CERN-TH-2001-041.

[20] W.-M. Yao *et al.*, "*Review of Particle Physics*," Journal of Physics G **33** (2006) 1+. http://pdg.lbl.gov.

[21] S. L. Glashow, J. Iliopoulos, and L. Maiani, "*Weak Interactions with Lepton-Hadron Symmetry*," Phys. Rev. **D2** (1970) 1285–1292.

[22] M. Kobayashi and T. Maskawa, "*CP Violation in the Renormalizable Theory of Weak Interaction*," Prog. Theor. Phys. **49** (1973) 652–657.

[23] H. Harari and M. Leurer, "*Recommending a Standard Choice of Cabibbo Angles and KM Phases for Any Number of Generations*," Phys. Lett. **B181** (1986) 123–128.

[24] **Particle Data Group**, C. Patrignani *et al.*, "*Review of Particle Physics*," Chin. Phys. **C40** (2016) no. 10, 100001.

[25] L.-L. Chau and W.-Y. Keung, "*Comments on the Parametrization of the Kobayashi-Maskawa Matrix*," Phys. Rev. Lett. **53** (1984) 1802.

[26] L. Wolfenstein, "*Parametrization of the Kobayashi-Maskawa Matrix*," Phys. Rev. Lett. **51** (1983) 1945.

[27] C. Jarlskog, "*Commutator of the Quark Mass Matrices in the Standard Electroweak Model and a Measure of Maximal CP Violation*," Phys. Rev. Lett. **55** (1985) 1039.

[28] R. Aleksan, B. Kayser, and D. London, "*Determining the quark mixing matrix from CP violating asymmetries*," Phys. Rev. Lett. **73** (1994) 18–20, `arXiv:hep-ph/9403341`.

[29] C. Jarlskog and R. Stora, "*Unitarity Polygons and CP Violation Areas and Phases in the Standard Electroweak Model*," Phys. Lett. **B208** (1988) 268–274.

[30] J. H. Christenson, J. W. Cronin, V. L. Fitch, and R. Turlay, "*Evidence for the 2π Decay of the K_2^0 Meson*," Phys. Rev. Lett. **13** (1964) 138–140.

[31] **Belle**, A. Abashian *et al.*, "*Measurement of the CP violation parameter $\sin 2\phi_1$ in B_d^0 meson decays*," Phys. Rev. Lett. **86** (2001) 2509–2514, `arXiv:hep-ex/0102018`.

[32] **Belle**, K. Abe *et al.*, "*Observation of large CP violation in the neutral B meson system*," Phys. Rev. Lett. **87** (2001) 091802, `arXiv:hep-ex/0107061`.

[33] **Belle**, K. Abe *et al.*, "*Observation of mixing induced CP violation in the neutral B meson system*," Phys. Rev. **D66** (2002) 032007, `arXiv:hep-ex/0202027`.

[34] **Belle**, K. Abe *et al.*, "*An Improved measurement of mixing induced CP violation in the neutral B meson system*," Phys. Rev. **D66** (2002) 071102, `arXiv:hep-ex/0208025`.

[35] **BaBar**, B. Aubert *et al.*, "*Measurement of CP violating asymmetries in B^0 decays to CP eigenstates*," Phys. Rev. Lett. **86** (2001) 2515–2522, `arXiv:hep-ex/0102030`.

[36] **BaBar**, B. Aubert *et al.*, "*Observation of CP violation in the B^0 meson system*," Phys. Rev. Lett. **87** (2001) 091801, `arXiv:hep-ex/0107013`.

[37] **BaBar**, B. Aubert *et al.*, "*A study of time dependent CP-violating asymmetries and flavor oscillations in neutral B decays at the $\Upsilon(4S)$*," Phys. Rev. **D66** (2002) 032003, `arXiv:hep-ex/0201020`.

[38] **BaBar**, B. Aubert *et al.*, "*Measurement of the CP-violating asymmetry amplitude* $\sin 2\beta$," Phys. Rev. Lett. **89** (2002) 201802, `arXiv:hep-ex/0207042`.

[39] **LHCb**, R. Aaij *et al.*, "*Test of lepton universality using $B^+ \to K^+\ell^+\ell^-$ decays*," Phys. Rev. Lett. **113** (2014) 151601, `arXiv:1406.6482`.

[40] **LHCb**, R. Aaij *et al.*, "*Test of lepton universality with $B^0 \to K^{*0}\ell^+\ell^-$ decays*," JHEP **08** (2017) 055, `arXiv:1705.05802`.

[41] **BaBar**, J. P. Lees *et al.*, "*Evidence for an excess of $\bar{B} \to D^{(*)}\tau^-\bar{\nu}_\tau$ decays*," Phys. Rev. Lett. **109** (2012) 101802, `arXiv:1205.5442`.

[42] **BaBar**, J. P. Lees *et al.*, "*Measurement of an Excess of $\bar{B} \to D^{(*)}\tau^-\bar{\nu}_\tau$ Decays and Implications for Charged Higgs Bosons*," Phys. Rev. **D88** (2013) no. 7, 072012, `arXiv:1303.0571`.

[43] **Belle**, M. Huschle *et al.*, "*Measurement of the branching ratio of $\bar{B} \to D^{(*)}\tau^-\bar{\nu}_\tau$ relative to $\bar{B} \to D^{(*)}\ell^-\bar{\nu}_\ell$ decays with hadronic tagging at Belle*," Phys. Rev. **D92** (2015) no. 7, 072014, `arXiv:1507.03233`.

[44] **Belle**, A. Abdesselam *et al.*, "*Measurement of the branching ratio of $\bar{B}^0 \to D^{*+}\tau^-\bar{\nu}_\tau$ relative to $\bar{B}^0 \to D^{*+}\ell^-\bar{\nu}_\ell$ decays with a semileptonic tagging method*," in *Proceedings, 51st Rencontres de Moriond on Electroweak Interactions and Unified Theories: La Thuile, Italy, March 12-19, 2016*. 2016. `arXiv:1603.06711`. `http://inspirehep.net/record/1431982/files/arXiv:1603.06711.pdf`.

[45] *Heavy Flavor Averaging Group*. `http://www.slac.stanford.edu/xorg/hfag/semi/winter16/winter16dtaunu.html`.

[46] **LHCb**, R. Aaij *et al.*, "*Measurement of the ratio of branching fractions $\mathcal{B}(\bar{B}^0 \to D^{*+}\tau^-\bar{\nu}_\tau)/\mathcal{B}(\bar{B}^0 \to D^{*+}\mu^-\bar{\nu}_\mu)$*," Phys. Rev. Lett. **115** (2015) no. 11, 111803, `arXiv:1506.08614`. [Erratum: Phys. Rev. Lett.115,no.15,159901(2015)].

[47] S. Weinberg, "*Implications of Dynamical Symmetry Breaking*," Phys. Rev. **D13** (1976) 974–996. [Addendum: Phys. Rev.D19,1277(1979)].

[48] L. Susskind, "*Lattice Models of Quark Confinement at High Temperature*," Phys. Rev. **D20** (1979) 2610–2618.

[49] K. G. Wilson, "*The Renormalization Group and Strong Interactions*," Phys. Rev. **D3** (1971) 1818.

[50] G. 't Hooft, "*Naturalness, chiral symmetry, and spontaneous chiral symmetry breaking*," NATO Sci. Ser. B **59** (1980) 135–157.

[51] E. Witten, "*Anomalous Cross-Section for Photon - Photon Scattering in Gauge Theories*," Nucl. Phys. **B120** (1977) 189–202.

[52] W. Zimmermann, "*Normal products and the short distance expansion in the perturbation theory of renormalizable interactions*," Annals Phys. **77** (1973) 570–601. [Lect. Notes Phys.558,278(2000)].

[53] K. G. Wilson, "*Nonlagrangian models of current algebra*," Phys. Rev. **179** (1969) 1499–1512.

[54] K. G. Wilson and W. Zimmermann, "*Operator product expansions and composite field operators in the general framework of quantum field theory*," Commun. Math. Phys. **24** (1972) 87–106.

[55] G. Buchalla, A. J. Buras, and M. E. Lautenbacher, "*Weak decays beyond leading logarithms*," Rev. Mod. Phys. **68** (1996) 1125–1144, `arXiv:hep-ph/9512380`.

[56] A. J. Buras and M. Munz, "*Effective Hamiltonian for B —¿ X(s) e+ e- beyond leading logarithms in the NDR and HV schemes*," Phys. Rev. **D52** (1995) 186–195, `arXiv:hep-ph/9501281`.

[57] M. Misiak, "*The $b \to se^+e^-$ and $b \to s\gamma$ decays with next-to-leading logarithmic QCD corrections*," Nucl. Phys. **B393** (1993) 23–45. [Erratum: Nucl. Phys.B439,461(1995)].

[58] M. Beneke, T. Feldmann, and D. Seidel, "*Exclusive radiative and electroweak $b \to d$ and $b \to s$ penguin decays at NLO*," Eur. Phys. J. **C41** (2005) 173–188, `arXiv:hep-ph/0412400`.

[59] W. Altmannshofer, A. J. Buras, D. M. Straub, and M. Wick, "*New strategies for New Physics search in $B \to K^*\nu\bar{\nu}$, $B \to K\nu\bar{\nu}$ and $B \to X_s\nu\bar{\nu}$ decays*," JHEP **04** (2009) 022, `arXiv:0902.0160`.

[60] M. Misiak and J. Urban, "*QCD corrections to FCNC decays mediated by Z penguins and W boxes*," Phys. Lett. **B451** (1999) 161–169, `arXiv:hep-ph/9901278`.

[61] G. Buchalla and A. J. Buras, "*The rare decays $K \to \pi\nu\bar{\nu}$, $B \to X\nu\bar{\nu}$ and $B \to l^+l^-$: An Update*," Nucl. Phys. **B548** (1999) 309–327, arXiv:hep-ph/9901288.

[62] Y. Sakaki, M. Tanaka, A. Tayduganov, and R. Watanabe, "*Testing leptoquark models in $\bar{B} \to D^{(*)}\tau\bar{\nu}$*," Phys. Rev. **D88** (2013) no. 9, 094012, arXiv:1309.0301.

[63] M. Wirbel, B. Stech, and M. Bauer, "*Exclusive Semileptonic Decays of Heavy Mesons*," Z. Phys. **C29** (1985) 637.

[64] N. Isgur and M. B. Wise, "*Relationship Between Form-factors in Semileptonic $\bar{B}$ and D Decays and Exclusive Rare $\bar{B}$ Meson Decays*," Phys. Rev. **D42** (1990) 2388–2391.

[65] A. Ali, P. Ball, L. T. Handoko, and G. Hiller, "*A Comparative study of the decays $B \to (K, K^*)\ell^+\ell^-$ in standard model and supersymmetric theories*," Phys. Rev. **D61** (2000) 074024, arXiv:hep-ph/9910221.

[66] O. Nachtmann, "*Elementary Particle Physics*," Springer-Verlag, 1990.

[67] G. C. Branco, L. Lavoura, and J. P. Silva, "*CP Violation*,".

[68] E. Leader and E. Predazzi, "*An Introduction to Gauge Theories and Modern Particle Physics*," p. 12. Cambridge University Press, 1996.

[69] **LHCb**, R. Aaij *et al.*, "*Differential branching fractions and isospin asymmetries of $B \to K^{(*)}\mu^+\mu^-$ decays*," JHEP **06** (2014) 133, arXiv:1403.8044.

[70] **LHCb**, R. Aaij *et al.*, "*Measurement of Form-Factor-Independent Observables in the Decay $B^0 \to K^{*0}\mu^+\mu^-$*," Phys. Rev. Lett. **111** (2013) 191801, arXiv:1308.1707.

[71] **LHCb**, R. Aaij *et al.*, "*Differential branching fraction and angular analysis of the decay $B_s^0 \to \phi\mu^+\mu^-$*," JHEP **07** (2013) 084, arXiv:1305.2168.

[72] J. Blumlein and R. Ruckl, "*Production of scalar and vector leptoquarks in e+ e- annihilation*," Phys. Lett. **B304** (1993) 337–346.

[73] H. Georgi and S. L. Glashow, "*Unity of All Elementary Particle Forces*," Phys. Rev. Lett. **32** (1974) 438–441.

[74] H. Fritzsch and P. Minkowski, "*Unified Interactions of Leptons and Hadrons*," Annals Phys. **93** (1975) 193–266.

[75] P. Langacker, "*Grand Unified Theories and Proton Decay*," Phys. Rept. **72** (1981) 185.

[76] H. Georgi, "*The State of the ArtGauge Theories*," AIP Conf. Proc. **23** (1975) 575–582.

[77] J. C. Pati and A. Salam, "*Lepton Number as the Fourth Color*," Phys. Rev. **D10** (1974) 275–289. [Erratum: Phys. Rev.D11,703(1975)].

[78] J. C. Pati and A. Salam, "*Unified Lepton-Hadron Symmetry and a Gauge Theory of the Basic Interactions*," Phys. Rev. **D8** (1973) 1240–1251.

[79] J. C. Pati and A. Salam, "*Is Baryon Number Conserved?*," Phys. Rev. Lett. **31** (1973) 661–664.

[80] O. U. Shanker, "*Flavor Violation, Scalar Particles and Leptoquarks*," Nucl. Phys. **B206** (1982) 253–272.

[81] O. U. Shanker, "*$\pi\ell$ 2, $K\ell$ 3 and $K^0 - \bar{K}0$ Constraints on Leptoquarks and Supersymmetric Particles*," Nucl. Phys. **B204** (1982) 375–386.

[82] J. L. Hewett and T. G. Rizzo, "*Low-Energy Phenomenology of Superstring Inspired E(6) Models*," Phys. Rept. **183** (1989) 193.

[83] D. B. Kaplan, "*Flavor at SSC energies: A New mechanism for dynamically generated fermion masses*," Nucl. Phys. **B365** (1991) 259–278.

[84] B. Gripaios, "*Composite Leptoquarks at the LHC*," JHEP **02** (2010) 045, `arXiv:0910.1789`.

[85] B. Schrempp and F. Schrempp, "*LIGHT LEPTOQUARKS*," Phys. Lett. **153B** (1985) 101–107.

[86] E. Baver and M. Leurer, "*Naturally light leptoquarks*," Phys. Rev. **D51** (1995) 260–264, `arXiv:hep-ph/9407324`.

[87] M. Leurer, "*A Comprehensive study of leptoquark bounds*," Phys. Rev. **D49** (1994) 333–342, `arXiv:hep-ph/9309266`.

[88] M. Leurer, "*New bounds on leptoquarks*," Phys. Rev. Lett. **71** (1993) 1324–1327, `arXiv:hep-ph/9304211`.

[89] W. Buchmuller and D. Wyler, "*Constraints on SU(5) Type Leptoquarks*," Phys. Lett. **B177** (1986) 377–382.

[90] S. Davidson, D. C. Bailey, and B. A. Campbell, "*Model independent constraints on leptoquarks from rare processes*," Z. Phys. **C61** (1994) 613–644, arXiv:hep-ph/9309310.

[91] R. N. Cahn and H. Harari, "*Bounds on the Masses of Neutral Generation Changing Gauge Bosons*," Nucl. Phys. **B176** (1980) 135–152.

[92] M. Kuze and Y. Sirois, "*Search for particles and forces beyond the standard model at HERA ep and Tevatron $p\bar{p}$ colliders*," Prog. Part. Nucl. Phys. **50** (2003) 1–62, arXiv:hep-ex/0211048. [Erratum: Prog. Part. Nucl. Phys.53,583(2004)].

[93] **CMS**, V. Khachatryan *et al.*, "*Search for Third-Generation Scalar Leptoquarks in the $t\tau$ Channel in Proton-Proton Collisions at $\sqrt{s}$ = 8 TeV*," JHEP **07** (2015) 042, arXiv:1503.09049. [Erratum: JHEP11,056(2016)].

[94] **CMS**, V. Khachatryan *et al.*, "*Search for pair production of third-generation scalar leptoquarks and top squarks in protonproton collisions at $\sqrt{s}$=8 TeV*," Phys. Lett. **B739** (2014) 229–249, arXiv:1408.0806.

[95] **CMS**, S. Chatrchyan *et al.*, "*Search for third-generation leptoquarks and scalar bottom quarks in pp collisions at $\sqrt{s} = 7$ TeV*," JHEP **12** (2012) 055, arXiv:1210.5627.

[96] **ATLAS**, G. Aad *et al.*, "*Search for third generation scalar leptoquarks in pp collisions at $\sqrt{s}$ = 7 TeV with the ATLAS detector*," JHEP **06** (2013) 033, arXiv:1303.0526.

[97] **ATLAS**, G. Aad *et al.*, "*Searches for scalar leptoquarks in pp collisions at $\sqrt{s}$ = 8 TeV with the ATLAS detector*," Eur. Phys. J. **C76** (2016) no. 1, 5, arXiv:1508.04735.

[98] **Particle Data Group**, K. A. Olive *et al.*, "*Review of Particle Physics*," Chin. Phys. **C38** (2014) 090001.

[99] **CDF**, D. Acosta *et al.*, "*Search for first-generation scalar leptoquarks in $p\bar{p}$ collisions at $\sqrt{s} = 1.96$ TeV*," Phys. Rev. **D72** (2005) 051107, arXiv:hep-ex/0506074.

[100] **CDF**, A. Abulencia *et al.*, "*Search for second-generation scalar leptoquarks in $p\bar{p}$ collisions at $\sqrt{s}$ = 1.96-TeV.*," Phys. Rev. **D73** (2006) 051102, arXiv:hep-ex/0512055.

[101] **D0**, V. M. Abazov *et al.*, "*Search for pair production of first-generation leptoquarks in p anti-p collisions at s**(1/2) = 1.96-TeV*," Phys. Lett. **B681** (2009) 224–232, arXiv:0907.1048.

[102] **D0**, V. M. Abazov *et al.*, "*Search for pair production of second generation scalar leptoquarks*," Phys. Lett. **B671** (2009) 224–232, arXiv:0808.4023.

[103] **CMS**, S. Chatrchyan *et al.*, "*Search for pair production of first- and second-generation scalar leptoquarks in pp collisions at $\sqrt{s} = 7$ TeV*," Phys. Rev. **D86** (2012) 052013, arXiv:1207.5406.

[104] **CMS Collaboration**, "*Search for Pair-production of Second generation Leptoquarks in 8 TeV proton-proton collisions.*," Tech. Rep. CMS-PAS-EXO-12-042, CERN, Geneva, 2013. https://cds.cern.ch/record/1542374.

[105] H. Murayama and T. Yanagida, "*A viable SU(5) GUT with light leptoquark bosons*," Mod. Phys. Lett. **A7** (1992) 147–152.

[106] G. Senjanovic and A. Sokorac, "*Light Leptoquarks in SO(10)*," Z. Phys. **C20** (1983) 255.

[107] D. Beirevi, S. Fajfer, N. Konik, and O. Sumensari, "*Leptoquark model to explain the B-physics anomalies, R_K and R_D*," Phys. Rev. **D94** (2016) no. 11, 115021, arXiv:1608.08501.

[108] M. Bauer and M. Neubert, "*Minimal Leptoquark Explanation for the $R_{D^{(*)}}$, R_K , and $(g-2)_g$ Anomalies*," Phys. Rev. Lett. **116** (2016) no. 14, 141802, arXiv:1511.01900.

[109] R. Alonso, B. Grinstein, and J. Martin Camalich, "*Lepton universality violation and lepton flavor conservation in B-meson decays*," JHEP **10** (2015) 184, arXiv:1505.05164.

[110] L. Calibbi, A. Crivellin, and T. Ota, "*Effective Field Theory Approach to bs(), BK(*) and BD(*) with Third Generation Couplings*," Phys. Rev. Lett. **115** (2015) 181801, arXiv:1506.02661.

[111] D. Beirevi, N. Konik, O. Sumensari, and R. Zukanovich Funchal, "*Palatable Leptoquark Scenarios for Lepton Flavor Violation in Exclusive $b \to s\ell_1\ell_2$ modes*," JHEP **11** (2016) 035, arXiv:1608.07583.

[112] I. Dorsner, S. Fajfer, J. F. Kamenik, and N. Kosnik, "*Can scalar leptoquarks explain the f(D(s)) puzzle?*," Phys. Lett. **B682** (2009) 67–73, arXiv:0906.5585.

[113] I. Dorner, S. Fajfer, A. Greljo, J. F. Kamenik, and N. Konik, "*Physics of leptoquarks in precision experiments and at particle colliders*," Phys. Rept. **641** (2016) 1–68, arXiv:1603.04993.

[114] I. Dorsner, S. Fajfer, and A. Greljo, "*Cornering Scalar Leptoquarks at LHC*," JHEP **10** (2014) 154, arXiv:1406.4831.

[115] I. Dorsner, J. Drobnak, S. Fajfer, J. F. Kamenik, and N. Kosnik, "*Limits on scalar leptoquark interactions and consequences for GUTs*," JHEP **11** (2011) 002, arXiv:1107.5393.

[116] S. Fajfer, J. F. Kamenik, I. Nisandzic, and J. Zupan, "*Implications of Lepton Flavor Universality Violations in B Decays*," Phys. Rev. Lett. **109** (2012) 161801, arXiv:1206.1872.

[117] I. Dorner, S. Fajfer, N. Konik, and I. Niandi, "*Minimally flavored colored scalar in $\bar{B} \to D^{(*)}\tau\bar{\nu}$ and the mass matrices constraints*," JHEP **11** (2013) 084, arXiv:1306.6493.

[118] I. Dorner, S. Fajfer, D. A. Faroughy, and N. Konik, "*Saga of the two GUT leptoquarks in flavor universality and collider searches*," arXiv:1706.07779.

[119] S. Fajfer and N. Konik, "*Vector leptoquark resolution of R_K and $R_{D^{(*)}}$ puzzles*," Phys. Lett. **B755** (2016) 270–274, arXiv:1511.06024.

[120] N. Kosnik, "*Model independent constraints on leptoquarks from $b \to s\ell^+\ell^-$ processes*," Phys. Rev. **D86** (2012) 055004, arXiv:1206.2970.

[121] J. M. Arnold, B. Fornal, and M. B. Wise, "*Phenomenology of scalar leptoquarks*," Phys. Rev. **D88** (2013) 035009, arXiv:1304.6119.

[122] J. P. Saha, B. Misra, and A. Kundu, "*Constraining Scalar Leptoquarks from the K and B Sectors*," Phys. Rev. **D81** (2010) 095011, arXiv:1003.1384.

[123] R. Mohanta, "*Effect of scalar leptoquarks on the rare decays of B_s meson*," Phys. Rev. **D89** (2014) no. 1, 014020, arXiv:1310.0713.

[124] F. S. Queiroz, K. Sinha, and A. Strumia, "*Leptoquarks, Dark Matter, and Anomalous LHC Events*," Phys. Rev. **D91** (2015) no. 3, 035006, arXiv:1409.6301.

[125] G. Hiller and I. Nisandzic, "*R_K and R_{K^*} beyond the standard model*," Phys. Rev. **D96** (2017) no. 3, 035003, arXiv:1704.05444.

[126] G. Hiller, D. Loose, and K. Schnwald, "*Leptoquark Flavor Patterns & B Decay Anomalies*," JHEP **12** (2016) 027, arXiv:1609.08895.

[127] I. de Medeiros Varzielas and G. Hiller, "*Clues for flavor from rare lepton and quark decays*," JHEP **06** (2015) 072, arXiv:1503.01084.

[128] G. Hiller and M. Schmaltz, "*R_K and future $b \to s\ell\ell$ physics beyond the standard model opportunities*," Phys. Rev. **D90** (2014) 054014, arXiv:1408.1627.

[129] D. Aristizabal Sierra, M. Hirsch, and S. G. Kovalenko, "*Leptoquarks: Neutrino masses and accelerator phenomenology*," Phys. Rev. **D77** (2008) 055011, arXiv:0710.5699.

[130] S. Davidson and S. Descotes-Genon, "*Minimal Flavour Violation for Leptoquarks*," JHEP **11** (2010) 073, arXiv:1009.1998.

[131] B. Gripaios, M. Nardecchia, and S. A. Renner, "*Composite leptoquarks and anomalies in B-meson decays*," JHEP **05** (2015) 006, arXiv:1412.1791.

[132] W. Buchmuller, R. Ruckl, and D. Wyler, "*Leptoquarks in Lepton - Quark Collisions*," Phys. Lett. **B191** (1987) 442–448. [Erratum: Phys. Lett.B448,320(1999)].

[133] A. J. Davies and X.-G. He, "*Tree Level Scalar Fermion Interactions Consistent With the Symmetries of the Standard Model*," Phys. Rev. **D43** (1991) 225–235.

[134] P. H. Frampton and B.-H. Lee, "*SU(15) GRAND UNIFICATION*," Phys. Rev. Lett. **64** (1990) 619.

[135] P. H. Frampton, "*Light leptoquarks as possible signature of strong electroweak unification*," Mod. Phys. Lett. **A7** (1992) 559–562.

[136] P. H. Frampton and T. W. Kephart, "*Higgs sector and proton decay in SU(15) grand unification*," Phys. Rev. **D42** (1990) 3892–3894.

[137] K. De Bruyn, R. Fleischer, R. Knegjens, P. Koppenburg, M. Merk, A. Pellegrino, and N. Tuning, "*Probing New Physics via the $B_s^0 \to \mu^+\mu^-$ Effective Lifetime*," Phys. Rev. Lett. **109** (2012) 041801, arXiv:1204.1737.

[138] C. Bobeth, M. Gorbahn, T. Hermann, M. Misiak, E. Stamou, and M. Steinhauser, "*$B_{s,d} \to l^+l^-$ in the Standard Model with Reduced Theoretical Uncertainty*," Phys. Rev. Lett. **112** (2014) 101801, arXiv:1311.0903.

[139] **CMS**, S. Chatrchyan *et al.*, "*Measurement of the B(s) to mu+ mu- branching fraction and search for B0 to mu+ mu- with the CMS Experiment*," Phys. Rev. Lett. **111** (2013) 101804, arXiv:1307.5025.

[140] **LHCb**, R. Aaij *et al.*, "*Measurement of the $B_s^0 \to \mu^+\mu^-$ branching fraction and search for $B^0 \to \mu^+\mu^-$ decays at the LHCb experiment*," Phys. Rev. Lett. **111** (2013) 101805, arXiv:1307.5024.

[141] **LHCb, CMS**, V. Khachatryan *et al.*, "*Observation of the rare $B_s^0 \to \mu^+\mu^-$ decay from the combined analysis of CMS and LHCb data*," Nature **522** (2015) 68–72, `arXiv:1411.4413`.

[142] **CDF**, T. Aaltonen *et al.*, "*Search for the Decays $B_s^0 \to e^+\mu^-$ and $B_s^0 \to e^+e^-$ in CDF Run II*," Phys. Rev. Lett. **102** (2009) 201801, `arXiv:0901.3803`.

[143] **LHCb Collaboration**, K. De Bruyn, "*Search for the rare decays $B_{(s)}^0 \to \tau^+\tau^-$*," Tech. Rep. LHCb-CONF-2016-011. CERN-LHCb-CONF-2016-011, CERN, Geneva, Sep, 2016. `https://cds.cern.ch/record/2220757`.

[144] A. K. Alok, A. Datta, A. Dighe, M. Duraisamy, D. Ghosh, and D. London, "*New Physics in b -¿ s mu+ mu-: CP-Violating Observables*," JHEP **11** (2011) 122, `arXiv:1103.5344`.

[145] A. Ali, E. Lunghi, C. Greub, and G. Hiller, "*Improved model independent analysis of semileptonic and radiative rare B decays*," Phys. Rev. **D66** (2002) 034002, `arXiv:hep-ph/0112300`.

[146] **BaBar**, J. P. Lees *et al.*, "*Measurement of the $B \to X_s l^+l^-$ branching fraction and search for direct CP violation from a sum of exclusive final states*," Phys. Rev. Lett. **112** (2014) 211802, `arXiv:1312.5364`.

[147] T. Inami and C. S. Lim, "*Effects of Superheavy Quarks and Leptons in Low-Energy Weak Processes k(L) —¿ mu anti-mu, K+ —¿ pi+ Neutrino anti-neutrino and K0 ¡—¿ anti-K0*," Prog. Theor. Phys. **65** (1981) 297. [Erratum: Prog. Theor. Phys.65,1772(1981)].

[148] J. Charles *et al.*, "*Current status of the Standard Model CKM fit and constraints on $\Delta F = 2$ New Physics*," Phys. Rev. **D91** (2015) no. 7, 073007, `arXiv:1501.05013`.

[149] Y. Grossman, Z. Ligeti, and E. Nardi, "*New limit on inclusive $B \to X_s$ anti-neutrino neutrino decay and constraints on new physics*," Nucl. Phys. **B465** (1996) 369–398, `arXiv:hep-ph/9510378`. [Erratum: Nucl. Phys.B480,753(1996)].

[150] **ALEPH**, R. Barate *et al.*, "*Measurements of BR (b —¿ tau- anti-nu(tau) X) and BR (b —¿ tau- anti-nu(tau) D*+- X) and upper limits on BR (B- —¿ tau- anti-nu(tau)) and BR (b—¿ s nu anti-nu)*," Eur. Phys. J. **C19** (2001) 213–227, `arXiv:hep-ex/0010022`.

[151] P. Biancofiore, P. Colangelo, and F. De Fazio, "*On the anomalous enhancement observed in $B \to D^{(*)}\tau\bar{\nu}_\tau$ decays*," Phys. Rev. **D87** (2013) no. 7, 074010, `arXiv:1302.1042`.

[152] S. Aoki *et al.*, "*Review of lattice results concerning low-energy particle physics*," Eur. Phys. J. **C74** (2014) 2890, arXiv:1310.8555.

[153] G. Buchalla and A. J. Buras, "*The rare decays $K^+ \to \pi^+ \nu \bar{\nu}$ and $K_L \to \mu^+ \mu^-$ beyond leading logarithms*," Nucl. Phys. **B412** (1994) 106–142, arXiv:hep-ph/9308272.

[154] G. Isidori and R. Unterdorfer, "*On the short distance constraints from K(L,S) —¿ mu+ mu-*," JHEP **01** (2004) 009, arXiv:hep-ph/0311084.

[155] I. Dorner, S. Fajfer, A. Greljo, J. F. Kamenik, N. Konik, and I. Niandic, "*New Physics Models Facing Lepton Flavor Violating Higgs Decays at the Percent Level*," JHEP **06** (2015) 108, arXiv:1502.07784.

[156] K. Cheung, W.-Y. Keung, and P.-Y. Tseng, "*Leptoquark induced rare decay amplitudes $h \to \tau^{\mp} \mu^{\pm}$ and $\tau \to \mu\gamma$*," Phys. Rev. **D93** (2016) no. 1, 015010, arXiv:1508.01897.

[157] S. Baek and K. Nishiwaki, "*Leptoquark explanation of $h \to \mu\tau$ and muon $(g-2)$*," Phys. Rev. **D93** (2016) no. 1, 015002, arXiv:1509.07410.

[158] L. Lavoura, "*General formulae for f(1) —¿ f(2) gamma*," Eur. Phys. J. **C29** (2003) 191–195, arXiv:hep-ph/0302221.

[159] M. Beneke and T. Feldmann, "*Symmetry breaking corrections to heavy to light B meson form-factors at large recoil*," Nucl. Phys. **B592** (2001) 3–34, arXiv:hep-ph/0008255.

[160] M. Beneke, T. Feldmann, and D. Seidel, "*Systematic approach to exclusive $B \to V l^+ l^-$, $V\gamma$ decays*," Nucl. Phys. **B612** (2001) 25–58, arXiv:hep-ph/0106067.

[161] C. Bobeth, G. Hiller, and D. van Dyk, "*More Benefits of Semileptonic Rare B Decays at Low Recoil: CP Violation*," JHEP **07** (2011) 067, arXiv:1105.0376.

[162] C. Bobeth, G. Hiller, D. van Dyk, and C. Wacker, "*The Decay $B \to K \ell^+ \ell^-$ at Low Hadronic Recoil and Model-Independent $\Delta B = 1$ Constraints*," JHEP **01** (2012) 107, arXiv:1111.2558.

[163] D. London, "*Extracting Weak Phases Cleanly from Charmless 3-Body B Decays*," in *7th International Workshop on the CKM Unitarity Triangle (CKM 2012) Cincinnati, Ohio, USA, September 28-October 2, 2012*. 2012. arXiv:1212.3221. http://inspirehep.net/record/1207267/files/arXiv:1212.3221.pdf.

[164] C. Bobeth, G. Hiller, and G. Piranishvili, "*Angular distributions of $\bar{B} \to \bar{K}\ell^+\ell^-$ decays*," JHEP **12** (2007) 040, `arXiv:0709.4174`.

[165] **LHCb**, R. Aaij *et al.*, "*Measurement of the isospin asymmetry in $B \to K^{(*)}\mu^+\mu^-$ decays*," JHEP **07** (2012) 133, `arXiv:1205.3422`.

[166] C. W. Bauer, S. Fleming, D. Pirjol, and I. W. Stewart, "*An Effective field theory for collinear and soft gluons: Heavy to light decays*," Phys. Rev. **D63** (2001) 114020, `arXiv:hep-ph/0011336`.

[167] A. Ali, G. Kramer, and G.-h. Zhu, "*$B \to K^+l^+l^-$ decay in soft-collinear effective theory*," Eur. Phys. J. **C47** (2006) 625–641, `arXiv:hep-ph/0601034`.

[168] K. S. M. Lee, Z. Ligeti, I. W. Stewart, and F. J. Tackmann, "*Extracting short distance information from $b \to sl^+l^-$ effectively*," Phys. Rev. **D75** (2007) 034016, `arXiv:hep-ph/0612156`.

[169] J. Charles, A. Le Yaouanc, L. Oliver, O. Pene, and J. C. Raynal, "*Heavy to light form-factors in the heavy mass to large energy limit of QCD*," Phys. Rev. **D60** (1999) 014001, `arXiv:hep-ph/9812358`.

[170] P. Ball and R. Zwicky, "*New results on $B \to \pi, K, \eta$ decay formfactors from light-cone sum rules*," Phys. Rev. **D71** (2005) 014015, `arXiv:hep-ph/0406232`.

[171] A. Khodjamirian, T. Mannel, A. A. Pivovarov, and Y. M. Wang, "*Charm-loop effect in $B \to K^{(*)}\ell^+\ell^-$ and $B \to K^*\gamma$*," JHEP **09** (2010) 089, `arXiv:1006.4945`.

[172] W.-S. Hou, M. Kohda, and F. Xu, "*Rates and asymmetries of B^{+-} decays*," Phys. Rev. **D90** (2014) no. 1, 013002, `arXiv:1403.7410`.

[173] P. Colangelo, F. De Fazio, P. Santorelli, and E. Scrimieri, "*Rare $B \to K^{(*)}$ neutrino anti-neutrino decays at B factories*," Phys. Lett. **B395** (1997) 339–344, `arXiv:hep-ph/9610297`.

[174] C. S. Kim, Y. G. Kim, and T. Morozumi, "*New physics effects in B —¿ K(*) neutrino neutrino decays*," Phys. Rev. **D60** (1999) 094007, `arXiv:hep-ph/9905528`.

[175] U. Egede, T. Hurth, J. Matias, M. Ramon, and W. Reece, "*New observables in the decay mode $\bar{B}_d \to \bar{K}^{*0}l^+l^-$*," JHEP **11** (2008) 032, `arXiv:0807.2589`.

[176] D. Melikhov, N. Nikitin, and S. Simula, "*Right-handed currents in rare exclusive B —¿ (K, K*) neutrino anti-neutrino decays*," Phys. Lett. **B428** (1998) 171–178, `arXiv:hep-ph/9803269`.

[177] W. Altmannshofer, P. Ball, A. Bharucha, A. J. Buras, D. M. Straub, and M. Wick, "*Symmetries and Asymmetries of $B \to K^* \mu^+ \mu^-$ Decays in the Standard Model and Beyond*," JHEP **01** (2009) 019, `arXiv:0811.1214`.

[178] P. Ball and R. Zwicky, "*$B_{d,s} \to \rho, \omega, K^*, \phi$ decay form-factors from light-cone sum rules revisited*," Phys. Rev. **D71** (2005) 014029, `arXiv:hep-ph/0412079`.

[179] C. Bobeth, A. J. Buras, F. Kruger, and J. Urban, "*QCD corrections to $\bar{B} \to X_{d,s} \nu \bar{\nu}$, $\bar{B}_{d,s} \to \ell^+ \ell^-$, $K \to \pi \nu \bar{\nu}$ and $K_L \to \mu^+ \mu^-$ in the MSSM*," Nucl. Phys. **B630** (2002) 87–131, `arXiv:hep-ph/0112305`.

[180] **LHCb**, C. Langenbruch, "*Latest results on rare decays from LHCb*," in *Proceedings, 50th Rencontres de Moriond Electroweak Interactions and Unified Theories: La Thuile, Italy, March 14-21, 2015*, pp. 317–324. 2015. `arXiv:1505.04160`. `http://inspirehep.net/record/1370442/files/arXiv:1505.04160.pdf`.

[181] B. Grinstein and D. Pirjol, "*Exclusive rare $B \to K^* \ell^+ \ell^-$ decays at low recoil: Controlling the long-distance effects*," Phys. Rev. **D70** (2004) 114005, `arXiv:hep-ph/0404250`.

[182] M. Beylich, G. Buchalla, and T. Feldmann, "*Theory of $B \to K^{(*)} \ell^+ \ell^-$ decays at high q^2: OPE and quark-hadron duality*," Eur. Phys. J. **C71** (2011) 1635, `arXiv:1101.5118`.

[183] G. Buchalla and G. Isidori, "*Nonperturbative effects in $\bar{B} \to X_s l^+ l^-$ for large dilepton invariant mass*," Nucl. Phys. **B525** (1998) 333–349, `arXiv:hep-ph/9801456`.

[184] B. Grinstein and D. Pirjol, "*Symmetry breaking corrections to heavy meson form-factor relations*," Phys. Lett. **B533** (2002) 8–16, `arXiv:hep-ph/0201298`.

[185] M. Bauer and M. Wirbel, "*Form-Factor Effects in Exclusive d and B Decays*," Z. Phys. **C42** (1989) 671.

[186] B. Stech, "*A Form-factor model for exclusive B and D decays*," Z. Phys. **C75** (1997) 245–251, `arXiv:hep-ph/9608297`.

[187] C. Bobeth, G. Hiller, and G. Piranishvili, "*CP Asymmetries in bar $B \to \bar{K}^* (\to \bar{K} \pi) \bar{\ell} \ell$ and Untagged $\bar{B}_s$, $B_s \to \phi (\to K^+ K^-) \bar{\ell} \ell$ Decays at NLO*," JHEP **07** (2008) 106, `arXiv:0805.2525`.

[188] U. Egede, T. Hurth, J. Matias, M. Ramon, and W. Reece, "*New physics reach of the decay mode $\bar{B} \to \bar{K}^{*0} \ell^+ \ell^-$*," JHEP **10** (2010) 056, `arXiv:1005.0571`.

[189] F. Beaujean, C. Bobeth, D. van Dyk, and C. Wacker, "*Bayesian Fit of Exclusive $b \to s\bar{\ell}\ell$ Decays: The Standard Model Operator Basis*," JHEP **08** (2012) 030, arXiv:1205.1838.

[190] F. Kruger and J. Matias, "*Probing new physics via the transverse amplitudes of $B^0 \to K^{*0}(\to K^-\pi^+)l^+l^-$ at large recoil*," Phys. Rev. **D71** (2005) 094009, arXiv:hep-ph/0502060.

[191] J. Matias, F. Mescia, M. Ramon, and J. Virto, "*Complete Anatomy of $\bar{B}_d - > \bar{K}^{*0}(- > K\pi)l^+l^-$ and its angular distribution*," JHEP **04** (2012) 104, arXiv:1202.4266.

[192] S. Descotes-Genon, J. Matias, M. Ramon, and J. Virto, "*Implications from clean observables for the binned analysis of $B - > K * \mu^+\mu^-$ at large recoil*," JHEP **01** (2013) 048, arXiv:1207.2753.

[193] T. Feldmann and J. Matias, "*Forward backward and isospin asymmetry for $B \to K^* l^+ l^-$ decay in the standard model and in supersymmetry*," JHEP **01** (2003) 074, arXiv:hep-ph/0212158.

[194] M. R. Ahmady, S. Lord, and R. Sandapen, "*Isospin asymmetry in $B \to K^*\mu^+\mu^-$ using AdS/QCD*," Phys. Rev. **D90** (2014) no. 7, 074010, arXiv:1407.6700.

[195] C. Bobeth, G. Hiller, and D. van Dyk, "*The Benefits of $\bar{B} - > \bar{K}^* l^+ l^-$ Decays at Low Recoil*," JHEP **07** (2010) 098, arXiv:1006.5013.

[196] **HPQCD**, H. Na, C. M. Bouchard, G. P. Lepage, C. Monahan, and J. Shigemitsu, "*$B \to Dl\nu$ form factors at nonzero recoil and extraction of $|V_{cb}|$*," Phys. Rev. **D92** (2015) no. 5, 054510, arXiv:1505.03925. [Erratum: Phys. Rev.D93,no.11,119906(2016)].

[197] S. Fajfer, J. F. Kamenik, and I. Nisandzic, "*On the $B \to D^*\tau\bar{\nu}_\tau$ Sensitivity to New Physics*," Phys. Rev. **D85** (2012) 094025, arXiv:1203.2654.

[198] A. Crivellin and S. Pokorski, "*Can the differences in the determinations of V_{ub} and V_{cb} be explained by New Physics?*," Phys. Rev. Lett. **114** (2015) no. 1, 011802, arXiv:1407.1320.

[199] B. Bhattacharya, A. Datta, D. London, and S. Shivashankara, "*Simultaneous Explanation of the R_K and $R(D^{(*)})$ Puzzles*," Phys. Lett. **B742** (2015) 370–374, arXiv:1412.7164.

[200] S. Bhattacharya, S. Nandi, and S. K. Patra, "*Optimal-observable analysis of possible new physics in $B \to D^{(*)}\tau\nu_\tau$*," Phys. Rev. **D93** (2016) no. 3, 034011, arXiv:1509.07259.

[201] C. Hati, G. Kumar, and N. Mahajan, "*$\bar{B} \to D^{(*)}\tau\bar{\nu}$ excesses in ALRSM constrained from B, D decays and $D^0 - \bar{D}^0$ mixing*," JHEP **01** (2016) 117, arXiv:1511.03290.

[202] Y. Sakaki, M. Tanaka, A. Tayduganov, and R. Watanabe, "*Probing New Physics with q^2 distributions in $\bar{B} \to D^{(*)}\tau\bar{\nu}$*," Phys. Rev. **D91** (2015) no. 11, 114028, arXiv:1412.3761.

[203] D. Becirevic, S. Fajfer, I. Nisandzic, and A. Tayduganov, "*Angular distributions of $\bar{B} \to D^{(*)}\ell\bar{\nu}_\ell$ decays and search of New Physics*," arXiv:1602.03030.

[204] N. Kosnik, D. Becirevic, and A. Tayduganov, "*Testing the Standard Model in $B \to D\tau\bar{\nu}$ decay with minimal theory input*," arXiv:1301.4037. [PoSConfinementX,244(2012)].

[205] D. Das, C. Hati, G. Kumar, and N. Mahajan, "*Towards a unified explanation of $R_{D^{(*)}}$, R_K and $(g-2)_\mu$ anomalies in a left-right model with leptoquarks*," Phys. Rev. **D94** (2016) 055034, arXiv:1605.06313.

[206] M. Duraisamy, P. Sharma, and A. Datta, "*Azimuthal $B \to D^*\tau^-\bar{\nu_\tau}$ angular distribution with tensor operators*," Phys. Rev. **D90** (2014) no. 7, 074013, arXiv:1405.3719.

[207] K. Hagiwara, M. M. Nojiri, and Y. Sakaki, "*CP violation in $B \to D\tau\nu_\tau$ using multipion tau decays*," Phys. Rev. **D89** (2014) no. 9, 094009, arXiv:1403.5892.

[208] R. Alonso, A. Kobach, and J. Martin Camalich, "*New physics in the kinematic distributions of $\bar{B} \to D^{(*)}\tau^-(\to \ell^-\bar{\nu}_\ell\nu_\tau)\bar{\nu}_\tau$*," Phys. Rev. **D94** (2016) no. 9, 094021, arXiv:1602.07671.

[209] R. Barbieri, G. Isidori, A. Pattori, and F. Senia, "*Anomalies in B-decays and $U(2)$ flavour symmetry*," Eur. Phys. J. **C76** (2016) no. 2, 67, arXiv:1512.01560.

[210] M. A. Ivanov, J. G. Krner, and C.-T. Tran, "*Analyzing new physics in the decays $\bar{B}^0 \to D^{(*)}\tau^-\bar{\nu}_\tau$ with form factors obtained from the covariant quark model*," Phys. Rev. **D94** (2016) no. 9, 094028, arXiv:1607.02932.

[211] M. Duraisamy and A. Datta, "*The Full $B \to D^*\tau^-\bar{\nu_\tau}$ Angular Distribution and CP violating Triple Products*," JHEP **09** (2013) 059, arXiv:1302.7031.

[212] A. Datta, M. Duraisamy, and D. Ghosh, "*Diagnosing New Physics in $b \to c\,\tau\,\nu_\tau$ decays in the light of the recent BaBar result*," Phys. Rev. **D86** (2012) 034027, arXiv:1206.3760.

[213] M. Tanaka and R. Watanabe, "*New physics in the weak interaction of $\bar{B} \to D^{(*)}\tau\bar{\nu}$*," Phys. Rev. **D87** (2013) no. 3, 034028, `arXiv:1212.1878`.

[214] M. Freytsis, Z. Ligeti, and J. T. Ruderman, "*Flavor models for $\bar{B} \to D^{(*)}\tau\bar{\nu}$*," Phys. Rev. **D92** (2015) no. 5, 054018, `arXiv:1506.08896`.

[215] X.-Q. Li, Y.-D. Yang, and X. Zhang, "*Revisiting the one leptoquark solution to the R($D^{()}$) anomalies and its phenomenological implications*," JHEP **08** (2016) 054, `arXiv:1605.09308`.

[216] B. Dumont, K. Nishiwaki, and R. Watanabe, "*LHC constraints and prospects for S_1 scalar leptoquark explaining the $\bar{B} \to D^{(*)}\tau\bar{\nu}$ anomaly*," Phys. Rev. **D94** (2016) no. 3, 034001, `arXiv:1603.05248`.

[217] B. Capdevila, A. Crivellin, S. Descotes-Genon, J. Matias, and J. Virto, "*Patterns of New Physics in $b \to s\ell^+\ell^-$ transitions in the light of recent data*," `arXiv:1704.05340`.

[218] M. Bordone, G. Isidori, and A. Pattori, "*On the Standard Model predictions for R_K and R_{K^*}*," Eur. Phys. J. **C76** (2016) no. 8, 440, `arXiv:1605.07633`.

[219] P. Gambino and C. Schwanda, "*Inclusive semileptonic fits, heavy quark masses, and V_{cb}*," Phys. Rev. **D89** (2014) no. 1, 014022, `arXiv:1307.4551`.

[220] S. L. Glashow, D. Guadagnoli, and K. Lane, "*Lepton Flavor Violation in B Decays?*," Phys. Rev. Lett. **114** (2015) 091801, `arXiv:1411.0565`.

[221] **CMS**, V. Khachatryan *et al.*, "*Search for Lepton-Flavour-Violating Decays of the Higgs Boson*," Phys. Lett. **B749** (2015) 337–362, `arXiv:1502.07400`.

[222] C.-J. Lee and J. Tandean, "*Minimal lepton flavor violation implications of the $b \to s$ anomalies*," JHEP **08** (2015) 123, `arXiv:1505.04692`.

[223] W. Altmannshofer and I. Yavin, "*Predictions for lepton flavor universality violation in rare B decays in models with gauged $L_\mu - L_\tau$*," Phys. Rev. **D92** (2015) no. 7, 075022, `arXiv:1508.07009`.

[224] A. Crivellin, G. D'Ambrosio, and J. Heeck, "*Explaining $h \to \mu^\pm\tau^\mp$, $B \to K^*\mu^+\mu^-$ and $B \to K\mu^+\mu^-/B \to Ke^+e^-$ in a two-Higgs-doublet model with gauged $L_\mu - L_\tau$*," Phys. Rev. Lett. **114** (2015) 151801, `arXiv:1501.00993`.

[225] A. Crivellin, L. Hofer, J. Matias, U. Nierste, S. Pokorski, and J. Rosiek, "*Lepton-flavour violating B decays in generic Z' models*," Phys. Rev. **D92** (2015) no. 5, 054013, `arXiv:1504.07928`.

[226] **LHCb**, R. Aaij *et al.*, "*First observation of the decay $B^+ \to \pi^+\mu^+\mu^-$*," JHEP **12** (2012) 125, `arXiv:1210.2645`.

[227] J. A. Bailey *et al.*, "*$B \to Kl^+l^-$ decay form factors from three-flavor lattice QCD*," Phys. Rev. **D93** (2016) no. 2, 025026, `arXiv:1509.06235`.

[228] A. Khodjamirian, T. Mannel, N. Offen, and Y. M. Wang, "*$B \to \pi\ell\nu_l$ Width and $|V_{ub}|$ from QCD Light-Cone Sum Rules*," Phys. Rev. **D83** (2011) 094031, `arXiv:1103.2655`.

[229] S. Davidson, G. Isidori, and S. Uhlig, "*Solving the flavour problem with hierarchical fermion wave functions*," Phys. Lett. **B663** (2008) 73–79, `arXiv:0711.3376`.

[230] M. Redi, "*Leptons in Composite MFV*," JHEP **09** (2013) 060, `arXiv:1306.1525`.

[231] **Muon g-2**, G. W. Bennett *et al.*, "*Measurement of the negative muon anomalous magnetic moment to 0.7 ppm*," Phys. Rev. Lett. **92** (2004) 161802, `arXiv:hep-ex/0401008`.

[232] J. P. Miller, E. de Rafael, and B. L. Roberts, "*Muon (g-2): Experiment and theory*," Rept. Prog. Phys. **70** (2007) 795, `arXiv:hep-ph/0703049`.

[233] I. Caprini, L. Lellouch, and M. Neubert, "*Dispersive bounds on the shape of anti-B —¿ D(*) lepton anti-neutrino form-factors*," Nucl. Phys. **B530** (1998) 153–181, `arXiv:hep-ph/9712417`.

List of Publications

Thesis Publications

1. ***"Scalar leptoquarks and the rare B meson decays"***, **S. Sahoo**, and R. Mohanta, Phys. Rev. D **91**, 094019 (2015), [arXiv:1501.05193].

2. ***"Study of the rare semileptonic decays $\bar{B}_d^0 \to \bar{K}^* l^+ l^-$ in scalar leptoquark model"***, **S. Sahoo**, and R. Mohanta, Phys. Rev. D **93**, 034018 (2015), [arXiv:1507.02070].

3. ***"Leptoquark effects on $b \to s\nu\bar{\nu}$ and $\bar{B} \to \bar{K} l^+ l^-$ decay processes"***, **S. Sahoo**, and R. Mohanta, New J. Phys. **18**, 013032 (2016) [arXiv:1509.06248].

4. ***"Explaining R_K and $R_{D^{(*)}}$ anomalies with vector leptoquark"***, **S. Sahoo**, R. Mohanta, and A. Giri, Phys. Rev. D **95** 035027 (2017) [arXiv:1609.04367].

5. ***"Rare semileptonic $B \to K(\pi) l_i^- l_j^+$ decay in vector leptoquark model"***, M. Duraisamy, **S. Sahoo**, and R. Mohanta, Phys. Rev. D **95**, 035022 (2017), [arXiv:1610.00902].

Other Publications

1. ***"Lepton flavor violating B meson decays via a scalar leptoquark"***, **S. Sahoo**, and R. Mohanta, Phys. Rev. D **93**, 114001 (2016) [arXiv:1512.04567].

2. ***"Effects of scalar leptoquark on semileptonic Λ_b decays"***, **S. Sahoo**, and R. Mohanta, New J.Phys. **18**, 093051 (2016) [arXiv:1607.04449].

3. ***"Study of the rare decays $B_{s,d}^* \to \mu^+ \mu^-$"***, **S. Sahoo**, and R. Mohanta, Jour. Phys. G **44**, 035001 (2017), [arXiv:1612.02543].

4. ***"New physics effects in charm meson decays involving** $c \to u l^+ l^- (l^\mp l^\pm)$" **transitions"**, **S. Sahoo**, and R. Mohanta, Eur. Phys. J. C **77**, 344 (2017), [arXiv:1705.02251].

5. ***"Impact of vector leptoquark on** $\bar{B} \to \bar{K}^* l^+ l^-$ **anomalies"***, **S. Sahoo**, and R. Mohanta, (Under review).

6. ***"Model independent investigation of rare semileptonic** $b \to u l \bar{\nu}_l$ **decay processes"***, **S. Sahoo**, A. Ray, and R. Mohanta, (Under review).

Conference Proceedings

1. ***"Scalar Leptoquarks and the Rare** B **Meson Decays"***, **S. Sahoo**, and R. Mohanta, Springer Proc. Phys. **174**, 221-226 (2016).

2. ***"Implications of lepton nonuniversality in the beauty sector"***, A. Giri, R. Mohanta, and **S. Sahoo**, J. Phys. Conf. Ser, **770**, 012031 (2016) [arXiv:1610.02659].

3. ***"Effects of Scalar Leptoquarks in** $b \to s$ **Transitions"***, R. Mohanta, and **S. Sahoo**, J. Phys. Conf. Ser, **770**, 012019 (2016).

4. ***"Impact of leptoquarks in semileptonic** B **decays"***, **S. Sahoo**, R. Mohanta, and A. Giri, PoS CKM2016, **145** (2017), [arXiv:1701.06768].

5. ***"Study of the rare decays** $B^*_{s,d} \to \mu^+ \mu^-$ **"***, **S. Sahoo**, and R. Mohanta, Proceedings of XXII DAE-BRNS High Energy Physics Symposium 2016 [arXiv:1706.10026] (To appear in springer proceedings).

Phenomenological Study of Rare Semileptonic B Meson Decays with Leptoquarks

ORIGINALITY REPORT

37%	9%	36%	2%
SIMILARITY INDEX	INTERNET SOURCES	PUBLICATIONS	STUDENT PAPERS

PRIMARY SOURCES

1	Suchismita Sahoo, Rukmani Mohanta, Anjan K. Giri. " Explaining the and anomalies with vector leptoquarks ", Physical Review D, 2017 Publication	8%
2	Suchismita Sahoo, Rukmani Mohanta. " Study of the rare semileptonic decays in scalar leptoquark model ", Physical Review D, 2016 Publication	7%
3	Suchismita Sahoo, Rukmani Mohanta. " Scalar leptoquarks and the rare meson decays ", Physical Review D, 2015 Publication	3%
4	Murugeswaran Duraisamy, Suchismita Sahoo, Rukmani Mohanta. " Rare semileptonic decay in a vector leptoquark model ", Physical Review D, 2017 Publication	3%
5	Sahoo, Suchismita, and Rukmani Mohanta. "Leptoquark effects on \$b\;\to	2%

\;s{\boldsymbol{\nu }}\bar{{\boldsymbol{\nu }}}$ and $B\;\to \;{{Kl}}^{+}{l}^{-}$ decay processes", New Journal of Physics, 2016.
Publication

6	Suchismita Sahoo, Rukmani Mohanta. " Lepton flavor violating meson decays via a scalar leptoquark ", Physical Review D, 2016 Publication	2%
7	Suchismita Sahoo, Rukmani Mohanta. "New physics effects in charm meson decays involving $$c \rightarrow u l^+ l^- (l_i^{\mp } l_j^{\,\pm \,})$$ c → u l + l - (l i ∓ l j ±) transitions", The European Physical Journal C, 2017 Publication	1%
8	pos.sissa.it Internet Source	1%
9	Bevan, A. J., B. Golob, Th. Mannel, S. Prell, B. D. Yabsley, H. Aihara, F. Anulli, N. Arnaud, T. Aushev, M. Beneke, J. Beringer, F. Bianchi, I. I. Bigi, M. Bona, N. Brambilla, J. Brodzicka, P. Chang, M. J. Charles, C. H. Cheng, H.-Y. Cheng, R. Chistov, P. Colangelo, J. P. Coleman, A. Drutskoy, V. P. Druzhinin, S. Eidelman, G. Eigen, A. M. Eisner, R. Faccini, K. T. Flood, P. Gambino, A. Gaz, W. Gradl, H. Hayashii, T. Higuchi, W. D. Hulsbergen, T. Hurth, T. Iijima,	<1%

This is to certify that the thesis entitled "Phenomenological study of rare semileptonic B meson decays with leptoquarks" has been screened by the Turnitin software at the library of University of Hyderabad. The software shows 37% similarity index out of which, 23% came from the candidates research articles related to this thesis and 3% came from her other research articles (published in Physical Review D, and European Journal of Physics C), which are not related to this thesis. The major part of remaining 11% might have come from the other articles, which has not been detected by the software. Therefore, this thesis is free from plagiarism.

Prof. Rukmani Mohanta
(Thesis Supervisor)